

Turnover of Suspended and Settled Organic Matter in Ports and Waterways

Zander, F.

DOI

[10.4233/uuid:f4d57842-9603-41aa-950b-1009ab3c3fe3](https://doi.org/10.4233/uuid:f4d57842-9603-41aa-950b-1009ab3c3fe3)

Publication date

2022

Document Version

Final published version

Citation (APA)

Zander, F. (2022). *Turnover of Suspended and Settled Organic Matter in Ports and Waterways*. [Dissertation (TU Delft), Delft University of Technology]. <https://doi.org/10.4233/uuid:f4d57842-9603-41aa-950b-1009ab3c3fe3>

Important note

To cite this publication, please use the final published version (if applicable). Please check the document version above.

Copyright

Other than for strictly personal use, it is not permitted to download, forward or distribute the text or part of it, without the consent of the author(s) and/or copyright holder(s), unless the work is under an open content license such as Creative Commons.

Takedown policy

Please contact us and provide details if you believe this document breaches copyrights. We will remove access to the work immediately and investigate your claim.

Turnover of Suspended and Settled Organic Matter in Ports and Waterways



Florian Zander

Turnover of Suspended and Settled Organic Matter in Ports and Waterways

Turnover of Suspended and Settled Organic Matter in Ports and Waterways

Dissertation

for the purpose of obtaining the degree of doctor

at Delft University of Technology

by the authority of the Rector Magnificus prof. dr. ir. T.H.J.J. van der Hagen

Chair of the Board for Doctorates

to be defended publicly on

Wednesday 6 July 2022 at 17:30 o'clock

by

Florian ZANDER

Master of Science in Geoscience

University of Hamburg, Germany

born in Hamburg, Germany

This dissertation has been approved by the promotor.

Composition of the doctoral committee

Rector Magnificus	Chairperson
Dr. habil. J. Gebert	Delft University of Technology, promotor
Prof. dr. ir. T.J. Heimovaara	Delft University of Technology, promotor

Independent members

Prof. dr. H. M. Jonkers	Delft University of Technology
Prof. dr. R. N. J. Comans	Wageningen University
Dr. J.E.E. von Beusekom	Helmholtz-Zentrum Hereon, Germany
Dr. habil. ir. C. Chassagne	Delft University of Technology
Dr. B.M. van Breukelen	Delft University of Technology
Prof. dr. ir. M. K. de Kreuk	Delft University of Technology, reserve member



MUDNET

Keywords: Sediment organic matter, river sediments, spatial variability, DOM fractions, organic matter decay rates, yield stress, organo-mineral complexes, carbon flux, temporal variability

Copyright © 2022 by F. Zander

An electronic version of this dissertation is available at <http://repository.tudelft.nl>.

Content

Glossary	XI
Summary	XIII
1 Introduction	17
1.1 Decomposition, stabilization and transformation of organic matter.....	17
1.2 Stabilization and mineralization.....	17
1.3 Classification and decomposition.....	19
1.4 Humification.....	20
1.5 Impact of organic matter on rheological and nautical properties.....	21
1.6 Investigation area: Elbe Estuary and Port of Hamburg.....	22
2 Research questions	25
3 Structure of results presentation	27
4 Field sampling and analysis methods	29
4.1 Field sampling.....	29
4.2 Laboratory analyses.....	30
5 Spatial variability of organic matter degradability in tidal Elbe sediments	33
Abstract	34
5.1 Introduction	35
5.2 Investigation area and sampling strategy	36
5.2.1 Investigation area.....	36
5.2.2 Sampling strategy.....	36
5.3 Methods	37
5.3.1 Anaerobic degradation of organic matter.....	37
5.3.2 Aerobic degradation of organic matter.....	37
5.3.3 Carbon stable isotopes.....	38
5.3.4 DNA concentration.....	38
5.3.5 Density fractionation.....	38
5.3.6 Standard properties of solids and pore water.....	38
5.3.7 Statistical evaluation of data.....	39
5.4 Results	39
5.4.1 Sediment properties.....	39
5.4.2 Degradation of organic matter.....	42
5.4.3 Relationship between abiotic sediment properties and organic matter degradation.....	45
5.5 Discussion	45
5.5.1 Sediment properties and degradation of organic matter.....	45
5.5.2 Source and stabilisation of organic matter in sediments.....	49
5.5.3 Transformation of nitrogen.....	50
5.6 Conclusions and outlook	51
Acknowledgements	52

References.....	52
6 Linking patterns of density, thermometric and carbon stable isotope fractions of organic matter to its lability in sediments of the tidal Elbe river	55
Abstract.....	56
6.1 Introduction	57
6.2 Materials and methods.....	58
6.3 Results.....	60
6.3.1 Origin and properties of investigated sediments	60
6.3.2 Extractable SOM fractions, field transect.....	63
6.3.3 Effect of temperature and time on anaerobic SOM decay and water-extractable SOM dynamics	65
6.3.4 Density fractions, carbon stable isotopes and thermometric fractions	67
6.4 Discussion.....	70
6.4.1 Stratification of biological and chemical indicators along the transect.....	70
6.4.2 Organic matter lability: chemical organic matter (SOM) fractions.....	71
6.4.3 Physical organic matter fractions and stable carbon isotopes	73
6.5 Conclusions	74
Acknowledgements	74
References.....	75
Supplementary material	77
7 Organic matter pools in sediments of the tidal Elbe river.....	79
Abstract.....	80
7.1 Introduction	81
7.2 Investigation area and sampling approach.....	82
7.3 Methods.....	83
7.3.1 Anaerobic and aerobic decay of sediment organic matter	83
7.3.2 Identification and quantification of differently degradable organic matter pools.....	84
7.4 Results.....	85
7.4.1 Sediment properties.....	85
7.4.2 Decay rates and sizes of organic matter pools.....	86
7.5 Discussion.....	91
7.5.1 Spatial trends of sediment organic matter (SOM) degradable pools	91
7.5.2 Organic matter decay rates and degradable shares in soils and sediments.....	92
7.5.3 Trends in time and with depth	93
7.6 Conclusions and outlook.....	93
Acknowledgements	94
References.....	94
8 Effects of organic matter degradation in cohesive sediment: Linking sediment rheology to spatio-temporal patterns of organic matter degradability	97
Abstract.....	98
8.1 Introduction	99

8.2	Materials and methods	99
8.2.1	Overview of material properties	100
8.2.2	Impact of SOM decay on rheological properties	100
8.2.3	Rheological characterization	100
8.3	Results	101
8.3.1	Effect of organic matter decay on sediment yield stress	101
8.3.2	Spatial and seasonal variation of yield stresses	102
8.3.3	Depth-differentiation of yield stresses.....	103
8.4	Discussion	105
8.4.1	General effects of SOM decay on static and fluidic yield stresses.....	105
8.4.2	Seasonal and spatial trends.....	107
8.5	Conclusions and outlook	107
	Acknowledgements	108
	Conflict of interest statement	108
	References	108
	Supplementary material	110
9	Temporal variability of SOM decay	111
9.1	Introduction	111
9.2	Results.....	111
9.3	Discussion.....	113
9.4	Conclusion.....	114
10	Carbon flux in the Port of Hamburg	115
10.1	Introduction	115
10.2	Approach.....	115
10.3	Results.....	116
10.4	Discussion.....	119
10.5	Conclusion.....	120
11	Overarching summary	121
11.1	Spatial variability of sediment organic matter decay	121
11.2	Influence of SOM decay on rheology under different redox conditions	122
11.3	Organic matter metamorphosis and organic matter pools.....	123
11.4	Answers to research questions	125
12	Reflection and prospects of the research	127
	References	129
A1	137
13	Effect of organic matter degradation in cohesive sediment: A detailed rheological analysis	137
	Abstract	138
13.1	Introduction	139
13.2	Experimental methods	139
13.2.1	Water content and bulk density.....	140

13.2.2	Degradation of organic matter	140
13.2.3	Impact of degradation time on rheological properties	140
13.2.4	Rheological characterization	140
13.3	Results and discussion	141
13.3.1	Stress ramp-up tests.....	141
13.3.2	Amplitude sweep tests.....	142
13.3.3	Frequency sweep tests.....	143
13.3.4	Time-dependence and structural recovery tests.....	144
13.3.5	Effect of degradation time	146
13.4	Conclusions	148
	Acknowledgments	148
	References.....	149
A2	151
14	Influence of anaerobic degradation of organic matter on the rheological properties of cohesive mud from different European ports	151
	Abstract.....	152
14.1	Introduction	153
14.2	Experimental Methods	153
14.2.1	Sample Collection.....	153
14.2.2	Wet Bulk Density, Particle Size Distribution and TOC Content.....	154
14.2.3	Anaerobic Degradation of Organic Matter.....	154
14.2.4	Rheological Characterization.....	154
14.3	Results and Discussion.....	155
14.3.1	Anaerobic Degradation Tests	155
14.3.2	Wet Bulk Density, Particle Size Distribution and TOC Content.....	155
14.3.3	Stress Ramp-Up Tests.....	155
14.3.4	Amplitude Sweep Tests	158
14.3.5	Frequency Sweep Tests	159
14.3.6	Time Dependent and Structural Recovery Tests	161
14.4	Conclusions	163
	Supplementary Materials.....	164
	Acknowledgments	165
	References.....	166
	Acknowledgements	167
	Curriculum Vitae.....	169
	List of publications.....	171

Glossary

CS	Consolidated sediment
DM	Dry matter
DOM	Dissolved organic matter
EPS	Extracellular polymeric substance
FM	Fluid mud
PS	Pre-consolidated sediment
RBS	River bed sediment
SOM	Sediment organic matter
SPM	Suspended particulate matter
TC	Total carbon
TIC	Total inorganic carbon
TOC	Total organic carbon

Summary

Organic matter plays a major role in global ecosystems and has several functions in terrestrial and marine environments. As organic matter impacts, among others, the rheological behaviour and settling rates of mineral sediment particles, it is of great relevance to the definition and maintenance of the nautical depth in ports and waterways. The microbial decay of organic matter leads to the emission of climate forcing gases like CO₂ and CH₄.

In this theses it will be provided fundamental insight in the behaviour of sediment organic matter in the aquatic river system. It presents analyses of field and laboratory experiments using sediment samples taken during 21 sampling campaigns between 2018 and 2020 in the Port of Hamburg, Germany. The focus lay on sampling locations with high sedimentation rates. It is investigated chemical, physical and biological parameters and their variability in space and over time. It quantifies the share of anaerobically and aerobically degradable sediment organic matter in a depth profile and along a transect of about 30 km within the tidal Elbe river.

Sediment organic matter at upstream and downstream locations is mainly allochthonous as it comes from the catchment (upstream) or from North Sea (downstream). Young organic matter, entering the system from upstream, has predominantly biogenic sources. Upstream organic matter originates from the catchment, containing plankton-derived and more easily degradable components. It was shown that the most upstream location was nourished primarily by upstream fluvial sediments. This location was characterised by the highest concentrations of chlorophyll a, microbial biomass, silicic acid, EPS, humic acids and hydrophilic organic matter, the most negative $\delta^{13}\text{C}$ signature and by the highest oxygen consumption rate, with decreasing trends towards downstream locations. At downstream locations, organic matter is mainly of allochthonous origin, entering the harbour mainly with the tidal flood current from the direction of the North Sea. The organic matter degradability was the lowest at downstream locations and organic matter was stabilised in organo-mineral associations. It is elucidated that spatial patterns of organic matter degradability can be explained by a source gradient. It was found that sediment organic matter lability is inversely linked to its stabilisation in organo-mineral complexes. The degradability gradient could be explained by different organic matter quality in relation to its origin. A fast, medium, slowly and non-degradable pool (pool 1 to pool 4) were identified based on the measured organic matter lability. Temporal and spatial variabilities (gradient and depth) were observed as well as seasonal changes of degradable organic matter pools. An age gradient was found with easily degradable material in top layers and increasing stabilization of organic matter in organo-mineral compounds with depth. The degradability was larger in upper sediment layers. It was also larger under aerobic conditions but the differences between aerobic and anaerobic decay decreased from upstream to downstream. The investigation area mostly comprised stabilised organic matter. On average around 20 % of TOC was anaerobically degradable and around 30% of TOC was aerobically degradable. Thermometric pyrolysis was shown to serve as a useful proxy to predict organic matter degradability in river sediments, with the Hydrogen-Index (HI) correlating well with degradability.

Further, it will be demonstrated that the sediment organic matter decay has a biological, chemical and physical effect on the shear strength. Degradation of organic matter significantly affects sediment strength, especially under the anaerobic conditions. The formation of gas bubbles under anaerobic conditions added an additional physical component to the effect of biological organic matter decay. The susceptibility of the sediment to yield stress changes might depend on the availability of easily

degradable organic matter. Pronounced spatial trends were found with higher changes in yield stress at upstream locations and lower yield stress changes at downstream locations.

Finally, this thesis will demonstrate the metamorphosis of sediment properties and sediment organic matter from its state in suspension to being part of the settled and consolidated sediment as well as from upstream to downstream. Temporal and spatial gradients were found for aerobic and anaerobic carbon fluxes as well as for potentially degradable organic carbon. A first draft of a carbon flux estimate originating from the microbial decay of organic matter from the investigation area is presented which can be used for future carbon foot printing assessments, for example for port maintenance activities.

1 Introduction

1.1 Decomposition, stabilization and transformation of organic matter

Organic matter plays a major role in terrestrial and oceanic biogeochemical cycles, (Burd et al., 2016). Organic matter has a critical function in the global carbon balance (Fageria, 2012). The emission of climate gases by organic matter decay affects global warming. Soil organic matter contains more than three times carbon than the atmosphere or terrestrial vegetation (Schmidt et al., 2011). Soil organic carbon serves as source and sink for nutrients and plays a vital role in maintenance of soil fertility (Khatoon et al., 2017). Thus, there is a need for a unified theory of controls on organic matter to holistically understand what drives the degradation of organic matter regardless of the ecosystem (Kothawala et al., 2021). A global carbon cycle can connect organic matter pools in soil, freshwater, and marine ecosystems with the atmosphere (Burd et al., 2016). It is crucial to incorporate inland waters into the carbon cycle and connect inland waters with other habitats in studies of carbon biogeochemistry. Travník et al. (2018) mentioned that inland waters have an impact on the carbon cycle by the emission of gases in the atmosphere.

The pathway of overall organic matter mineralization is described as the movement of organic matter from soils through inland waters to coastal systems (Burd et al., 2016). Rapid mineralization happens near the sediment surface (soils) or water surface (oceans) returning CO₂ back to the atmosphere. Soil organic matter is a complex mixture of molecules with different physicochemical properties (Tadini et al., 2015). According to Guggenberger (2005), the organic matter decomposition process in soils is regulated by three groups of factors: the physicochemical environment, the quality of the resource and the acting decomposer organisms. Intrinsic properties and thermodynamics (i.e., organic matter composition, electron acceptors, type and concentration of metabolic intermediates) influences the organic matter degradability as well as kinetics (i.e., temperature and physical protection) and transport processes (i.e., bioturbation, bioirrigation and sedimentation rate) (Arndt et al., 2013).

Guggenberger (2005) describes the following mechanisms from the input of plant and animal residues (*deposition*) to the stabilised organic matter (*stabilization*): The organic carbon is transferred to another chemical structure caused by enzymatic attack or chemical reactions (*transformation*). *Decomposition* describes the breakdown of organic macromolecules. This process is usually mediated by micro-organisms and includes depolymerization and oxidation reactions for example *hydrolysis* using water to break down molecules. Whereas *mineralization* is the microbial conversion into inorganic constituents of organic matter. Moreover, carbon of organic residues is transformed and converted to humic substances through biochemical and abiotic processes (*humification*) and incorporated in microbial biomass producing resynthesized organic matter (*assimilation*). Decreasing the potential for mineralization of organic matter via biological, chemical, or physical processes is called *stabilization*.

1.2 Stabilization and mineralization

Stabilized organic matter comprises strongly morphologically transformed substances without macroscopically perceptible tissue structures stabilized against mineralization (low turnover rate) (Blume et al., 2016). The mineralization of organic matter (complete microbial decomposition) forms inorganic substances (CH₄, CO₂, H₂O) and releases nutrients (e.g., magnesium, iron, nitrogen, sulphur, phosphorous). Organic matter is also important for the binding of inorganic and organic pollutants and regulates their bioavailability (Blume et al., 2016). The carbon content of organic matter varies within individual substance classes with an average carbon content of around 50 %. Polysaccharides contain

about 40 % carbon and lipids about 70 % carbon (Blume et al., 2016). During the decomposition, most of the carbon is liberated as CO₂, whereas nitrogen is initially mainly stored in the microbial biomass. In the long term, more than 95 % of nitrogen is stabilized within organic matter. Carbon/nitrogen (C/N) ratios change from 25-70 for plant residues to 6-9 for soil biota and microbial products associated with soil minerals (Paul, 2016). Consequently, the C/N ratio of the organic matter becomes increasingly narrow during the organic matter degradation, reaching values of 10–12 in intensively processed soils (Blume et al., 2016). With organic matter of low C/N ratio, cumulative respiration is higher than with high C/N organic matter. Therefore, Nguyen and Marschner (2016) concludes that microbial biomass and nitrogen and phosphorous availability are mainly influenced by the proportion of low or high C/N organic matter input. The degree of decomposition of the organic matter can modify the correlation between carbon, nitrogen and phosphorous net mineralization rates and the organic matter stoichiometry in organic horizons of temperate forests (Heuck and Spohn, 2016). Organic matter decomposition can therefore be predicted from its intrinsic C/N ratios and those of labile inputs (Qiao et al., 2016, subtropical forest). Phytoplankton and zooplankton have a smaller C/N ratio (around six) than freshly deposited marine organic matter (around ten). Selective degradation of organic matter components decreases C/N values already in the water column. Compared to vascular plants, algae do not have cellulose but are rich in proteins. Therefore, the C/N ratio of terrestrial biomass is often higher than of marine biomass. In marine ecosystems, a clear separation between marine and terrestrial organic matter is not possible and even deep-sea sediments can still contain terrestrial organic matter (Schulz and Zabel, 2006). The organic matter transformation is important for ecological processes, regulating the nutrient cycling and ecosystem carbon balance. Many authors focussed on the organic matter transformation for soils (i.e., Rahman et al., 2018; Reichenbach et al., 2021; Wieder et al., 2015; Frouz, 2018; Poirier et al., 2018; Riggs et al., 2015; Fernandes et al., 2020; Li et al., 2019; 2020) and for sediments (Müller et al., 2018; Zhang et al., 2018; Seelen et al., 2019). While approaches to investigate organic matter quality and stability in terrestrial soils are plentiful, only few studies are available for freshwater sediments.

Organic matter mineralization shows the highest rates from the decomposition of fresh organic matter and the turnover of the microbial biomass, namely, readily decomposable substances like polysaccharides (Blume et al., 2016). The decomposition of organic matter can form dissolved organic matter. Rates of organic matter mineralization are low when carbon has been transferred into the stable fraction, e.g., by the sorption of dissolved organic matter (Blume et al., 2016). Organo-mineral compounds are mineral products formed by biological activity, dead and decaying organisms, or non-biological organic compounds. They can be characterized by pyrolysis, (thermo)chemolysis and ¹³C-NMR spectroscopy (Kögel-Knabner et al., 2008). High biological activity increases the formation of organo-mineral compounds, because microorganisms constantly form reactive organic substances. Microorganisms forming organo-mineral complexes, are involved in the weathering of minerals and subsequent release of elements like iron and aluminium (Violante and Caporale, 2015). Organic matter stabilization can result from the separation of the substrate from the decomposers (i.e. access by microorganisms and enzymes), preventing further degradation. The mineral phase is considered to be the most important for the formation of organo-mineral compounds, because micro-aggregates are formed by clay minerals and iron- and aluminium-(hydr)oxides (Totsche et al., 2018). Organic substance, especially microbial polysaccharides and proteins, is stabilized and protected from microbial degradation through interactions with fine-grained minerals. The interactions with organic matter particles in the clay fraction (clay minerals, iron oxides) lead to the formation of stable clay-organic matter associations. Therefore, organic carbon stabilization with fine particles is crucial for

long-term carbon sequestration (Singh et al., 2018). The binding between minerals and organic substances depends on the type and surface charge of the mineral as well as on the type and charge of the functional groups in the organic matter. This is influenced by the pH value and base saturation. Dependent on the mineral's surface charge, the pH value and the base saturation, binding of organic matter onto the mineral phase can happen through ligand exchange. Moreover, through ionic bondings between organic cations and the negative charges of clay minerals, weak interactions (hydrogen bonds, Van der Waals interactions, hydrophobic interactions) or complex formation with metal cations (Blume et al., 2016). If stabilized organic matter exists in the form of organo-mineral compounds, it can be isolated from the mineral share of the sediment using particle size and density fractionation (Blume et al., 2016).

1.3 Classification and decomposition

Classification of organic matter quality and its degradability in terrestrial soils has been approached by various methods of chemical and physical fractionation, as reviewed by Lützow et al. (2007). Lehmann and Kleber (2015) described the soil organic matter as a continuum of progressively decomposing organic compounds. Grasset et al. (2021) showed that the extent of methane production could be well predicted by the quantity of particular organic matter and its quality, the latter assessed with the C/N ratio. In Kögel-Knabner et al. (2008) and Cheeke et al. (2013), the combination of fractionation, incubation, and chemical characterization methodologies were used to focus on complex interactions of organic matter ecosystem functioning. Further methods of organic matter classification were described and/or applied in Helfrich et al. (2007), Shen et al. (2018), Kögel-Knabner (2018), Hoffland et al. (2020), Gebert et al. (2006), Wakeham and Canuel (2016) and Zander et al. (2020). During the stabilization process, light, easily degradable organic matter is removed and organic matter is transformed into the heavy density fraction by organic matter mineralization. Although the method of density fractionation was already used in 1950 (Henin and Turc), recent literature still uses density fractionation for classification. It was used for soils by Baldock and Skjemstad (2000), Six and Paustian (2014), Adams et al. (2018), Schnecker et al. (2016), Plaza et al. (2019), Diochon et al. (2016), Viret and Grand (2019), Zander et al. (2020) and reviewed by Gao et al. (2019). For sediments, only a few recent studies used the density fraction, namely, Wakeham and Canuel (2016), Cui et al. (2016), Ke et al. (2018, sludge) and Winkler et al. (2020). Non-degradable organic matter, found in the heavy density fraction, is also called recalcitrant.

Recalcitrant organic matter consists of macromolecular components of plants or microorganisms not readily decomposable by microorganisms due to their chemical structures (e.g., aromatic plant constituents or lignin). Another important step for biological decomposition of organic matter is the hydrolysis of solid organic matter by hydrolytic enzymes such as aminopeptidase, chymotrypsin, and glucosidase as mentioned in Yoshikawa et al. (2017). In general, the following stability sequence can be derived for organic compounds originating from plants, already found similarly in Waksman et al. (1928): sugars, starches, proteins < celluloses < lignins, wax, resins, tannins (Blume et al., 2016). The decomposition of sugars, starches, proteins, hemicellulose or cellulose, and non-lignified parts in general takes place most rapidly (Berg and McLaugherty, 2020). Lignocellulose is degraded much more slowly as well as already decomposed material, namely, peat, manure or compost. Hemicellulose degradation occurs prior to cellulose degradation (Devaux et al., 2018). Organic matter in subaquatic soils, with plants not containing lignocellulose, is more strongly decomposed than soils in nearshore marine environments (Blume et al., 2016). Wilkinson in 1958 already assumed that polysaccharides (cellulose, hemicellulose) and proteins serve as a carbon and energy source for microorganisms and

are fully metabolized. After extracellular enzymatic hydrolysis, the resulting monomer or dimer fragments are absorbed by microorganisms and oxidized by heterotrophic bacteria as a source of energy. Lignin does not serve as a carbon or energy source for microorganisms because it has a low energy gain for microorganisms (Blume et al., 2016). For bacteria, the complete oxidation of lignin is highly exothermic and the microbial degradation of lignin requires an alternative energy source (Zhu et al., 2017). Lignin is the most important and common aromatic organic compound with a share of up to 30% of plant biomass (Zhu et al., 2017). Moreover, lignin is a major component of humic acid in soils (Datta et al., 2017). Fungi, breaking lignin polymers and opening up fresh zones of organic matter, cannot survive in anaerobic conditions. Therefore, large parts of the organic matter will not be available for further decomposition.

The end products of organic matter mineralization in aerobic environments with dissolved phases are H₂O and CO₂, while the associated mineral salts are taken up by bacteria or released. The same products can be generated under anaerobic conditions when other oxidizing agents (electron acceptors) such as nitrate, sulphate, manganese (IV) or iron (III) are available. Moreover, under anaerobic conditions, methane can be produced. For anaerobic oxidation of methane in marine sediments, terminal electron acceptors such as nitrate, nitrite, manganese (IV) or iron (III) are more energetically favourable than sulphate (Yang et al., 2021). Kristensen et al. (1994, sediments) found that the aerobic carbon decay was about ten times faster than under anaerobic conditions. Whereas McKew et al. (2013, estuarine sediments) showed that anaerobic microorganisms can rapidly utilise labile biofilm dissolved organic matter (DOM) and extracellular polymeric substances at the same rates as the aerobic community. Generally, under anaerobic organic matter decay, microorganisms gain less energy than with aerobic decay. Furthermore, anaerobic decomposition is slower and usually incomplete. When aerobic microbial activity exceeds the rate of oxygen supply, oxygen depleted zones are formed in the water column (Rabalais et al., 2010; Geerts et al., 2017). Under anaerobic conditions, frequently prevailing in fine-grained sediments, methane (CH₄) is produced as well. The anaerobic organic matter decay produces methane that has a global warming potential which is 56 times that of CO₂ (for the coming 20 years). The poor solubility of methane in water led to entrapped gas in the sediment, resulting in changes to both the rheological properties (chapter 1.5) and density. The methane production, resulting from anaerobic sediment organic matter decay, increases linearly with the quantity of phytoplankton-derived and terrestrially-derived organic matter (Grasset et al., 2021). The methane production correlates positively with the amount of organic matter supply and negatively with the C/N ratio (Grasset et al., 2021). In upper sea sediment layers, Stevenson et al. (2020) found aerobic processes, reactive organic carbon and highest abundances of bacteria and archaea. Whereas in deeper sediment layers, they found microorganisms involved in nitrate/nitrite and iron/manganese reduction across the oxic-anoxic redox boundary and dominance of sulphate reducers.

1.4 Humification

The definition of humification and humic substances depends on the analytical capabilities to elucidate the structure of biomolecules (Guggenberger, 2005). Humic substances isolated from soils of different pedogenesis differ strongly in their chemical structural composition (Kögel-Knabner, 2000). Humic substances can be isolated from soils by strong alkali extraction and then further differentiated into acid soluble (fulvic acid) and acid-insoluble materials (humic acids). Straathof et al. (2014) and Straathof and Comans (2015) chemically extracted DOM components to evaluate the quality of organic matter in composts. Schellekens et al. (2017) extracted solid and aquatic samples to investigate molecular structures of humic and fulvic acids. Hayes et al. (2017) concluded that all organic matter

components are decomposable, but at different rates. They found that humic components were relatively resistant to decomposition. Humin has an aliphatic nature that might be attributable to lipids that comprise a significant portion of its organic components (Rice, 2001). Humin mainly consists of aliphatic hydrocarbons (Hayes et al., 2017), namely, aromatic and carbohydrate carbon (Rice, 2001). The gradient of humification degree increased with depth in Amazonian soils with deeper horizon presenting a higher amount of aromatic groups in the structure of humin (Tadini et al., 2015). The humification process had no direct relation with the age of the organic matter. In Hayes et al. (1989), at least 50% of soil organic carbon was described as humic substances. Humic substances in soils representing around 20–50% of organic matter structure (Tadini et al., 2015). Similar shares were found in Straathof et al. (2014) for compost. For tidal fluvial sediments, humic substances have not been deeply investigated yet.

As part of the natural carbon cycle, the labile part of organic matter is also subject to microbial degradation. The impact of microorganisms on the marine carbon cycle as investigated in Worden et al. (2015) should be incorporated in the global carbon cycle. The diversity of microbial communities influences the organic matter degradation (Suominen et al., 2021, anaerobic conditions). Marine DOM contains in total about 660×10^{15} g carbon, one thousand times more carbon than all living organisms in the oceans combined (Hansell et al., 2009 in Dittmar, 2015). Freshly produced DOM is highly degradable and consumed within days after production (Dittmar, 2015), the same is true for inland waters (Catalan et al., 2016, in Ward et al., 2017). Phytoplankton can play a significant role for the settling of fine-grained sediment as the chlorophyll a concentration correlates strongly with the suspended sediment concentration (Deng et al., 2019). Within the river-continuum (Vannote et al., 1980), fine-grained sediments in shallow upstream areas can be expected to show high net primary production compared to light-deficient areas in deeper and/or more turbulent waters showing low net primary production. Fine grained sediments with high organic matter content are mainly found in the sampling area of this study, as explained in chapter 1.6.

1.5 Impact of organic matter on rheological and nautical properties

The relevance of organic matter for the rheological and mechanical properties of sediments and soils suggests that the degradation of organic matter should provoke inverse (i.e., destabilizing) effects.

Sediment-bound organic matter influences sediment properties that are relevant for navigation and maintenance of ports and waterways, such as rheology (Wurpts and Torn, 2005; Shakeel et al., 2019, 2022a), settling and consolidation behaviour (Sills and Gonzalez, 2001; Jommi et al., 2019). Organic matter interacts with the sediment mineral phase through Van der Waal's or Coulombic forces. Further, organic matter can enhance settlement of suspended particulate matter (SPM) by bridging mineral particles and thereby promoting floc formation (Deng et al., 2019). Moreover, organic matter enlarge the diameter of particles, neutralize surface charges or reduce repulsive forces between charged particles (Lagaly and Dékány, 2013).

Rheological properties on fluvial or tidal sediments have barely been investigated. On the one hand, Wurpts and Torn (2005) postulated that microbially formed extracellular polymeric substances (EPS) decrease yield point and viscosity of saline fluid mud layers in Emden seaport. On the other hand, Shakeel et al. (2019) showed that organic matter increased the yield points (shear stresses) of freshwater Elbe sediments at a given density. Gerbersdorf et al. (2008) described that the colloidal and bound EPS moieties showed a strong correlation with the critical shear stress for erosion over sediment depth. EPS have been shown to profoundly influence bedform dynamics, increasing the time for development of bedforms for small quantities of EPS (Malarkey et al., 2015; Parsons et al., 2016). EPS

network can enhance the cohesive strength of sediments by embedding particles and permeating void spaces. Moreover, EPS can offer additional ionic binding sites and cross-linkages (Gerbersdorf et al., 2008). Both, microalgal and bacterial biomass show strong correlations with the colloidal and bound EPS carbohydrate fractions. Therefore, Gerbersdorf et al. (2008) concluded that microalgae and bacteria influence the properties of the sediment by binding fine-grained sediment.

Miryahyaei et al. (2020) found a linear relationship between rheological properties and the hydrolysis rate in anaerobic digestion. With decreasing hydrolysis rate the rheological properties changes, namely the flow consistency index, yield stress, and viscoelastic moduli. Further, they investigated the efficiency of organic matter removal and found that a decrease in the hydrolysis rate was associated with an increase in yield stress. Markgraf et al. (2012) found that for wet soils, an increased organic matter content provided greater resistance to deformation and improved soil elastic properties. This allowed greater deformation before a yield point was reached.

Besides the effect of organic matter on stress-strain relationships in soils and sediments, the production of methane gas during its degradation under anaerobic conditions can lead to technical problems like impeded nautical depth finding by reflection of sonic waves on gas bubbles. Sills and Gonzalez (2001) and Jommi et al. (2019) have demonstrated strong reduction in shear stresses by gas originating from organic matter decay. Next to its climate-forcing potential, methane also increases the risk of explosion in the suction head and on board of trailing suction hopper dredgers. From various perspectives it is therefore of interest to understand the drivers and mechanisms of organic matter decay in river sediments.

1.6 Investigation area: Elbe Estuary and Port of Hamburg

Freshwater sediment organic matter originates from both natural (eroded terrestrial topsoils, plant litter, planktonic and benthic organisms) and anthropogenic (surface runoff, sewage waste) sources. The Elbe River has a catchment area of around 148.000 km² (Boehlich and Strotmann, 2008) in the Czech Republic, Poland, Austria and Germany. The Port of Hamburg is a fresh water harbour. Brackish water can be found between river-km 655 and river-km 680 (from source, river mouth around river-km 730), depending on the tide and the river discharge (Boehlich and Strotmann, 2008). Sediment reaches the harbour from two directions. From upstream, terrestrial and riverine organic matter is transported with the current toward the harbour area whereas from downstream, marine algae are transported into the harbour with tide. From downstream, the Elbe river estuary is subject to two daily tidal cycles (Rolinski, 1999). Fine sediments enter the harbour area with an on average 3.8 m tidal hub at the Hamburg St. Pauli monitoring station. Distinctive flood dominance from Glückstadt (river-km 675) to Hamburg (river-km 630) leads to a net import of sediment from downstream (“tidal pumping”). The asymptotic tidal periods with a stronger flood period and a weaker ebb period leads to the accumulation of sediments in the harbour area (Weilbeer, 2014) as can be seen at the main sampling locations in Figure 1. High sedimentation rates of material imported from both directions result in shallow water depths in navigation channels and harbour basins (Boehlich and Strotmann, 2008).

In the eastern part of the harbour, a decrease in water depth of about 10 m from the main harbour area to shallower parts of Elbe River is found in upstream direction around location P1 (southern river stream) and location P3 (northern river stream, both Figure 1). The depth differences along the river lead to an accumulation of fine grained sediments in deeper main harbour area. In general, the share of fine grained sediments increases in the main harbour area from downstream to upstream (location P9 to P1, Zander et al., 2020).

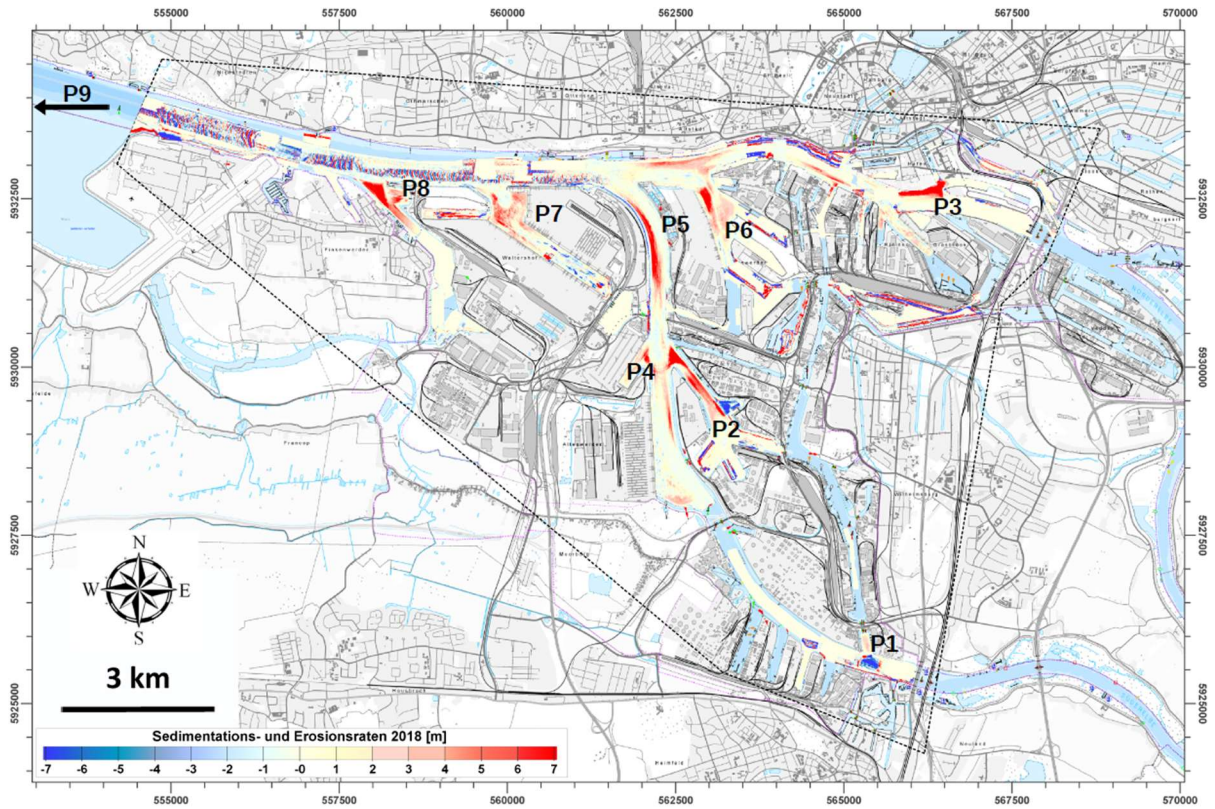


Figure 1 Sedimentation and erosion rates in the sampling area for location P1 to P9 (river-km 615 to 643) for the range between 15th April and 15th June 2018, Port of Hamburg, Germany. Red areas show high sedimentation rates, figure modified from Hamburg Port Authority (HPA).

2 Research questions

This thesis investigates patterns and mechanisms of lability and stability or recalcitrance of sediment organic matter towards microbial degradation. Research was guided by the following questions:

1. Which spatial gradients are found in the Hamburg Port area?
2. What drives organic matter decay processes?
3. How can organic matter be classified in the harbour area?
4. What is the influence of organic matter decay on the rheological behaviour of sediments ?
5. What are the temporal patterns of biological parameters and organic matter decay in the investigated area?

These generic questions are further detailed in the individual results chapters in which also the corresponding hypotheses are presented.

3 Structure of results presentation

Chapters 5 to 8 represent the four manuscripts prepared for peer-reviewed journal publications which form the main body of this thesis:

Chapter 5

Zander F, Heimovaara T, Gebert J (2020) Spatial variability of organic matter degradability in tidal Elbe sediments. *Journal of Soils and Sediments* 20, 2573- 2587. doi.org/10.1007/s11368-020-02569-4

This paper presents spatial sediment organic matter (SOM) degradability patterns in the Port of Hamburg and investigates correlations with standard analytical properties.

Chapter 6

Zander F, Comans RNJ, Gebert J (2022a) Linking patterns of density, thermometric and carbon stable isotope fractions of organic matter to its lability in sediments of the tidal Elbe river. Manuscript submitted to *Applied Geochemistry* (November 2021), under revision.

This research investigates SOM properties along a tidal Elbe River transect using dissolved organic matter (DOM) fractions, density fractions, carbon stable isotopes and thermometric pyrolysis (Rock Eval 6©).

Chapter 7

Zander F, Gröngröft A, Eschenbach A, Heimovaara T Gebert J (2022b) Organic matter pools in sediments of the tidal Elbe river. Manuscript submitted to *Limnologica* (November 2021), accepted for publication on 8 June 2022.

In this manuscript, the share of anaerobically and aerobically degradable SOM along a transect through the Port of Hamburg and in a depth profile are quantified. This study analyses the reactivity of organic matter pools along the river transect based on the biodegradation reaction rates.

Chapter 8

Zander F, Shakeel A, Kirichek A, Chassagne C, Gebert J (2022c) Effects of organic matter degradation in cohesive sediment: Linking sediment rheology to spatio-temporal patterns of organic matter degradability. *Journal of Soils and Sediments*. doi.org/10.1007/s11368-022-03155-6

Here, the authors analyse how gas generation affects sediment density, viscosity and shear strength, thereby impacting detection and maintenance of the navigable depth.

Chapter 9 provides a deeper view on the temporal variability of SOM decay to complete the temporal results made in Zander et al. (2022b).

Chapter 10 introduces a method of calculating carbon fluxes in the Port of Hamburg in relation to sedimentation, in situ temperatures and data on organic matter degradability, to evaluate the carbon emissions per time unit and location.

Chapter 11 includes the overarching discussion of the results presented in this dissertation answering the research questions.

In the **annex**, the following manuscripts with co-authorship can be found:

Shakeel A, Zander F, de Kerk J-W, Kirichek A, Gebert J, Chassagne C (2022a) Effect of organic matter degradation in cohesive sediment: A detailed rheological analysis. *Journal of Soils and Sediments*. doi.org/10.1007/s11368-022-03156-5

Shakeel A, Zander F, Kirichek A, Gebert J, Chassagne C (2022b) Influence of anaerobic degradation of organic matter on the rheological properties of cohesive mud from different European ports. *Journal of Marine Science and Engineering* 10(3):446. doi.org/10.3390/jmse10030446

4 Field sampling and analysis methods

Chapter 4.1 and 4.2 give a general overview over parameters and methods used in the field and by different laboratories that contributed data to the BIOMUD project. The description of specific methods such as related to fractionation of DOM, incubation experiments, and biogeochemical sediment and water characterization can be found in the method section of the respective manuscripts (Zander 2020; 2022a; 2022b; 2022c) that constitute chapters 0 to 0 of this thesis. The approach to estimate carbon fluxes is explained in the respective chapter 9.3.

4.1 Field sampling

The sampling in the Port of Hamburg was conducted between April 2018 and November 2020 at locations with high sedimentation rates (Table 1, Figure 1 and Zander et al., 2020). There were nine main sampling locations between river-km 616 and 643 (location P1 to P9). Additional, upstream and downstream locations (river-km 598 and 679) were sampled in June and September 2019 to broaden the view of SOM fluxes in the Elbe River. In 2018, an overview of the complete harbour transect was made (results in Zander et al., 2020) whereas in 2019, the focus was primarily on a few harbour basins of main interest for the harbour sediment management. In 2020, the frequency of sampling campaigns was increased to investigate seasonal changes in SOM decay in greater detail. The total number of samples was around 400.

Table 1 Overview of sampling campaigns in the main harbour area in the years 2018 to 2020. Note: in June and September 2019 (“5+”) samples were taken further upstream and downstream of the Port of Hamburg.

Campaign	Year	Month	Number of sampled locations	Layers sampled
0	2018	April	3	SPM, FM, PS, CS
1	2018	June	9	SPM, FM, PS, CS
2	2018	July	9	SPM, FM, PS, CS
3	2018	August	9	SPM, FM, PS, CS
4	2018	September	9	SPM, FM, PS, CS
5	2018	November	9	SPM, FM, PS, CS
6	2019	March	3	SPM, FM, PS, CS
7	2019	Mai	5	SPM, FM, PS, CS
8	2019	June	5+	SPM, FM, PS, CS
9	2019	July	5	SPM, FM, PS, CS
10	2019	August	3	SPM, FM, PS, CS
11	2019	September	5+	SPM, FM, PS, CS
12	2019	November	3	SPM, FM, PS, CS
13	2020	April	2	FM, PS
14	2020	Mai	3	FM, PS
15	2020	Mai	3	FM, PS
16	2020	June	3	FM, PS
17	2020	July	3	FM, PS
18	2020	August	3	FM, PS
19	2020	September	3	FM, PS
20	2020	September	3	FM, PS
21	2020	November	3	FM, PS

The sampling took place with a 1 m Frahmplot corer (Figure 2), placed in the sediment at several depths to sample the complete thickness of up to several meters. The sediment layers were identified visually and by on-board measurements of density (Anton Paar density meter DMA 35). From top to bottom a four-layer-system was identified (Zander et al., 2020), starting with the aqueous suspended particulate matter (SPM) followed by the fluid mud (FM), representing the lutocline. Below the FM layer, a pre-consolidated sediment (PS) followed. PS layers can be described as a non-fluidic sediment layer in the initial stages of consolidation, representing the topmost, freshly settled material. The lowest layer was the completely consolidated CS layer. A detailed description of the four-layer system is found in Zander

et al. (2020). Figure 3 shows schematically the formation of layers of different rheological properties in the transition zone between the water phase and the genuine river bed.

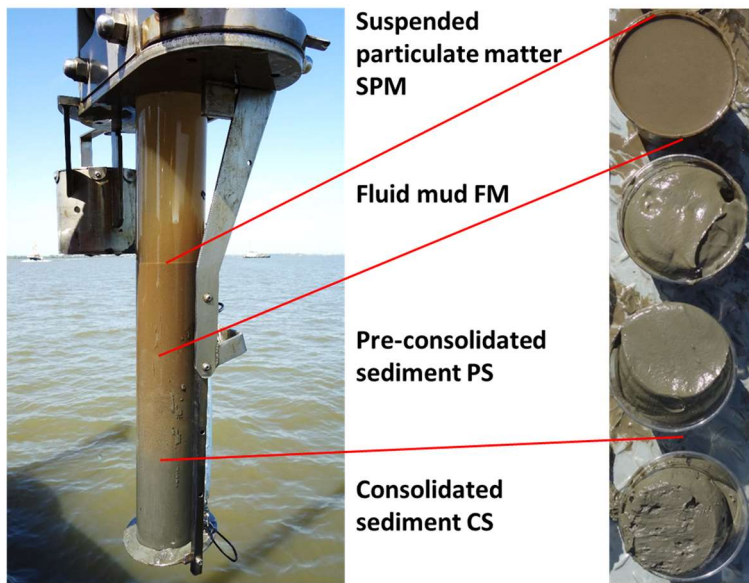


Figure 2 Frahmplot core sampler of 1 m length (left) with four-layer-system separated in sample buckets (right). From top to bottom with suspended particulate matter (SPM), fluid mud (FM), pre-consolidated sediment (PS) and consolidated sediment (CS).

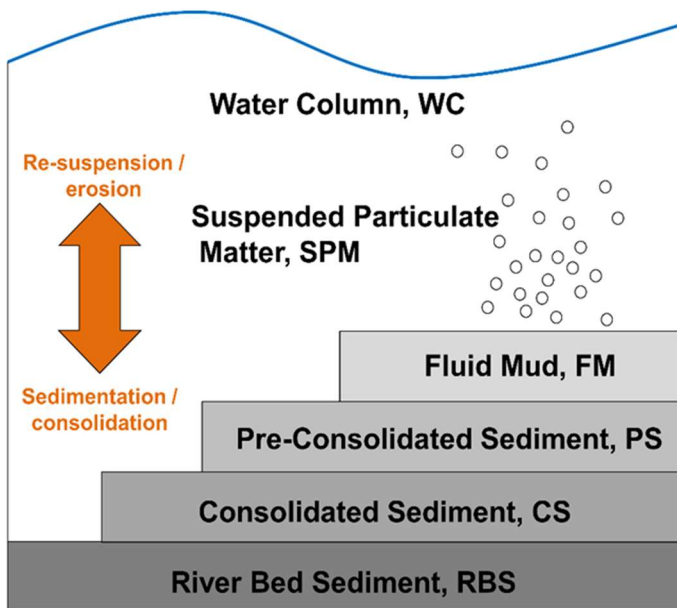


Figure 3 Scheme of sediment layers from top to bottom: suspended particulate matter (SPM), fluid mud (FM), pre-consolidated sediment (PS) consolidated sediment (CS) and river bed sediment (RBS).

4.2 Laboratory analyses

The analyses used in this thesis (Figure 4) were performed at the following institutions and laboratories. If not stated differently, solids were analysed. TU Delft, BIOMUD project (aerobic and anaerobic SOM decay, further biogeochemical sediment properties), Hamburg Port Authority (biogeochemical water properties), limnological institute dr. Nowak (standard biogeochemical sediment properties), Agrolab laboratory (grain size analysis), University of Kiel (microbial population), Biocenter Klein Flottbek (EPS), Soil Science Institute of the University of Hamburg (aerobic SOM decay, chemical sediment properties, isotopes, density fractions, mineralogical composition), Wageningen

University and Research (WUR, organic matter fractions), Deltares (Rock Eval pyrolysis), University of Twente (clay analyses) and Department of Hydraulic Engineering at TU Delft in the framework of the project RHEOMUD (rheological properties).

The applied method of sediment incubation, described in Zander et al. (2020), tried to reproduce the biological degradability of SOM as happening in situ. The idea of this long-term incubation method was to get a detailed overview of the SOM decay. Samples could be taken at several states of the incubation process and biogeochemical properties were analysed, namely, gas composition, redox conditions, rheological properties, physical and chemical fractions.

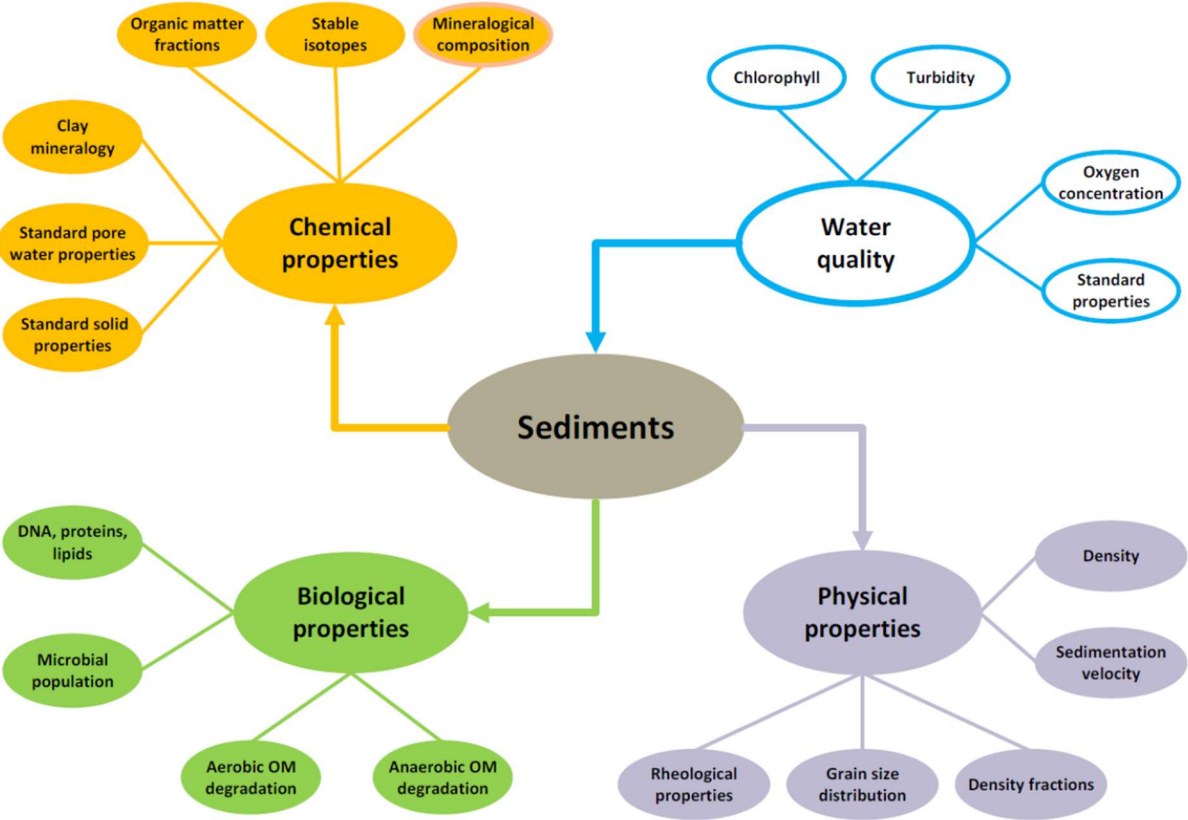


Figure 4 Schematic overview of data used in this thesis, analysed by different laboratories, sediment properties marked by colour, yellow: chemical, green: biological, grey: physical as well as water properties circled in blue.

5 Spatial variability of organic matter degradability in tidal Elbe sediments

Florian Zander¹ • Timo Heimovaara¹ • Julia Gebert¹

¹Delft University of Technology, Department of Geoscience & Engineering, Stevinweg 1, 2628 CN Delft, The Netherlands

Corresponding author: Florian Zander, f.zander@tudelft.nl

Abstract

Purpose: The microbial turnover of sediment organic matter (OM) in ports and waterways impacts water quality, silt depth finding and presumably also rheological properties as well as greenhouse gas emissions, especially if organic carbon is released as methane. As a consequence, sediment management practices as a whole are affected. This study aimed to discern spatial OM degradability patterns in the Port of Hamburg and investigated correlations with standard analytical properties as a basis for future predictive modelling.

Materials and methods: Sediments in the Port of Hamburg were repeatedly sampled at nine locations along an east-west transect using a 1 m corer. In a stratified sampling approach, layers of suspended particulate matter (SPM), fluid mud (FM), pre-consolidated sediment (PS) and consolidated sediment (CS) were identified and individually analysed for long-term aerobic and anaerobic degradation of organic matter, DNA concentration, stable carbon isotope signature, density fractions and standard solids and pore water properties.

Results and discussion: The investigation area was characterised by a distinct gradient with a 10-fold higher OM degradability in upstream areas and lower degradability in downstream areas. Concomitantly, upstream locations showed higher DNA concentrations and more negative $\delta^{13}\text{C}$ values. The share of bulk sediment in the heavy density fraction as well as the proportion and absolute amount of organic carbon were significantly larger at downstream locations. A depth and hence age-related gradient was found at individual locations, showing higher degradability of the upper, younger material, concomitant with higher DNA concentration, and lower OM turnover in the deeper, older and more consolidated material. Deeper layers were also characterised by higher concentrations of pore water ammonium, indicative of anaerobic nitrogen mineralisation.

Conclusions: Organic matter lability is inversely linked to its stabilisation in organo-mineral complexes. The observed degradability gradient is likely due to different OM quality in relation to its origin. Downstream OM enters the system with the tidal flood current from the direction of the North Sea whereas upstream locations receive OM originating from the catchment, containing more autochthonous, plankton-derived and more easily degradable components. At individual sampling points, depth-related degradability gradients reflect an age gradient, with easily degradable material in top layers and increasing stabilization of OM in organo-mineral compounds with depth.

Keywords Dredging • Fluid mud • Organic matter degradation • Organo-mineral complexes • Respiration

5.1 Introduction

Sources of organic matter in riverine sediments can be natural or anthropogenic. Examples of natural sources are eroded terrestrial topsoils and plant litter, supplying allochthonous organic matter, or planktonic and pelagic biomass, yielding autochthonous organic matter, whereas urban sewage and surface runoff reflect anthropogenic allochthonous sources. Under aerobic conditions, the microbial degradation of organic matter with oxygen as terminal electron acceptor releases carbon dioxide (CO₂), whereas under anaerobic conditions organic carbon is additionally released as methane (CH₄). Estuarine systems emit CO₂ into the atmosphere at rates that are quantitatively significant for the global carbon cycle (Borges and Abril 2012). Streams and rivers are responsible for the dominant share of global CO₂ emissions from inland waters (Raymond et al., 2013). Intense aerobic turnover of organic matter can cause oxygen minimum zones in the water body. Because of the poor solubility of methane in water, methanogenesis results in the formation of gas bubbles which are either entrapped within the sediment or released by ebullition through the overlaying water column. Gas bubbles produced from anaerobic degradation of organic matter in sediments are assumed to decrease sediment density, viscosity and shear strength and to delay sedimentation and consolidation. Gas bubbles may obstruct sonic depth finding and therefore maintenance of the navigable depth and increase dredging costs by requiring the operation of degassing units on trailer suction hopper dredgers (Wurpts and Torn 2005). Lastly, anaerobic degradation of organic matter in sediments leads to the release of the potent greenhouse gas methane. The magnitude and rate of anaerobic organic matter degradation depends on the organic matter content and degradability as well as the prevailing environmental (e.g. temperature) and geochemical (e.g. types of electron acceptors) conditions (Arndt et al., 2013).

The water depth in the Port of Hamburg, one of the biggest ports in Europe, is strongly affected by a tidal range of approximately 3.8 m. The port receives sediments, suspended and sediment-bound organic matter both from the upstream catchment and from the North Sea, the latter due to tidal pumping (Boehlich and Strotmann 2008). The resulting sediment load in combination with the presence of low-flow areas within port basins or the formation of eddies at turn-offs causes hotspots of sedimentation and hence respective dredging efforts to maintain the nautical depth. Due to the possible effects of sediment organic matter turnover highlighted above, quantification of the lability of organic matter at focal points of sedimentation plays an important role for optimising sediment management. In light of this, the aim of this study was to investigate the spatial variability of organic matter degradability in the Port of Hamburg and to examine possible correlations with standard analytical geochemical properties as prerequisite for the prediction of location-specific behaviour of organic matter, supporting spatially differentiated management of sediments. It was hypothesized that:

1. Stabilisation of sediment organic matter in organo-mineral complexes increases with age and therefore with depth as well as along a transportation gradient.
2. Ageing of sediments decreases organic matter lability and therefore changes biodegradation kinetics as well as the distribution of organic matter over different density fractions.
3. An upstream-downstream decreasing gradient of organic matter degradability exists as labile organic matter enters the harbour mainly from upstream through algal biomass, adding a more rapidly degradable pool.

5.2 Investigation area and sampling strategy

5.2.1 Investigation area

The Port of Hamburg (Figure 5) is a tidal port located approximately 100 km inland from the North Sea. The sampling points (P1 to P9) mostly reflect key locations of maintenance of the nautical depth, with high sedimentation rates and hence increased dredging effort. Further, the sampling points represent a gradient from upstream to downstream. They feature different hydromorphological properties with respect to their the distance to the main fairway, the geometry of the harbour basin and the extent of flow-through of water (see Table 2).

Table 2 Characterisation of sampling points.

Nr.	River-km	Coordinates (WGS 84)		Length of basin	Distance to centre of main fairway
		° N	° E		
-	km			m	m
P1	616	53.477625	9.984925	300	300
P2	619	53.511615	9.949098	2300	1000
P3	620	53.538433	10.000369	1400	200
P4	621	53.516918	9.935416	600	400
P5	623	53.529945	9.938585	-	0
P6	624	53.538188	9.949979	2300	400
P7	627	53.533910	9.905856	2400	700
P8	629	53.538894	9.881215	2700	700
P9	643	53.567833	9.679490	-	0

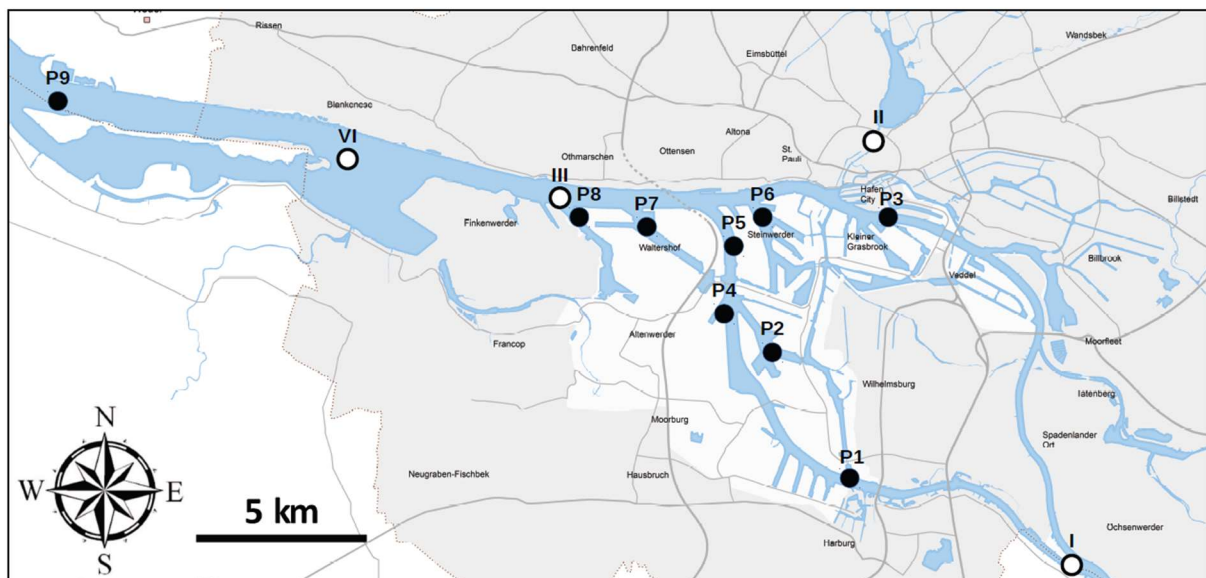


Figure 5 Investigation area (Port of Hamburg) with sampling locations (small dots) between river km 616 (P1, upstream) and 643 (P9, downstream), the big dots show the sampling location of the Hamburg Hamburg Serviceportal (compare section 4.2) (source: adapted from Hamburg Port Authority).

5.2.2 Sampling strategy

In 2018, sediment samples were taken with a core sampler (volume ca. 10 l) at nine locations in the Port of Hamburg (Figure 5) in June, August, September and November. The goal of the sampling strategy was to include the most upstream and the most downstream location as well as the major sedimentation areas in the Port of Hamburg. Additionally, sampling aimed at analysing variability with depth (see section 4.3) and time (not presented in this study). In a vertical cut, four layers were

distinguished between the upper (water) and the lower (riverbed) boundary: suspended particulate matter (SPM), fluid mud (FM), pre-consolidated sediment (PS) and consolidated sediment (CS). While SPM layers still fully represents the aqueous phase, FM is the first layer below the lutocline, still showing fluidic but already non-Newtonian properties. This layer is not always present. The lutocline was identified visually, seconded by on-board measurements of density (Anton Paar density meter DMA 35). Below the FM layer follows pre-consolidated sediment (PS) which can be described as a non-fluidic sediment layer in the initial stages of consolidation, representing the topmost, freshly settled material. This layer is most pronounced in areas of high sedimentation rates. Below follows the consolidated sediment (CS) layer, defined as a firm, aged sediment layer of reduced water content. The described stratification was accompanied by a pronounced redox gradient with SPM still in an oxidised state but FM, PS and CS material usually in a reduced state with values decreasing with depth (see Figure 11). In the core sampler, the depth of each layer was determined with reference to the lutocline (Wolanski 1988), located between suspended particulate matter and fluid mud. In a stratified sampling approach, several cores were taken at each location, layers were separated, homogenised and stored cool in air-tight containers until they were processed. Suspended particulate matter was pumped from the top of the core on the vessel and centrifuged in the laboratory.

5.3 Methods

5.3.1 Anaerobic degradation of organic matter

Depending on the available sample mass, the water content and the expected gas production rate, 20 g (SPM), 100 (FM) or 200 g fresh sample (PS and CS) were placed in triplicates into 100 ml (SPM), 250 ml (FM) or 500 ml glass bottles (PS and CS). The bottle headspace was flushed with 100% N₂ to establish anaerobic conditions and incubated at 36 °C in dark. For quantification of gas production an automated low gas flow measuring device (Gas Endeavour, Bioprocess Control, Sweden) was used for samples from PS and CS layers and a pressure gauge for samples from SPM and FM layers. After gas production had reached a level of below 2 ml d⁻¹, considered as the lower limit for measurements with the Gas Endeavour device, the long-term gas production for pre-consolidated and consolidated layers were continued with the pressure gauge.

The anaerobic (anoxic) degradation of organic matter was quantified based on the release of carbon into the gas phase. According to the oxidation-reduction reactions taking place with decreasing redox potential and decreasing enthalpy, organic carbon is first released as CO₂ from the reduction of nitrate, manganese, iron, and sulphate. After the depletion of these terminal electron acceptors (TEAs), carbon is additionally released as CH₄. Gas phase carbon was quantified applying the ideal gas law using the gas composition, the headspace volume, the incubation temperature, and the pressure inside the bottle. The total amount of generated gas equals the sum of CO₂ and CH₄ produced and was expressed as mass unit of carbon released per mass unit of organic carbon (as present in the original sample), hence indicating the degradability of the organic carbon independent of its absolute amount. Gas chromatographic analyses did not detect any other gases. Values measured after 21 days (G₂₁) and after 100 days (G₁₀₀) were used as standard benchmarks.

5.3.2 Aerobic degradation of organic matter

To determine the degradation of organic matter under aerobic (oxic) conditions, in this paper also referred to as “respiration”, 15 g of homogenised fresh sample were incubated in 1 l glass bottles at 20 °C in dark with a headspace consisting of atmospheric air. The sample was distributed on the bottom of the bottles in a layer of only a few mm thickness in order to minimize limitations to the diffusion of

oxygen into the sample. To avoid the limitation of OM degradation by elevated CO₂ levels, the bottle headspace was flushed with synthetic air after CO₂ concentrations had reached three vol.% in the gas phase, then measurements were resumed. Applying the ideal gas law, the amount of degraded carbon was calculated using the concentration of CO₂ as measured by gas-chromatographic analysis and the bottle headspace volume. Respiratory C-release was related to mass unit organic carbon present in the sample at the beginning of the incubation and calculated for the benchmark times of 21 days (R₂₁) and 100 days (R₁₀₀).

5.3.3 Carbon stable isotopes

The δ¹³C-values of the sediment organic matter were determined with an isotope-ratio mass spectrometer (Delta V; Thermo Scientific, Dreieich, Germany) coupled to an elemental analyzer (Flash 2000; Thermo Scientific). Prior to analysis, samples were treated with phosphoric acid (43%, 80 °C for 2 h) to release inorganic carbon. Values are expressed relative to Vienna Pee Dee Belemnite (VPDB) using the external standards IAEA IAEA-CH7 (-31.62 ‰ vs. VPDB) and IVA soil 33802153 (27.46‰ vs. VPDB).

5.3.4 DNA concentration

Isolation of genomic DNA was performed using the “Quick-DNA Fungal/Bacterial Microprep” kit (<https://www.zymoresearch.eu/quick-dna-fungal-bacterial-kit>) following the procedure indicated by the supplier, with the following minor modifications: for better cell lysis, 5 µl lysozyme (2000 µg ml⁻¹) and 5 µl proteinase K (200 µg ml⁻¹) were added to the sample. Genomic DNA was eluted in 27 µl distilled water into a 1.5 ml reaction tube. The eluate was passed through the same filter a second time. Isolated DNA was suspended over night at 4 °C. DNA concentrations were measured using an Implen NanoPhotometer NP80 (Implen GmbH, München, Germany) at 260 nm (Cryer et al., 1975).

5.3.5 Density fractionation

Density fractionation was carried out using LUDOX[®] HS-40 colloidal silica suspension in water (Sigma-Aldrich) with a cut-off density of 1.4 g cm⁻³. The procedure is based on the method first presented by van den Pol-van Dasselaar and Oenema (1999), adapted from Meijboom (1995), and also applied by Gebert et al. (2006) on riverine sediments in a previous study. In brief, fresh sediment samples were placed in glass beakers, mixed with an excess of Ludox[®] at a density of 1.4 g cm⁻³ and stirred thoroughly. Light material < 1.4 g cm⁻³ accumulated at the surface and was separated from heavy material > 1.4 g cm⁻³, sinking to the bottom, by decantation. The two fractions were washed with distilled water and oven-dried at 105 °C for subsequent physical and chemical analyses (see section 3.6).

5.3.6 Standard properties of solids and pore water

The analysis of solids properties included total nitrogen (TN, DIN EN 16168), total organic carbon (TOC, both DIN ISO 10694), water content (WC, DIN ISO 11465), redox potential (Eh, DIN 38404), particle size distribution (DIN ISO 11277), oxygen consumption after three hours (AT_{3h}, TV-W/I 1994), phosphorus (P) and sulphur (S, both DIN ISO 11885), pH-value (pH, DIN EN 15933) and electrical conductivity (EC, DIN EN 27888). The following parameters were measured in filtrated pore water: dissolved organic carbon (DOC, DIN EN 1484), ammonium (NH₄⁺, DIN ISO 11732), phosphate (PO₄³⁻, DIN ISO 6878) and sulphate (SO₄²⁻, DIN ISO 10304).

5.3.7 Statistical evaluation of data

Linear regression analyses were carried out to detect possible interrelations between sediment properties and parameters of organic matter degradation. Statistical significance of Pearson's coefficient r was accepted for a probability of error $p < 0.01$ for a two-sided test. The time course of carbon release from anaerobic and aerobic organic matter degradation was described by exponential fitting. The number of considered phases was increased until the coefficient of determination no longer improved and was highest for a two- or three-phase system, depending on the degradation state of the sample. For most of the samples, a three-phase exponential fit best described the data (Eq. 1, OriginPro2019).

$$y = A1 * \exp(-x/t1) + A2 * \exp(-x/t2) + A3 * \exp(-x/t3) + y0 \quad \text{Eq. 1}$$

With $A1, A2, A3$ = initial value in each phase

x = time in days

$t1, t2, t3$ = degradation rate constant

$y0$ = total cumulative anaerobically degraded organic matter.

For the comparison between samples and for the correlation with sediment properties, benchmark values of carbon release under aerobic (R) and under anaerobic (G) conditions after 21 days (R_{21}, G_{21}) and 100 days (R_{100}, G_{100}) were used.

5.4 Results

5.4.1 Sediment properties

The thickness of the investigated pre-consolidated layer PS, the first freshly deposited material below the lutocline, was between 15 cm and 30 cm (Table 3). Except for the most downstream point P9, all samples showed a very high content of fines $< 63 \mu\text{m}$ (sum of clay and silt) of up to 97% of the total mass. Sediment texture varied between clay (P4, most clay) to sandy clay loam (P9, most sand; FAO 2006). The sand-dominated texture at P9, and high sand contents at P5, reflect the fact that both are situated within the main flow channel (Table 2) where flow rates are higher, limiting sedimentation of fines. Correspondingly, these locations showed the lowest TOC contents. Concentrations of nitrogen (TN) and organic carbon (TOC) varied strongly between 0.2 % and 1.0 % (TN) and 2.0 % and 7.6 % (TOC) and were highest upstream and lowest downstream. The TOC-to-TN ratio was 10-fold higher at the downstream location (P9). The water content, phosphorus and electric conductivity showed similar patterns with increased values upstream and lower values downstream. NH_4^+ in the pore water was strongly increased at upstream point P1 (up to 70 times) compared to other locations; PO_4^{3-} was increased two-fold. Inversely, the sulphate concentration was around five-fold higher at downstream location P9 compared to upstream location P1.

Organic matter degradation leads to transformation and stabilization of the remaining organic matter in organo-mineral complexes with silt and clay, which causes a shift in the distribution of organic carbon towards higher density fractions. Compared to the bulk sediment (Table 3), the light fraction was enriched in organic matter, showing TOC contents of up to 14%. By contrast, TOC contents in the heavy fraction only reached up to 1.6% (data not shown). Between 40% and 50% of the total mass was found in the light fraction at upstream sampling point P1, comparing to only 5% to 20% at downstream sampling point P9 (Figure 6, upper panel). In combination, between 80% and 90% of the organic carbon were found in the light density fraction at upstream point P1, whereas at downstream point P9 this share was 30-80% (Figure 6, lower panel). Although the fractionated mass was often enriched in the

heavy fraction, the share of TOC was always higher in the light fraction, with one exception for location P9 (CS layer from November 2018).

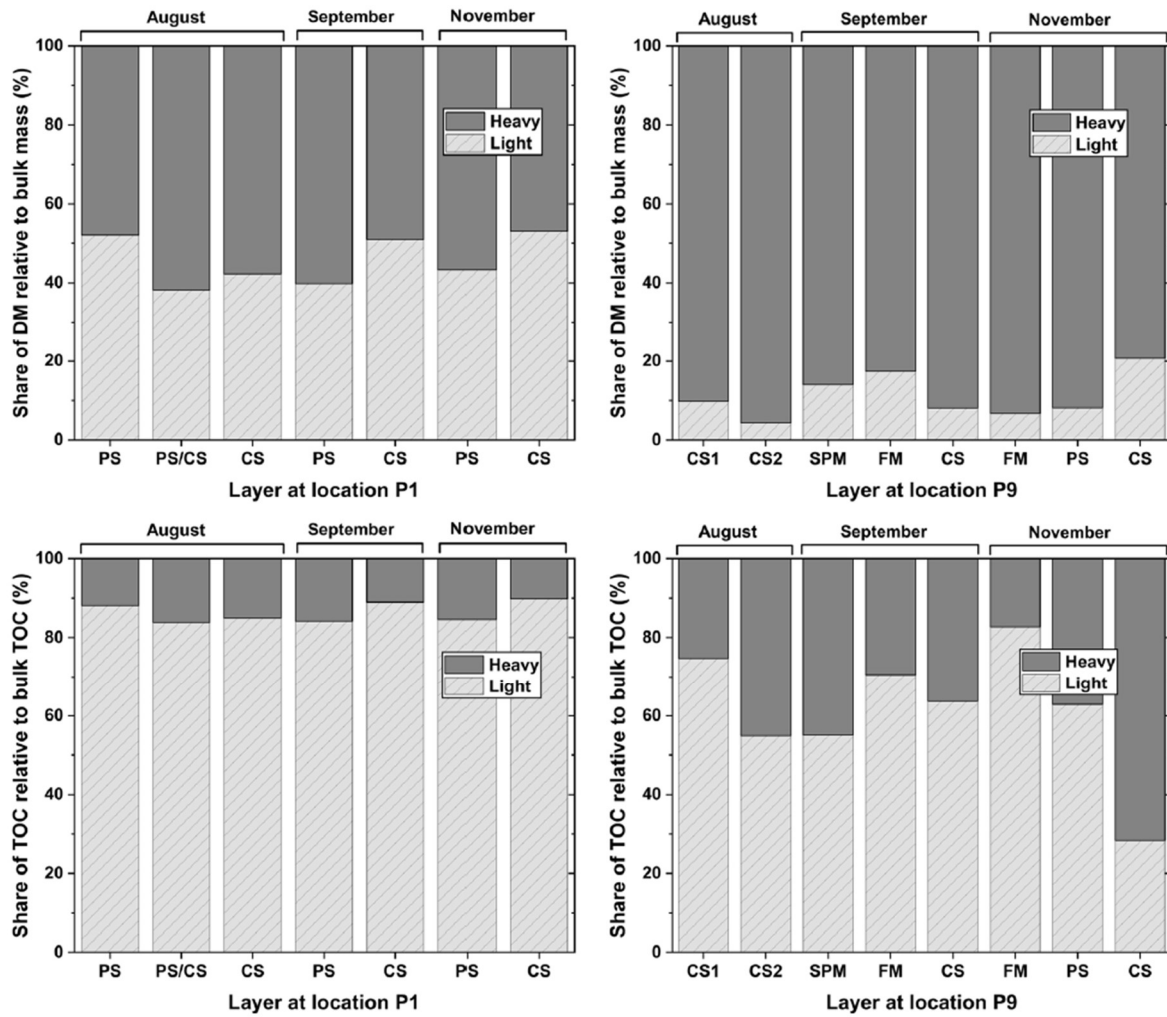


Figure 6 Share of total dry mass (DM, upper panel) and of total organic carbon (TOC, lower panel) in the light ($< 1.4 \text{ g cm}^{-3}$) and heavy ($> 1.4 \text{ g cm}^{-3}$) density fraction at points P1 (upstream, left) and P9 (downstream, right). FM = fluid mud, PS = pre-consolidated sediment, CS = consolidated sediment, samples taken in August, September and November.

Table 3 Abiotic properties of pre-consolidated (PS) layers (solids) and the corresponding pore water by example of the sampling campaign from June 2018.

	P1	P2	P3	P4	P5	P6	P7	P8	P9
Depth b.l. (cm)	5-25	5-35	5-20	5-30	0-30	10-30	0-25	0-20	10-30
TN (%)	1.0	0.6	0.6	0.6	0.3	0.5	0.5	0.5	0.2
TOC (%)	7.6	4.4	4.4	4.3	2.2	3.9	3.6	3.8	2.0
TOC/TN (% % ⁻¹)	7.6	7.6	7.2	7.4	8.5	8.3	7.7	8.4	10.0
WC (% DM)	495	371	359	342	169	299	293	366	158
Eh (meV)	-226	-280	-315	-280	-256	-300	-280	-360	-173
Clay (< 2 µm, %)	50	51	48	56	23	47	43	46	20
Silt (2 - 63 µm, %)	44	46	48	36	45	45	45	47	27
Sand (> 63 µm, %)	6	3	4	8	32	8	12	7	53
P (mg g _{DM} ⁻¹)	2120	1650	1640	1610	930	1510	1500	1510	840
S (mg g _{DM} ⁻¹)	4540	4750	4660	4530	2850	4630	4560	4590	2620
pH (-)	7.5	7.4	7.5	7.6	7.6	7.5	7.6	7.7	8.0
EC (µS cm ⁻¹)	2250	1945	1817	2020	1768	1792	1680	1627	1371
DOC (mg l ⁻¹)	41	27	56	37	21	23	15	17	20
NH ₄ ⁺ (mg l ⁻¹)	200	23	39	29	9	10	6	6	3
PO ₄ ³⁻ (mg l ⁻¹)	0.15	0.10	0.12	0.12	0.09	0.15	0.08	0.10	0.07
SO ₄ ²⁻ (mg l ⁻¹)	23	9	5	5	100	19	100	100	120

TN = total nitrogen; TOC = total organic carbon; WC = water content; Eh = redox potential, LOI = loss on ignition; P = phosphorus; S = sulphur; EC = electric conductivity; DOC = dissolved organic carbon; NH₄⁺ = ammonium, PO₄³⁻ = orthophosphate; SO₄²⁻ = sulphate; **bold** = min. and max. values; b.l. = below lutocline

The contrast between upstream and downstream properties was also reflected by the stable isotope signature and the concentration of DNA. The organic matter at the downstream location P9 was enriched in ¹³C (Figure 7, left panel); moreover, at all locations the heavy density fraction was enriched in ¹³C compared to the light density fraction (Figure 7, right panel). Also, an increased concentration of DNA was found in the sediment at upstream point P1 (location RV at river-km 616) compared to downstream point P9 (location SW at river-km 643) (Figure 8). While for the δ¹³C values no clear differentiation with depth could be identified, DNA concentrations showed a clear depth-related gradient with highest values in the youngest layers (fluid mud) and the lowest values in the oldest material (consolidated sediment).

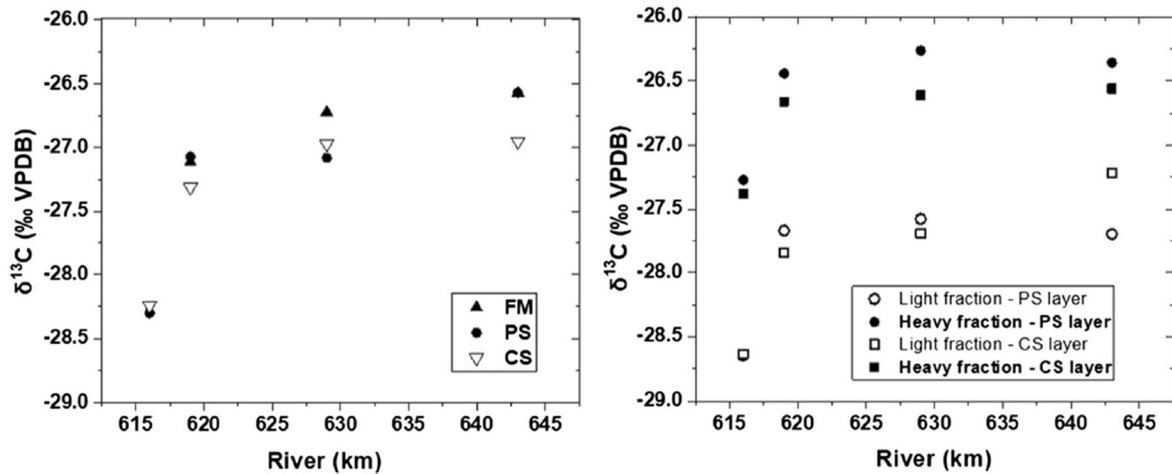


Figure 7 $\delta^{13}\text{C}$ signature of fluid mud (FM), pre-consolidated (PS) and consolidated sediment (CS) on the original sample (left panel) and on the density-fractionated samples (only PS and CS, right panel) over the sampling transect East (km 616) - West (km 643) for the locations P1, P2, P8 and P9, samples taken in November 2018. Left: Bulk sample, right: light ($< 1.4 \text{ g cm}^{-3}$) and heavy ($> 1.4 \text{ g cm}^{-3}$) density fractions.

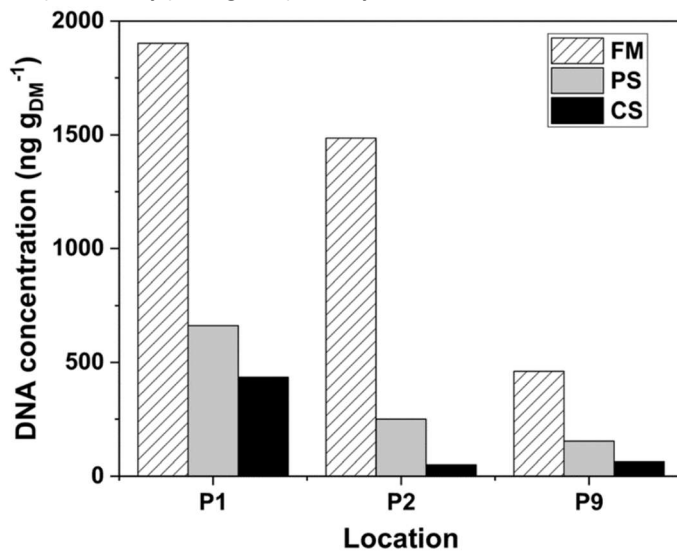


Figure 8 DNA concentration in fluid mud (FM), pre-consolidated (PS) and consolidated sediment (CS) for locations RV, RT and SW in June 2018.

5.4.2 Degradation of organic matter

An example of cumulated release of carbon from the anaerobic degradation of organic matter is shown in Figure 9 for the most upstream (P1) and the most downstream (P9) location for pre-consolidated (PS) layers with averages of three parallel measurements. In spite of the significant differences in absolute levels of carbon release (about four times higher at P1 after 160 days), the time course for both the samples shown here and all other samples followed the same asymptotic pattern with decreasing rates over time. The time course of carbon release by aerobic respiration followed the same pattern over time: however, the amount of carbon released when oxygen was available as terminal electron acceptor was threefold compared to carbon release under anaerobic conditions (Figure 10).

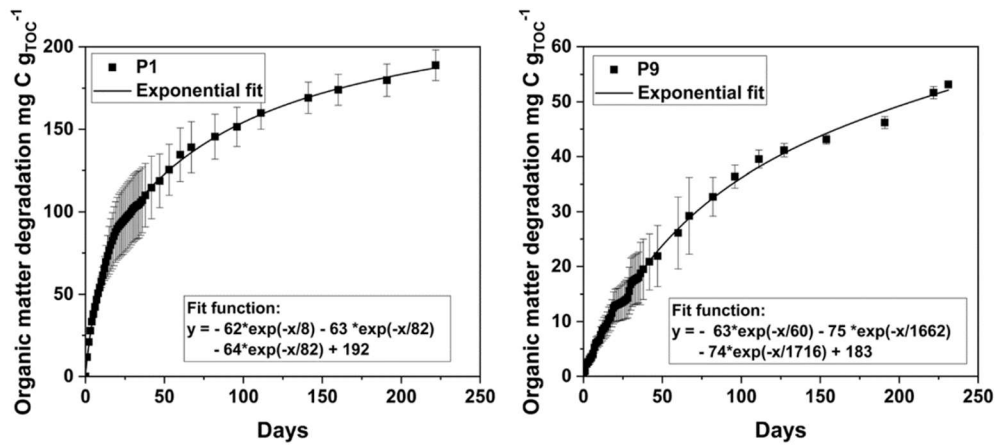


Figure 9 Time course of organic matter degradation under anaerobic conditions by example of pre-consolidated samples from location P1 (left) and P9 (right) taken in June 2018, line: exponential fit with equation. Data points = average of three parallels, error bars = maximum and minimum.

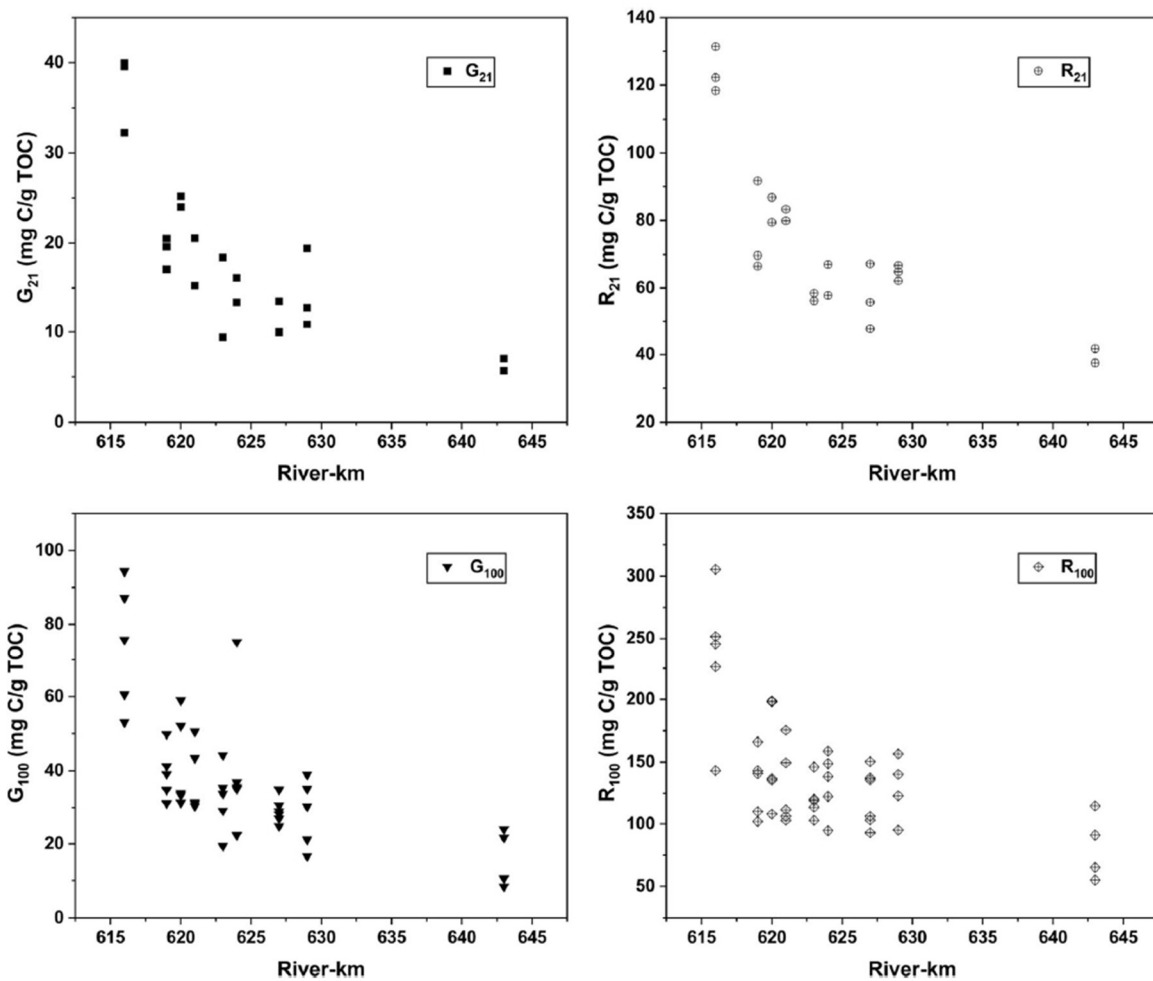


Figure 10 Cumulative C release from pre-consolidated sediment, measured over 21 and 100 days under aerobic (R) and anaerobic (G) conditions shown over the sampling transect East (km 616) - West (km 643), data from campaign one to five. Both the degradation (carbon release normalised to dry mass) and the degradability (carbon release normalised to mass unit TOC) of organic matter followed a marked gradient with higher values upstream and lower rates downstream (Figure 10). The following key differences were observed between the sampling locations regarding degradation and degradability of organic matter (Table 4):

- 10 to 30 times higher carbon release (per g DW) from anaerobic organic matter degradation (G_{21} , G_{100}) and up to 10-fold increased carbon release (per g DW) from aerobic degradation (R_{21} , R_{100}) related to dry mass at the upstream location P1 compared to the downstream location P9.
- The consumption of oxygen within three hours was higher at location P1 compared to P9 by the factor of seven (AT_{3h} , P1: $2.0 \text{ g O}_2 \text{ kg}_{\text{DW}}^{-1}$, P9: $0.4 \text{ g O}_2 \text{ kg}_{\text{DW}}^{-1}$).
- Higher degradability of organic matter at location P1, with a factor of 2.5 to seven compared to location P9 for both aerobic (R_{21} , R_{100}) and anaerobic (G_{21} , G_{100}) conditions.

Besides the upstream-downstream gradient of organic matter degradability, a depth- and therefore age-related gradient was also observed at the individual sampling points (Figure 11). Both anaerobic and aerobic (not shown) degradation of carbon per unit TOC decreased with increasing depth and hence age, coinciding with increased in situ concentrations of pore water ammonia (Figure 12, left panel) and more negative redox potentials (Figure 12, right panel) in deeper layers.

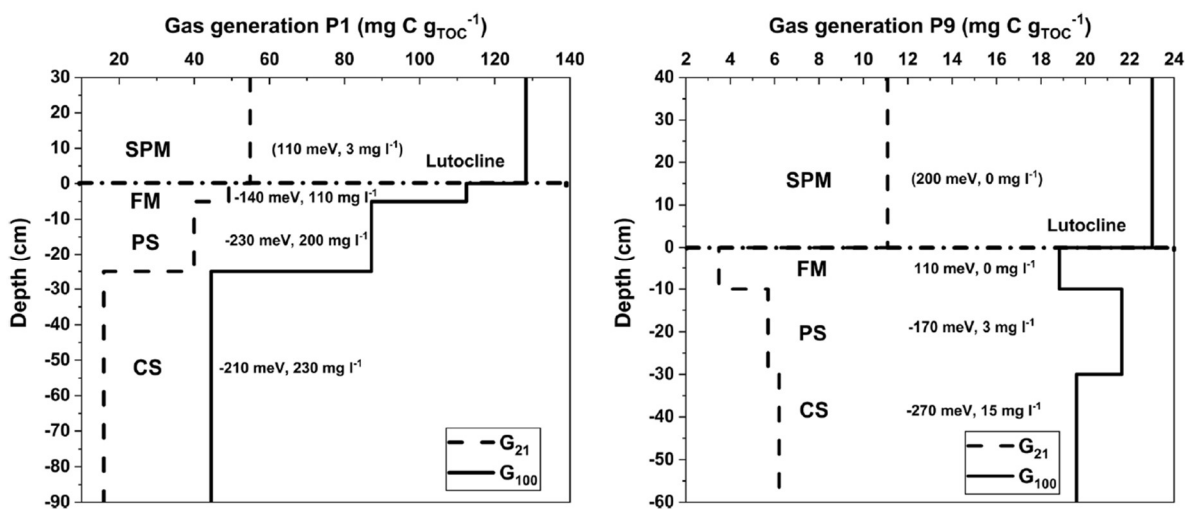


Figure 11 Cumulative organic matter degradation under anaerobic conditions (G) over depth for 21 days (G_{21}) and 100 days (G_{100}) with redox potential (meV) and ammonium concentration in pore water (mg l^{-1}) at location P1 and P9 per layer (SPM - CS), depth below lutocline, samples taken in June 2018, values in brackets calculated from other campaigns.

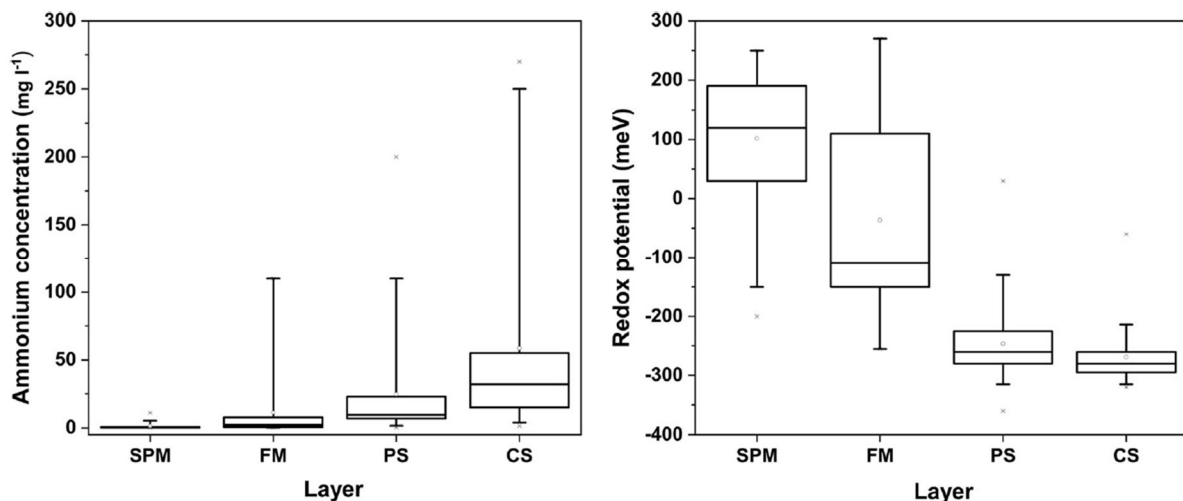


Figure 12 Depth profiles of redox potential and pore water concentration of ammonia (NH_4^+) at the time of sampling for selected sampling points, samples taken in June 2018. Square symbol = mean, line = median, box = 25th-75th percentile, whisker = 5th-95th percentile, cross = 1st-99th percentile, line symbol = minimum and maximum.

Table 4 Cumulative carbon release from anaerobic (G) and aerobic (R) degradation of organic matter of pre-consolidated (PS) layers after 21 and 100 days by example of the sampling campaign from June 2018.

	P1	P2	P3	P4	P5	P6	P7	P8	P9
R ₂₁ (mg C gTOC ⁻¹)	118	92	87	83	56	58	56	67	42
R ₁₀₀ (mg C gTOC ⁻¹)	245	110	199	106	120	149	136	140	91
G ₂₁ (mg C gTOC ⁻¹)	40	20	25	21	9	13	10	11	6
G ₁₀₀ (mg C gTOC ⁻¹)	87	50	59	51	29	36	29	30	22
R ₂₁ (mg C gDM ⁻¹)	9.0	4.0	3.8	3.6	1.2	2.3	2.0	2.5	0.8
R ₁₀₀ (mg C gDM ⁻¹)	18.6	4.9	8.7	4.6	2.6	5.8	4.9	5.3	1.8
G ₂₁ (mg C gDM ⁻¹)	3.0	0.9	1.1	0.9	0.2	0.5	0.4	0.4	0.1
G ₁₀₀ (mg C gDM ⁻¹)	6.6	2.2	2.6	2.2	0.6	1.4	1.0	1.2	0.4
AT _{3h} (g O ₂ kgDM ⁻¹)	2.0	1.6	1.6	1.5	0.7	1.2	0.3	1.1	0.4

R₂₁/R₁₀₀ and G₂₁/G₁₀₀ = cumulative C release by aerobic and anaerobic organic matter degradation after 21/100 days; AT_{3h} = oxygen consumption after three hours, DM = dry matter; **bold** = min. and max. values

5.4.3 Relationship between abiotic sediment properties and organic matter degradation

Correlation analyses showed strong relationships between parameters reflecting carbon release by aerobic and anaerobic degradation of organic matter (R and G) and individual sediment properties (**Error! Reference source not found.**). Both processes were strongly positively related to TN and TOC contents as well as to water content and inversely related to the ratio of TOC to TN. Further, organic matter degradation was positively related to clay content, total phosphorus, total sulphur, dissolved organic carbon and pore water ammonium, but negatively to sand content and pore water sulphate. Aerobic and anaerobic degradability of organic matter were correlated well with each other, with values for Pearson's *r* of 0.85 or greater, both for short-term (after 21 days) and long-term (100 days) periods, indicating the same principal governing factors behind the two processes.

5.5 Discussion

5.5.1 Sediment properties and degradation of organic matter

5.5.1.1 Sediment properties

Both the abiotic sediment properties as well as organic matter degradation and degradability and DNA content in the investigation area were subject to a pronounced spatial gradient. In general, upstream sediments featured a higher organic matter content (reflected by higher TOC and TN contents) with a lower TOC-TN-ratio, higher total sulphur and phosphorus and higher concentrations in pore water of dissolved organic carbon, ammonium and phosphate. The higher solute concentration was reflected by a higher electric conductivity upstream, while downstream samples showed higher sulphate content, indicating increase of marine influence. The sulphate concentration in the sediment pore water can be influenced by two processes: the input of sulphate from marine origin through the stream water and the reduction of pore water sulphate under anaerobic conditions. Oxygen saturation of the water and hence higher redox potentials can be promoted by turbulence as induced by a stronger current (location P9 in the main fairway, Figure 11). This can be seen from also higher turbidity values (Table 5, position IV), showing three-times higher turbidity values than at location P1 (compare position I). The water temperature, affecting organic matter decay by its influence on the biological activity, did not vary between the locations. The influence of tributaries (Alster: 6 m³ s⁻¹ runoff, Bille: 4 m³ s⁻¹) to the total flow (on average in 2017 around 500 m³ s⁻¹) is negligible.

Concurrent with the gradient in sediment properties, both, the mass-related release of carbon from the anaerobic and aerobic degradation of sediment organic matter as well as the degradability of the organic matter also decreased in the downstream direction. In terms of possible greenhouse gas emissions this gradient means that sediments from the upstream location P1 can, within 21 days, produce up to 30 times the amount of methane and carbon dioxide per unit dry mass of dredged sediment than sediments from the downstream location P9. Carbon release under aerobic conditions was around three to five times higher compared to anaerobic conditions (Figure 10), one reason being the higher energy gain when oxygen is available as terminal electron acceptor. Cumulative oxygen consumption values in this study, normalised to 20 °C, were in agreement with Spieckermann et al. (2018) who sampled at a similar location (near location P2) in 20 to 40 cm sediment depth.

5.5.1.2 Correlation between sediment properties and organic matter degradability

Statistically significant correlations were found between standard analytical sediment parameters and the degradation and degradability of organic matter (**Error! Reference source not found.**). Organic matter degradability (R and G are expressed in carbon release per unit TOC) correlated most strongly with total organic carbon, indicating that in the investigated system higher organic matter content also means a higher share of degradable organic matter. Degradability was inversely related to the ratio of TOC to TN, confirming the findings of Gebert et al. (2019) for degradation of organic matter in landfilled dredged sediment, suggesting lower degradability with decreasing contents of nitrogen per unit organic carbon. An inverse relationship can be expected because the nitrogen to carbon ratio in the decomposer biomass is higher than in soil (sediment) organic matter and litter, creating a constant demand for nitrogen (Berg and McClaugherty 2003). In terrestrial soils, decomposition rates for litter were thus also found to be positively linked to the TN/TOC ratio (Manzoni et al., 2008) and negatively to the TOC/TN ratio (e.g. van Dijk 1980). The strong correlation between sediment water content (WC) and TOC ($r = 0.95$) and TN ($r = 0.93$) contents reflects the fact that the youngest, most freshly settled material is the least consolidated one (highest water content) and at the same time the one with the least extent of organic matter decomposition, featured by (still) higher TOC and TN contents. From thermodynamic considerations (for a review see Arndt et al., 2013) it appears plausible that pore water sulphate correlated negatively with organic matter degradability, as the reduction of sulphate is energetically favourable compared to methanogenesis. In a study investigating gas production of sediments from ten federal German waterways, Gebert et al. (2006) found the lag phase until methane production commenced to be strongly correlated to the concentrations of inorganic electron acceptors such as sulphate in the pore water.

5.5.1.3 Organic matter quality

All systems with high organic carbon sedimentation rates, high internal primary production and anoxic bottom waters have a high CH₄ emission potential (Grasset et al., 2018). Indeed, the strongest CH₄ production potential was found for the sediments at the highly anoxic locations of this study (e.g. location P1, Figure 11). Grasset et al. (2018) attributed low CH₄ production from sediment to a low availability of labile compounds, comparable with downstream location P9 showing low concentrations in the light density fraction (Figure 6) and high CH₄ to the addition of fresh organic carbon to anoxic sediments. The same study showed that planktonic biomass (autochthonous organic carbon) was faster degradable than terrestrial biomass (allochthonous organic carbon). This suggests that, as also shown by Schoel et al. (2014, see section 5.2), the organic carbon input at more upstream locations in the investigation area is dominated by autochthonous (phytoplankton, zooplankton) organic carbon, complementing the already mineral-phase bound and hence less degradable organic

carbon pool. Other studies also related carbon release to organic matter quality and hence degradability, using different indicators. For example, White et al. (2002) described different classes of organic matter compounds that correlated positively (primary and secondary polysaccharides) or negatively (phenolic precursors, lignin, proteins, and lipids) to the cumulative respiration. Further, Dai et al. (2002) could link carbon emission to the presence of easily degradable components such as polysaccharides. Straathof et al. (2014) found the concentration of the hydrophilic DOC fraction to correlate positively with respiration rates measured for compost. In this study, higher chlorophyll concentrations, indicative of higher phytoplankton biomass, are assumed to explain the higher degradability of organic matter seen at the downstream location P1.

Table 5 Water parameters at the date of the sampling in June 2018 with location and river-km of this study and the sampling positions of Hamburg Serviceportal (2019).

This study		HH-Service		WT	O ₂	TB	CH	pH
Location	River-km	Position	River-km	°C	mg l ⁻¹	FNU	µg l ⁻¹	-
P1	616	I	610	18	9.0	19	118	8.4
P3	620	II	622	25	3.8	12	20	7.8
P8	629	III	629	19	4.3	39	13	7.6
P9	643	IV	636	20	4.9	57	nd	7.5

WT = water-temperature; O₂ = oxygen concentration; TB = turbidity and CH = total chlorophyll concentration; **bold** = min. and max. values; nd = not determined

Table 6 Pearson's coefficient r for correlations between aerobic and anaerobic organic matter degradation referred to g TOC and material properties for pre-consolidated layers (n ≥ 25). Shaded = Pearson's coefficient r significant on a confidence level of 99.99%, bold and dark shaded: Pearson's coefficient r > 0.85.

TN	TOC	TOC/TN	R ₂₁	R ₁₀₀	G ₂₁	G ₁₀₀	WC	Eh	Clay	Silt	Sand	AT _{3h}	P	S	EC	DOC	NH ₄ ⁺	PO ₄ ³⁻	SO ₄ ²⁻
-	0.99	-0.72	0.92	0.87	0.85	0.84	0.95	-0.33	0.67	0.30	-0.68	0.81	0.89	0.65	0.56	0.51	0.82	-0.16	-0.64
	-	-0.68	0.91	0.88	0.85	0.85	0.93	-0.30	0.68	0.30	-0.68	0.77	0.91	0.65	0.53	0.54	0.81	-0.16	-0.59
		-	-0.71	-0.65	-0.63	-0.62	-0.78	0.57	-0.77	-0.42	0.80	-0.62	-0.67	-0.72	-0.42	-0.29	-0.43	0.26	0.64
R ₂₁			-	0.91	0.86	0.87	0.92	-0.40	0.63	0.21	-0.60	0.75	0.79	0.52	0.43	0.60	0.76	-0.14	-0.64
R ₁₀₀			-	-	0.83	0.85	0.85	-0.40	0.53	0.27	-0.55	0.71	0.72	0.50	0.31	0.73	0.72	-0.10	-0.61
G ₂₁			-	-	-	0.98	0.80	-0.40	0.55	0.21	-0.53	0.74	0.73	0.50	0.36	0.58	0.72	-0.13	-0.63
G ₁₀₀			-	-	-	-	0.79	-0.38	0.51	0.21	-0.50	0.74	0.72	0.47	0.31	0.64	0.72	-0.07	-0.62
WC			-	-	-	-	-	-0.37	0.78	0.32	-0.77	0.78	0.87	0.73	0.46	0.42	0.69	-0.17	-0.57
Eh			-	-	-	-	-	-	-0.50	-0.55	0.61	-0.32	-0.38	-0.52	-0.16	-0.38	-0.08	0.45	0.46
Clay			-	-	-	-	-	-	-	0.23	-0.92	0.56	0.81	0.88	0.28	0.33	0.29	-0.18	-0.41
Silt			-	-	-	-	-	-	-	-	-0.60	0.33	0.50	0.60	0.17	-0.01	0.12	-0.10	-0.32
Sand			-	-	-	-	-	-	-	-	-	-0.57	-0.83	-0.92	-0.29	-0.25	-0.28	0.18	0.45
AT _{3h}			-	-	-	-	-	-	-	-	-	-	0.67	0.60	0.42	0.44	0.57	-0.09	-0.67
P			-	-	-	-	-	-	-	-	-	-	-	0.81	0.54	0.35	0.68	-0.29	-0.56
S			-	-	-	-	-	-	-	-	-	-	-	-	0.27	0.20	0.24	-0.24	-0.50
EC			-	-	-	-	-	-	-	-	-	-	-	-	-	0.14	0.67	-0.40	-0.42
DOC			-	-	-	-	-	-	-	-	-	-	-	-	-	-	0.43	-0.05	-0.45
NH ₄ ⁺			-	-	-	-	-	-	-	-	-	-	-	-	-	-	-	-0.14	-0.51
PO ₄ ³⁻			-	-	-	-	-	-	-	-	-	-	-	-	-	-	-	-	-
SO ₄ ²⁻			-	-	-	-	-	-	-	-	-	-	-	-	-	-	-	-	0.22

TN = total nitrogen; TOC = total organic carbon; R₂₁(R₁₀₀)/G₂₁(G₁₀₀) = aerobic and anaerobic organic matter degradation after 21(100) days; WC = water content; Eh = redox potential, AT_{3h} = oxygen consumption after three hours, LOI = loss on ignition; P = phosphorus; S = sulphur; EC = electric conductivity; DOC = dissolved organic carbon; NH₄⁺ = ammonium; PO₄³⁻ = phosphate; SO₄²⁻ = sulphate

5.5.2 Source and stabilisation of organic matter in sediments

Organic matter in soils and sediments is stabilised by formation of organo-mineral complexes which reduce its accessibility to biological degradation and hence to mineralization (Baldock and Skjemstad 2000; Six and Paustian 2014; Gao et al., 2019). Conversely, non-complexed organic matter is more labile, i.e. prone to mineralisation and has been found to be associated with microbial biomass C and N (Bu et al., 2012). The increased share of light fraction organic carbon upstream was seconded by a markedly higher concentration of DNA, indicative of a higher biomass content, as shown by Agnieszka et al. (2012) and Rehman et al. (2016). The gradient in DNA content supports the assumption a higher share of biomass-based degradable organic matter in the upstream area, as also suggested by the higher chlorophyll values in the water phase (Table 5). The chlorophyll concentration was nine times higher near the upstream location P1 (position I) compared to the more downstream location P8 (near position III; Hamburg Serviceportal 2019). It is assumed that at individual sampling locations the lower contents of DNA in deeper layers result from the mineralisation (decay) of the increasingly buried organisms without new biomass being introduced. The lower biomass levels are then maintained over time as the conditions such as scarcity of terminal electron acceptors (more negative redox potentials, Figure 12) and poor rates of diffusive exchange of metabolites pose boundaries to biological activity. A markedly higher share of light fraction organic carbon was found at the upstream location P1, while the downstream location P9 was dominated by heavy fraction organic carbon (Figure 6). This suggests that the lower degradability of downstream organic matter results from an higher level of association with the mineral phase and that upstream organic matter was characterised by a higher share in light-fraction, easily accessible biogenic share of organic matter. The latter is corroborated by the aforementioned elevated levels of chlorophyll and therefore an increased share of biomass-based degradable organic matter in the upstream area. For landfilled Elbe sediment that had undergone several years to decades of organic matter degradation, Gebert et al. (2019) found over 93% of the bulk mass and over 80% of the organic carbon to be associated with the heavy fraction. Together, these data suggest a transition of organic carbon from the more accessible (light) to the less accessible (heavy) fraction and hence progressive stabilization of organic matter in organo-mineral complexes with increasing mineralisation and hence age.

The findings were supported by the carbon isotopic signature, with a greater share of ^{12}C in the bulk sample from upstream and an enrichment in ^{13}C downstream. Organic matter components containing the lighter isotope ^{12}C are degraded at a higher rate than those containing ^{13}C , causing an enrichment of ^{13}C and therefore an increase in the $\delta^{13}\text{C}$ signature with age (overview in Wang et al., 2015) and hence an increased level of organic matter stabilisation. Together with the distribution of TOC over the light and heavy density fractions, this again points at aged, more stabilised organic matter at the downstream location. However, the isotopic signature is also influenced by the origin of the organic matter. For example, plant species following the C3-assimilation pathway have an average $\delta^{13}\text{C}$ value of -27 ‰, species assimilating via the C4-pathway an average $\delta^{13}\text{C}$ value of -14 ‰, whereas marine organic matter typically has $\delta^{13}\text{C}$ values varying between -20 ‰ and -22 ‰ (Schulz and Zabel 2006). Lammers et al. (2017) found $\delta^{13}\text{C}$ values between 10.5 ‰ and 23.5 ‰ for eukaryotic phytoplankton in a shallow Dutch lake. The observed isotopic gradient can therefore reflect a higher age of the downstream sediment organic matter or a different origin. As point P9 (PS-layer: -26.6 ‰, Figure 7) is characterized by input of downstream sediments carried in direction of the harbour with the flood tide and point P1 (PS-layer: -28.3 ‰, Figure 7) is dominated by input from the upstream catchment with higher algal biomass in the water phase (see chlorophyll concentrations in Table 5), a source-based gradient over the investigation area is likely.

The $\delta^{13}\text{C}$ signature was expected to increase with depth due to a preferred consumption of ^{12}C by microorganisms. Likewise, it was expected that the share of carbon in the heavy density fraction would increase with depth. Both was only partly found, for example for the samples from November 2018 at location P9 (Figure 6, lower right panel). It is assumed that the absence of a clear depth-related trend is due to the naturally dynamic hydro-morphological situation (variable current, tide, dredging activities, etc.), confounding depth gradients that would be visible if they reflected an age gradient of exactly the same original material. However, the assumption that heavy fraction organic carbon reflects the older, more stabilised and therefore less degradable pool was supported by the fact that heavy density fraction organic carbon showed an enrichment in ^{13}C compared to the organic carbon found in the light density fraction (Figure 7, right panel).

Schoel et al. (2014) showed that phytoplankton plays an important role for the concentration of dissolved oxygen in the Elbe. Also, Thorp and Delong (2002) described phytoplankton as the main driver of heterotrophic organic carbon cycling for eutrophic rivers. In line with the river continuum concept (Vannote et al., 1980), Schoel et al. (2014) demonstrated super-saturation with oxygen due to enhanced net primary production in the shallow and eutrophic upstream parts of the Elbe and light-deficiency induced decay of algal biomass by zooplankton grazing in the significantly deeper waters of the Hamburg Port area, inducing oxygen minimum zones. Concurrent to phytoplankton biomass, biological oxygen demand (BOD) and oxygen saturation plummeted within the Hamburg Port area, a trend is seen in the gradient of decreasing degradability of organic matter in downstream direction demonstrated in this study (Figure 10). Within the harbour area, the river continuum concept is difficult to apply due to the strong tidal influence, additional urban afflux from streets, creeks, sewages or surface runoff as well as massive interventions like the removal of entire habitats (organisms, organic matter, etc.) by dredging.

Spatial variability of organic matter (degradation) with location and/or depth were also found in several other environments, for example in estuaries (Middelburg et al., 1996), mineral soils (Fang et al., 2005), intertidal sediments (Beck et al., 2008), lakes (Natchimuthu et al., 2015) and coastal wetlands (Yousefi Lalimi et al., 2018). Middelburg et al. (1996) found the spatial variability of organic matter mineralization in intertidal sediments to be mainly caused by differences in the organic matter lability. As in our study, Yousefi Lalimi et al. (2018) and Fang et al. (2005) found a depth gradient of decreasing decomposition rates in (marsh) soil layers. The results from Fang et al. (2005) indicated that soil basal respiration rate is closely related to variations in available carbon pools occurring at different soil depths, also hypothesized in our study. Beck et al. (2008) described that products of organic matter remineralisation (e.g. DOC, NH_4^+ , PO_4^{3-}) increased with depth in pore waters of intertidal flat sediments, which can be also seen in this study (e.g. NH_4^+ , Figure 12).

The higher upstream degradability can be caused by a higher degradability of the organic matter itself, reflecting an intrinsic chemical property, or by more favourable environmental conditions such as increased availability of nutrients or both. In this study, the longitudinal gradient of organic matter degradability correlates with a gradient in decreasing nutrient concentrations, as seen from the contents in pore water phosphate and also total phosphorus (Table 3).

5.5.3 Transformation of nitrogen

Upstream locations showed stronger accumulation of NH_4^+ in the pore water (Table 3, Figure 11), reflecting nitrogen mineralisation under anaerobic conditions, in line with higher degradability of upstream organic matter. The advanced state of organic matter degradation in deeper lying and therefore older layers was also seen by a depth gradient of increasing ammonium concentrations in the pore water (Figure 12). This was most pronounced at point P1, where also both the highest organic

matter turnover (related to dry weight of sample) and the highest degradability (related to mass unit organic carbon) were found.

Sanders et al. (2018) measured dissolved inorganic nitrogen in water samples of the stream along a gradient within the Elbe River in May 2013. Sampling locations included points near to points P1, P3, P6, P8 and P9 of this study. When comparing the two data sets, it is found that ammonium (NH_4^+) concentrations in the pore water (Table 3, layer PS) were 20 to 240 times higher compared to the concentrations in the water column, while nitrite concentrations (NO_2^-) were increased by only 2.5- to 12-fold and nitrate concentrations (NO_3^-) were partly even lower in the pore water compared to the water column (0.1- to 1.4-fold difference). Altogether, this indicates the dominance of anaerobic nitrogen mineralisation in the sediment, leading to the observed accumulation of ammonium, with denitrification being less relevant. Brockmann (1994) found decreased concentrations of dissolved organic nitrogen and dissolved organic phosphorus between Elbe river kilometres 630 and 770 towards the sea, mainly due to dilution with sea water. The decrease of the particulate organic matter concentration and the turbidity-organic matter-ratio in downstream direction was explained with organic matter degradation in the upper estuary and dilution with inorganic suspended particulate matter (SPM) from the lower estuary.

5.6 Conclusions and outlook

The time-course of organic matter degradation in long-term experiments showed the presence of differently available pools whose increasing depletion leads to an exponential decay of organic matter reactivity. The investigation area was characterised by a distinct gradient of sediment abiotic properties and organic matter lability, with higher degradability upstream and lower degradability downstream. Upstream locations were characterised by a higher concentration of DNA, a higher share of organic carbon in the light density fraction (i.e. not stabilized in organo-mineral complexes) and lower (more negative) $\delta^{13}\text{C}$ values. This supports the hypothesis of sediment and organic matter properties being determined by a spatial stratification of the source organic matter and the conditions impacting sediment properties at any individual location along the stream. Data suggest that at downstream locations, organic matter is mainly of allochthonous origin (e.g. eroded soils, plant litter), entering the port mainly with the tidal flood current from the direction of the North Sea whereas upstream locations receive sediments and organic matter predominantly originating from the Elbe catchment, with an additional greater share of autochthonous organic matter (planktonic biomass), earmarked by a lighter organic carbon (less ^{13}C). In between, sediments are of mixed origin, the magnitude of the individual upstream and downstream shares depending on the prevalent hydrodynamic conditions. Upstream, the suspended particulate matter feeding sedimentation contains more easily degradable components such as algal biomass, already suggested by higher chlorophyll concentrations in the water column, and reflected by a higher share of total mass in the sediment's lighter density fraction. Downstream, a higher level of mineralization and therefore of stabilization of the input organic matter is evidenced by an increased share of organic carbon bound to the mineral phase and lower aerobic and anaerobic degradability. Whether the observed gradient is solely due to the assumed differences in input organic matter or whether an age gradient from upstream to downstream overlays the source pattern, cannot be determined at this moment. Ongoing clay mineralogical analyses of downstream and upstream sediments shall help to further elucidate the question.

Density fractionation appears to be a promising qualitative tool which can explain the presence of differently degradable organic matter pools in sediments. Future chemical fractionation will show

whether these pools can be related to intrinsic organic matter chemical quality. While it became clear that degradability and density distribution are closely linked, the hypothesis that ageing (and hence increased mineralization and stabilization) leads to a shift towards increasing association of organic matter with the mineral phase could not be directly verified by the depth and hence age profiles at the individual sampling locations of this study. This is assumed to be due to depth profiles not representing a chronosequence of the very same settled material. Future experiments investigating the change in density distribution on one sample with ongoing incubation shall help to investigate this hypothesis. The good correlation of organic matter degradability with standard analytical parameters such as TN and TOC may allow predictions of turnover using data on simple abiotic sediment properties. Additionally, the chlorophyll concentration might play an important role in the organic matter degradation. The significantly higher degradability of organic matter under aerobic compared to anaerobic conditions in combination with the marked spatial stratification of degradability provides the basis for the assessment of climate impact of dredging and relocation measures, but also for the quantification of potential greenhouse gas emissions from port areas without intervention. Upcoming investigations will reveal the temporal variability of organic matter quality (fractions of dissolved organic carbon) and degradability in greater detail. All of the above will feed into the development of a process-based model predicting organic matter turnover in the Port of Hamburg in time and space. Benefits of this study will include increased process knowledge on organic matter degradation behaviour as a basis for implementing adaptive sediment management, positively impacting the water quality and possibly reducing greenhouse gas emissions.

Acknowledgements

This study was funded by Hamburg Port Authority and carried out within the project BIOMUD, a member of the MUDNET academic network www.tudelft.nl/mudnet/. Aerobic respiration, organic carbon contents in density fractions and stable isotopes were measured by the Institute of Soil Science (Prof. Dr. Annette Eschenbach, Dr. Alexander Gröngröft and Dr. Christian Knoblauch, respectively), DNA concentrations were measured by the Institute of Botany (Dr. Ines Krohn), both University of Hamburg.

References

- Agnieszka W, Zofia S, Aleksandra B, Artur B (2012) Evaluation of Factors Influencing the Biomass of Soil Microorganisms and DNA Content. *Open J of Soil Sci* 2:64-69
- Arndt S, Jørgensen BB, LaRowe DE, Middelburg JJ, Pancost RD (2013) Quantifying the degradation of organic matter in marine sediments: A review and synthesis. *Earth Sci Rev* 123:53-86
- Baldock JA, Skjemstad JO (2000) Role of the soil matrix and minerals in protecting natural organic materials against biological attack. *Org Geochem* 31:697-710
- Beck M, Dellwig O, Liebezeit G, Schnetger B, Brumsack HJ (2008) Spatial and seasonal variations of sulphate, dissolved organic carbon, and nutrients in deep pore waters of intertidal flat sediments. *Estuar Coast Shelf S* 79:307-316
- Berg B, McLaugherty CA (2003) *Plant Litter: Decomposition, Humus Formation, Carbon Sequestration*. Springer, Berlin
- Boehlich MJ, Strotmann T (2008) The Elbe Estuary. *Die Küste, Arch Res Technol North Sea Baltic Coast* 74:288-306
- Borges AV, Abril G (2012) Carbon Dioxide and Methane Dynamics in Estuaries. Elsevier. ESCO 00504.
- Brockmann UH (1994) Organic matter in the Elbe estuary. *Aquatic Ecol* 28:371-381
- Bu X, Ruan H, Wang L, Ma W, Ding J, Yu X (2012) Soil organic matter in density fractions as related to vegetation changes along an altitude gradient in the Wuyi Mountains, southeastern China. *Appl Soil Ecol* 52:42-47
- Cryer D, Eccleshall R, Marmur J (1975) Isolation of yeast DNA. Prescott DM (ed.), *Method Cell. Biol.* 12:39-44
- Dai XY, White D, Ping CL (2002) Comparing bioavailability in five Arctic soils by pyrolysis-gas chromatography/mass spectrometry. *J Anal App Pyrol* 62:249-258
- DIN 38404 (2012) German standard methods for the examination of water, waste water and sludge - Physical and physico-chemical parameters (group C) - Calculation of the calcit saturation of water. Beuth, Berlin, Germany
- DIN EN 1484 (1997) Water analysis - Guidelines for the determination of total organic carbon (TOC) and dissolved organic carbon (DOC). Beuth, Berlin, Germany
- DIN EN 15933 (2012) Sludge, treated biowaste and soil - Determination of pH. Beuth, Berlin, Germany
- DIN EN 16168 (2012) Sludge, treated biowaste and soil - Determination of total nitrogen using dry combustion method. Beuth, Berlin, Germany
- DIN EN 27888 (1993) Water quality; determination of electrical conductivity. Beuth, Berlin, Germany
- DIN ISO 6878 (2004) Water quality - Determination of phosphorus - Ammonium molybdate spectrometric method. Beuth, Berlin, Germany
- DIN ISO 10304 (2009) Water quality - Determination of dissolved anions by liquid chromatography of ions - Part 1: Determination of bromide, chloride, fluoride, nitrate, nitrite, phosphate and sulfate. Beuth, Berlin, Germany
- DIN ISO 10694 (1995) Soil quality - Determination of organic and total carbon after dry combustion (elementary analysis). Beuth, Berlin, Germany
- DIN ISO 11277 (2009) Soil quality - Determination of particle size distribution in mineral soil material - Method by sieving and sedimentation. Beuth, Berlin, Germany

- DIN ISO 11465 (1993) Soil quality - Determination of dry matter and water content on a mass basis - Gravimetric method. Beuth, Berlin, Germany
- DIN ISO 11732 (2005) Water quality - Determination of ammonium nitrogen - Method by flow analysis (CFA and FIA) and spectrometric detection. Beuth, Berlin, Germany
- DIN ISO 11885
- Fang C, Smith P, Moncrieff JB, Smith JU (2005) Similar response of labile and resistant soil organic matter pools to changes in temperature. *Nature* 433:57-59
- Food and Agriculture Organization of the United Nations (FAO) (2006) Guidelines for Soil Description. 4th Edn. United Nations. Rome
- Gao J, Mikutta R, Jansen B, Guggenberger G, Vogel C, Kalbitz K (2019) The multilayer model of soil mineral-organic interfaces – a review. *J Plant Nutr Soil Sci* 000:1-15
- Gebert J, Knoblauch C, Gröngroft A (2019) Gas production from dredged sediment. *Waste Manage* 85:82-89
- Gebert J, Köthe H, Gröngroft A (2006) Methane formation by dredged sediment. *J Soils Sediments* 6:75-83
- Grasset C, Mendonca R, Saucedo GV, Bastviken D, Roland F, Sobek S (2018) Large but variable methane production in anoxic freshwater sediment upon addition of allochthonous and autochthonous organic matter. *Limnol Oceanogr* 63:1488-1501
- Hamburg Serviceportal (2019) HamburgService – Wassergüte-Auskunft
<https://gateway.hamburg.de/hamburggateway/fvp/fv/BSU/wasserguete/wfWassergueteAnfrageListe.aspx?Sid=37#>. Accessed:2 May 2019
- Lammers JM, Reichart GJ, Middelburg JJ (2017) Seasonal variability in phytoplankton stable carbon isotope ratios and bacterial carbon sources in a shallow Dutch lake: *Limnol Oceanogr* 62:2773–2787
- Manzoni S, Jackson RB, Trofymow JA, Porporato A (2008) The global stoichiometry of litter nitrogen mineralization. *Science* 321:684-686
- Meijboom FW, Hassink J, van Noordwijk M (1995) Density fractionation of soil macroorganic matter using silica suspensions. *Soil Biol Biochem* 27:1109-1111
- Middelburg JJ, Klaver G, Nieuwenhuize J, Wielemaker A, de Haas W, Vlugg T, van der Nat JFWA (1996) Organic matter mineralization in intertidal sediments along an estuarine gradient. *Mar Ecol Prog Ser* 132:157-168
- Natchimuthu S, Sundgren I, Galfalk M, Klemmedtsson L, Crill P, Danielsson A, Bastviken D (2015) Spatio-temporal variability of lake CH₄ fluxes and its influence on annual whole lake emission estimates. *Limnol Oceanogr* 61:13–26
- Raymond P, Hartmann J, Lauerwald R, Sobek S, McDonald C, Hoover M, Butman D, Striegl R, Mayorga E, Humborg C, Kortelainen P, Dürr H, Meybeck M, Ciais P, Guth P (2013) Global carbon dioxide emissions from inland waters. *Nature* 503:355-359
- Rehman Ku, Ying Z, Andleeb S, Jiang Z, Olajide EK (2016) Short Term Influence of Organic and Inorganic Fertilizer on Soil Microbial Biomass and DNA in Summer and Spring. *J Northeast Agric Univ* 23:20-27
- Schoel A, Hein B, Wyrwa J, Kirchesch V (2014) Modelling Water Quality in the Elbe and its Estuary –Large Scale and Long Term Applications with Focus on the Oxygen Budget of the Estuary. *Die Kueste* 81:203-232
- Schulz HD, Zabel M (2006) Marine Geochemistry. Springer Berlin Heidelberg New York. ISBN-10 3-540-32143-8
- Sander R (2015) Compilation of Henry's law constants (version 4.0) for water as solvent. *Atmos Chem Phys* 15:4399-4981
- Sanders T, Schoel A, Dähnke K (2018) Hot Spots of Nitrification in the Elbe Estuary and Their Impact on Nitrate Regeneration. *Estuar and Coasts* 41:128-138
- Six J, Paustian K (2014) Aggregate-associated soil organic matter as an ecosystem property and a measurement tool. *Soil Biol Biochem* 68:A4-A9
- Spieckermann MJ, Gröngroft A, Eschenbach A (2018) Zeitliche Änderung des O₂-Zehrungspotentials von Sedimenten aus dem Hamburger Hafen. Rostocker Baggergutseminar. <https://www2.auf.uni-rostock.de/ll/baggergut/rbs10/pdf/Spieckermann.pdf>. Accessed:30 May 2019
- Straathof AL, Chincari R, Comans RNJ, Hoffland E (2014) Dynamics of soil dissolved organic carbon pools reveal both hydrophobic and hydrophilic compounds sustain microbial respiration. *Soil Biol Biochem* 79:109-116
- Straathof AL, Comans RNJ (2015) Input materials and processing conditions control compost dissolved organic carbon quality. *Bioresource Technol* 179:619–623
- Thorpe JM and DeLong MD (2002) Dominance of autochthonous autotrophic carbon in food webs of heterotrophic rivers. *Oikos* 96:3:543-550
- Van den Pol-van Dasselaar A, Oenema O (1999) Methane production and carbon mineralisation of size and density fractions of peat soils. *Soil Biol Biochem* 31:877-886
- Van Dijk H (1980) Survey of Dutch organic matter research with regard to humification and degradation rates in arable land. Land Use Seminar on Soil Degradation, Wageningen, 13-15
- Vannote RL, Minshall WG, Cummins KW, Sedell JR, Cushing CE (1980) The river continuum concept. *Can J Fish Aquat Sci* 37:130-37
- Wang G, Jia Y, Li W (2015) Effects of environmental and biotic factors on carbon isotopic fractionation during decomposition of soil organic matter. *Sci Rep* 5:11043
- White DM, Garland DS, Dai X, Ping, CL (2002) Fingerprinting soil organic matter in the arctic to help predict CO₂ flux. *Cold Reg Sci and Technol* 35:185-194
- Wirth H (1980) Sedimentologie und Geochemie von Elbschwebstoffen zwischen Schnackenburg und Hamburg. Diplomarbeit Fachbereich Geowissenschaften, Universität Hamburg
- Wolanski E, Chappell J, Ridd P, Vertessy R (1988) Fluidization of mud in estuaries. *J Geophys Res* 93:2351-2361
- Wurpts R Torn P (2005) 15 Years Experience with Fluid Mud: Definition of the Nautical Bottom with Rheological Parameters. *Terra et Aqua* 99:22-32
- Yousefi Lalimi F, Silvestri S, D'Alpaos A, Roner M, Marani M (2018) The Spatial Variability of Organic Matter and Decomposition Processes at the Marsh Scale. *J Geophys Res-Bioge* 123:3713-3727

6 Linking patterns of density, thermometric and carbon stable isotope fractions of organic matter to its lability in sediments of the tidal Elbe river

F. Zander¹, R.N.J. Comans², J. Gebert¹

¹Faculty of Civil Engineering and Geosciences, Department of Geoscience and Engineering, Delft University of Technology, 2628 CN Delft, the Netherlands

²Soil Chemistry and Chemical Soil Quality Group, Wageningen University, 6708 PB, Wageningen, the Netherlands.

Corresponding author: Florian Zander, f.zander@tudelft.nl

Abstract

Degradability of organic matter in river sediments differs in relation to origin and age. In order to explain previously observed spatial patterns of organic matter degradability and stabilization, this study investigated sediment organic matter (SOM) properties along a tidal Elbe river transect using dissolved organic matter (DOM) fractions, density fractions, carbon stable isotopes and thermometric pyrolysis (Rock Eval 6©). These properties were linked to SOM decay rates and biological indicators such as chlorophyll a and silicic acid in the water phase, and sediment-bound extrapolymeric substances (EPS), microbial biomass and oxygen consumption. Sediment source gradients were established using the concentration of Zn in the fraction < 20 µm as proxy.

The specific Zn concentration showed that the most upstream location was nourished primarily by upstream fluvial sediments while the other locations carried a downstream signature. The upstream location was also characterised by the highest concentrations of chlorophyll a, microbial biomass, silicic acid, EPS, humic acids and hydrophilic DOM, the most negative $\delta^{13}\text{C}$ signature and by the highest oxygen consumption rate, with decreasing trends towards downstream locations. This trend was reiterated by decreasing SOM lability from upstream to downstream, an increasing share of total SOM found in the acid-base-extractable fractions and a decreasing share of carbon in the light density fractions. Thermometric pyrolysis revealed the highest H index (easily degradable SOM) for the most upstream location and the ratio of the I index (immature SOM) to the R index (refractory SOM) to correlate positively with measured SOM decay rates.

This study shows that spatial patterns of SOM degradability can be explained by a source gradient, with young organic matter entering the system from upstream from predominantly biogenic sources, while downstream sources (North Sea sediment) deliver more refractory SOM that is stabilised in organo-mineral associations to a higher extent. In the investigated sediments, dissolved organic matter represented 0.23 to 1.20% of the TOC from anaerobically degradable SOM, while 4.10 to 11.46% TOC was liberated as CO_2 and CH_4 after long-term incubation (250 days). Thermometric pyrolysis is shown to serve as a useful proxy to predict SOM degradability in river sediments, with the Hydrogen-Index (HI) correlating well with degradability and the relationship between the I-Index and R-Index changing consistently towards lower I-Indices and higher R-Indices with increasing degree of SOM stabilization.

Keywords: Sediment organic matter; anaerobic and aerobic degradability; chemical and physical DOM and SOM fractions

6.1 Introduction

Marine dissolved organic matter contains in total about 660×10^{15} g carbon, one thousand times more carbon than all living organisms in the oceans combined (Hansell et al., 2009 in Dittmar, 2015). Most of the freshly produced dissolved organic matter (DOM) is highly degradable and consumed within days after production (Dittmar, 2015), and the same is true for inland waters (Catalan et al., 2016, in Ward et al., 2017). To advance understanding of the carbon balance along the river continuum (Vannote et al., 1980) and to predict organic matter decay, it is of interest to research mechanisms of SOM stabilization and to find proxies to assess its lability. Next to its role in the aquatic carbon cycle, sediment-bound organic matter (SOM) influences sediment properties that are relevant for navigation and maintenance of ports and waterways, such as rheological (Wurpts and Torn, 2005; Shakeel et al., 2019, 2022) or settling and consolidation behaviour (Sills and Gonzalez 2001; Jommi et al., 2019). While approaches to investigate SOM quality and stability in terrestrial soils are plentiful, only few studies are available for freshwater sediments.

The classification of organic matter quality and its degradability in terrestrial soils has been approached by various methods of chemical and physical fractionation, as reviewed by Lützow et al. (2007). Lehmann and Kleber (2015) described the soil organic matter as a continuum of progressively decomposing organic compounds. Grasset et al. (2021) showed that the extent of methane production could be well predicted by the quantity of particular organic matter and its quality, the latter assessed with the C/N ratio. Helfrich et al. (2007) and Shen et al. (2018), for example, used chemical fractionation to isolate stable soil organic matter from different agricultural and forest soils and to assess the influence of different land uses on the organic matter quality and quantity of soils. It has been attempted to cluster the different behaviour of functional organic matter pools of different degradability based on physical and chemical organic matter fractions. Kögel-Knabner (2018) reviewed molecular methods in SOM research. Hoffland et al. (2020) concluded that in terms of the eco-functionality of organic matter in soils especially the non-degradable (recalcitrant) fraction of organic matter is under-researched.

For sediments, Gebert et al. (2006) found that maximum anaerobic SOM decay rates in ten fluvial sediments correspond to the amount of carbon in the light density fraction ($< 1.4 \text{ g cm}^{-3}$). Wakeham et al. (2016) identified unevenly distributed organic matter (no trend in age) among density fractions in riverine delta sediments with the biggest share of SOM (TOC and mass) in the meso-density fraction ($1.6\text{-}2.5 \text{ g cm}^{-3}$). Zander et al. (2020) found pronounced spatial gradients of SOM degradability (higher degradability upstream, lower degradability downstream) in the tidal freshwater part around the port of Hamburg which correlated with patterns of ^{13}C enrichment and an increased share of TOC in the heavy density fraction downstream.

This study investigates possible causes of the observed spatial gradient (source and/or age gradient) with different approaches by linking the size of physical and chemical SOM and DOM (dissolved organic matter) fractions, and further biotic and abiotic properties in sediments of the tidal Elbe (Figure 2) to SOM degradability. SOM degradability is defined as the share of carbon released by microbial degradation under aerobic or anaerobic conditions with respect to total TOC. It is hypothesized that

1. SOM lability along the investigated transect is dependent on SOM origin and age: fresh planktonic, easily degradable biomass feeds organic matter stocks from upstream while less degradable organic matter is older and stabilized in organo-mineral complexes. These can form in situ as a result of progressive SOM degradation (ageing) or are as such imported from sources like eroded upstream and downstream alluvial soils and from North Sea sediment.

2. SOM chemical and physical fractions can be related to biological and physico-chemical sediment processes.
3. With increasing incubation temperature and incubation time, larger shares of DOM fractions will be produced (DOM fractions as a product of SOM decay).
4. Light density fractions decrease and $\delta^{13}\text{C}$ values increase with progressive SOM decay and mirror the spatial trend of SOM degradability along the investigated transect.

While Zander et al. (2020) give an overview of the spatial and depth gradients of SOM degradability, carbon stable isotopes, density fractions and DNA in extrapolymeric substances observed in the investigation area, this study focuses on SOM fractions observed in situ, their change in relation to SOM decay and their relation to selected biotic and abiotic sediment properties.

6.2 Materials and methods

Investigation area and sampling approach

Sediment samples for this study were collected from different locations along a transect of around 30 river kilometres (P1 = river km 616, P9 = river km 646, Figure S1) through the Port of Hamburg (site description in Zander et al., 2020) using one meter core sampler ('Frahmplot'). On board, the core was divided into three layers based on differences in visual consistency and strength: fluid mud (FM), pre-consolidated sediment (PS), and consolidated sediment (CS), from top to bottom. Average sediment properties at sampling locations P1 to P9 (Figure 2) as well as their depth-related differentiation have been characterised in Zander et al. (2020).

In this study, samples from the locations P1, P2, P6, P8 and P9 were analysed for SOM fractions. Sample selection was based on differences in location, depth and measured SOM degradability. Samples from additional other locations were analysed for further physicochemical and biological parameters, including extrapolymeric substances, microbial biomass, silicic acid, chlorophyll, carbon stable isotopes, Rock-Eval pyrolysis, aerobic and anaerobic SOM decay rates.

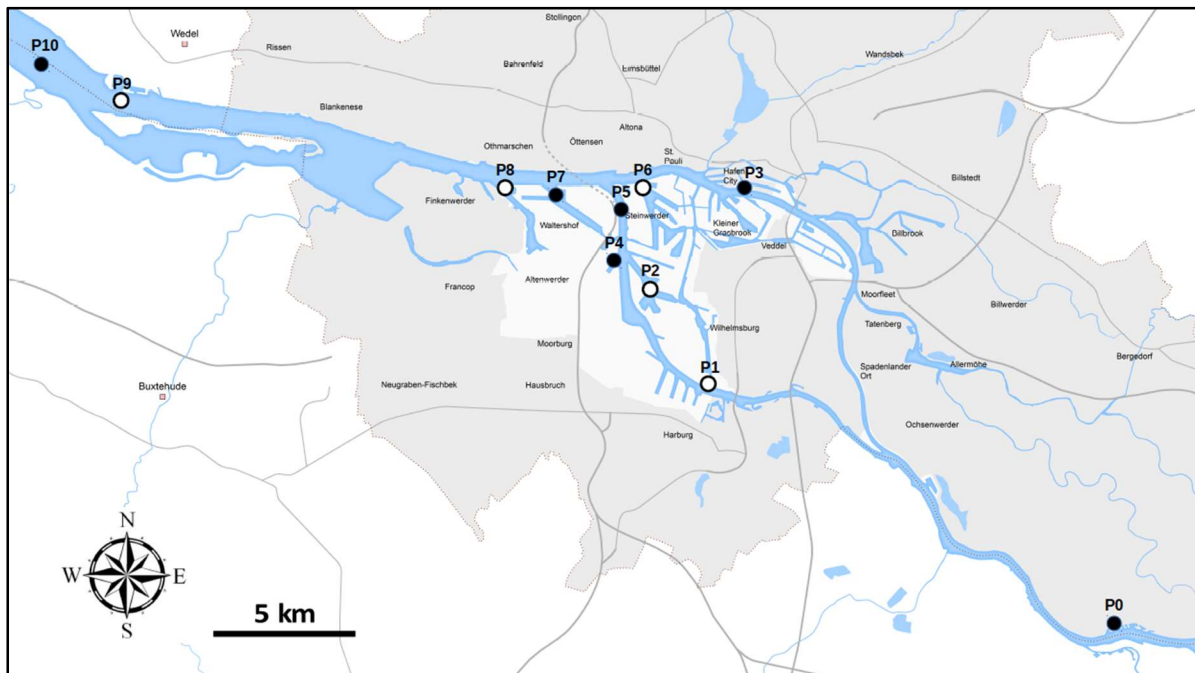


Figure 13 Investigation area around the Port of Hamburg (adapted from Hamburg Port Authority) with sampling locations between river km 598 (P0, upstream) and 646 (P10, downstream). White circles represent the sampling locations investigated in this study. Further information on sampling sites and sampling strategy in Zander et al. (2020).

Organic matter fractions

Water- and acid-base-extractable SOM fractions were analysed on a subset of 16 samples collected in 2018 (for properties, see Table 6). Water-extractable SOM is assumed to resemble the DOM fraction of these sediments. Organic matter was extracted on two aliquots using firstly, a water extracted (ratio sediment to water was 1:2) and, secondly, a sequential acid-base-extraction (procedures described in detail in Van Zomeren and Comans, 2007). This acid-base fractionation method uses aggregation/precipitation and dissolution properties of natural organic matter established by the International Humic Substances Society (IHSS) to determine acid-base-extractable DOM humic acid (HA), fulvic acid (FA), hydrophobic neutrals (HoN) and hydrophilic acids (Hi) as described in Straathof et al. (2014).

In brief, the starting solution of the total extracted DOC was acidified to pH 1 using 6 M HCl, the acidified solution was then centrifuged, separating the HA from the supernatant. The pellet of HA was re-dissolved in a base solution of 0.1 M KOH and subsequently measured as DOC on a Segmented Flow Analyser (SFA), while the remaining supernatant was then equilibrated with the resin DAX-8 (SigmaAldrich) for 1 h at 220 rpm horizontal shaking at a 1:5 resin to solution ratio. This equilibration step pulled hydrophobic FA and HoN compounds out of solution by binding them to the surface of the hydrophobic resin. The compounds that remained in solution are operationally defined as hydrophilic acids and their concentration was measured as DOC on an SFA. Finally, the resin separated from the Hi fraction was equilibrated in 0.1 M KOH, re-dissolving the FA pool. The concentration of FA was also measured as DOC on an SFA while the concentration of the remaining HoN pool was calculated by determining the proportion of the DOC which was not re-dissolved from the resin (as it remains bound to the resin even under alkaline conditions).

The recovery rate was between 78% and 87% for the acid-base-extraction and 80% to 97% for the water-extraction. For both extractions, the fractions have been normalized to 100% recovery relative to total DOC.

Density fractions

The procedure is based on the method first presented by van den Pol-van Dasselaar and Oenema (1999), adapted from Meijboom et al. (1995), and also applied by Gebert et al. (2006) on riverine sediments in a previous study. The samples were placed in glass beakers, mixed with an excess of LUDOX[®] HS-40 colloidal silica suspension in water (Sigma-Aldrich) with a cut-off density of 1.4 g cm⁻³ and stirred thoroughly. Light material < 1.4 g cm⁻³ accumulated at the surface and was separated from heavy material > 1.4 g cm⁻³, sinking to the bottom, by decantation. The two fractions were washed with distilled water and oven-dried at 105 °C for subsequent physical and chemical analyses (see Section 3.3). More details are given in Zander et al. (2020).

Carbon stable isotopes

The $\delta^{13}\text{C}$ -values of the sediment organic matter were determined with an isotope-ratio mass spectrometer (Delta V; Thermo Scientific, Dreieich, Germany) coupled to an elemental analyser (Flash 2000; Thermo Scientific). Prior to analysis, samples were treated with phosphoric acid (43%, 80 °C for 2 h) to release inorganic carbon. Values are expressed relative to Vienna Pee Dee Belemnite (VPDB) using the external standards IAEA IAEA-CH7 (-31.62 ‰ vs. VPDB) and IVA soil 33802153 (27.46‰ vs. VPDB).

Organic matter decay rates

The detailed description of the methods to measure aerobic and anaerobic organic carbon release and to calculate the corresponding decay rates can be found in Zander et al. (2020). In brief, the time course of cumulated carbon release (CH₄-C and CO₂-C) was described by one phase or two phase exponential decay fits (OriginPro2019). Two phase functions were split into two single functions with different organic matter decay kinetics. For each function, the organic matter decay rate B (mg C g_{TOC}⁻¹ d⁻¹) was derived by calculating the derivative of the sum function. The daily decay rates were calculated from the derivative of the exponential fit of the cumulative curve.

Response of anaerobic SOM decay and SOM fractions to different temperatures of SOM decay

Temperature sensitivity experiments were performed to quantify differences in SOM decay rates and subsequent DOM fraction patterns in relation to temperature for aerobic and anaerobic conditions. To this end, sediment samples from a long term temperature experiment (between 5 and 42 °C) were analysed for DOM fractions to simulate different decay behaviours on the same samples for the same incubation time, but with temperature as the only one changing parameter. The incubation treatment is described in Zander et al. (2020).

Rock-Eval pyrolysis

The Rock-Eval 6[®] method was used to further characterise SOM, especially the share of hydrocarbon and oxygen bearing components. In brief, the sample is first pyrolysed and subsequently oxidised, both steps using a temperature ramp, and the resulting release of hydrocarbons, CO and CO₂ are quantified with a flame ionisation and infrared detector. The method is described in detail Sebag et al. (2016) and Oliveira et al. (2017). In brief, analyses were carried out with 30 to 100 mg of powdered samples using a Rock-Eval 6 pyrolyzer manufactured by Vinci Technologies. Phase one was a pyrolysis in an inert N₂ atmosphere starting at a temperature of 200 °C until 650 °C with a heating rate of 25 °C/min, phase two included thermal decomposition in an oxidized atmosphere starting at a temperature of 400 °C until 850 °C with the same heating rate (Sebag et al., 2016). The Hydrogen Index (HI), a proxy for more labile organic matter, was calculated by integrating the amounts of hydrocarbons normalized to the amount of total organic carbon (Lafargue et al., 1998). The I-index, assessing the preservation of thermally labile immature organic fraction and the R index, assessing the contribution of thermally stable refractory organic fraction corresponding to the most persistent or refractory SOM fraction were defined by Sebag et al. (2006; 2016).

Other parameters

Chlorophyll a concentration as an indicator for planktonic biomass was measured in situ with a CTD probe (CTD90, Sea&Sun, data provided by Hamburg Port Authority) in the near-bottom water column. For the points P0 and P10 (Figure 17), chlorophyll data were gathered from FGG Elbe data portal (2020), chlorophyll concentration from 2017 to 2020 near location P8 was obtained from Hamburg Serviceportal (2020, Figure 17). Methods for silicic acid, EPS-DNA concentration and standard properties of solids and pore water are given in Zander et al. (2020).

6.3 Results

6.3.1 Origin and properties of investigated sediments

Selected abiotic and biotic properties of the 16 samples in focus of this study are given in Table 6, average values for the same properties of all samples collected in 2018 are described in Zander et al. (2020). Clear differences between upstream and downstream sediment properties are illustrated by location P9 (downstream, sample W3, W13 and W14) showing the lowest values for total nitrogen (TN,

0.2% DM, W3), total organic carbon (TOC, 1.8% DM, W3), anaerobically degradable SOM (Degradable AN, 9%, W3), clay (15%, W13), silt (26%, W3), water content (WC, 95% DM, W3), light density fraction (LF, 7% DM-bulk, W13), oxygen consumption after 3 h (AT_{3h}, 0.4 g O₂ kg_{DW}⁻¹, W13) and silicic acid (SA, 13 mg l⁻¹, W13) and high values at location P1 (upstream, sample W4, W5, W8 and W9) for TN (1.0% DM, W4), TOC (6.8% DM, W9), silt (56%, W9), B2 (4.9 mg C g_{TOC}⁻¹ day⁻¹, W8), WC (520% DM, W4), light density fraction (LF, 53% DM-bulk, W9), microbial biomass (MB, 6208 mg kg_{DM}⁻¹, AT_{3h} (3.1 g O₂ kg_{DW}⁻¹, W4), SA (44 mg l⁻¹, W9). silicic acid (SA, 13 mg l⁻¹, W13) and high values at location P1 (upstream, sample W4, W5, W8 and W9) for TN (1.0% DM, W4), TOC (6.8% DM, W9), silt (56%, W9), B2 (4.9 mg C g_{TOC}⁻¹ day⁻¹, W8), WC (520% DM, W4), light density fraction (LF, 53% DM-bulk, W9), microbial biomass (MB, 6208 mg kg_{DM}⁻¹, AT_{3h} (3.1 g O₂ kg_{DW}⁻¹, W4), SA (44 mg l⁻¹, W9).

Table 6 Abiotic and biotic sediment properties of samples selected for this study. W1 to W16 = sample ID.

	W1	W2	W3	W4	W5	W6	W7	W8	W9	W10	W11	W12	W13	W14	W15	W16
Position (-)	P6	P6	P9	P1	P1	P6	P6	P1	P1	P2	P2	P2	P9	P9	P6	P6
Sampling date (-)	aug-18	aug-18	sep-18	sep-18	sep-18	sep-18	sep-18	nov-18	nov-18	nov-18	nov-18	nov-18	nov-18	nov-18	nov-18	nov-18
Layer (-)	PS	PS	CS	PS	CS	PS	CS	PS	CS	FM	PS	CS	PS	CS	PS	CS
Depth b.l. (cm)	0-20	20-35	25-50	0-15	15-50	0-20	20-45	0-20	20-50	0-10	10-40	40-80	10-30	30-65	0-30	30-70
TN (% DM)	0.4	0.4	0.2	1.0	0.9	0.4	0.4	0.8	1.0	0.4	0.5	0.5	0.2	0.2	0.4	0.4
TOC (% DM)	3.5	3.6	1.8	6.6	6.7	3.1	3.3	5.7	6.8	3.8	3.9	3.9	1.8	1.8	3.1	3.3
TOC/TN (% % ⁻¹)	8	8	11	7	7	8	8	7	7	9	8	8	11	11	9	8
Degradable AN (%)	24	19	9	24	20	16	11	16	14	15	14	12	13	19	50	12
Clay (<2 µm, %)	43	44	16	45	47	38	41	48	38	48	46	51	15	16	38	34
Silt (2-63 µm, %)	47	48	26	47	45	37	46	48	56	46	48	39	29	34	45	45
Sand (>63 µm, %)	9	8	58	8	7	25	13	4	7	6	7	10	56	50	18	21
WC (% DM)	295	260	95	520	393	265	235	408	362	321	278	242	115	103	242	192
Eh (meV)	-310	-300	-265	-250	-220	-260	-290	-280	-240	-190	-260	-300	30	-60	-140	-280
pH (-)	7.4	7.4	7.3	7.1	6.7	7.4	7.3	7.2	6.6	7.4	7.4	7.1	7.4	7.3	7.4	7.3
LF (% DM-bulk)	35	19	8	40	51	18	26	43	53	24	24	25	7	8	24	27
HF (% DM-bulk)	65	81	92	60	49	82	74	57	47	76	76	75	93	92	76	73
MB (mg kg _{DM} ⁻¹)	nd	nd	nd	4886	3475	nd	nd	4275	6208	3069	2595	2950	nd	nd	nd	nd
AT _{3h} (g O ₂ kg _{DM} ⁻¹)	1.5	1.2	0.7	3.1	1.9	1.0	0.8	2.4	2.4	1.3	1.4	1.3	0.4	0.4	0.7	0.7
Silicic acid (mg l ⁻¹)	24	29	30	40	26	26	31	32	44	17	25	37	13	19	19	37

b.I. below lutocline, FM fluid mud, PS pre-consolidated sediment, CS consolidated sediment, TN total nitrogen, TOC total organic carbon, both for anaerobic incubation, Degradable AN anaerobically degradable SOM, WC water content, Eh redox potential, LF and HF light and heavy density fraction, MB microbial biomass, AT_{3h} oxygen consumption after 3 h, nd not determined. Average values has been shown in Zander et al. (2020) for depth, total nitrogen, total organic carbon, grain size analyses, water content, redox potential, pH and oxygen consumption after 3 h.

To estimate the shares of upstream and downstream material in the total sediment mix found at each location, the concentration of Zn in the particle size fraction < 20 µm was used as a proxy, differing significantly between upstream (higher concentrations) and North Sea material (lower concentrations; Kappenberg and Fanger, 2007 in Beusekom et al., 2021). Figure 14 (left) shows that from a downstream point of view the sediments are dominated by North Sea material until Elbe km 619 (P2, 400 mg Zn kg_{DW}⁻¹ in fraction < 20 µm), transported into the port by so called tidal pumping (Schwartz et al., 2015), while locations further upstream of this point are characterised by upstream sediments with larger Zn concentration (P1 and P0: 650 and 850 mg Zn kg_{DW}⁻¹). In the water phase, the chlorophyll a concentration generally decreased from upstream (P0) to downstream (P10, Figure 14, right). The small figure shows how chlorophyll varies seasonally by example of continuous measurements near location P8 (Hamburg Serviceportal, 2020), indicating a multi-peak algae bloom with generally higher values in the warmer seasons, decreasing towards winter. In 2018, the first peak occurred exceptionally early.

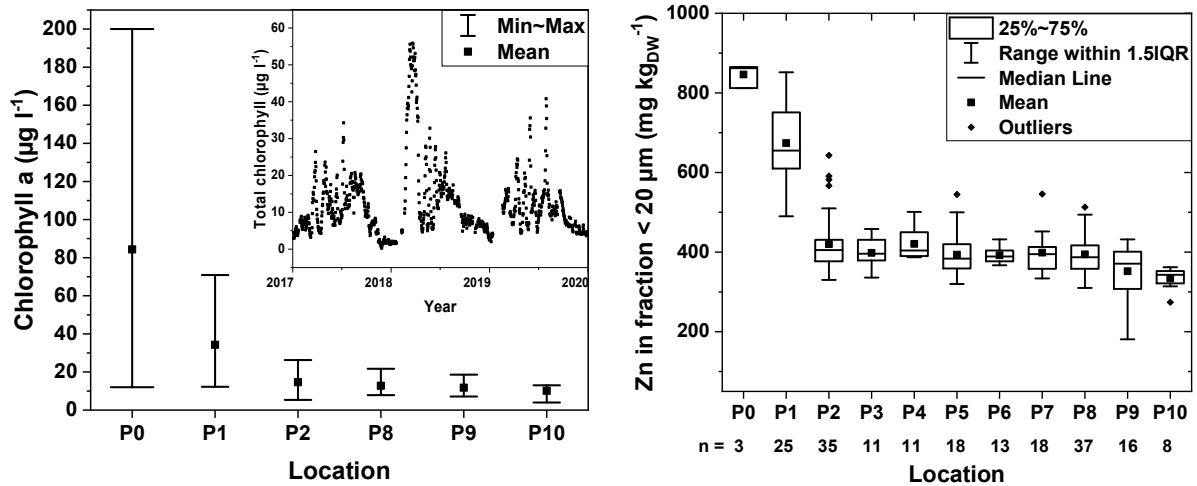


Figure 14 Left: in situ chlorophyll concentration from upstream (P0) to downstream (P10) in 2018 ($n = 5$). Squares = average values, error bars = maximum, minimum. Data for P0 and P10: FGG Elbe data portal (2020), total chlorophyll concentration from 2017 to 2020 (small Figure): Hamburg Serviceportal (2020), near location P8. Right: concentration of Zn in the particle size fraction $< 20 \mu\text{m}$ along the investigated transect for PS and CS layers from 2018 and 2019, P0 = river-km 579, P10 = river-km 646.

At downstream locations, i.e. P8 to P10, the lowest concentration of silicic acid (indicative of the algae group of diatoms), microbial biomass, oxygen consumption after three hours ($\text{AT}_{3\text{h}}$) and extrapolymeric substances (EPS) was found (Figure 15). These trends align with the trend of decreasing SOM degradability (Figure 16), and decreasing shares of water-extractable SOM hydrophilics, increasing shares of water-extractable fulvic acids and hydrophobic neutrals and an increasing ratio of acid-base-extractable to water-extractable hydrophilics (see Figure 17).

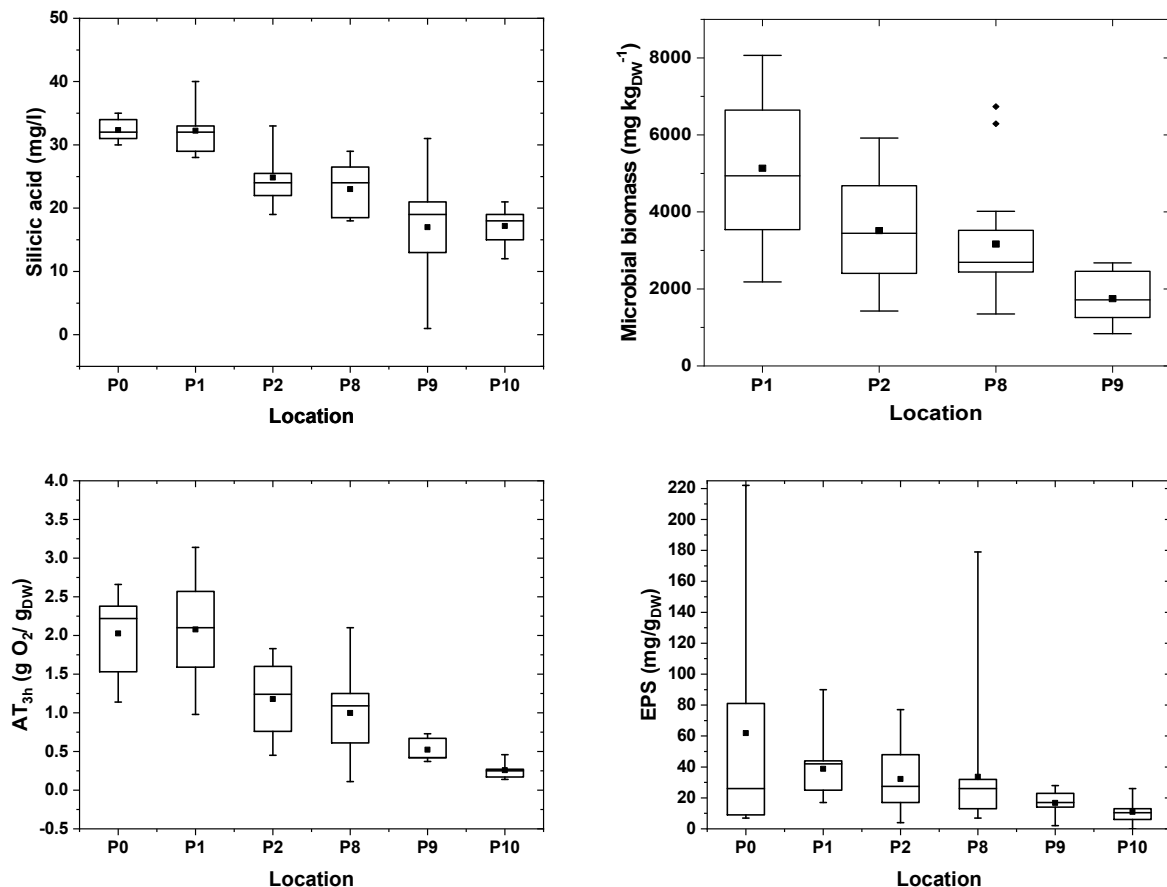


Figure 15 Silicic acid, microbial biomass, oxygen consumption after three hours (AT_{3h}) and extrapolymeric substances (EPS) concentration from upstream to downstream i.e. location P0 to P10, PS layers for all parameters analysed out of microbial biomass: PS and CS layers, $n \geq 6$. Lines = median values, squares = mean values, boxes = 25th and 75th percentile.

As almost all sediment samples were characterised by negative redox potentials (Table 6), decay rates for anaerobic SOM degradation were considered in this study. SOM decay rates declined asymptotically over time of incubation (compare Zander et al., 2020). Figure 16 shows that for the short-term decay (Figure 16, upper panel), a large range of decay rates (i.e. large differences) was found, whereas for the long-term decay, only a small range of rates (i.e. high similarity between samples) was detected (Figure 16, lower panel). Over time, the decay behaviour along the transect thus becomes more similar.

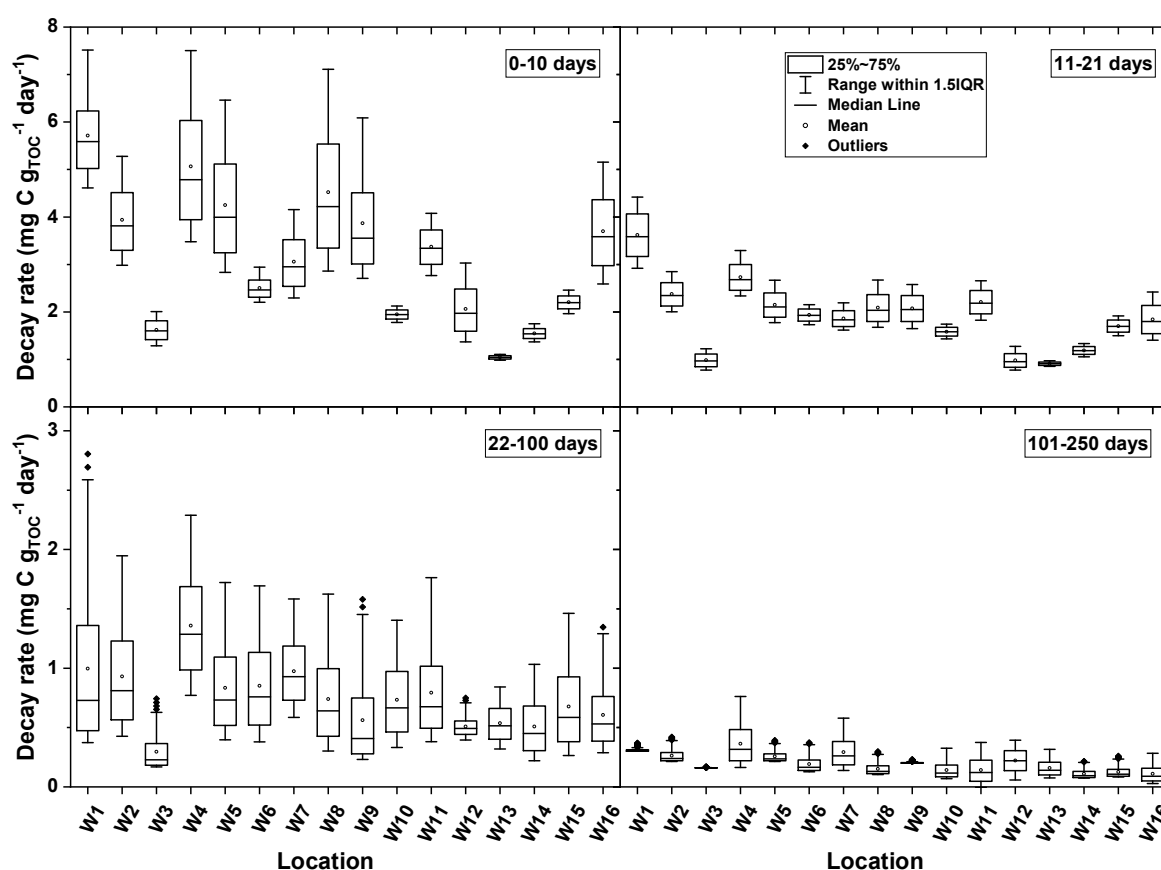


Figure 16 Anaerobic decay rates for 16 samples, per sample averaged over 0-10, 11-21, 22-100 and 101-250 days. Note the different y-axis in the lower part of the figure.

6.3.2 Extractable SOM fractions, field transect

Water-extractable and acid-base-extractable SOM fractions were analysed on a subset of 16 samples from 2018 (for properties, see Table 6). The concentration of all fractions were found to decrease strongly from upstream to downstream locations in the water-extractable SOM (Figure 17, left). At all locations, all water-extractable SOM fractions, except for the hydrophobic neutrals (HoN), increased with depth from the upper FM/PS layers to the lower CS layers, this change being most pronounced at upstream locations. For the HoN fraction, this pattern was also found at upstream location P1. With the acid-base extraction, up to $80 \text{ mg C g}_{\text{TOC}}^{-1}$ of SOM were liberated (Figure 17, middle column) at location P1, exceeding water-extractable SOM concentrations in all fractions by about one order of magnitude. The spatial and depth-related trends described for the water-extractable fraction were

inversed for the acid-base-extractable fraction, increasing from 60 mg C g_{TOC}⁻¹ (P1) to 160 mg C g_{TOC}⁻¹ (P9).

Humic acids (HA) were the largest contributor to extractable SOM at all locations, making up around 50% to 60% of water- and acid-base-extractable SOM. The ratio between acid-base-extractable and water-extractable SOM (AB/W) increased in downstream direction for all fractions with the exception of the HoN fraction (Figure 17, right). The ratio between the acid-base fraction and the water-extractable fraction can be interpreted as a dimensionless solid/liquid partitioning coefficient, which was found to be between 5 and 60 for total water-extractable SOM, and the HA and FA fraction. The largest differences in the partitioning coefficients of the SOM fractions between upstream (P1) and downstream (P9) locations were found for the HA fraction (factor 5 to 50) and the Hi fraction (factor 20 to 200). Together, these results indicate an increase in the share of mineral-bound SOM towards downstream and changes in the contribution of individual fractions to total water-extractable SOM along the transect. By the example of material from pre-consolidated (PS) layers, the latter is detailed in Figure 17.

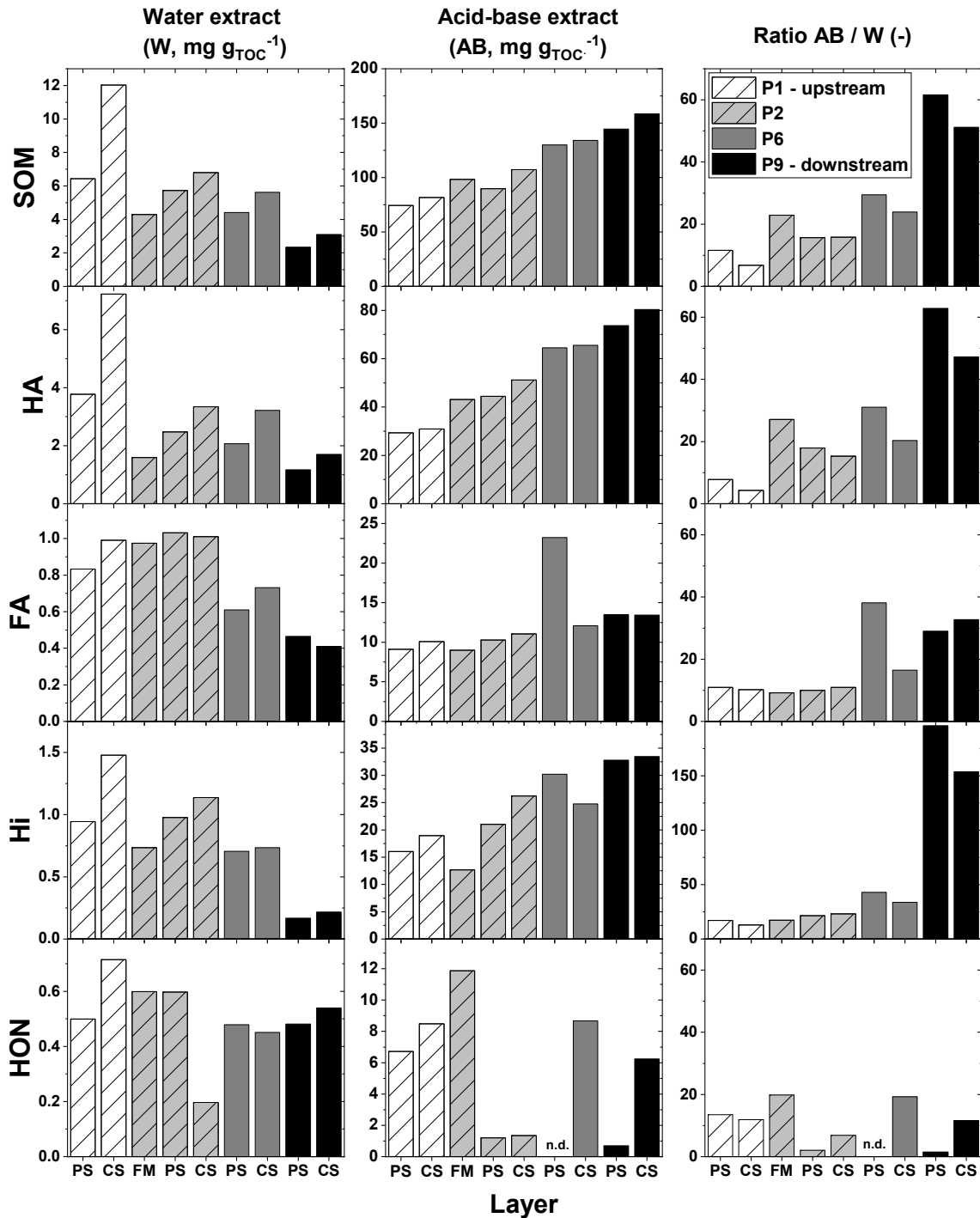


Figure 17 Water-extractable SOM fractions (left), acid-base-extractable SOM fractions (middle) and ratio between acid-base and water-extractable SOM (right). Total extracted SOM, HA (humic acid), FA (fulvic acid, Hi (hydrophilic acid), HoN (hydrophobic neutrals), concentrations are normalised to total organic carbon (TOC). Observe differently scaled y-axes. n.d. = not determined.

6.3.3 Effect of temperature and time on anaerobic SOM decay and water-extractable SOM dynamics

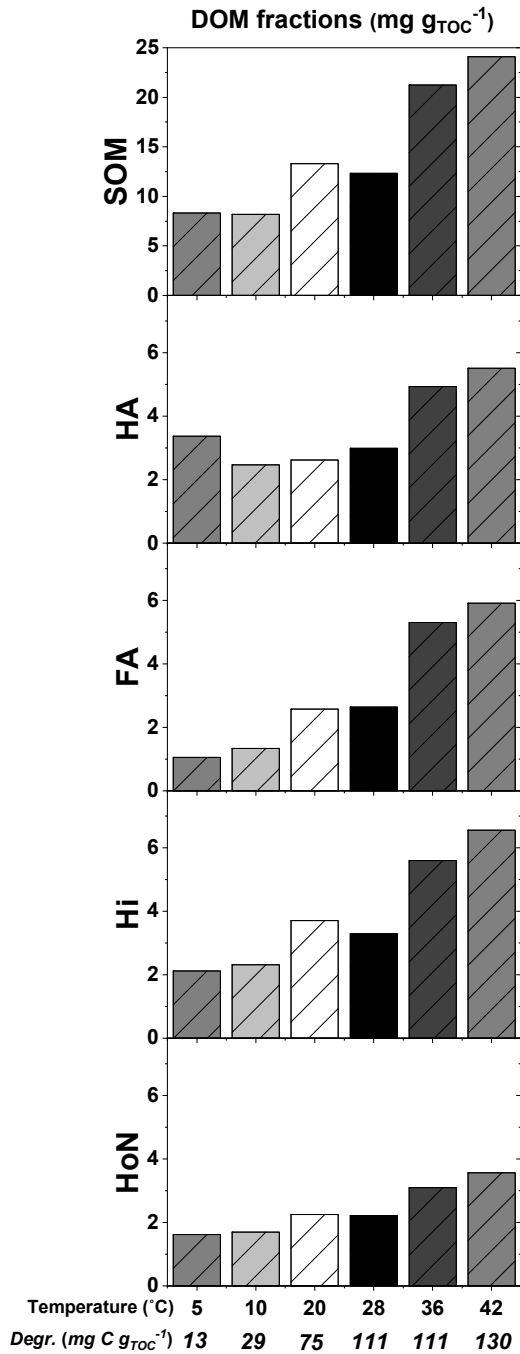
Water-extractable SOM fractions were analysed in aliquots of a sediment sample that had been incubated under anaerobic conditions at temperatures between 5 and 42 °C for 865 days. Due to the temperature-dependency of SOM degradation, sampling at a given point in time allowed to capture different states of degradation of the same original sample. The levelling off of the cumulative SOM

decay curve (plateau), caused by declining degradation rates, was reached earlier at higher incubation temperatures (data not shown). Cumulative C release varied between 13 mg C g_{TOC}⁻¹ at 5 °C and 130 mg C g_{TOC}⁻¹ at 42 °C (Figure 18, left), i.e. between 1.3% and 13% of TOC.

The total water-extractable SOM and the concentration of the individual fractions increased with increasing incubation temperature (Figure 18, left). From 5 to 42 °C, the FA fraction increased by a factor of 6 and the Hi fraction increased by a factor of 3. Total water-extractable SOM and the HoN fraction showed a similar trend but to a smaller extent, making up between 8.2 and 24.1 mg C g_{TOC}⁻¹ after 865 days of anaerobic incubation. After 865 days of anaerobic incubation at 42 °C, i.e. the temperature yielding the most exhaustive SOM decay, 24.1 mg C g_{TOC}⁻¹, were transferred into DOM whereas 130 mg C g_{TOC}⁻¹ was transferred into gas (CO₂, CH₄). For the other samples analysed in this study (incubated anaerobically for 250 days, Table 6), the values were lower due to the shorter incubation period, i.e. between 2.3 and 12 mg C g_{TOC}⁻¹ were transferred into DOM and 41.0 to 114.6 mg C g_{TOC}⁻¹ into gas.

The second experiment, investigating the time course of SOM release using a constant incubation temperature (36 °C) showed that concentrations of total water-extractable SOM and the FA, Hi and HoN fractions increased clearly over time of incubation. Total water-extractable SOM increased from 3 to 5 mg C g_{TOC}⁻¹ (3 to 45 days), and total cumulatively degraded SOM from 1 to 16 mg C g_{TOC}⁻¹ (Figure 18, right).

Temperature gradient, 865 days



Time gradient, 36 °C

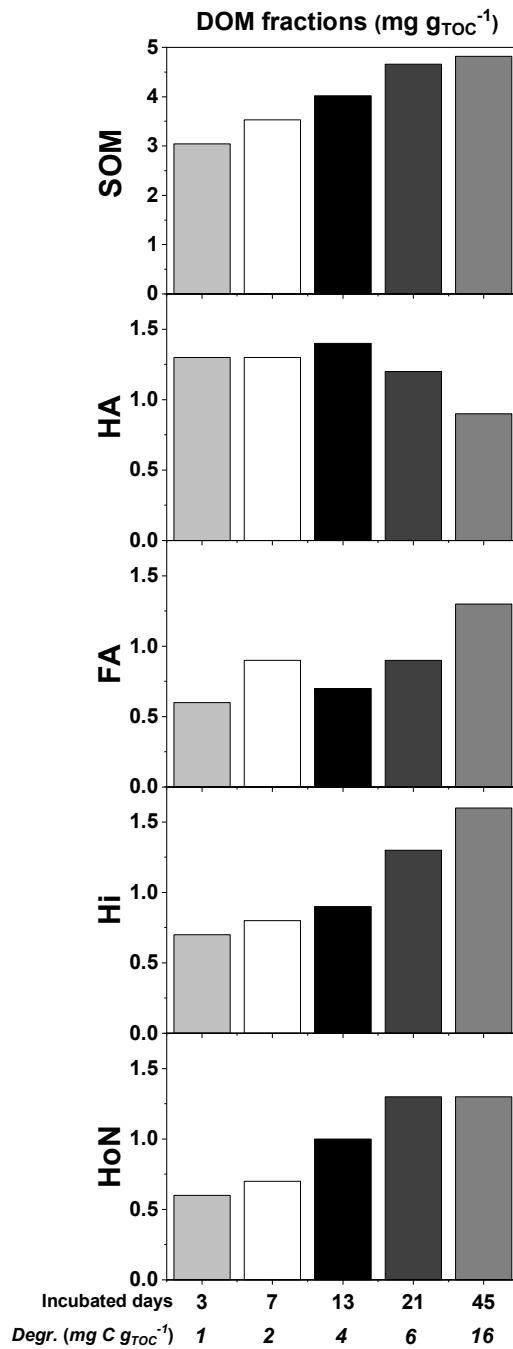


Figure 18 Left: Water-extractable SOM fractions with different incubation temperatures (5 to 42 °C) after 865 days of incubation, samples taken in November 2018. Right: water-extractable SOM fractions incubated at 36 °C for different time steps (3 to 45 days), both for PS layers of location P7, samples taken in November 2020. Total water-extractable SOM, HA (humic acid), FA (fulvic acid), Hi (hydrophilic acids), HoN (hydrophobic neutrals) concentrations are normalised to total organic carbon (TOC). Degr. = cumulatively degraded TOC, expressed as mg C g_{TOC}⁻¹ at given temperature or days.

6.3.4 Density fractions, carbon stable isotopes and thermometric fractions

The share of TOC in the light density fraction, assumed to represent the more easily degradable organic matter, mostly showed a decreasing trend from upstream (location P1) to downstream (location P9) for all sediment layers (Figure 19, left), e.g. from about 80% (P1) to 55% share of bulk-TOC (P9) for CS

layers. In order to investigate whether the observed spatial patterns in density fractions could be caused by progressive SOM decay (ageing), the share of TOC in the light density fraction was also investigated in samples that had been incubated anaerobically in the laboratory for 250 days and compared to the density fraction distribution found for the respective fresh sample. After 250 days, on average > 90% of degradable SOM had decayed, estimated by asymptotic curve fitting. After SOM decay in sediments from both upstream (P2) and downstream (P8) locations, a strong decrease in light density fraction TOC was found (Figure 19, right). These results confirm that preferential decay of unbound SOM contributes to the observed downstream decreasing share of SOM in the light density fraction.

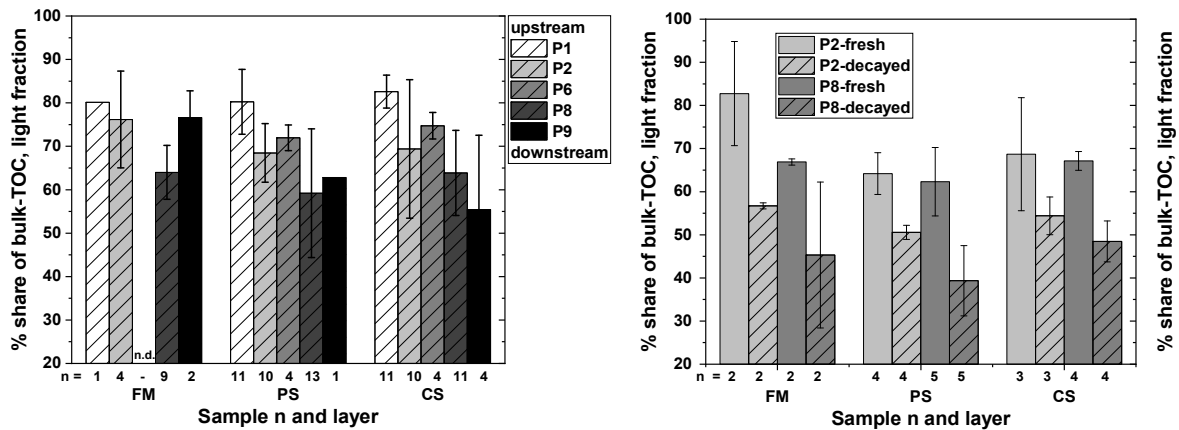


Figure 19: Left: share of total organic carbon (TOC) in the light density fraction ($< 1.4 \text{ g cm}^{-3}$) at different locations for FM, PS and CS layers. Right: share of total organic carbon (TOC) in the light density fraction ($< 1.4 \text{ g cm}^{-3}$) at locations P2 and P8 for FM, PS and CS layers for fresh samples (pure bars) and decayed samples (250 days of anaerobic incubation, lined bars). For both figures: errors show standard deviation, sample n written below, samples taken in 2018 and 2019, n.d. = not determined.

In all samples, the decrease in light fraction TOC with SOM decay was accompanied by an enrichment in heavy carbon (^{13}C), indicating preferential degradation of ^{12}C -containing and relative enrichment of ^{13}C -bearing components (Figure 20, left). On average, $\delta^{13}\text{C}$ values had increased in degraded samples by 0.7 ‰ VPDB for upstream location P2 and by 0.6 ‰ VPDB for downstream location P8, compared to the respective fresh samples. Location P1, characterised by the highest SOM degradability (see grey bars Figure 20, left), also showed the lowest $\delta^{13}\text{C}$ values of both the fresh and the decayed sample. Less pronounced differences were observed between location P2 and location P8. In field samples, sediment from location P2 to location P9 was enriched in ^{13}C compared to samples from P1, yielding a difference of about around 1 ‰ VPDB (Figure 20, right). As the sample number per location comprises samples taken at several points in time, the pattern appears stable over time.

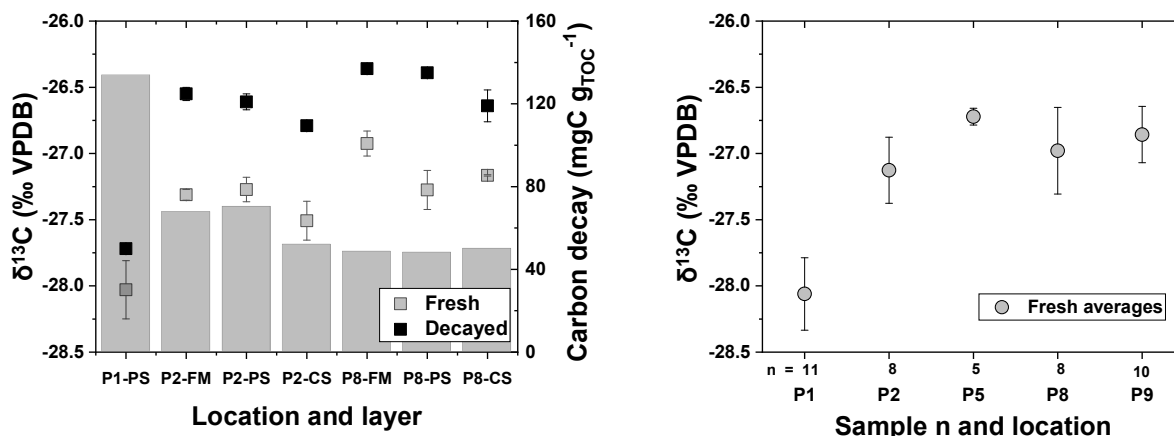


Figure 20: Left: Averages of stable carbon isotope signatures before (fresh) and after (decayed) 250 days of anaerobic SOM decay for three sediment layers (FM, PS, CS) at location P1, P2 and P8. Samples taken in November 2018, errors show standard deviation, $n = 2$, grey transparent bars show total carbon decay. Right: fresh sample average stable carbon isotope signatures for FM, PS and CS layers at locations P1, P2, P5, P8 and P9, samples from 2018. Values are expressed relative to Vienna Pee Dee Belemnite (VPDB).

The suitability of the Rock-Eval 6© method was investigated as a further proxy to describe sediment organic matter stability/lability. The Hydrogen Index, representing more labile organic matter, was higher at location P1 and decreased within the harbour transect (Figure 21, top left), consistent with the trend of an increasing SOM stability reflected by the previously presented parameters (Table 6). A depth gradient was not observed. The I-index (immature organic fraction) and R-index (refractory fraction or persistent SOM, both, Sebag et al., 2006) showed an inverse linear relationship with all measured samples on a single line ($R^2 = 0.998$), and with upstream location P1 (triangles) showing larger I-indices and lower R-indices (Figure 21, top right). The Hydrogen Index (HI, immature organic fraction) correlated better with cumulative aerobic carbon decay after 21 days (Figure 21, bottom right) than with the cumulative anaerobic decay after 21 days (bottom left). For one sample (location P1), the Rock-Eval analysis was repeated after long-term laboratory incubation. It is seen that the organic matter decay led to a shift of the I-index and the R-index towards the less easily degradable SOM from locations P2 to P9 (Figure 21, top right).

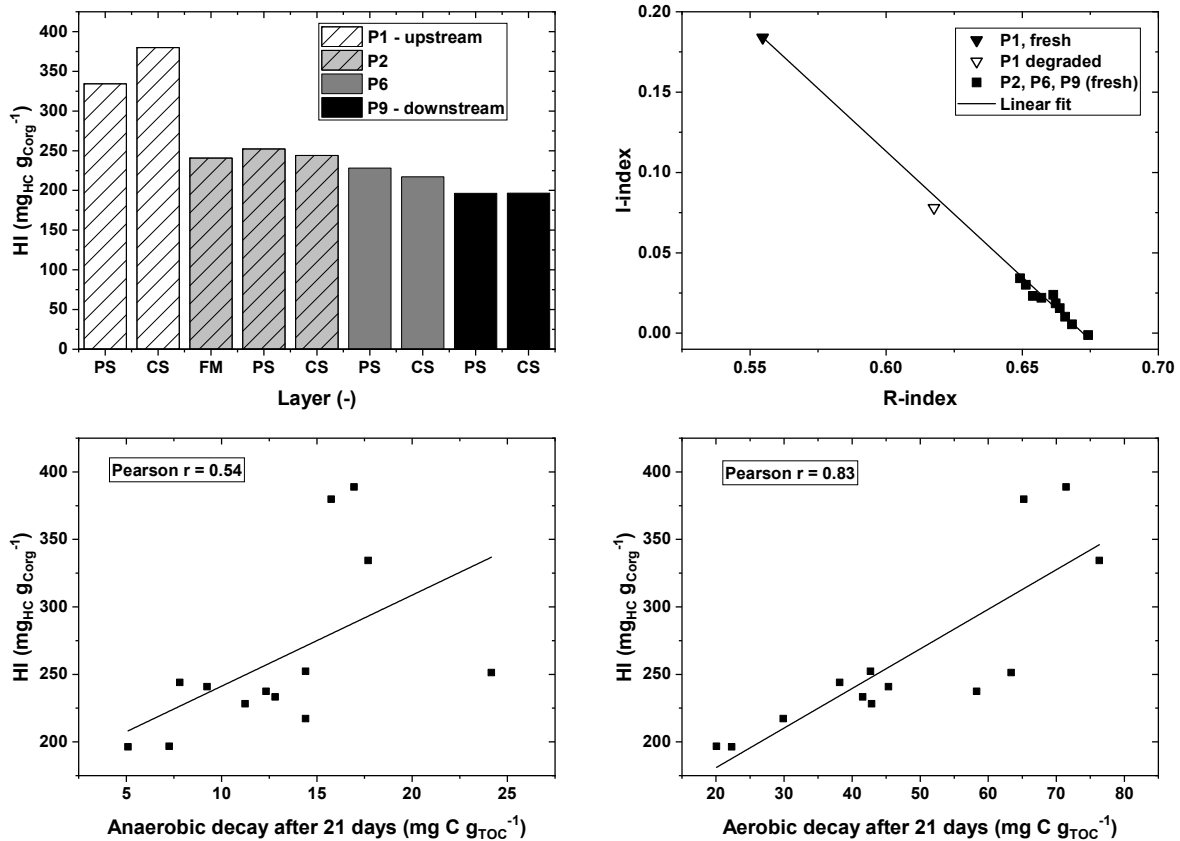


Figure 21 Rock-Eval 6 parameters measured in fresh and degraded sediment samples. Hydrogen Index (HI, up left, samples from November 2018). I-index versus R-index (up right), HI index versus anaerobic (down left) and aerobic decay after 21 days (down right), samples from 2018, see Table 6. Filled triangle: fresh sediment P1 location, open triangle: degraded sediment P1 location, sample from November 2018. Filled squares: P2, P6 and P9 location (fresh). I-index and R-index analysed according to Sebag et al. (2016).

6.4 Discussion

Consistent differences in water-extractable SOM fractions, carbon stable isotope signatures and stability indices obtained from Rock Eval pyrolysis have been identified in sediment samples from upstream to downstream locations. The gradual changes in these SOM properties are likely to originate from a gradient of upstream input of easily degradable, phytoplanktonic organic matter and to underlie the previously observed differences in short-term SOM decay rates (Figure 16).

6.4.1 Stratification of biological and chemical indicators along the transect

Zander et al. (2020) showed SOM degradability to decrease from upstream to downstream locations in the Port of Hamburg. This aligned with a decrease of chlorophyll a, indicating an upstream driven input of fresh algal biomass (Deng et al., 2019 and Schoel et al., 2014; Figure 15), as well as a decrease in silicic acid, indicative of a gradient in presence of siliceous biota, and a decrease in microbial biomass and extrapolymeric substances (Figure 15). Upstream locations are therefore characterised by higher input of easily degradable organic matter, reflected by a higher share of water-extractable hydrophilic acids that represent more easily degradable DOM (Straathof et al., 2014; Figure 17) and a lower ratio of acid/base to water-extractable SOM compared to downstream locations (Figure 17 and Figure 18). The latter reflects a downstream stronger SOM binding to the sediment and thus a lower bioavailability of organic matter, which is in turn consistent with the downstream decreasing share of light density (i.e., non-mineral-bound) organic matter (Figure 19). The pronounced decline in SOM degradability

from upstream to downstream locations in the Port of Hamburg further corresponded to a decline in short-term oxygen consumption (AT_{3h} , Figure 15) from upstream to downstream locations.

Along the Elbe river, the specific concentration of Zn in the particle size fraction of $< 20 \mu\text{m}$ followed a typical stratification with average values up to $850 \text{ mg Zn kg}_{\text{DW}}^{-1}$ found in sediments upstream of Hamburg and average values of $400 \text{ mg Zn kg}_{\text{DW}}^{-1}$ typical for sediments transported into the harbour from the North Sea by tidal pumping (Figure 14, right). Reese et al. (2019) clustered the Elbe River sediments from upstream (river km 580) to downstream (river km 740) in four clusters by using a multi-element fingerprinting and isotopic tracer approach. According to Reese et al. (2019), sediment from about river km 580 to 615 carries the fluvial signal of the Elbe River, whereas sediment from about river km 615 to 700 was described as a mixture of marine and fluvial sediment. The specific Zn concentrations found in the samples analysed in this project confirm those findings. It is hence assumed that sediments, including sediment organic matter, at location P1 are dominated by the fluvial signature, while sediments from location P2 onwards (river km 619, Figure 20, right) reached the upstream harbour area from downstream by tidal pumping (Schwartz et al., 2015) and to a lesser extent by transport from upstream to downstream. Therefore, the properties of sediment organic matter at locations downstream of P1 not only result from the decay of upstream SOM ('age gradient') but also reflect downstream SOM transported into the investigation area and thus a source gradient. As these sediments receive less input from (upstream) fresh, easily degradable biogenic organic matter (richer in ^{12}C), their organic matter is older, more degraded and bound in organo-mineral complexes, as evidenced by an enrichment in $\delta^{13}\text{C}$ (Figure 20), a lower share of TOC in the low-density fraction (Figure 19), and a higher ratio of acid-base over water-extractable SOM (Figure 17 and Figure 18).

The idea of similar SOM origin for locations downstream of P2, expected from the spatial distribution of the fine fraction Zn content (Figure 14) was supported by the fact that the I-index and the R-index for samples from P2 to P9 clustered around very similar values (high R indices, low I indices, Figure 21, top right) while the most upstream sample (P1) was characterised by a low R index (persistent, i.e. old SOM) and high I index (immature, i.e. fresh SOM). As a result of SOM degraded in this sample, the relationship between immature and persistent SOM shifted towards the signature of the more downstream samples, corroborating the stability/maturity gradient also indicated by the other parameters (stable isotopes, density fractions, degradation rates), see also discussion in section 4.3.

6.4.2 Organic matter lability: chemical organic matter (SOM) fractions

According to Bongiorno et al. (2019), hydrophilic SOM (Hi) mainly comprises the soluble fractions of total organic carbon (TOC), primarily composed of root and microbial exudates and products of hydrolysis and leachates of SOM. In the investigated sediments, the hydrophilic SOM fraction (Hi) correlated strongly positively with the share of easily degradable organic matter, represented by mass of sediment in the light density fraction (Pearson's $r = 0.92$) and negatively with mineral-bound organic matter (heavy density fraction, not shown). According to Straathof et al. (2014), hydrophilic compounds can provide a readily available carbon source to the microbial community. It is therefore assumed that along the investigated gradient the Hi fraction can be regarded as an indicator for labile organic matter, present in higher concentrations due to biogenic input (as discussed above) at upstream locations (water-extraction, Figure 17, left). In this study, the Hi concentration dropped with decreasing organic matter lability (increasing stabilization) along the transect, which matches the findings of Straathof et al. (2014).

The decreasing share of water-extractable SOM from upstream to downstream (Figure 17, left) is assumed to be related to (1) the progressive decay of easily available organic matter, i.e. less strongly

bound to the mineral phase and water-extractable, as the sediment travels along the transect (age gradient) and (2) to the higher input of easily degradable organic matter upstream (source gradient), evidenced by higher upstream chlorophyll concentrations, higher microbial biomass, silicic acid and EPS (Table 6). This interpretation implies that SOM originating from downstream sources a priori contains less Hi.

In comparison to labile hydrophilic SOM compounds, hydrophobic SOM compounds (particularly fulvic acids, FA, and hydrophobic neutrals, HoN) have been associated with lower carbon turnover rates (Straathof et al., 2014). This was also seen in this study as FA and HoN concentrations increased with decreasing organic matter degradability from upstream to downstream locations (Figure 17, left). These more hydrophobic components are assumed to represent the less-easily degradable SOM fraction which undergoes little change in the short or intermediate term, i.e., during the time of sediment organic matter transport from upstream to downstream. The results clearly indicate the different composition of SOM along the transect.

The increasing ratio between acid-base and water-extractable SOM concentrations from upstream to downstream (Figure 17, right) is consistent with the higher share of mineral bound SOM downstream, that is liberated by the acid-base-extraction and considered not available for microbial SOM decay. At upstream locations, the share of degradable, water-extractable SOM was higher, confirming that less SOM was bound to the mineral phase than at the more downstream locations. The ratio of Hi liberated by the acid-base-extraction to Hi in the water extractable fraction was highest for the most downstream location P9, supporting the concept that the Hi fraction is preferably degraded and therefore detected less in the water-extractable fraction at sites with less input of fresh organic matter, i.e. dominated by older organic matter (Figure 17, right). At location P9, Hi still represents a minor share of about 20% of the sediment-bound organic matter, which is dominated by the humic (HA, FA and HON) SOM fractions (Figure 17, middle). The increasing concentration of these hardly soluble, acid-base extractable total SOM fractions along the transect, coinciding with an increasing contribution of the heavy density SOM fraction (Figure 19), confirmed that downstream locations are characterized by more mineral-associated, strongly bound SOM.

In the absence of data on water-extractable or acid-base-extractable SOM from fluvial sediments, data from soils and compost are used for comparison. Bongiorno et al. (2019) reported a share of water-extractable SOM between 0.06% to 0.40% of TOC for European soils. Lundquist et al. (1999) and Haynes (2005) found between 0.05% and 0.40% of TOC for agricultural African soils, and Straathof et al. (2014) reported 0.09% and 0.61% of TOC for composts. In this study, compared with the literature above, relatively high values of water-extractable SOM were found, i.e. between 0.2% and 1.2% of TOC.

Due to the hypothesis that DOM represents a net product of SOM decay, total SOM, and the fractions HA, FA, Hi and HoN were also analysed after having incubated sediment at temperatures between 5 °C and 42 °C and after different degradation times during long-term incubation at 36 °C. With higher incubation temperature, both the SOM decay rates and the concentration of the water-extractable SOM fractions increased (Figure 18, left), showing that DOM (as represented by water-extractable SOM) was formed as a product of SOM decay (3rd hypothesis). The increase in total water-extractable SOM as well as in all individual fractions, with time (Figure 18, left) was supporting the strong spatial trends in depth (FM to CS layers) and location (upstream to downstream, water and acid-base extraction, Figure 17). Also, increasing incubation time led to an increased concentration of all fractions (Figure 18, right). Knowing that with stronger SOM decay the concentration of the water-extractable

fractions increased (Figure 18), downstream locations (P8 and P9) showed clear indications for a more advanced SOM decay with less available easily degradable (i.e., hydrophilic) SOM.

6.4.3 Physical organic matter fractions and stable carbon isotopes

At downstream locations, the light density fraction was less dominant than at the upstream locations (Figure 9), as already described in Zander et al. (2020). Downstream, a greater share of organic matter was associated with the mineral phase, reflecting in a larger share of organic carbon in the heavy density fraction, thus reducing SOM accessibility to degradation (Baldock and Skjemstad 2000; Six and Paustian 2014; Gao et al., 2019). Positive correlations were seen between the share of sediment in the light density fraction and water-extractable SOM fractions HA, FA and (less) HoN with Pearson's r of 0.89 (HA), 0.87 (FA) and 0.58 (HoN) as well as silicic acid (Pearson's $r = 0.71$) and microbial biomass (Pearson's $r = 0.66$). For water-extractable Hi, strong correlations were not observed, assuming that this might be the result of the rapid degradation of water-extractable Hi.

The enrichment of ^{13}C in the organic matter at locations downstream of P1 is consistent with a higher extent of SOM decay, as also found for soils (e.g. Wang et al., 2015), strengthening the hypothesis of predominance of already degraded organic matter at downstream locations, also evidenced by lower degradation rates (Zander et al., 2020). The relationship between ^{13}C -enriched and degraded SOM was corroborated by the higher amounts of ^{13}C found in the SOM after long-term (> 500 days) decay in the laboratory (enrichment in $\delta^{13}\text{C}$, Figure 20, left), indicating the preferential decay of ^{12}C -containing SOM constituents. SOM at location P1 (Figure 20, left) showed the highest decay rates but the lowest shift towards ^{13}C concentrations. This observation could be explained by the fact that the extent of isotopic fractionation declines with increasing reaction rates (Chanton et al., 2008; Gebert and Streese-Kleeberg, 2017).

Lowest $\delta^{13}\text{C}$ values (Figure 20, left), meaning smallest share of mineralized SOM, proved the first hypothesis of fresh planktonic, easily degradable biomass fed organic matter stocks from upstream. An (expected) enrichment of $\delta^{13}\text{C}$ with depth was not found (Figure 20, left), which may be related to the fact that the samples shown in Figure 20 (right) were taken at the end of the year (November). The main sedimentation events occur in the summer months, implying that the sampled material had already undergone partial depletion of the most degradable SOM throughout the year, possibly leading to a similar isotopic signature than found for the layer underneath. Moreover, direct comparison of depth-related phenomena assumes that the deposited material does not vary over time and that dredging interventions do not disturb the profile. For both reasons, conclusions relying on the assumptions of an intact depth profile have to be drawn with reservation.

The upstream-downstream decreasing trend of the Hydrogen Index (HI) (Figure 21), representing the easily degradable SOM (Sebag et al., 2016), was in line with the trends of SOM degradability (Zander et al., 2020), the extractable SOM fractions (Figure 17) and the stable carbon isotope signatures (Figure 20). Larger I-indices and lower R-indices, as found at location P1, are indicative of more labile biological compounds (Sebag et al., 2016). Sebag et al. (2016) analysed >1300 samples with the Rock Eval method and plotted the immature organic fraction representing I-index and the persistent SOM representing R-index. Compared to the identified relationships in that paper, the ratio of I-index and R-index found in this study was comparable to A-horizons of Leptosols/Ferralsols and B-horizons of Cambisols. Location P1 showed the most similar R-indices and I-indices to A and Bh-horizons. The ratio of I-indices to R-indices of the harbour sediments of this study are best represented by those found for organo-mineral horizons by Sebag et al. (2016), supporting the findings that larger shares of SOM (at most locations > 50% DM-bulk, Table 6) in downstream locations are indeed found in the heavy density

fraction. Positive correlations between short-term respiration after 21 days (R21) and the Rock-Eval parameters, i.e. Hydrogen Index (HI, Pearson $r = 0.83$) and I-index (Pearson $r = 0.76$), reveal that both, HI and I-index, can indeed serve as a proxy for the more easily degradable organic matter in these sediments, and, with the results in Figure 21, show the connection between these two approaches of carbon classification.

6.5 Conclusions

In the investigated transect within the tidal Elbe river, sediment-bound organic matter is imported both from downstream as well as from upstream areas whereas fresh, labile organic matter enters the system from upstream, as indicated by the gradients in chlorophyll a and silicic acid. The gradient in the specific Zn concentration in the particle size fraction $< 20 \mu\text{m}$ indicated that the upstream location P1 being nourished primarily from upstream fluvial sediments while the other locations carried a stronger downstream signature. The decreasing SOM degradability from upstream to downstream was accompanied by an increasing share of SOM bound in organo-mineral associations, evidenced by lower shares of SOM detected in the light density fraction, enrichment in ^{13}C , a higher ratio of acid-base to water-extractable SOM and lower Hi-indices.

The decrease of biological parameters, i.e. chlorophyll a, microbial biomass, silicic acid concentration, EPS concentration and oxygen consumption indicated a change in organic matter composition from upstream to downstream. SOM lability decreased from upstream to downstream, evidenced by an increased share of total SOM found in the acid-base-extractable fractions downstream. The proposed gradient of SOM lability is corroborated by the decrease of carbon in the light density fractions in sediments with older, more decayed and hence stabilized organic matter, and from upstream to downstream. The enrichment of ^{13}C in the organic matter at downstream locations also confirmed a higher extent of decay, strengthening the hypothesis of already degraded organic matter dominating at downstream locations. This study further confirmed this hypothesis by the large enrichment of ^{13}C in laboratory-decayed sediment samples. Thermometric pyrolysis (Rock Eval 6©) further confirmed the trends indicated by the stable carbon isotope signatures and patterns in extractable SOM fractions, with the Hydrogen Index relating well to SOM decay rates and the relationship between I and R-index supporting the findings that a significant share of downstream SOM is bound in organo-mineral complexes. These RE6 indices may therefore serve as powerful proxies for SOM lability/stability in river and estuarine sediments.

Potential products of SOM decay (Hi, FA, HA and total water-extractable fraction) correlated with the SOM decay rates. Larger concentrations of water-extractable SOM fractions were found with increasing temperature and/or increasing incubation time, confirming the assumption that these compounds represent products rather than sources of SOM decay.

Acknowledgements

This study was funded by Hamburg Port Authority and carried out within the project BIOMUD, a member of the MUDNET academic network www.tudelft.nl/mudnet/. Carbon contents in density fractions and stable isotopes were measured by the Institute of Soil Science (Prof Dr Annette Eschenbach, Dr Alexander Gröngröft and Dr Christian Knoblauch, respectively). Rock Eval 6 © analyses were performed by Deltares through Dr Martine Kox.

References

- van Beusekom, J., Sander, S. T., Fehling, D., Schulz, G., Minutolo, F., Neumann A., Bold S., Dähnke K. 2021. Long-term SPM dynamics in the Elbe estuary and adjacent coastal zone: Interactions with phytoplankton underestimated? Helmholtz-Zentrum Geestacht. Mudnet conference 2021
- Bongiorno G., Büneemann, E.K., Oguejiofor, C.U., Meier, J., Gort, G., Comans, R., Mäder, P., Brussaard, L., de Goede, R. 2019. Sensitivity of labile carbon fractions to tillage and organic matter management and their potential as comprehensive soil quality indicators across pedoclimatic conditions in Europe. *Eco Indic* 99, 38–50
- Catalán, N., Marcé, R., Kothawala, D.N., Tranvik, L.J. 2016. Organic carbon decomposition rates controlled by water retention time across inland waters. *Nat Geosci* 9, 501–504. doi: 10.1038/ngeo2720
- Chanton, J.P., Powelson, D.K., Abichou, T., Fields, D., Green, R. 2008. Effect of Temperature and Oxidation Rate on Carbon-isotope Fractionation during Methane Oxidation by Landfill Cover Materials *Environ Sci Technol*, 42, 7818–7823
- Deng Z., He, Q., Safar, Z., Chassagne, C. 2019. The role of algae in fine sediment flocculation: In-situ and laboratory measurements. *MarGeol* 413, 71–84
- Dittmar, T. 2015. Reasons Behind the Long-Term Stability of Dissolved Organic Matter. *Biogeochemistry of Marine Dissolved Organic Matter*, doi: <http://dx.doi.org/10.1016/B978-0-12-405940-5.00007-8>
- FGG Elbe data portal. 2020. <https://www.elbe-datenportal.de/>. Accessed: 18. April 2020.
- Gebert J., Köthe, H., Gröngroft, A. 2006. Prognosis of Methane Formation by River Sediments. *J Soil Sediments* 6 (2), 75 – 83
- Gebert, J., Streese-Kleeberg, J. 2017. Coupling Stable Isotope Analysis with Gas Push-Pull Tests to Derive In Situ Values for the Fractionation Factor associated with the Microbial Oxidation of Methane in Soils. *Soil Sci Soc Am J* 81, 1107–1114, doi:10.2136/sssaj2016.11.0387
- Grasset, S., Moras, S., Isidorova, A., Couture, R.-M., Linkhorst, A., Sobek, S. 2021. An empirical model to predict methane production in inland water sediment from particular organic matter supply and reactivity. *Limnol Oceanogr* 9999 1–13, doi: 10.1002/lno.11905
- Hamburg Serviceportal. 2020. HamburgService – Wassergüte-Auskunft <https://gateway.hamburg.de/hamburggateway/fvp/fv/BSU/wasserguete/wfWassergueteAnfrageListe.aspx?Sid=37#>. Accessed: 11. March 2020
- Hansell, D.A., Carlson, C.A., Repeta, D.J., Schlitzer, R., 2009. Dissolved organic matter in the ocean: a controversy stimulates new insights. *Oceanography* 22, 202–211
- Haynes, R.J., 2005. Labile organic matter fractions as central components of the quality of agricultural soils: an overview. *Adv Agron* 85, 221-268.
- Helfrich, M., Flessa, H., Mikutta, R., Dreves, A., Ludwig, B. 2007. Comparison of chemical fractionation methods for isolating stable soil organic carbon pools. *Eur J Soil Sci* 58, 1316–1329
- Hoffland, E., Kuyper, T.W., Comans, R.N.J., Creamer, R.E. 2020. Eco-functionality of organic matter in soils. *Plant and Soil* 455, 1–22, doi: <https://doi.org/10.1007/s11104-020-04651-9>
- Jommi, C., Murano, S., Trivellato, E., Zwanenburg, C. 2019. Experimental results on the influence of gas on the mechanical response of peats. *Géotechnique* 69, 9, 753–766, doi: <https://doi.org/10.1680/jgeot.17.P.148>
- Kappenberg, J., Fanger, H.-U. 2007 Sedimenttransportgeschehen in der tidebeeinflussten Elbe, der Deutschen Bucht und in der Nordsee. GKSS report 2007/20; ISSN 0344–9629
- Kögel-Knabner, I., Rumpel, C. 2018 Advances in Molecular Approaches for Understanding Soil Organic Matter Composition, Origin, and Turnover: A Historical Overview. *Advances in Agronomy* 149, 1-48, doi: <https://doi.org/10.1016/bs.agron.2018.01.003>
- Lafargue, E., Marquis, F., Pillot, D., 1998. Rock-Eval 6 applications in hydrocarbon exploration, production, and soil contamination studies. *Oil & Gas Sci Techn* 53 (4), 421–437
- Lehmann, J., Kleber, M. 2015. The contentious nature of soil organic matter. *Nature* 528, doi:10.1038/nature16069
- Von Lütow, M., Kögel-Knabner, I., Ekschmitt, K., Flessa, H., Guggenberger, G., Matzner, E., Marschner, B. 2007. SOM fractionation methods: Relevance to functional pools and to stabilization mechanisms. *Soil Biol Biochem* 39, 2183–2207
- Lundquist, E.J., Jackson, L.E., Scow, K.M., 1999. Wet-dry cycles affect dissolved organic carbon in two California agricultural soils. *Soil Biol Biochem* 31, 1031-1038.
- Meijboom, F.W., Hassink, J., van Noordwijk, M. 1995. Density fractionation of soil macroorganic matter using silica suspensions. *Soil Biol Biochem* 27, 1109–1111
- Oliveira, B.R.F., Smit, M.P.J., van Paassen, L.A., Grotenhuis, J.T.C., Rijnaarts, H.H.M. 2017. Functional properties of soils formed from biochemical ripening of dredged sediments—subsidence mitigation in delta areas. *J Soil Sediments* 17, 286–298. <https://doi.org/10.1007/s11368-016-1570-7>
- Reese, A., Zimmermann, T., Pröfrock D., Irrgeher J. 2019. Extreme spatial variation of Sr, Nd and Pb isotopic signatures and 48 element mass fractions in surface sediment of the Elbe River Estuary - Suitable tracers for processes in dynamic environments? *Sci Total Environ* 668, 512–523
- Schoel, A., Hein, B., Wyrwa, J., Kirchesch, V. 2014. Modelling water quality in the Elbe and its estuary—Large Scale and Long Term Applications with Focus on the Oxygen Budget of the Estuary. *Die Kueste* 81: 203–232
- Schwartz, R., Eichweber, G., Entelmann, I., Keller, I., Rickert-Niebuhr, K., Röper, H., Wenzel, C. 2015. Aspects of pollutant sediment management in the tidal Elbe. *HW* 59, H.6, doi: 10.5675/HyWa_2015,6_9
- Sebag, D., Disnar, J.-R., Guillet, B., Di Giovanni, C., Verrecchia, E.P., Durand, A., 2006. Monitoring organic matter dynamics in soil profiles by 'Rock-Eval pyrolysis': bulk characterization and quantification of degradation. *Eur J Soil Sci* 57 (3), 344–355
- Sebag, D., Verrecchia, E.P., Cécillon, L., Adatte, T., Albrecht, R., Aubert, M., Bureau, F., Cailleau, G., Copard, Y., Decaens, T., Disnar, J.-R., Hetényi, M., Nyilas, T., Trombino, L. 2016. Dynamics of soil organic matter based on new Rock-Eval indices. *Geoderma* 284, 185–203
- Shakeel, A., Kirichek, A., Talmon, A., Chassagne, C. 2021. Rheological analysis and rheological modelling of mud sediments: What is the best protocol for maintenance of ports and waterways?. *Estuar Coast Shelf S* 257, 107407
- Shakeel, A., Kirichek, A., Chassagne, C. 2019. Is density enough to predict the rheology of natural sediments? *Geo-Mar Lett* 39, 427–434, doi: <https://doi.org/10.1007/s00367-019-00601-2>
- Shen, Q, Suarez-Abelenda, M., Camps-Arbestain, M., Pereira, R.C., McNally, S.R., Kelliher, F.M. 2018. An investigation of organic matter quality and quantity in acid soils as influenced by soil type and land use. *Geoderma* 328, 44–55

- Sills, G.C., Gonzalez, R. Consolidation of naturally gassy soft soil. 2001. *Geotechnique* 51, 7, 629-639
- Straathof, A.L., Chincarini, R., Comans, R.N.J., Hoffland, E. 2014. Dynamics of soil dissolved organic carbon pools reveal both hydrophobic and hydrophilic compounds sustain microbial respiration. *Soil Biol Biochem* 79, 109-116
- Van den Pol-van Dasselaar A, Oenema, O. 1999. Methane production and carbon mineralisation of size and density fractions of peat soils. *Soil Biol Biochem* 31, 877-886
- Vannote, R.L., Minshall, W.G., Cummins, K.W., Sedell, J.R., Cushing, C.E. 1980. The river continuum concept. *Can J Fish Aquat Sci* 37: 130-137
- Van Zomeren, A., Comans, R.N.J. 2007. Measurement of Humic and Fulvic Acid Concentrations and Dissolution Properties by a Rapid Batch Procedure. *Environ Sci Technol* 41, 6755-6761
- Wakeham, S.G., Canuel, E.A. 2016. The nature of organic carbon in density-fractionated sediments in the Sacramento-San Joaquin River Delta (California). *Biogeosciences* 13, 567-582
- Wang, G., Jia, Y., Li, W. 2015. Effects of environmental and biotic factors on carbon isotopic fractionation during decomposition of soil organic matter. *Sci Rep* 5, 11043
- Ward, N.D., Bianchi, T.S., Medeiros, P.M., Seidel, M., Richey, J.E., Keil, R.G., and Sawakuchi, H.O. 2017. Where Carbon Goes When Water Flows: Carbon Cycling across the Aquatic Continuum. *Frontiers in Marine Science* 4, 7, doi: 10.3389/fmars.2017.00007
- Wurpts, R., Torn, P. 2005. 15 Years Experience with Fluid Mud: Definition of the Nautical Bottom with Rheological Parameters. *Terra et Aqua*, 99
- Zander, F., Heimovaara, T., Gebert, J. 2020. Spatial variability of organic matter degradability in tidal Elbe sediments. *J Soil Sediments*. Special issue, doi: <https://doi.org/10.1007/s11368-020-02569-4>

Supplementary material

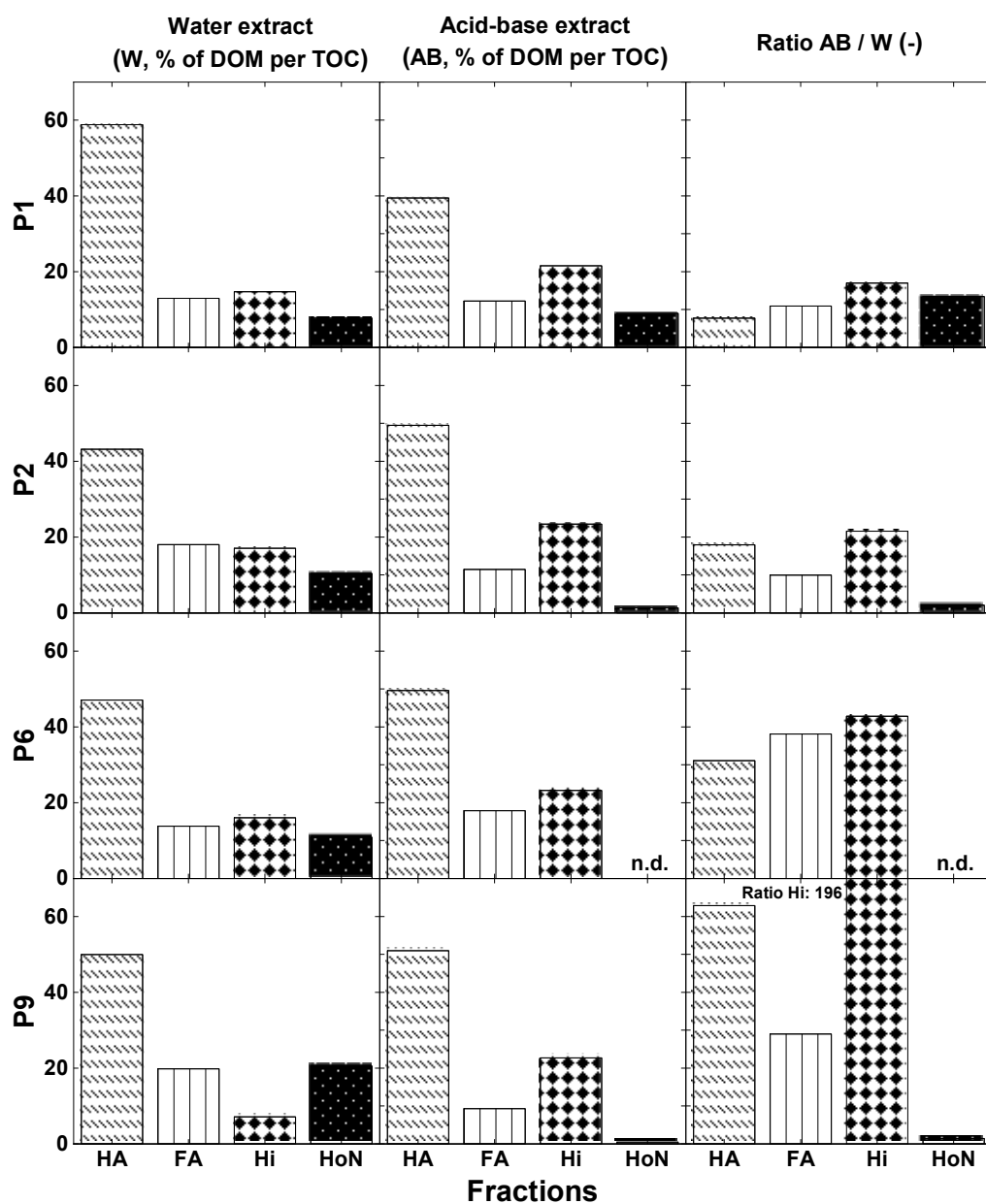


Figure S1 Shares of water-extractable SOM per total organic carbon (TOC) (left), share of acid-base-extractable SOM (middle) and ratio between acid-base and water-extractable SOM for PS layers at location P1 (upstream), P2, P6 and P9 (downstream). HA humic acid, FA fulvic acid, Hi hydrophilics, HoN hydrophobic neutrals. n.d. = not determined.

7 Organic matter pools in sediments of the tidal Elbe river

F. Zander¹, A. Groengroeft², A. Eschenbach², T.J. Heimovaara¹, J. Gebert¹

¹Delft University of Technology, Dept. Geoscience and Engineering, Stevinweg 1, 2628 CN Delft, The Netherlands

²University of Hamburg, Dept. Department of Earth Sciences, Allende-Platz 2, 20146 Hamburg, Germany

Email

Florian Zander: f.zander@tudelft.nl

Alexander Gröngroeft: Alexander.Groengroeft@uni-hamburg.de

Annette Eschenbach: Annette.Eschenbach@uni-hamburg.de

Timo J. Heimovaara: T.J.Heimovaara@tudelft.nl

Julia Gebert: Email: j.gebert@tudelft.nl

Corresponding author:

Florian Zander

Faculty of Civil Engineering and Geosciences, Department of Geoscience & Engineering,
Delft University of Technology,

Stevinweg 1, 2628 CN Delft, The Netherlands

Email: f.zander@tudelft.nl

Abstract

Anaerobic sediment organic matter decay generates methane, delays sediment consolidation, reduces sediment density, viscosity and shear strength, all impacting the sediment rheological parameters and the navigable depth. This study quantifies the share of anaerobically and aerobically degradable sediment organic matter (SOM) in a depth profile and along a transect through the tidal river Elbe in the section of the Port of Hamburg. From exponential organic matter decay functions, organic matter decay rates ($\text{mg C g}_{\text{TOC}}^{-1} \text{d}^{-1}$) were derived and clustered with a K-Means Cluster Analysis. The reactivity of different (kinetic) organic matter pools along the river transect were characterized based on their biodegradation rates. A fast, medium, slowly and non-degradable pool (pools 1 to 4) were identified based on the measured organic matter lability. SOM lability decreased from upstream to downstream, evidenced by the decreasing amount of the easily degradable pool 1 material from upstream to downstream. The size of the slowly degradable pool 3, assumed to be associated with SOM bound to the mineral particles, did not show any spatial gradient and was therefore thought to represent a baseline share of hardly accessible SOM in the investigation area (about 12%-16% of TOC). Total degradability thus appears to be governed by the amount of SOM present in addition to this basis (pool 3), which in turn follows a source gradient and an age gradient from upstream to downstream. The recalcitrant pool 4 was the largest at any part of the harbour, for any depth, and for both, anaerobic and aerobic conditions (about 75%-85% of TOC). This indicates that the sediment in the investigation area, including the uppermost, i.e. fluidic and freshly settled layers, mostly comprises stabilised organic matter and contributes largely to storage of organic carbon. Differently sized anaerobic SOM pools with depth were observed as well as seasonal changes of the easily degradable SOM pool 1. The degradability was larger in upper sediment layers, it was also larger under aerobic conditions (by about 10% of TOC) but the differences between aerobic and anaerobic decay decreased from upstream to downstream.

Keywords: Organic matter decay rates, organic matter lability, recalcitrance, spatial variability, river sediments

7.1 Introduction

Organic matter interacts with the sediment mineral phase through Van der Waal's or Coulombic forces. By bridging mineral particles and thereby promoting floc formation (Deng et al., 2019), organic matter can enhance settlement of suspended particulate matter (SPM). Shakeel et al. (2019) showed that organic matter increased the yield points (shear stresses) of freshwater Elbe sediments at a given density while Wurpts and Torn (2005) contend that microbially formed extrapolymeric substances (EPS) decrease yield point and viscosity of saline fluid mud layers in Emden seaport. EPS have been shown to profoundly influence bedform dynamics, increasing the time for development of bedforms for small quantities of EPS (Malarkey et al., 2015; Parsons et al., 2016). Sills and Gonzalez (2001) and Jommi et al. (2019) have demonstrated strong reduction in shear stresses by gas originating from organic matter decay. The (anaerobic) decay of organic matter leads to the generation of methane gas, delays sediment consolidation, reduces sediment density, viscosity and shear strength (Shakeel et al., 2022; Zander et al., 2022), impacting flow properties and therefore the navigable depth. Given the effects organic matter can exert on the physical behaviour of fine-grained sediment (mud), it is of interest to assess its lability, or, inversely, its stability or recalcitrance towards microbial degradation.

Microbial degradation of sediment organic matter (SOM) is part of the natural aquatic carbon cycle. SOM degradation depends on the amount of organic matter, its lability, the environmental conditions driving microbial activity and the availability of terminal electron acceptors (for a review see Arndt et al., 2013). Phyto- and zooplankton biomass is an important source of labile organic matter in aquatic systems (van Duyl et al., 1999; Tillmann et al., 2000; Wolfstein et al., 2000), providing autochthonous, easily degradable organic matter (Grasset et al., 2018) to the system. Boyd et al. (2013) showed this fraction to be readily degraded under both, anoxic and oxic, conditions. Similarly, McKew et al. (2013) found that in estuarine sediments, the anaerobic community could rapidly utilise labile biofilm DOC and EPS at the same rates as the aerobic community. For the investigated transect through the Port of Hamburg, the source area for labile organic matter is the non-tidal shallow, eutrophic upstream river section with enhanced net primary production, whereas the significantly deeper waters of the Hamburg Port area are characterized by light-deficiency induced decay of algal biomass and zooplankton grazing (Schoel et al., 2014). For a section of about 200 km upstream of the Port of Hamburg, Kamjunke et al. (2021) coupled phytoplankton biomass to solar irradiation and low river discharge, inducing less mixing within the water column, and showed that it was hampered by nutrient dynamics only when biomass concentrations were high. In downstream sections of the Elbe River, the share of particulate organic material decreased, indicating decomposition in the upper estuary and dilution with inorganic SPM from the lower estuary (Brockmann, 1994). Easily degradable organic matter of marine phytoplankton origin hardly reaches the investigated section as it is already degraded during its upstream-directed passage through the zone of maximum turbidity (Wolfstein and Kies, 1999).

In addition to autochthonous, labile organic matter the investigation area also receives allochthonous organic matter bound to mineral particles originating from the North Sea with (Kappenberg and Fanger, 2007; Zander et al., 2020), due to its location in the tidal section of the Elbe river. This share is stabilized in organo-mineral complexes in which organic matter is less accessible to microbial decay (Baldock and Skjemstad 2000; Six and Paustian 2014; Gao et al., 2019). Although significantly lower carbon release rates can therefore be expected from the microbial decay of this organic matter fraction, its high mass as part of the mineral sediment inventory makes it an important pool in the

overall sediment carbon budget. For many estuaries, fundamental data gaps hamper the understanding of the connectivity of terrestrial, aquatic and marine carbon budgets (Ward et al., 2015). Larger shares of organic matter can be degraded under aerobic conditions than under anaerobic conditions due to larger energy gain under aerobic redox state. When organic matter is degraded under aerobic conditions in the water column or close to the sediment-water interface and the aerobic microbial activity exceeds the rate of oxygen supply, oxygen depleted zones can form in the water column (Rabalais et al., 2010). Die-off of upstream riverine phytoplankton in downstream areas led to oxygen depleted zones in the Elbe river (Geerts et al., 2017). Grasset et al. (2021) found that the methane production, resulting from anaerobic sediment organic matter decay, increased linearly with the quantity of phytoplankton-derived and terrestrially-derived organic matter. The methane production correlated strongly and positively with the amount of organic matter supply and negatively with the C/N ratio. Technical problems arising from methane-enriched sediment include impeded nautical depth finding due to reflection of sonic waves and risks of explosion in the suction head and on board of trailing suction hopper dredgers. From various perspectives it is therefore of interest to understand the drivers and mechanisms of organic matter decay in river sediments as well as the size of degradable organic matter pools.

Earlier investigations, using sediment data from the Port of Hamburg from 2018, revealed spatial gradients of SOM decay in the tidal Elbe river around the Port of Hamburg, with a gradient of decreasing SOM decay from upstream to downstream and with depth/age (Zander et al., 2020). SOM decay kinetics in all layers mostly showed an asymptotic behaviour with rates decreasing exponentially over time. For many samples, the data were best described by applying multiphase (mostly two phase) exponential fits. It was suggested that over time of incubation, separate organic matter pools with different decay rate constants and hence different lability become dominant. This study quantifies the share of anaerobically and aerobically degradable organic matter along a transect through the Port of Hamburg, part of the tidal Elbe river (Figure 2), and thereby provides a novel basis for future carbon budgeting studies within the investigation area. This study identifies the reactivity and size of different (kinetic) organic matter pools along the river transect based on their biodegradation rates using a three year observation period. SOM decay is defined as the amount of sediment organic carbon released by microbial decay. This decay can happen under different environmental boundary conditions such as temperature and redox state. The latter was investigated by measuring the carbon release by microbial SOM decay under anaerobic and aerobic conditions in the laboratory. It was hypothesized that

4. A recalcitrant, non-degradable, carbon pool can be found in the harbour sediments. This pool is larger under anaerobic conditions and smaller under aerobic conditions.
5. As organic matter production is higher at upstream areas, more easily degradable organic matter (labile pool) is found upstream.
6. Downstream, a greater share of carbon is found in both, the slowly degradable and the recalcitrant organic matter pool.
7. Upper sediment layers contain more easily degradable carbon. Hence a larger share of the total carbon can be found in this labile pool.

7.2 Investigation area and sampling approach

Eleven locations within the tidal Elbe River around the Port of Hamburg (Figure 1) were sampled on average every two months in the period 2018-2020., with locations P1 to P9 presenting sedimentation hotspots requiring enhanced maintenance activity by the port. At each location, between three and

five sediment cores per sampling event were retrieved using a core sampler ('Frahmplot'; Shakeel et al., 2020). For each core, up to four (if present) different layers were distinguished from top to bottom: suspended particulate matter (SPM), fluid mud (FM), pre-consolidated sediment (PS), and consolidated sediment (CS). These layers were separated and a mixed sample per layer prepared from the respective material of the multiple cores. In this study, data on organic matter decay rates and organic matter pool sizes is presented for all samples from 2018 and 2019, amounting to a total of $n = 294$. Samples were transported to the laboratory under cool conditions in air-tight containers and processed swiftly upon arrival in the laboratory.

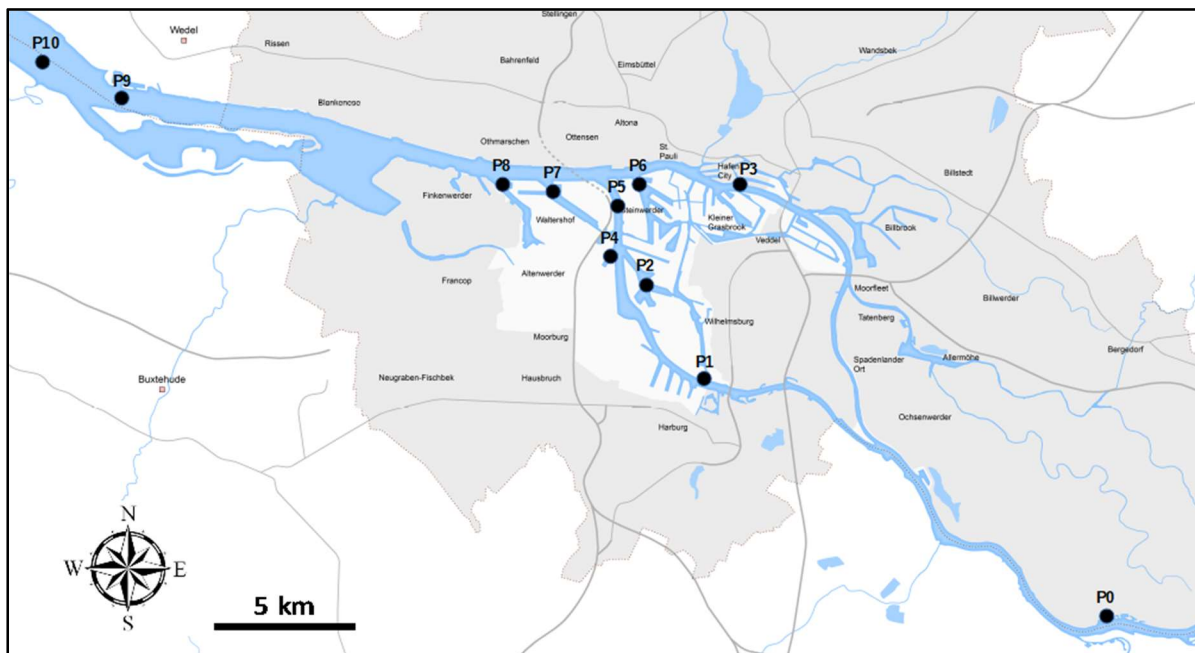


Figure 22: Investigation area around the Port of Hamburg (adapted from Hamburg Port Authority) with sampling locations between river km 598 (P0, upstream) and 646 (P10, downstream). Further information on sampling sites and sampling strategy in Zander et al. (2020).

7.3 Methods

Standard sediment properties (see Table 7) were analysed according to the methods listed in Zander et al. (2020).

7.3.1 Anaerobic and aerobic decay of sediment organic matter

SOM decay was assessed by measuring carbon release into the gas phase over time upon incubation of the samples in the laboratory in closed glass bottles sealed with butyl rubbers toppers under anaerobic and aerobic conditions for more than 250 days.

To analyse SOM decay under *anaerobic conditions*, the bottle headspace was purged with N_2 and subsequently incubated at 36 °C in the dark. The elevated experimental temperature was chosen to warrant exhaustive decay of organic matter within the time frame of the experiment (see Figure 2) in order to assess degradability of sediment organic matter as accurately as possible. The pressure in the bottles, increasing due to the produced gases (methane and carbon dioxide, CH_4 and CO_2), was measured manually with a pressure gauge (LEX1, Keller) which was connected to the bottle headspace using a needle pierced through the stopper. The frequency of measurements was adapted to the gas production rate and decreased from daily intervals at the beginning of the incubation to monthly intervals at the end. The carbon gas production was calculated from the increase in headspace

pressure in combination with gas chromatographic analyses of headspace composition. The values are reported as the sum of CH₄-C and CO₂-C measured in the gas phase and the share of CO₂-C dissolved in the aqueous phase. The latter was calculated using the CO₂ concentration, the volume of water, the pressure in the bottle headspace and the temperature-corrected solubility of CO₂ in water as given by Henry's constant (given in Sander, 2015). For some samples, measurements were carried out for at least 500 days until cumulative carbon release approximated a plateau, in other words, they decreased to very low rates.

Aerobic SOM decay was quantified on separate aliquots at an incubation temperature of 20 °C. The bottle headspace was flushed with atmospheric air in the beginning of the measurements and as soon as a concentration of 2.5% CO₂ in the bottle headspace was reached. Carbon release was calculated from the increase in the concentration of headspace CO₂, measured by gas chromatography, considering dissolution of CO₂ as described above. The sample n was n = 268 for anaerobic samples and n = 243 for aerobic samples.

In order to compare anaerobic and aerobic decay rates, all anaerobic SOM decay rates were normalised to a temperature of 20 °C based on data from a separate temperature experiment (Li, 2018). The temperature coefficient function was used $Q_{16} = (R_2/R_1)$ with R₁ and R₂ as the released carbon at the given temperature (i.e., R₁ at 20 °C and R₂ at 36°C). This coefficient was applied to the time steps of interest, namely, 10, 21, 50, 150 and 250 days.

7.3.2 Identification and quantification of differently degradable organic matter pools

The time course of cumulative carbon release was described by single rate or dual rate exponential decay functions (Eq. 1 and 2), performed with OriginPro2019, with the choice based on the function with the higher coefficient of determination. Dual rate exponential decay functions were split into two single functions with different organic matter decay kinetics as shown in Figure 23. The total cumulative degraded organic matter (mg C g_{TOC}⁻¹) is the sum of the pool size of each function (y₀, Eq. 3). For each function, the organic matter decay rate (R, mg C g_{TOC}⁻¹ d⁻¹) was derived by multiplying the decay rate constant (k) and the pool size (M₀, Eq. 4). All decay rates were clustered with a K-Means Cluster Analysis (OriginPro2019), considering the total cumulative degraded organic matter (y₀). It was used a method of vector quantization with minimum sum of squares to assign observations to groups. Observations were partitioned into clusters (k) in which each observation belongs to the cluster with the nearest mean (cluster centre). The distance between an observation and a cluster was calculated from the Euclidean distance between the observation and the cluster centre. The cut-off values separating each cluster of decay rates were used to define fast, medium and slowly degrading SOM pools (mg C g_{TOC}⁻¹), results seen in Figure 24. The half-lives were calculated from the time constant multiplied with the natural logarithm of two. The fourth, recalcitrant pool (not biologically available) was calculated from the difference between the total TOC concentration and the sum of pools 1 to 3. The recalcitrant pool was always classified as pool 4 (last pool) even when less than three pools were determined. An example for a dual rate cumulative function of fast and slow organic matter decay is shown in Figure 23 for upstream and downstream location (P1 and P9, left and right).

$$M = -M_0 * \exp(-k*t) + y_0 \quad \text{Eq. 1}$$

$$M = -M_{0a}*\exp(-k_a*t) - M_{0b} * \exp(-k_b*t) + y_0 \quad \text{Eq. 2}$$

$$Y_0 = M_{0a} + M_{0b} \quad \text{Eq. 3}$$

$$R = -M_0 * k \quad \text{Eq. 4}$$

with

M_0 = total pool size of each function (a or b) in $\text{mg C g}_{\text{TOC}}^{-1}$

k = decay rate constant in d^{-1}

t = time in days (d)

y_0 = total cumulative degraded organic matter in $\text{mg C g}_{\text{TOC}}^{-1}$

R = decay rate in $\text{mg C g}_{\text{TOC}}^{-1} \text{d}^{-1}$

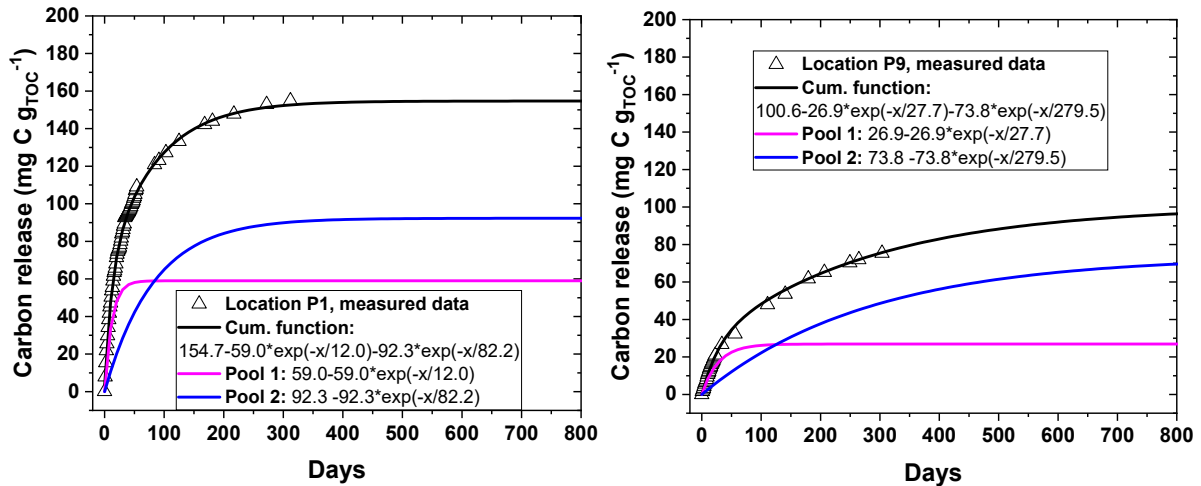


Figure 23 Example of a dual rate cumulative function of organic matter decay with fitting functions per individual pool for upstream location P1 (left) and downstream location P9 (right) and average values of three parallels of cumulative carbon release.

7.4 Results

7.4.1 Sediment properties

Table 7 shows mean abiotic properties of all sediment layers and the corresponding pore water from 2018 and 2019. Sediments properties, methods described in Zander et al. (2020), are quite similar in the main part of the harbour (location P2 to P8). Total nitrogen, total organic carbon, silt, loss on ignition, phosphorus, pH, electric conductivity, dissolved organic matter, ammonium, phosphate and sulphate showed similar ranges in the harbour area. Clear differences are seen between the boundary locations P1 (upstream) and P9 (downstream) with highest values found at P1 for total nitrogen, total organic carbon, electrical conductivity, nutrients and silt (Table 7, bold). Location P9 reflecting the site with the highest sand content and the lowest concentration of these parameters.

Table 7 Abiotic properties of all sediment layers and the corresponding pore water from 2018 and 2019, SD: standard deviation. TN total nitrogen, TOC total organic carbon, WC water content, Eh redox potential, LOI loss on ignition, P phosphorus, S sulphur, EC electric conductivity, DOC dissolved organic carbon, NH_4^+ ammonium, PO_4^{3-} phosphate, Chl a chlorophyll a, Silicic acid, SO_4^{2-} sulphate. Minimum and maximum means in bold. Overall mean in italic.

	Upstream																		Downstream	
	Overall	P1		P2		P3		P4		P5		P6		P7		P8		P9		
	Mean	Mean	SD	Mean	SD	Mean	SD	Mean	SD	Mean	SD	Mean	SD	Mean	SD	Mean	SD	Mean	SD	
TN (%)	0.5	0.8	0.2	0.5	0.1	0.5	0.1	0.5	0.1	0.4	0.1	0.4	0.0	0.4	0.1	0.4	0.0	0.3	0.1	
TOC (%)	4.0	6.4	0.8	4.2	0.5	4.2	0.6	4.0	0.5	3.1	0.9	3.7	0.3	3.5	0.5	3.8	0.3	2.7	1.0	
TOC/TN (%/%)	8.6	8.1	4.3	8.3	1.1	7.8	0.6	7.9	0.5	9.2	1.7	8.3	0.2	8.4	0.5	8.7	0.8	9.8	1.3	
WC (% _{DM})	387	508	276	425	369	380	286	332	163	341	427	300	138	267	84	446	692	294	207	
Eh (meV)	-174	-212	91	-217	116	-187	174	-190	164	-183	152	-182	166	-171	177	-188	132	-38	180	
Clay (< 2 µm, %)	38	39	9	43	8	47	5	41	6	31	8	42	3	38	5	41	8	27	14	
Silt (2 - 63 µm, %)	46	52	8	50	5	47	3	46	5	43	9	45	3	45	3	49	5	39	8	
Sand (> 63 µm, %)	16	9	7	7	5	6	3	13	4	26	15	13	5	17	5	11	7	34	19	
LOI (%)	12	17	4	12	3	14	3	12	3	10	2	12	3	11	3	12	3	8	3	
P (mg C/g _{TOC})	1522	2199	213	1636	179	1472	235	1550	145	1227	204	1428	88	1448	121	1510	113	1039	307	
S (mg C/g _{TOC})	4791	4907	896	5004	1383	4967	2104	5083	1665	4088	1325	5222	2577	4965	1793	5265	2491	3638	1399	
pH (-)	7.3	7.3	0.2	7.5	0.2	7.6	0.2	7.5	0.2	7.6	0.2	7.5	0.2	7.5	0.1	7.5	0.2	7.7	0.2	
EC (µS/cm)	1794	2147	865	1832	566	1748	445	1919	530	1627	404	1761	596	1754	372	1790	471	1481	283	
DOC (mg/l)	27	45	66	30	28	27	18	28	22	22	14	23	13	19	12	24	12	15	10	
NH ₄ ⁺ (mg/l)	27	100	99	21	27	18	20	25	21	9	11	14	12	13	15	15	39	4	5	
PO ₄ ³⁻ (mg/l)	0.11	0.08	0.07	0.09	0.06	0.10	0.06	0.11	0.09	0.13	0.08	0.12	0.07	0.11	0.04	0.10	0.08	0.16	0.07	
Chl a (mg/l)	19	38	27	16	11	40	21	16	9	19	15	14	11	13	8	10	5	10	6	
Silicic acid (mg/l)	21	26	13	21	12	22	12	24	12	17	10	22	11	22	13	20	11	14	11	
SO ₄ ²⁻ (mg/l)	81	57	52	81	57	66	60	65	53	88	54	69	60	88	49	87	54	114	43	

7.4.2 Decay rates and sizes of organic matter pools

A K-means cluster analysis (see method section) was used to differentiate the data set on decay rates for anaerobic (Figure 24, left) and aerobic SOM decay (Figure 24, right) and to quantify the size of the according organic matter pools. It was chosen to separate three clusters with corresponding decay rates B1, B2, B3 considering the overall range of the decay rates. The decay rates for anaerobically degrading SOM varied between 0.1 mg C g_{TOC}⁻¹ d⁻¹ and 29 mg C g_{TOC}⁻¹ d⁻¹ (Figure 24, left) with cut-offs between pool 1 and pool 2 at 5.2 mg C g_{TOC}⁻¹ d⁻¹, and between pool 2 and pool 3 at 2.2 mg C g_{TOC}⁻¹ d⁻¹. For aerobic decay (Figure 24, right), the range of decay rates was between 0.1 mg C g_{TOC}⁻¹ d⁻¹ and 26 mg C g_{TOC}⁻¹ d⁻¹ and the cut-off values yielded between pool 1 and pool 2 at 5.5 mg C g_{TOC}⁻¹ d⁻¹, and between pool 2 and pool 3 at 2.4 mg C g_{TOC}⁻¹ d⁻¹. Hence, both, the decay rates as well as the cut-off values to separate individual pools were very similar for anaerobic and aerobic decay. The average half-lives were between 1.7 days (B1) to 61 days (B3) for anaerobic decay (Figure 24, left) and between 1.3 days (B1) and 96 days (B3) for aerobic decay (Figure 24, right).

The following analyses aimed at quantifying the share of degradable SOM under aerobic and anaerobic conditions and differentiating this share into pools characterized by different degradation kinetics. However, it is not suggested that the identified aerobically and anaerobically degradable SOM pools represent different physical entities.

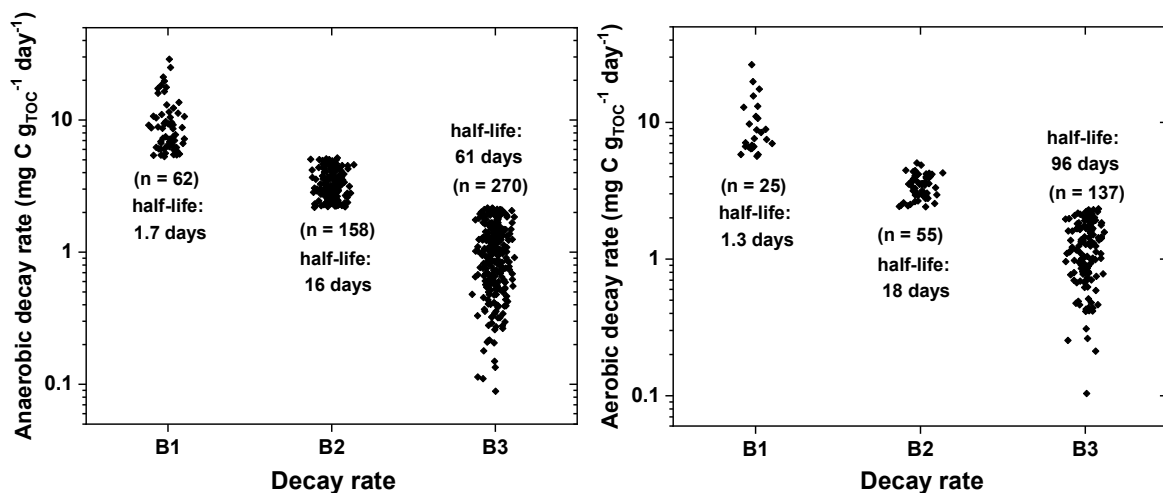


Figure 24 K-means Cluster Analysis differentiated the data set into three clusters with decay rates (B1, B2, B3) and averaged half-lives, of anaerobically (left) and aerobically (right) incubated samples (250 days), normalised to 20 °C. Samples collected from locations P1-P9 during 12 campaigns in the period 2018-2019. Sample n for anaerobic decay n = 490, sample n for aerobic decay n = 217.

Under aerobic conditions, SOM pool 1 was found mainly at upstream locations P1 and P2 (Figure 25, top left). The size of pool 2 strongly decreased from upstream to downstream locations from around 250 to 50 mg C g_{TOC}^{-1} whereas pool 3 was mostly similar along the transect, only location P1 showing slightly higher values (bottom left). For upstream locations, the total share of degradable SOM (sum of pool 1, pool 2 and pool 3) was higher than at downstream locations, as seen from the increase of the mean share of the stable pool 4 from 680 to 850 mg C g_{TOC}^{-1} from upstream (P1) to downstream locations (P9, Figure 25, bottom right).

Comparing aerobic and anaerobic decay conditions, aerobic decay showed a larger share of degradable organic matter (Figure 25 and Figure 26, sum of pool 1, pool 2 and pool 3). The aerobic decay exceeding the anaerobically degradable share by around 100 mg C g_{TOC}^{-1} at location P1. At downstream location P9, the anaerobically and aerobically degradable share was about equal.

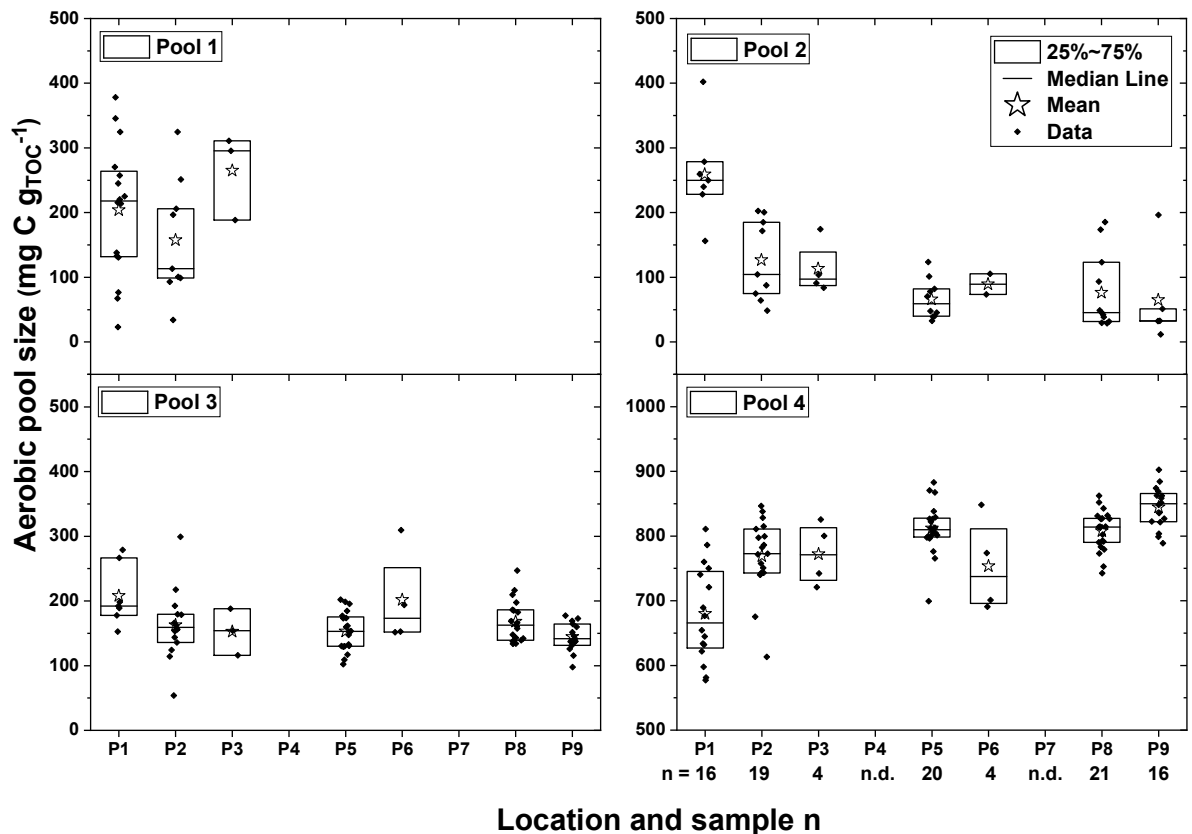


Figure 25 Size of aerobically degradable SOM pools ($\text{mg C g}_{\text{TOC}}^{-1}$) per location for four pools and all layers, samples taken in 2018 and 2019. Consider the differently scaled y-axis for the non-degradable pool 4 (bottom right). Lines = median values, stars = mean values, boxes = 25th and 75th percentile, n.d. = not determined. The sample n is valid for pool 4, because not all pools appeared for each sample.

Under anaerobic conditions, samples with the most rapidly degrading SOM pool 1, corresponding to decay rate B1, were found mainly at upstream locations P1 and P2 (Figure 26, top left). The largest size of pool 2 was at P5 and P9 (Figure 26, top right). The size of pool 3 was mostly similar along the transect, slightly decreasing from upstream to downstream (bottom left). At upstream location P1, the total share of degradable SOM (sum of carbon in pools 1 to 3) was higher than at intermediate and downstream locations. This was indicated by the significantly (non-paired t-test: 0.0003) lower amount of carbon in the non-degradable (stable) pool 4 (Figure 26, bottom right). At upstream location P1, 240 $\text{mg C g}_{\text{TOC}}^{-1}$ were anaerobically degradable (760 $\text{mg C g}_{\text{TOC}}^{-1}$ non-degradable) whereas at downstream location P9, only 160 $\text{mg C g}_{\text{TOC}}^{-1}$ were anaerobically degradable (840 $\text{mg C g}_{\text{TOC}}^{-1}$ non-degradable).

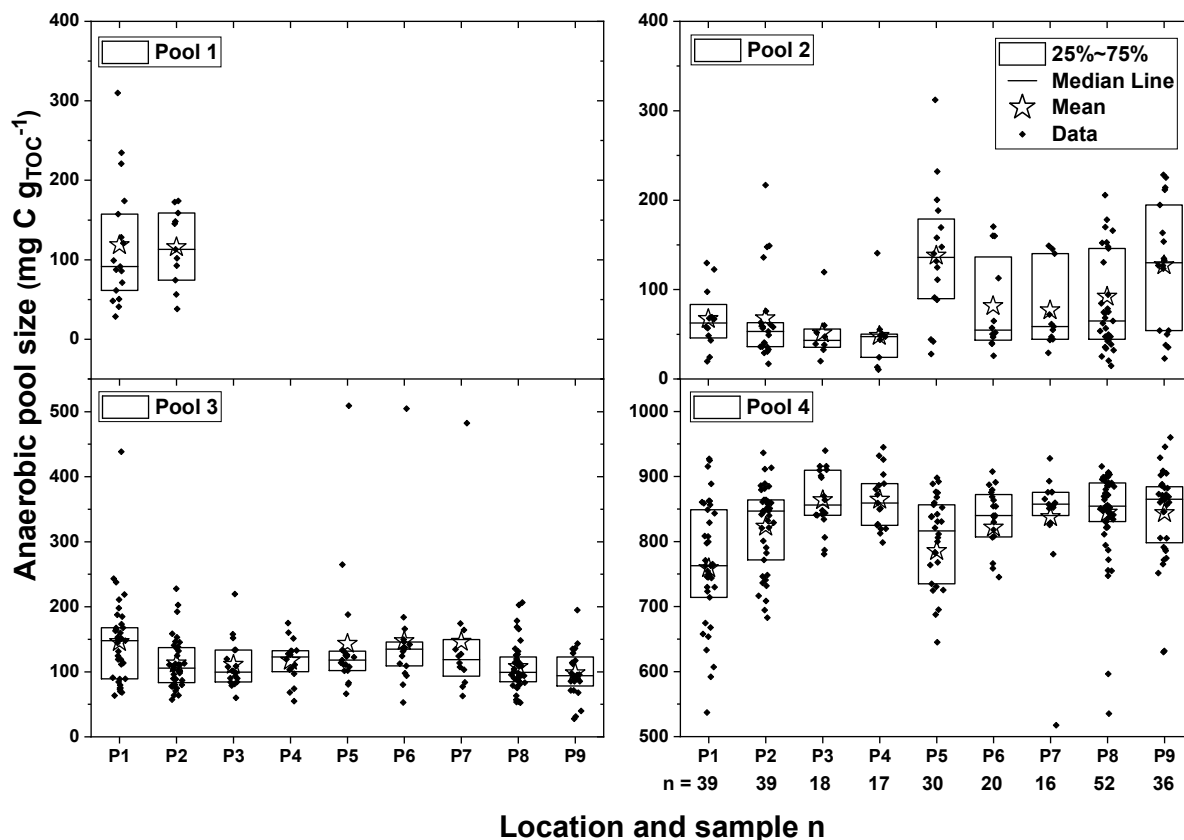


Figure 26 Size of anaerobically degradable SOM pools ($\text{mg C g}_{\text{TOC}}^{-1}$) per location for four pools and all layers, samples taken in 2018 and 2019. Consider the differently scaled y-axis for the non-degradable pool 4 (bottom right). Lines = median values, stars = mean values, boxes = 25th and 75th percentile. The sample n is valid for pool 4, because not all pools appeared for each sample.

In terms of depth profiles, fluid mud (FM) on average had a share of around 39 % (anaerobic conditions, Figure 27, left) and 34% (aerobic conditions, Figure 27, right) of degradable carbon (i.e., the sum of pool 1, pool 2 and pool 3), whereas consolidated sediment (CS) harboured 28 % of anaerobically and 30% of aerobically degradable carbon (Figure 27). For anaerobic decay (Figure 27, left), the share of pool 1 and pool 2 was largest for FM layers, pool 4 increased with depth (FM to CS) from 61 % to 72 %. For aerobically degradable SOM pools (Figure 27, right), no pool 1 was observed for CS layers, depth related trends were less pronounced than for anaerobic SOM pools. The initial average TOC content was 3.9 % for FM and pre-consolidated sediment (PS) layers and 3.7 % for CS layers.

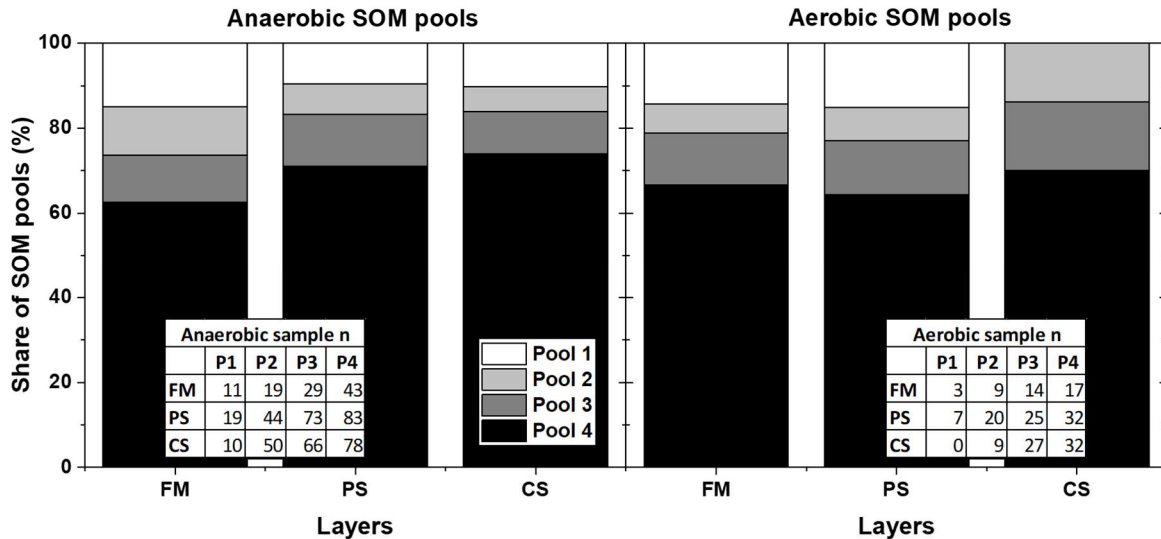


Figure 27 Relative share of the four sediment organic matter pools (pool 1-4) per layer (FM, PS, CS) from all locations, samples from 2018 and 2019. Left: anaerobically degraded SOM pools, right: aerobically degraded SOM pools.

Location P1 is the least disturbed location in the Port of Hamburg in terms of dredging and was therefore considered the best choice to investigate time and depth-related trends. Redox potentials revealed mostly anaerobic conditions in the sediment package. Hence, Figure 28 focusses on the time- and depth-related trends for anaerobic SOM decay at location P1. A clear seasonal trend was observed for the size of the easily degradable pool 1. The size of pool 1 increased from 45 mg C g_{TOC}^{-1} in March to 220 mg C g_{TOC}^{-1} in June, followed by a decrease towards the end of the year (Figure 28, left). This trend was less pronounced at other locations and not detectable in other pools. The average pool sizes decreased with depth (SPM to CS layer) for pool 1 and pool 2 (Figure 28, right). For pool 1 and pool 2, the degradable SOM was mainly found in SPM and PS layers (Figure 28, right) whereas pool 3 showed similar pool sizes for all layers.

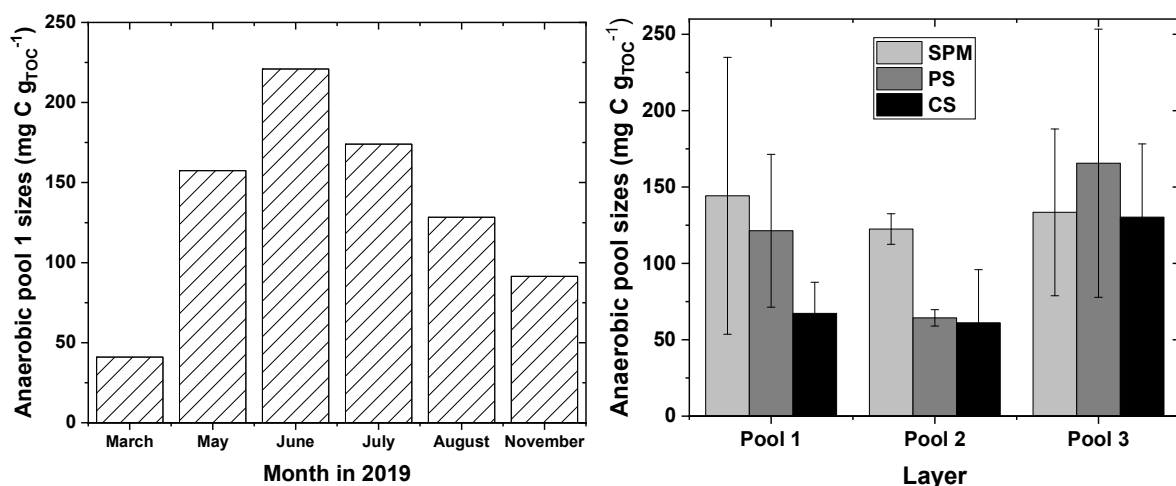


Figure 28 The anaerobically degradable pool 1 from March to November 2019 (left) and average ($n = 12$, 2018 and 2019) anaerobic pool sizes for SPM, PS and CS layers for pool 1, pool 2 and pool 3 (right), both at location P1.

7.5 Discussion

7.5.1 Spatial trends of sediment organic matter (SOM) degradable pools

Organic matter can be viewed as a continuum of successively degrading compounds (Lehman and Kleber, 2015). This study attempts to cluster this succession of degradability in freshwater sediments of the Elbe river by separating a fast (P1), medium (P2) and slowly (P3) degradable organic matter pool with half-lives of hours to days, days to weeks and weeks to months (Figure 24). It was assumed that the decay rates of easily degradable (i.e., freshly settled riverine organic matter) are high and decay rates of older (i.e., more mineral-bound organic matter) are low. The decay rates were used to define and quantify the differently degradable organic matter pools. A recalcitrant pool 4, which was considered not biologically available, was calculated from the difference between the total TOC concentration and the sum of pools 1 to 3.

The recalcitrant average share ranged mostly between 65 to 85% (aerobic conditions, Figure 25, bottom right) and 75 to 85% of TOC (anaerobic conditions, Figure 26, bottom right). This indicated that in most samples the greatest part of SOM was stable and not available to microbial decay. On average, about 10% more SOM was degradable when oxygen was available as terminal electron acceptor. This could be explained by the more favourable thermodynamics with the larger energy gain of the aerobic degradation pathway and the fact that under anaerobic conditions hydrolysis and fermentation of structurally complex organic matter are rate-limiting (Kristensen, 1995). Complete mineralization as well as degradation of larger molecules (i.e., lignin) is only accomplished under aerobic conditions. Further, estrogens, phthalates and surfactants are rapidly decomposed under aerobic conditions (Blume et al., 2016) but not under anaerobic conditions. Correspondingly, the recalcitrant pool 4 was larger under anaerobic conditions. At upstream location P1, largest differences between aerobic and anaerobic decay was found for pool 1 and pool 2. From upstream to downstream, the differences between aerobic and anaerobic pool sizes decreased. In an earlier study on dewatered and recently landfilled dredged sediment from the Port of Hamburg, the anaerobically degradable share amounted to only 3 to 11% of the organic carbon (Gebert et al., 2019). Hence a higher share of up to 89-97% of TOC to be present in the recalcitrant pool. It is plausible that for the dewatered and landfilled sediment the degradable SOM fraction is smaller than for the freshly sampled sediment analysed in this study. Pre-treatment and several years of landfilling will have led to further depletion of degradable SOM under first aerobic (during dewatering) and subsequently under anaerobic (landfilling) conditions.

The apparent lack of an aerobically and aerobically degradable pool 1 at downstream locations (Figure 25, top left) was interpreted as a successive depletion of easily degradable organic matter as the sediment passes through the harbour area. This could be explained by the correspondingly larger share of easily degradable organic matter at location P1. A strong decrease in the aerobically available pool 2 was observed along the transect (Figure 25, top right), mirrored by an increase in the recalcitrant pool 4 (Figure 25, bottom right). Both under aerobic and under anaerobic conditions, the size of the slowly degradable pool 3 did not show a spatial gradient (Figures 4 and 5, bottom left). It is hypothesised that this pool constitutes a basis of about 150 to 200 mg C g_{TOC}^{-1} (aerobic conditions, 15 to 20 % of TOC) and 100 to 150 mg C g_{TOC}^{-1} (anaerobic conditions, 10 to 15% of TOC) of mineral-bound slowly degradable SOM of predominantly downstream origin at all sampling locations. This pool does not contribute significantly to carbon release in the short or intermediate time scales when sediment is naturally transported from upstream to downstream.

About half of the high anaerobic and aerobic decay rates (B1, Figure 24, left and right) were found at location P1, reflecting the dominance of the easily degradable organic matter (pool 1) at upstream

locations (Figure 26, top left), resulting from the upstream input of biomass. Correspondingly, the recalcitrant pool 4 was smaller by approximately 100 mg C g_{TOC}⁻¹ at upstream location P1 compared to location P9 (Figure 26 and Figure 25, bottom right). The largest share of the mineral bound organic matter reaches the harbour from downstream with the tide, as indicated by the concentration of Zn in the particle size fraction < 20 µm (Kappenberg and Fanger, 2007), showing elevated concentrations and therefore an upstream signature only at locations P0 and P1 (Table 7). Reese et al. (2019) clustered sediment of the Elbe River as fluvial (to river km 615) and as a mixture of marine and fluvial (between river km 615 and 700). They based their clusters on element fingerprinting and isotopic tracer approaches. These findings are corroborated by higher upstream oxygen consumption rates (Spieckermann et al., 2021), higher upstream shares of organic carbon bound in the low density fraction and lower δ¹³C values (Zander et al., 2020), and further by increased values of parameters representing phytoplankton biomass such as chlorophyll a and silicic acid (Table 7). Also, increased concentrations of solid phase nutrients (phosphorus, sulphur, nitrogen) and carbon were found at upstream location P1. Hence, the spatial patterns of SOM degradability found in this study are directly linked to source gradients of labile autochthonous planktonic biomass, adding a small, but very reactive organic matter fraction of upstream origin to the larger part of recalcitrant organic matter from downstream.

7.5.2 Organic matter decay rates and degradable shares in soils and sediments

In this section, comparisons of decay rates and SOM pool sizes with literature will be made. It is evident that organic matter decay in terrestrial soils is governed by different environmental conditions (i.e., degree of saturation, redox potential, temperature) and different sources of organic matter input. Both, terrestrial soils and sediments, however, comprise older, mature organic matter stabilized in organo-mineral complexes as well as fresh, immature and easily degradable organic matter originating from microbial, plant or animal biomass. Moreover, sediment organic matter also comprises eroded topsoil organic matter, while terrestrial soils in the river catchment originate from river deposits during flooding.

For various terrestrial soils, Haynes (2005) listed values of potentially degradable carbon for soils between 0.8 and 12% of TOC, mostly between 5 and 15% of TOC. The sediments of this study showed, compared to Haynes (2005), higher values of degradable carbon under anaerobic conditions, namely, on average between 13 and 23% of TOC (compare inverse values of pool 4, Figure 26). These values can be explained by the continuous input of young, biogenic, less degraded organic matter, reaching the sediments in the investigation area from the upstream parts of the river (Schoel et al., 2014). According to a review of von Lützow et al. (2007), high soil organic matter decay rates represent microbial biomass and are typically found in the lighter density fraction.

In agreement with findings from McKew et al. (2013), the rates of carbon release by microbial decay of sediment organic matter were similar under aerobic and anaerobic conditions (Figure 24). In the literature, mean residence times (MRT) of degradable organic matter are given with 30 to 87 years for soils under corn cultivation (Schiedung et al., 2017). For forest soils, the MRT was between 10 and 30 years for temperatures between 7 °C and 13 °C (Garten et al., 2006). Oades (1988) mentioned MRTs between 4 to 200 years for various soils. In this study, the mean residence times for degradable organic matter (not shown) were around three to five years if decay rates were normalised to 20 °C and between 30 and 40 years if decay rates were normalized to 10 °C. This indicates the presence of younger, more easily degradable organic matter (i.e., phytoplankton with low MRT) when compared to the MRT of the already partly mineralized older organic matter of terrestrial soils mentioned above.

The MRT of this study (3 to 5 years, 20°C) showed a similar order of magnitude as the half-life (2.5 ± 4.7 years) of organic matter previously measured for inland waters (Catalán et al., 2016, 20°C).

7.5.3 Trends in time and with depth

In the investigated harbour area, sedimentation dynamics are influenced by maintenance dredging, disturbing the natural development of sediment depth profiles. Therefore, depth-related assumptions are made with reservation. Examples of depth-related patterns for various sediment parameters (i.e., SOM decay, carbon stable isotopes, DNA in extrapolymeric substances, pore water NH_4^+ concentration) were given in Zander et al. (2020). It was assumed that decreasing trends of observed SOM decay (rates) with depth are due to decreasing degradability of in situ SOM in older (deeper) sediment layers. This assumption was supported by the share of organic matter in differently degradable pools (Figure 27, left). Under anaerobic conditions, the largest share of degradable carbon was found in the fluid mud samples, decreasing with depth and hence age of the sediment. Therefore it was assumed that due to carbon decay, occurring in situ before sediment sampling, the share of degradable carbon is lower at depth. The depth gradient clearly showed larger shares of easily degradable SOM in upper layers (SPM and PS) and more decayed SOM in deeper layers (CS). This was true for the more easily degradable pools 1 and 2 (Figure 28, right). Increased pool 1 sizes (Figure 28, left) between spring and summer indicated an upstream growth of phytoplankton (Deng et al., 2019; Schoel et al., 2014). Similarly, Grossart et al. (2004) found seasonal patterns in a tidal flat ecosystem, namely, high sediment resuspension in November and phytoplankton-related processes influencing bacterial dynamics in May. Subsequent input of fresh organic matter at upstream locations (P1) was also indicated by increased chlorophyll a and silicic acid concentrations at location P1 (Table 1). This was supported by a diminishing share of easily degradable SOM between summer and autumn, in other words, a decreasing pool 1 in the second part of the year. It was assumed that the input of fresh SOM in March from upstream was still low due to high winter discharge, in combination with still low irradiation (Kamjunke et al., 2021), low water and sediment temperatures. A similar seasonal pattern was also described for the sediment oxygen consumption potential in the investigation area (Spieckermann et al., 2021) with highest oxygen consumption values for the summer months due to a larger of easily degradable biomass.

7.6 Conclusions and outlook

This paper is the first one to provide quantitative data on the mass of carbon that can be released from microbial decay of organic matter and to quantify its differently degradable shares in tidal sediments. SOM lability along a transect of 30 river kilometres though the Elbe around the Port of Hamburg decreased from upstream to downstream, evidenced by the decreasing amount of the easily degradable pool 1 material from upstream to downstream. The slowly degradable pool 3, assumed to be associated with SOM bound in organo-mineral complexes, is spread more or less equally along the investigated transect, constituting a similar share of predominantly marine origin at all locations. Total degradability thus appears to be governed by the amount of reactive SOM present in addition to this basis (pool 1, 10 to 15% and pool 2, 5 to 10%), which in turn follows a source gradient and an age gradient from upstream to downstream. The recalcitrant pool 4 comprised by far the largest part of TOC in any part of the harbour, indicating that for both, anaerobic and aerobic conditions, the sediment organic matter for the largest part is stable. The sediments therefore contribute significantly to organic carbon storage in the investigation area. The size of the anaerobically degradable SOM pools decreased with depth and hence age of organic matter and varied seasonally in relation to the variability of

upstream net primary production. Total SOM degradability was larger under aerobic than under anaerobic conditions by about 10% of TOC but the differences between aerobic and anaerobic decay decreased from upstream to downstream. The upper sediment layers, characterised by the highest amount of young organic matter, still showed a large share of poorly degradable and recalcitrant SOM (pools 3 and 4). This suggests that in the investigated system organic matter, even in the suspended and fluidic particle phases, is already significantly degraded or stabilized in organo-mineral associations. The size of the differently degradable organic matter pools and the degradation rates can be used to quantify carbon fluxes from microbial decay of sediment organic matter in the tidal Elbe river, using in situ temperatures and the known temperature dependency of anaerobic and aerobic decay.

Acknowledgements

This study was funded by Hamburg Port Authority and carried out within the project BIOMUD, a member of the MUDNET academic network www.tudelft.nl/mudnet/.

References

- Arndt, S.B.B. Jørgensen, D.E. LaRowe, J.J. Middelburg, R.D. Pancost, P. Regnier. 2013. Quantifying the degradation of organic matter in marine sediments: A review and synthesis. *Earth Sci Reviews* 123, 53–8, doi: <http://dx.doi.org/10.1016/j.earscirev.2013.02.008>
- Baldock JA, Skjemstad JO. 2000. Role of the soil matrix and minerals in protecting natural organic materials against biological attack. *Org Geochem* 31:697-710. doi.org/10.1016/S0146-6380(00)00049-8
- Blume HP, Brümmer GW, Fleige H, Horn R, Kandeler E, Kögel-Knabner I, Kretzschmar R, Stahr K, Wilke B-M, Scheffer F, Schachtschabel P (2016) *Soil Science*. Berlin Heidelberg Springer-Verlag. doi.org/10.1007/978-3-642-30942-7
- Boyd, A. McKew, Alex J. Dumbrell, Joe D. Taylor, Terry J. McGenity & Graham J.C. Underwood. 2013. Differences between aerobic and anaerobic degradation of microphytobenthic biofilm-derived organic matter within intertidal sediments. *FEMS Microbiol Ecol* 84, 495–50, doi: 10.1111/1574-6941.12077
- Brockmann, UH (1994) Organic matter in the Elbe Estuary. *Netherlands J of Aquatic Ecol* 28(3-4):371-381, doi: <https://doi.org/10.1007/BF02334207>
- Catalán, N, Marcé, R., Kothawala, D.N., Tranvik, L.J. 2016. Organic carbon decomposition rates controlled by water retention time across inland waters. *Nat Geosci* 9, doi: 10.1038/NNGEO2720
- Deng, Z, He, Q., Safar, Z., Chassagne, C. 2019. The role of algae in fine sediment flocculation: In-situ and laboratory measurements. *Mar Geol* 413, 71–84
- Gao J, Mikutta R, Jansen B, Guggenberger G, Vogel C Kalbitz K (2019) The multilayer model of soil mineral–organic interfaces—a review. *J*
- Garten, C.T., Hanson, P.J. 2006. Measured forest soil C stocks and estimated turnover times along an elevation gradient. *Geoderma* 136 342–352
- Gebert, J, Köthe, H., Gröngroft, A. 2006. Prognosis of Methane Formation by River Sediments. *J Soils & Sediments* 6, 2, 75–83
- Gebert, J., Knoblauch, C., Gröngroft, A. 2019. Gas production from dredged sediment. *Waste Manage* 85, 82-89, doi: <https://doi.org/10.1016/j.wasman.2018.12.009>
- Geerts, L, Cox, T.J.S., Maris, T., Wolfstein, K., Meire, P., Soetaert, K. 2017. Substrate origin and morphology differentially determine oxygen dynamics in two major European estuaries, the Elbe and the Schelde. *Estuar Coast Shelf S* 191, 157-170
- Grasset, S., Moras, S., Isidorova, A., Couture, R.-M., Linkhorst, A., Sobek, S. 2021. An empirical model to predict methane production in inland water sediment from particular organic matter supply and reactivity. *Limnol Oceanogr* 9999, 2021, 1–13, doi: 10.1002/lno.11905
- Grossart H-P, Brinkhoff T, Martens T, Duerselen C. (2004) Tidal dynamics of dissolved and particulate matter and bacteria in a tidal flat ecosystem in spring and fall. *Limnol Oceanogr* 49(6):2212–2222
- Haynes, R.J., 2005. Labile organic matter fractions as central components of the quality of agricultural soils: an overview. *Adv Agron* 85, 221-268
- Jommi, C, Muraro, S., Trivellato, E., Zwanenburg, C. 2019. Experimental results on the influence of gas on the mechanical response of peats. *Géotechnique* 69, 9, 753–766, doi: <https://doi.org/10.1680/jgeot.17.P.148>
- Kamjunke N, Rode M, Baborowski M, Kunz JV, Zehner J, Borchardt D, Weitere M (2021) High irradiation and low discharge promote the dominant role of phytoplankton in riverine nutrient dynamics. *Limnol and Oceano* 66:2648-2660.
- Kappenberg J, Fanger H-U (2007) Sedimenttransportgeschehen in der tidebeeinflussten Elbe, der Deutschen Bucht und in der Nordsee. GKSS report 2007/20; ISSN 0344–9629
- Kristensen, E. 1995. Aerobic and anaerobic decomposition of organic matter in marine sediment: which is fastest? *Limnol Oceanogr* 40, 1430-1437
- Lehman, J., Kleber, M. 2015. The contentious nature of soil organic matter. *Nature* 528, 60-68
- Li, X. 2018. Investigation of Gas Generation by Riverine Sediments: Production Dynamics and Effects of Sediment Properties. M.Sc. thesis. Delft University of Technology
- Von Lütow, M., Koegel-Knabner, I., Ekschmitt, K., Flessa, H., Guggenberger, G., Matzner, E., Marschner, B. 2007. SOM fractionation methods: Relevance to functional pools and to stabilization mechanisms. *Soil Biol Biochem* 39, 2183–2207
- Malarkey, J., Jaco H. Baas, J.H., Julie A. Hope, J.A., Rebecca J. Aspden, R.J., Daniel R. Parsons, D.R., Jeff Peakall, J., Paterson, D.M., Schindler, R.J., Ye, L., Lichtman, I.D., Bass, S.J., Davies, A.G., Manning, A.J., Thorne, P.D. 2015. The pervasive role of biological cohesion in bedform development. *Nature Commun* 6, 6257, doi: 10.1038/ncomms7257
- McKew, B.A., Dumbrell, A.J., Taylor J.D., McGenity, T.J., Underwood, G.J.C. 2013. Differences between aerobic and anaerobic degradation of microphytobenthic biofilm-derived organic matter within intertidal sediments. *FEMS Microbiol Ecol* 84, 495–509

- Oades J.M. 1988. The retention of organic matter in soils. *Biogeochemistry* 5, 35-70
- Parsons, D.R., Schindler, R.J., Hope, J.A., Malarkey, J., Baas, J.H., Peakall, J., Manning, A.J., Ye, L., Simmons, S., Paterson, D.M., Aspden, R.J., Bass, S.J., Davies, A.G., Lichtman, I.D., Thorne, P.D. 2016. The role of biophysical cohesion on subaqueous bed form size. *Geophys Res Lett* 43, 1566–1573, doi:10.1002/2016GL067667
- Rabalais, N.N., Diaz, R.J., Levin, L.A., Turner, R.E., Gilbert, D., Zhang, J. 2010. Dynamics and distribution of natural and human-caused hypoxia. *Biogeosciences* 7, 585–619
- Sander, R. 2015. Compilation of Henry's law constants (version 4.0) for water as solvent. *Atmos Chem Phys* 15, 4399–4981, doi:10.5194/acp-15-4399-2015
- Schiedung, H., Tilly, N., Hütt, C., Welp, G., Brüggemann, N., Amelung, W. 2017. Spatial controls of topsoil and subsoil organic carbon turnover under C3–C4 vegetation change. *Geoderma* 303 44–51
- Schoel, A, Hein B.,Wyrwa J., Kirchesch V. 2014. Modelling water quality in the Elbe and its estuary –Large Scale and Long TermApplications with Focus on the Oxygen Budget of the Estuary. *Die Kueste* 81, 203–232
- Shakeel, A., Kirichek, A., Chassagne, C. 2019. Is density enough to predict the rheology of natural sediments? *Geo-Mar Lett* 39, 427–434, doi: <https://doi.org/10.1007/s00367-019-00601-2>
- Shakeel, A., Kirichek, A., Chassagne, C. 2020. Rheological analysis of natural and diluted mud suspensions. *J Non-Newton Fluid* 286, 104434, doi:10.1016/j.jnnfm.2020.104434
- Shakeel A, Zander F, de Kerk J-W, Kirichek A, Gebert J, Chassagne C. 2022. Effect of organic matter degradation in cohesive sediment: A detailed rheological analysis. *J Soil Sediment* doi.org/10.1007/s11368-022-03156-5 (accepted for publication 30 January 2022)
- Sills G.C., Gonzalez R. 2001. Consolidation of naturally gassy soft soil. *Geotechnique* 51, 7, 629-639
- Six J, Paustian K. 2014. Aggregate-associated soil organic matter as an ecosystem property and a measurement tool. *Soil Biol Biochem* 68:A4-A9. doi.org/10.1016/j.soilbio.2013.06.014
- Spieckermann M, Gröngröft A, Karrasch M, Neumann A, Eschenbach A (2021) Oxygen Consumption of Resuspended Sediments of the Upper Elbe Estuary: Process Identification and Prognosis. *Aquat Geochem* (2021). doi.org/10.1007/s10498-021-09401-6
- Tillmann U, Hesse K-J, Colijn F (2000) Planktonic primary production in the German Wadden Sea. *J Plankton Res* 22:1253–1276.
- van Duyl FC, de Winder B, Kop AJ, Wollenzien U (1999) Tidal coupling between carbohydrate concentrations and bacterial activities in diatom-inhabited intertidal mudflats. *Mar Ecol Prog Ser* 191:19–32.
- Ward, N.D., Krusche, A.V., Sawakuchi, H.O., Brito, D.C., Cunha, A.C., Moura, J.M.S., da Silva, R., Yager, P.L., Keil, R.G., Richey, J.E. 2015. The compositional evolution of dissolved and particulate organic matter along the lower Amazon River—Óbidos to the ocean. *Mar Chem* 177, 244–256
- Wolfstein K, Kies L (1999) Composition of suspended particulate matter in the Elbe estuary: implications for biological and transportation processes. *Deutsche Hydrografische Zeitschrift*, 51(4):453-463.
- Wolfstein K, Colijn F, Doerffer, R (2000) Seasonal dynamics of microphytobenthos biomass and photosynthetic characteristics in the northern German Wadden Sea, obtained by the photosynthetic light dispensation system. *Estuar Coast Shelf Sci* 51:651–662.
- Wurpts, R., Torn, P. 2005. 15 Years Experience with Fluid Mud: Definition of the Nautical Bottom with Rheological Parameters. *Terra et Aqua* 99
- Zander, F., Heimovaara, T., Gebert, J. 2020. Spatial variability of organic matter degradability in tidal Elbe sediments. *J Soils Sediments*, 20, 2573–2587, doi: <https://doi.org/10.1007/s11368-020-02569-4>
- Zander F, Shakeel A, Kirichek A, Chassagne C, Gebert J. 2022. Effects of organic matter degradation in cohesive sediment: Linking sediment rheology to spatio-temporal patterns of organic matter degradability. *J Soil Sediment*. <https://doi.org/10.1007/s11368-022-03155-6> (accepted for publication 30 January 2022)

8 Effects of organic matter degradation in cohesive sediment: Linking sediment rheology to spatio-temporal patterns of organic matter degradability

F. Zander¹, A. Shakeel^{2,3}, A. Kirichek², C. Chassagne², J. Gebert¹

¹Section of Geo-Engineering, Department of Geoscience and Engineering, Faculty of Civil Engineering & Geosciences, Delft University of Technology, Stevinweg 1, 2628 CN Delft, The Netherlands

²Section of Environmental Fluid Mechanics, Department of Hydraulic Engineering, Faculty of Civil Engineering & Geosciences, Delft University of Technology, Stevinweg 1, 2628 CN Delft, The Netherlands

³Department of Chemical, Polymer & Composite Materials Engineering, University of Engineering & Technology, Lahore, KSK Campus, 54890 Pakistan

Corresponding author: Florian Zander, f.zander@tudelft.nl

Abstract

Purpose:

Sediment organic matter (SOM) influences settling and thus the rheological behavior of suspended particles by enhancing flocculation or reducing surface charges by forming organo-mineral complexes that facilitate particle-particle interactions in consolidating sediments. It was, therefore, assumed that the microbial degradation of SOM and its spatio-temporal variability would affect sediment rheological properties and enhance port maintenance dredging and navigability of ports and waterways.

Methods:

To investigate this effect, samples were taken at six locations along a transect of 30 river kilometers through the Port of Hamburg, Germany, during nine sampling campaigns within two years. The collected samples were divided into different layers based on the differences in visual consistency and strength. For analysis of SOM degradability, the samples were incubated in the laboratory for 250 days in glass bottles under aerobic and anaerobic conditions, measuring the CO₂ and CH₄ concentrations using gas chromatography and the pressure increase in the bottle headspace. Yield stress was analyzed before and after the dissolved organic matter (DOM) decay with a HAAKE MARS I rheometer (Thermo Scientific, Germany) with Couette geometry. Standard properties of solids and pore water were also analyzed.

Results:

Shear strength decreased upon SOM decay under both anaerobic and aerobic conditions. Under anaerobic conditions, organic matter decay reduced static and fluidic yield stress to an average of 74% and 79% of the fresh sample values. Consolidated layers at lower depths showed the highest absolute decrease in fluidic yield stress of up to -110 Pa due to larger amount of particles, and hence degradable organic matter was high in these layers. Pronounced spatial trends with higher changes in yield stress at upstream locations and lower yield stress changes at downstream locations, coincided with higher SOM degradability gradient upstream, supporting the assumption that the susceptibility of the sediment to yield stress changes depending on the availability of easily degradable organic matter.

Conclusion:

Degradation of organic matter significantly affects sediment strength, especially under the anaerobic conditions, even when the mass loss of organic matter mass loss is small. Seasonal variability in yield stress changes upon SOM decay indicate that the site-specific responses were modulated by overarching seasonal effects impacting the entire investigation area. It was assumed that during an anaerobic decay, the formation of gas bubbles added an additional physical component to the effect of biological SOM decay.

Keywords: spatial variability, organic matter deagradation, cohesive sediment, yield stress

8.1 Introduction

Sediment organic matter (SOM) originates from both natural (e.g. eroded terrestrial topsoils, plant litter, planktonic and benthic organisms) and anthropogenic (e.g. surface runoff, sewage waste) sources. The presence of organic matter can expedite suspended particle settling by flocculation through bridging between the mineral particles, creating larger diameter particles or by surface charge neutralization, reducing the repulsive forces between the charged particles (Lagaly and Dékány, 2013). As a result, the sediment strength increases with increasing amount of organic matter at the same bulk density (Shakeel et al., 2019).

Phytoplankton can play a significant role in the settling of fine-grained sediment by facilitating the bridging effect (Deng et al., 2019). Correspondingly, fine-grained sediment is expected to behave differently in shallow areas, upstream within the river-continuum (Vannote et al., 1980) of high net primary production compared to light-deficient areas in deeper and/or more turbulent waters. The existence of organic matter in sediments is known to significantly influence the rheological and cohesive properties of sediments (Shakeel et al., 2019; Wurpts and Torn 2005).

As part of the natural carbon cycle, the labile part of SOM is also subject to microbial degradation. Under aerobic conditions, SOM degradation results in the production of carbon dioxide (CO₂) while under anaerobic conditions, frequently prevailing in fine-grained sediments, methane (CH₄) is also produced. Particularly, CH₄ can remain entrapped in the sediment and affect its rheological properties and density due to the poor solubility of methane in water. The non-degraded part of SOM forms complexes with the mineral phase, leading to its stabilization and physical shielding and transfer of SOM into the heavy density fraction (Baldock and Skjemstad 2000; Six and Paustian 2014; Gao et al., 2019; Zander et al., 2020). Given the role of organic matter for the sediment's rheological properties, it can be expected that, next to the absolute SOM content, its degradability (inversely) influences these properties. In the investigated transect through the Port of Hamburg in the tidal Elbe river, SOM decay has been shown to follow trends in space, in time and with depth (Zander et al., 2020).

It is therefore hypothesized that:

8. Sediment yield stresses are influenced by sediment organic matter decay with seasonal and spatial trends;
9. The rheology is dependent on the sediment density and the amount of decayed sediment organic matter;
10. Anaerobically decayed samples display greater changes in rheological properties than aerobically decayed samples due to bubble formation.

8.2 Materials and methods

In this study, natural sediment samples were collected from different locations along a transect of around 30 river kilometers (P1 = river km 616, P9 = river km 646, Figure S2, supporting information) through the Port of Hamburg (site description found in Zander et al., 2020) using a 1 m core sampler ('Frahmplot') in the years 2019-2020. The collected samples were divided into different stratigraphic layers (fluid mud, pre-consolidated and consolidated sediment) based on the differences in their visual consistency and strength for further analysis. The layers did not show constant thickness, but always had the same stratigraphic order as the FM layer that was not always present.

8.2.1 Overview of material properties

Methods for standard properties of solids and pore water are given in Zander et al. (2020). Some basic properties of the sediments investigated in this study are summarized in Table S1 (supporting information). Minimum and maximum values of selected parameters were total nitrogen (TN, 0.3-0.9%, downstream location P9 and upstream location P1), total organic carbon (TOC, 2.4-6.3%, P9 and P1), clay (31-43%, P5 and P8), sand (5-27%, P1 and P5) and extracellular polymeric substance (EPS, 2-32 g kg_{DM}⁻¹, P9 and P1), highlighting the pronounced spatial gradient found along the transect. Negative redox potentials indicate anaerobic conditions at all the investigated sites.

8.2.2 Impact of SOM decay on rheological properties

Degradation of sediment organic matter was performed by using the methodology reported in Zander et al. (2020). Sediment samples were incubated for 250 days in glass bottles under aerobic and anaerobic conditions, measuring the CO₂ and CH₄ concentrations with gas chromatographic analyses and the pressure increase in the bottle headspace. From these, the amounts of released CO₂-C and CH₄-C were calculated and normalized to total organic carbon (TOC). Before and after the 250 days of incubation, rheological analyses were performed.

8.2.3 Rheological characterization

Static yield stress was obtained from the first decline in viscosity as a function of shear stress, which is linked to the breakage of the inter-connected network of flocs. On the other hand, the second decline in viscosity (i.e. fluidic yield stress) was associated to the breakage of reorganized flocs into smaller flocs or individual particles upon further shearing (Shakeel et al., 2022). The rheological analysis of both fresh and degraded mud samples was performed using a HAAKE MARS I rheometer (Thermo Scientific, Germany) with concentric cylinder (Couette) geometry (gap width = 1 mm). The mud samples were gently homogenized before each rheological experiment and a waiting time of 3–5 min was adopted before the test to minimize the disturbances created by the cylinder. The rheological experiments were performed at 20 °C, maintained by a Peltier controller system. In order to check the repeatability, all the experiments were performed in duplicate and the repeatability error was less than 2%. More details can be found in Shakeel et al. (2019).

Density and water contents were measured directly before analyzing the yield stress. The samples' moisture did in principle not change within the air tight incubation containers and were checked by weighing the containers. If water was lost, for example due to re-flushing of samples with air during aerobic incubation, demineralized water was added to compensate for this loss before yield stresses were measured. If the water content changes (fresh sample compared to degraded sample after the rheological analyses) still was higher than 5%, the sample was discarded since density strongly influence the yield stress.

All investigated samples showed a two-step yielding behavior, with the two yield points defined as static τ_s and fluidic yield stress τ_f (Shakeel et al., 2020a). The change in yield stress is the difference between the initial yield stress (fresh sample, τ_{s,f_fresh}) and the yield stress of degraded samples (τ_{s,f_deg}) with $\tau_{s,f}$ = static and fluidic yield stress. In this paper, this change is expressed as:

$$\Delta\tau_{s,f} = \tau_{s,f_deg} - \tau_{s,f_fresh} \quad \text{Eq. 1}$$

The percentage of the degraded sample's yield stress related to the fresh sample's yield stress is given by:

$$\frac{\tau_{s,f_deg}}{\tau_{s,f_fresh}} \times 100 (\%) \quad \text{Eq. 2}$$

and the percentage of yield stress change in relation to the original value (fresh sample) by:

$$\frac{|\Delta\tau_{s,f}|}{\tau_{s,f_fresh}} \times 100 (\%) \quad \text{Eq. 3.}$$

8.3 Results

8.3.1 Effect of organic matter decay on sediment yield stress

Cumulative degradation of sediment organic matter followed a multiphase exponential decay function (Zander et al., 2020). After 250 days of laboratory incubation, degradation rates for most samples were extremely low, meaning that the cumulative increase of released carbon reached a plateau. The loss of organic carbon during this exhaustive laboratory incubation under anaerobic conditions ranged between 30 and 215 mg C g_{TOC}⁻¹, i.e. between 3 and 21.5% of the organic carbon was available for microbial degradation (minimum and maximum, Figure 29, top left). Under aerobic conditions, the maximum release of organic carbon ranged between 91 and 344 mg C g_{TOC}⁻¹, i.e. 9.1 and 34.4% (Figure 29, top right). In situ, anaerobic conditions are dominant, indicated by negative redox potentials (see Table S1, supporting information).

For the vast majority of samples, organic matter degradation under anaerobic conditions led to a decline in strength, and therefore in static and fluidic yield stresses as characteristic values for a two-step yielding behaviour (Shakeel et al., 2020a). On average, the yield stresses of anaerobically decayed SOM decreased to 74% of the original value for static yield stress (SYS) and to 79% in case of the fluidic yield stress (FYS, both Figure 29, bottom). For aerobically decayed samples, a less strong effect was observed, i.e. on average a decrease to 93% of the original value for SYS and to 98% for FYS (note: 100% means that the decayed sample had the same YS value than the initial sample). For some samples, organic matter decay led to an increase in strength (values > 100% in Figure 29, bottom). The overall variability of yield stress values was much larger for aerobic than for anaerobic SOM decay.

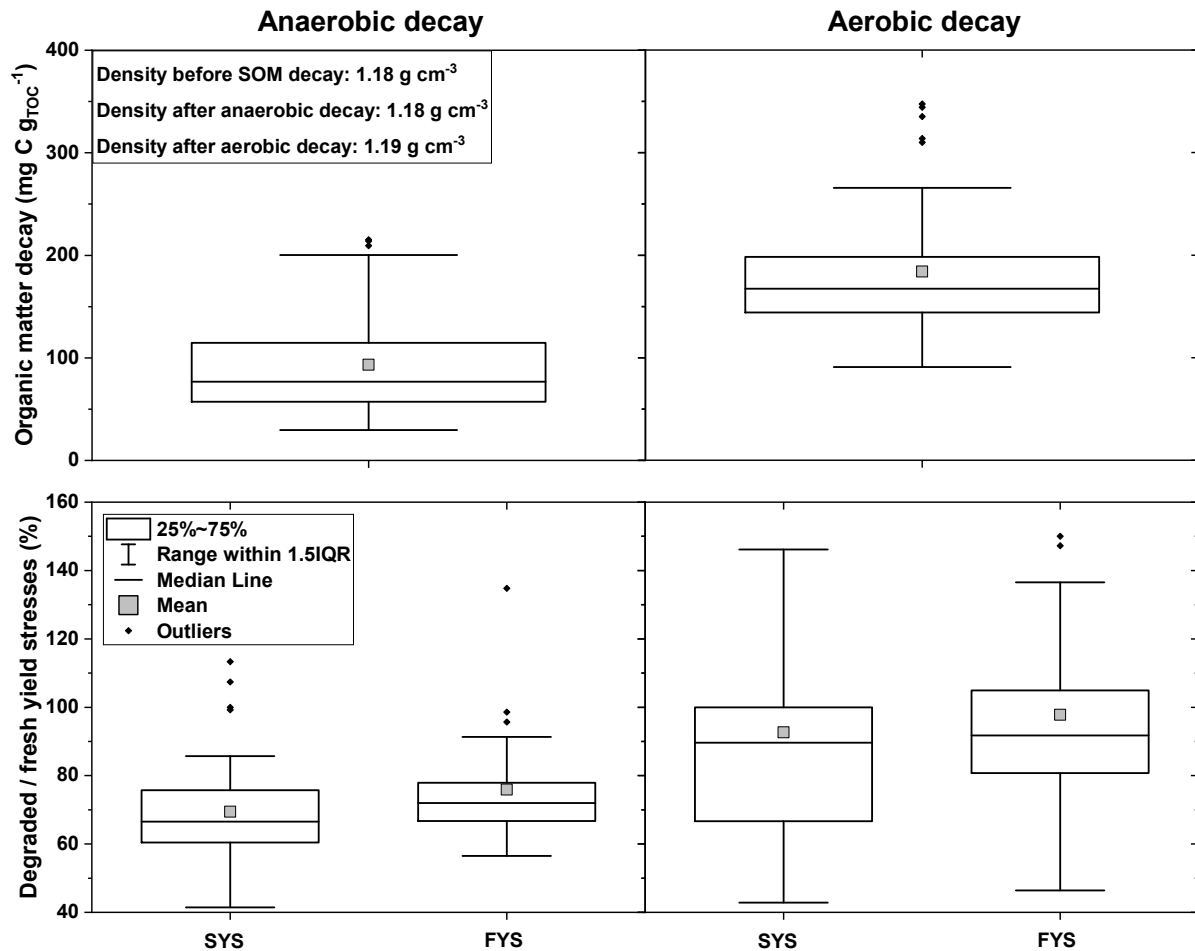


Figure 29 Cumulative carbon release by organic matter decay over 250 days (top) and corresponding yield stress of degraded sample in relation to fresh sample (in % of yield stress of fresh sample, Eq. 2, bottom) for anaerobic decay (AN, bottom left, $n = 95$) and aerobic decay (AE, bottom right, $n = 66$), all layers and locations samples in 2019 and 2020. 100% = decayed sample had the same YS value than the initial sample. 1.5IQR = factor 1.5 of the interquartile range (25%-75%).

8.3.2 Spatial and seasonal variation of yield stresses

Independent of sampling location or sampling depth (layer), it was found that the higher the strength of the fresh sample, the larger the decrease in strength upon degradation of organic matter, shown for the fluidic yield stress in Fig. 2. As carbon content and degradability are subject to both a seasonal variation and a spatial trend (Zander et al. 2020), it was hypothesized that these patterns would also be reflected in the effect of organic matter decay on the rheological properties.

If the dataset is divided by date of sampling (Figure 30, left), with each sampling date including all sampled locations and layers, it is seen that the ratio between the initial yield stresses and the change of yield stresses are reversed for each date with high Pearson's coefficients ($P \geq 0.85$) except for the campaign in June 2020 (20-jun, $P: -0.59$). This suggests that the sediment properties at all locations along the transect follow a similar principal temporal trend. If the dataset is divided by location of sampling (Figure 30, right), including all sampling dates for each location, a similar inverse relationship between initial yield stresses and the change of yield stresses is seen, with even higher Pearson's coefficients ($P \geq 0.9$), except for the location P8 ($P: -0.75$). For most of the samples, the slopes of change in yield stress over initial yield stress were more negative (steeper) in 2019 than in 2020 (Figure 30, left) and more negative at upstream compared to downstream locations (P1 and P2, Figure 30, right). This suggests that the sediment properties at each location differ distinctly from one another and also

maintain these differences over time. A similar pattern could be observed for the static yield stress (not shown here). Trends were less pronounced for aerobically decayed samples.

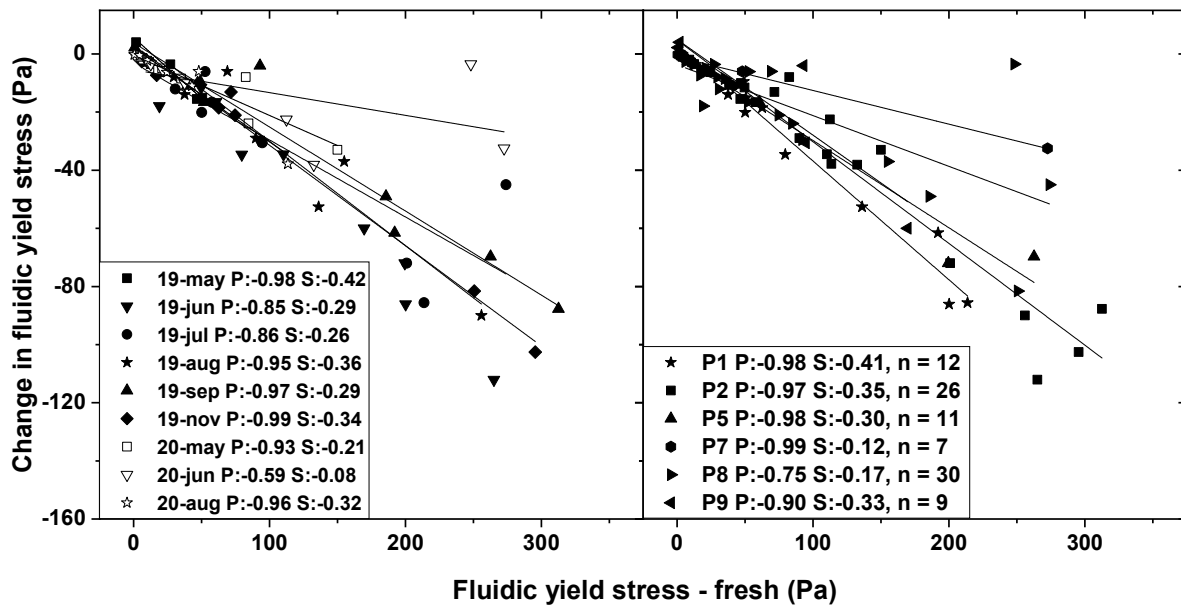


Figure 30 Relationship between fluidic yield stress of fresh samples $\tau_{f, fresh}$ and the change in yield stresses (Eq. 1) of anaerobically incubated samples (250 days) from 2019 and 2020. Left: closed symbols = 2019, open symbols = 2020, Pearson's coefficient r (P) and slope (S) given per sampling date (all locations, $n = 10$, left) and per location (all months, right) for chosen locations, all layers.

8.3.3 Depth-differentiation of yield stresses

If the data set is differentiated per depth, clear differences for the change in yield stress can be observed between the layers fluid mud (FM), pre-consolidated sediment (PS) and consolidated sediment (CS). The largest absolute change of yield stresses $\Delta\tau_{s,f}$ (Figure 31, top) was observed for the denser, i.e. deeper and more consolidated sediments (CS) layers. FM layers showed a larger but more scattered relative change of the static yield stresses upon decay (Figure 31, bottom). On average, the change in fluidic yield stresses were about threefold larger than the change in static yield stresses. Considering the relative change in yield stress (Figure 31, bottom), the change was about 60 to 90% for all layers. A few samples from FM layers showed an increase in yield stress.

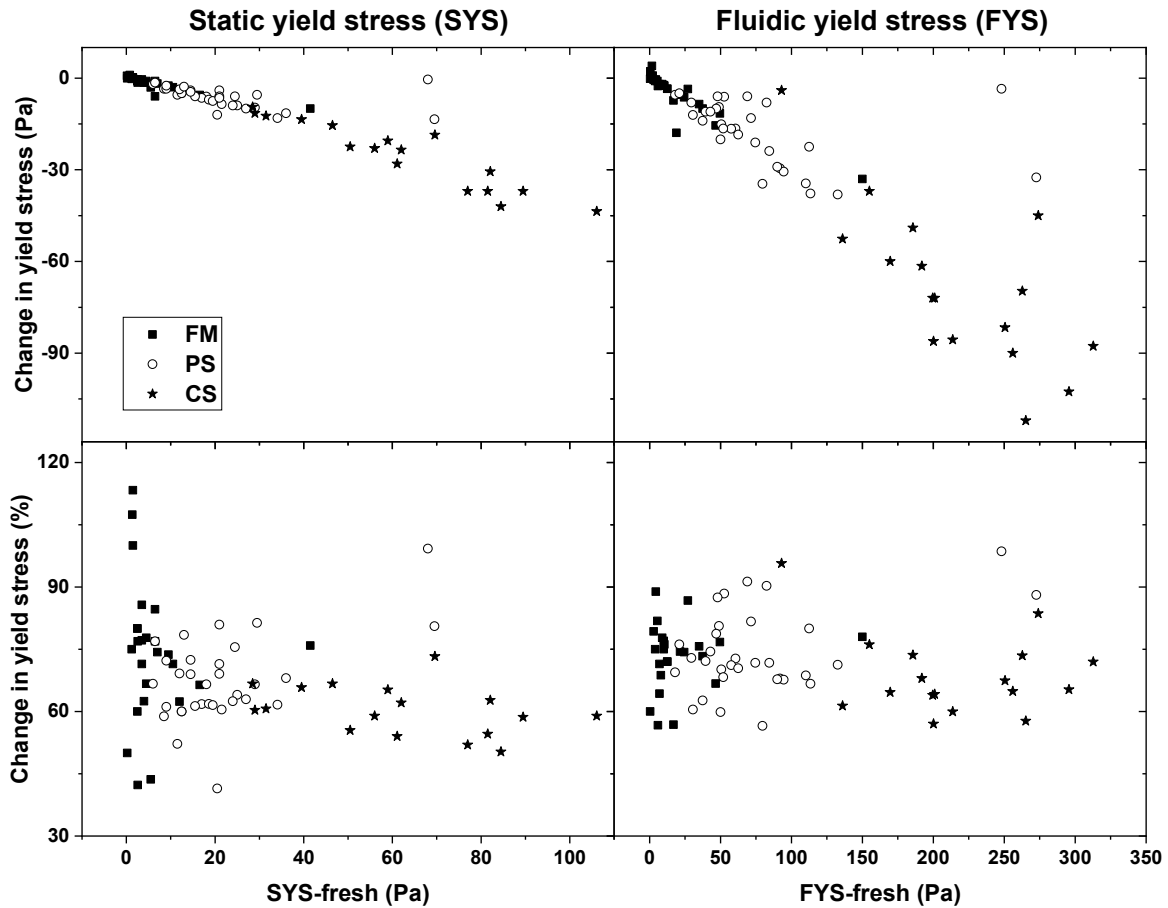


Figure 31 Relationship between initial yield stresses of fresh samples and the change of the yield stresses upon organic matter degradation for 250 days for FM, PS and CS layers, given in Pa (degraded – fresh, Eq. 1, top) and in % of fresh sample (Eq. 3, bottom). Left: static yield stress (SYS), right: fluidic yield stress (FYS), samples from all locations and all layers.

Due to the fact that the absolute change in yield stresses was the largest and showed the largest range for CS layers (Figure 31, top), data from these layers were used to investigate a possible spatial trend in more detail (Figure 32). The change of fluidic yield stress (and also of static yield stress, not depicted) showed clear decrease from upstream to downstream locations for anaerobic SOM decay (Figure 32, left) and a partial increase for aerobic decay (Figure 32, right); i.e. the differences between initial yield stress and yield stress of decayed sediments were smaller at downstream locations.

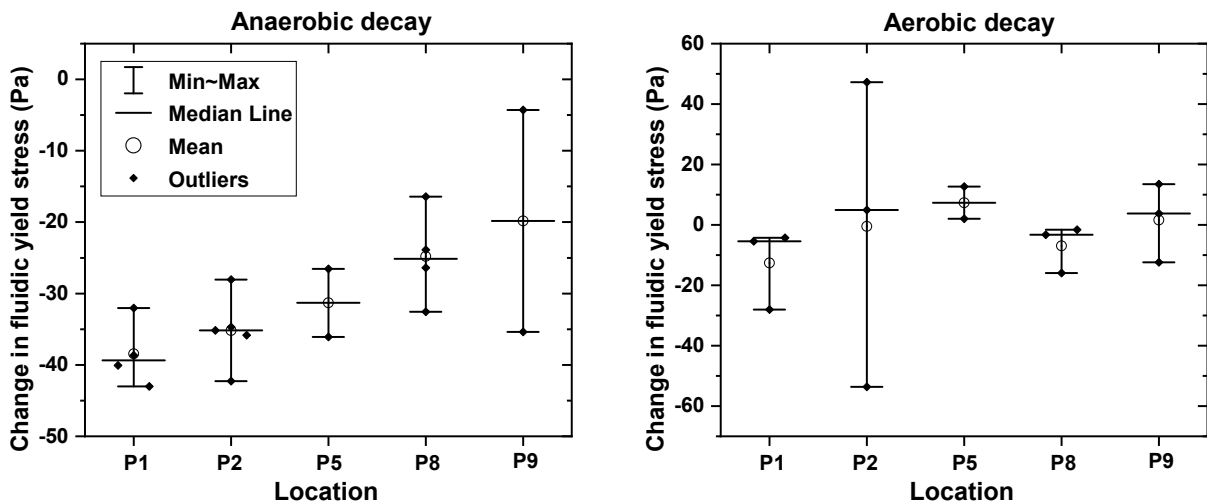


Figure 32 Change in fluidic yield stresses $\Delta\tau_f$ (Eq. 1) after SOM decay (250 days) for consolidated (CS) layers from 2019 under anaerobic conditions (left) and under aerobic conditions (right) for location P1, P2, P5, P8 and P9.

The higher the extent of anaerobic SOM decay, the larger the change in fluidic yield stresses (Figure 33). This pattern remained similar for different incubation times (21 and 250 days), during which the magnitude of change in fluidic yield stress did not change anymore. The largest spread in yield stress response to SOM decay as well as its decline appeared to result from cumulative decay of up to about 10 mg C g_{TOC}⁻¹ (21 days) and 60 mg C g_{TOC}⁻¹ (250 days), and remained on a low level beyond these thresholds. The yield stress decreased by 4 to 43 % of the initial value (all incubation times) with a cumulative SOM decay between 3 to 29 mg C g_{TOC}⁻¹ (21 days), and 30 to 121 mg C g_{TOC}⁻¹ (250 days). For FM and PS layers these trends were less pronounced, for aerobically decayed samples, these trends were not seen.

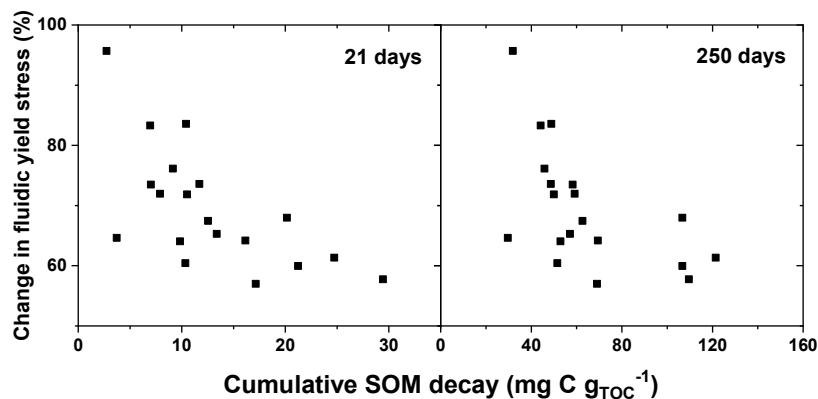


Figure 33 Relationship between cumulative anaerobic SOM decay of CS layers from 2019 after 21 and 250 days and the relative change in fluidic yield stresses (degraded – fresh, in % of the yield stress of the fresh sample, Eq. 3) upon SOM decay (250 days).

8.4 Discussion

8.4.1 General effects of SOM decay on static and fluidic yield stresses

Exhaustive decay of the degradable share of sediment organic matter led to a significant reduction in yield stresses, evidenced by a strong decrease in static and fluidic yield stresses. The effect was more pronounced for decay under anaerobic than under aerobic experimental conditions. In situ, mainly anaerobic conditions prevailed, caused by high oxygen consumption rates in the top few mm of the sediment deposit (Spieckermann, 2021) and evidenced by negative redox potentials (Zander et al., 2020 and Table S1, supporting information). Hence, SOM degradation in the bulk sediment occurs under anaerobic conditions, leading to the release of carbon as CH₄ and CO₂. Both anaerobic and aerobic SOM decay clearly led to a significant decrease in yield stresses (Figure 29), however, under aerobic conditions the effect was less pronounced and more scattered. It is hypothesized that the decrease in yield stresses upon SOM decay has a biological and a physical component, with microbial breakdown of organic bridging between particles reducing particle-particle interactions and presence of gas resulting from anaerobic decay causing the physical effect of decreasing bulk density, leading to further decline in yield stress. The later was supported by Jommi et al. (2019) who found that the presence of gas must be accounted for when studying the reduction in shear stresses by organic matter decay. It was found that the SOM decay caused a significant decrease in the rheological properties including yield stress, crossover amplitude, complex modulus and thixotropic hysteresis area (Shakeel et al., unpublished data). For the given data set, the changes in density during the period of incubation

observed in this study were only minor, which means that the detected changes in the rheological behavior are not caused by changes in the material's density.

In literature, higher yield stress values of fine grained sediments were typically associated to either higher density or higher organic matter content (Van Kessel and Blom; 1998; Soltanpour and Samsami, 2011; Xu and Huhe 2016; Shakeel et al., 2019; 2020a; Shakeel et al., unpublished data) with organic matter assumed to result in a stronger structure, i.e. higher yield stresses, of fine-grained sediment (Shakeel et al., 2019). Shear stresses of long-term incubated (250 days) samples correlated best with long-term SOM degradability, seen in Figure 33 (right), where anaerobic SOM decay led to larger change in fluidic yield stresses. During the initial decay of 10 or 60 mg C g_{TOC}^{-1} (corresponding to 21 or 250 days of incubation), the yield stresses decreased with an increasing amount of SOM degraded. The variability is assumed to be due to the variable amount of (easily) degradable SOM in the sample. When SOM decay progressed beyond this threshold, the yield stress did no longer decrease but remained on a low level. It is therefore concluded that the initial SOM decay is most relevant for the yield stress change, breaking up the organic bridging between particles (for a conceptual model see Shakeel et al., 2020b). In a parallel study investigating the structural recovery of sheared samples, it could be shown that after breakdown of SOM the samples exhibit a better recovery after shearing (Shakeel et al., unpublished data). This is due to the fact if the SOM bridges are broken, the elastic properties of the samples are greatly reduced, and, in line with what is observed for sediment samples without organic matter, these samples can fully recover their pre-shearing state. This corroborates the findings of this study that the decline in yield stresses is an effect of the initial phase of SOM breakdown, weakening or destroying organic bridging between mineral particles.

While the top fluidic sediment layers (FM) show the lowest absolute yield stress change, their average relative change upon SOM degradation was slightly larger than for the other layers but also scattered the most (Figure 31). Reasons for the large scatter of the more liquid (FM) layers could be the variable degree of aging (in situ SOM decay) of FM layers and therefore changing properties during the year, or dredging interventions such as water injection dredging (WID) that lead to the formation of WID-induced FM with a different behavior than undisturbed, naturally formed FM layers. Moreover, FM layers are highly affected by the water movement (tide, large vessels, etc.). These FM layers also contain the highest share of organic carbon in the light density fraction, SOM degradability and SOM pools (Zander et al (a), unpublished data), corroborating the relevance of easily degradable organic matter for the effects of SOM decay on the rheological behavior of sediments. This is also supported by the absolute decrease in yield stresses as a response to SOM degradation from upstream (P1) to downstream (P9) locations (shown for consolidated layers in Figure 33), coinciding with decreasing patterns of SOM degradability, microbial biomass, and an increase of carbon bound in the hardly degradable heavy density fraction (Zander et al (b), unpublished data). The more dense layers (i.e. CS layers) showed the largest change between the initial and the decayed yield stress (Figure 31). This appears plausible as more consolidated sediments have more mass, and hence more degradable carbon per unit volume than less consolidated or fluidic sediments, leading to a higher absolute reduction of yield stresses. Jommi et al. (2019) described that gas in peat layers led to a dramatic reduction of the mobilized (load below maximum) shear strength, although the ultimate (maximum) shear strength was hardly affected.

Although the average mass removed by anaerobic SOM decay after 250 days was only 0.6% DM (15% SOM decay with 4% TOC per DM, Zander et al. (b), unpublished data), a strong decrease in yield stresses was observed. Interestingly, under aerobic conditions (0.8% DM), the influence of the SOM

decay on rheological properties was less, despite the absolute mass of SOM removed being higher (0.8%), supporting the assumption that the effect of gas bubbles formed under anaerobic conditions being responsible for an added physical effect, causing a further decline in yield stresses. Under aerobic conditions, precipitation of iron and manganese oxides supporting cementation processes and therefore the stabilization of particles. This was assumed to lead to larger shear stresses of the aerobically incubated sediments.

8.4.2 Seasonal and spatial trends

The ratio between the initial yield stresses and the change in yield stresses of anaerobically incubated samples showed a linear trend for each sampling date (see Figure 30, left), assuming that yield stresses were influenced by the seasonally changing boundary conditions affecting content and quality of organic matter, such as input of fresh SOM, SOM degradability, sedimentation rates or dredging. Schoel et al. (2014) found seasonally changing (easily degradable) algae biomass concentrations in the Elbe River and it were observed seasonal changes in easily degradable SOM pools (Zander et al. (b), unpublished data). The more negative slopes of changes in yield stress upon SOM decay over yield stress of the freshly sampled sediments in 2019 compared to 2020 (Figure 30, left) suggest that in 2019, the sediments in the investigation area contained a larger share of easily degradable organic matter. Although locations P2 and P8 showed similar TOC and clay content (Table S1), they showed different behavior in yield stresses due to their different amount of easily degradable organic matter available at these locations. At upstream location P2, a larger share of upstream driven SOM reached this location compared to the more downstream-input driven location P8 (also explained in Zander et al., 2020). At upstream locations, a higher concentration of algae in the water column, represented by the chlorophyll a concentration (Zander et al. 2020) was detected, the measured degradability of SOM was higher, and a larger share of the light density fraction was found. Therefore, it is assumed that a larger share of easily degradable SOM, i.e. low molecular weight substances like cellulose and a smaller share of slowly degradable SOM, i.e. high molecular substances like lignin, are present at upstream locations.

The spatial trends of the yield stress change (Figure 32) coincide with the known stratification of organic matter degradability, with higher degradability in upstream locations and lower degradability in downstream samples. For all locations, the slopes for the ratio between the initial yield stresses and the change in yield stresses of anaerobically incubated samples were negative (Figure 30, right), meaning the SOM decay led to a decrease in yield stresses. Upstream locations (P1 and P2) had the most negative slopes, and showed the greatest absolute changes in yield stress for consolidated layers (Figure 32, left), reflecting the higher share of easily available organic matter and the largest amount of degradable carbon at these sites (Zander et al. (b), unpublished data). Per location, the slopes of the lines, correlating the change in fluidic yield stress (degraded – initial) and the initial fluidic yield stress varied within the range of -0.12 and -0.41 (Figure 30, right). This shows that the influence of organic matter degradation on sediment strength differs per sampling location, too. At the upstream locations (P1 and P2), more easily degradable SOM was available (Zander et al. 2020), and therefore, the differences of the fluidic yield stress between fresh and degraded samples was larger (Figure 32).

8.5 Conclusions and outlook

This study showed that under anaerobic conditions, shear strengths were decreased strongly after microbial SOM decay, whereas the effect under aerobic conditions was lower, in spite of the fact that the absolute amount of organic matter decayed under aerobic conditions was higher. It is concluded

that this effect reflects the combination of the biological effect of SOM degradation and the physical effect of entrapment of gas bubbles in the sediment, furthering the reduction of strength. Degradation of organic matter significantly affects sediment strength, especially under the anaerobic conditions prevailing in situ, even when the mass of organic matter removed is only little, here around 0.6% of dry matter. The effect sets in predominantly in the initial phases of degradation, which are assumed to be responsible for the break-down of organic bridging between mineral particles, thereby reducing the particle-particle interactions. A larger absolute change in yield stresses was seen with increasing depth, with gassy consolidated (CS) layers showing the largest decrease in yield stresses, owing to the fact that more consolidated sediments contain more mass, and hence degradable carbon per unit volume. CS layers showed the most distinct spatial trend, i.e. the decreasing change in static and fluidic yield stresses from upstream to downstream, coinciding with a gradient of decreasing SOM degradability. Hence, larger changes in yield stresses were seen at locations with high SOM decay, highlighting site-specific response of the rheological behavior due to site-specific availability of degradable organic matter. Seasonal trends with all sites along the transect following similar trends were also found, indicating that the investigation area as a whole is impacted by temporally changing factors such as the availability of easily degradable organic matter.

Acknowledgements

This study was funded by Hamburg Port Authority and carried out within the project BIOMUD and RHEOMUD, members of the MUDNET academic network www.tudelft.nl/mudnet/. Deltares is acknowledged for the use of the HAAKE MARS I rheometer. The authors thank dr. Susan Buisma-Yi for proofreading the manuscript.

Conflict of interest statement

The authors have no conflict of interest to disclose.

References

- Baldock JA, Skjemstad JO (2000) Role of the soil matrix and minerals in protecting natural organic materials against biological attack. *Organic Geochem* 31:697-710. [https://doi.org/10.1016/S0146-6380\(00\)00049-8](https://doi.org/10.1016/S0146-6380(00)00049-8)
- Deng Z, He Q, Safar Z, Chassagne C (2019) The role of algae in fine sediment flocculation: In-situ and laboratory measurements. *Mar Geol* 413:71–84. <https://doi.org/10.1016/j.margeo.2019.02.003>
- Gao J, Mikutta R, Jansen B, Guggenberger G, Vogel C, Kalbitz K (2019) The multilayer model of soil mineral-organic interfaces – a review. *J Plant Nutr Soil Sci* 000:1–15. <https://doi.org/10.1002/jpln.201900530>
- Jommi C, Muraro S, Trivellato E, Zwanenburg C (2019) Experimental results on the influence of gas on the mechanical response of peats. *Géotechnique* 69(9):753–766. <https://doi.org/10.1680/jgeot.17.P.148>
- Lagaly G, Dékány I (2013) Chapter 8 - Colloid Clay Science. In: Bergaya F, Lagaly G (Editors), *Developments in Clay Science*. Elsevier, 243-345.
- Schoel A, Hein B, Wyrwa J, Kirchesch V (2014) Modelling water quality in the Elbe and its estuary – Large Scale and Long Term Applications with Focus on the Oxygen Budget of the Estuary. *Die Kueste* 81:203–232. <https://hdl.handle.net/20.500.11970/101692>. Accessed on 6th December 2021
- Shakeel A, Kirichek A, Chassagne C (2019) Is density enough to predict the rheology of natural sediments? *Geo-Mar Lett* 39:427-434. <https://doi.org/10.1007/s00367-019-00601-2>
- Shakeel A, Kirichek A, Chassagne C (2020a) Rheological analysis of mud from Port of Hamburg, Germany. *J Soil Sediment* 20:2553-2562. <https://doi.org/10.1007/s11368-019-02448-7>
- Shakeel A, Kirichek A, Chassagne C (2020b) Yield stress measurements of mud sediments using different rheological methods and geometries: An evidence of two-step yielding. *Marine Geol* 427:106247. <https://doi.org/10.1016/j.margeo.2020.106247>
- Shakeel A, Zander F, de Kerk J-W, Kirichek A, Gebert J, Chassagne C (2022) Effect of organic matter degradation in cohesive sediment: A detailed rheological analysis. *J Soil Sediment* doi.org/10.1007/s11368-022-03156-5 (accepted for publication 30 January 2022)
- Six J, Paustian K (2014) Aggregate-associated soil organic matter as an ecosystem property and a measurement tool. *Soil Biol Biochem* 68:A4-A9. <https://doi.org/10.1016/j.soilbio.2013.06.014>
- Soltanpour M, Samsami F (2011) A comparative study on the rheology and wave dissipation of kaolinite and natural Hendijan Coast mud, the Persian Gulf. *Ocean Dynamics* 61:295-309. <https://doi.org/10.1007/s10236-011-0378-7>
- Spieckermann MJ (2021) Controls of Oxygen Consumption of Sediments in the Upper Elbe Estuary. Dissertation. University of Hamburg. *Hamburger Bodenkundliche Arbeiten* 101. ediss.sub.uni-hamburg.de/handle/ediss/9129. Accessed on 6th December 2021

- Van Kessel T, Blom C (1998) Rheology of cohesive sediments: comparison between a natural and an artificial mud. *J Hydraul Res* 36:591-612. <https://doi.org/10.1080/00221689809498611>
- Vannote RL, Minshall WG, Cummins KW, Sedell JR, Cushing CE (1980) The river continuum concept. *Can J Fish Aquat Sci* 37:130–137. <https://doi.org/10.1139/f80-017>
- Wurpts R, Torn P (2005) 15 years experience with fluid mud: definition of the nautical bottom with rheological parameters. *Terra et Aqua: International Journal on Public Works, Ports and Waterways Developments*
- Xu J, Huhe A (2016) Rheological study of mudflows at Lianyungang in China. *Int J Sediment Res* 31:71-78. <https://doi.org/10.1016/j.ijsrc.2014.06.002>
- Zander F, Heimovaara T, Gebert J (2020) Spatial variability of organic matter degradability in tidal Elbe sediments. *J Soil Sediment* 20:2573-2587. <https://doi.org/10.1007/s11368-020-02569-4>
- Zander, F., Comans, R.N.J., Gebert, J. (2022a) Linking patterns of organic matter, density, thermometric and carbon stable isotope fractions to organic matter lability in sediments of the tidal Elbe river. (submitted to *Appl Geochem*)
- Zander, F., Gröngroft, A., Eschenbach, A., Heimovaara, T., Gebert, J. (2022b) Organic matter pools in sediments of the tidal Elbe river. (accepted for publication on 8 June 2022)

Supplementary material

Table S1 Average material properties for the mainly observed locations (P1, P2, P5, P8, P9) for PS layers from 2019 and 2020.

	P1	P2	P5	P8	P9
Sample n	6	16	6	19	1
TN (%)	0.9	0.5	0.3	0.4	0.3
TOC (%)	6.3	4.0	3.7	3.8	2.4
WC (%DM)	449	371	314	331	216
Dry weight (%)	18	23	25	24	32
Eh (meV)	-277	-255	-259	-261	-200
Clay (< 2 μm , %)	41	43	39	41	31
Silt (2 - 63 μm , %)	54	51	49	50	42
Sand (> 63 μm , %)	5	7	12	8	27
Density-bulk (g cm^{-3})	1.29	1.37	1.40	1.38	1.51
pH (-)	7.1	7.4	7.3	7.3	7.3
Silicic acid ($\text{mg kg}_{\text{DM}}^{-1}$)	140	78	69	76	41
EPS ($\text{g kg}_{\text{DM}}^{-1}$)	32	24	28	26	2

TN total nitrogen, TOC total organic carbon, WC (%DM) water content in % dry matter, Eh redox potential, EPS extracellular polymeric substance

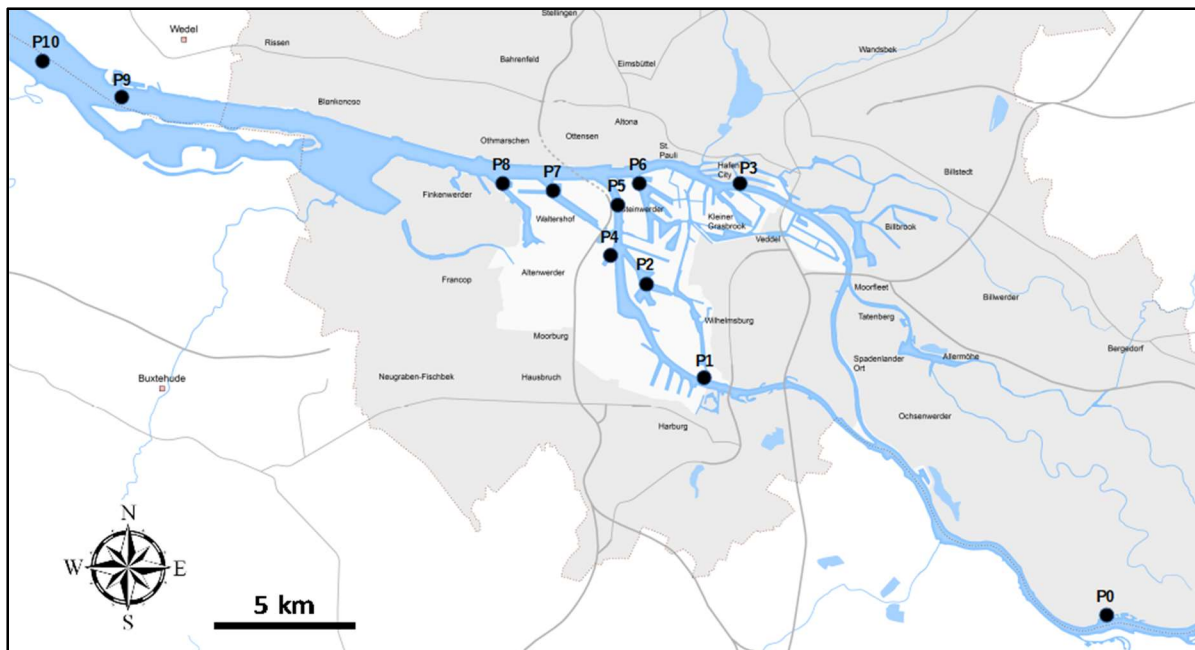


Figure S2 Investigation area around the Port of Hamburg (adapted from Hamburg Port Authority) with sampling locations between river km 598 (P0, upstream) and 646 (P10, downstream). Further information on sampling sites and sampling strategy in Zander et al. (2020).

9 Temporal variability of SOM decay

9.1 Introduction

The input of planktonic biomass into the system varies over the season and was approximated by the concentration of chlorophyll measured in the water column. In this chapter it will be analysed whether the temporal variability of the input of easily degradable planktonic biomass reflects in the degradability of sediment organic matter. The data of chlorophyll a were provided by water quality measurements of the public sector (Hamburg Serviceportal). The chlorophyll measuring locations were at Bunthaus (near location P0, see chapter 6.2) and at Seemannshöft (near location P8). Data about the dissolved organic matter was provided by limnological institute dr. Nowak. Further data were measured by TU Delft.

9.2 Results

Near upstream location P0, the chlorophyll a concentration (Figure 34, left) peaked in spring for all years (2018 to 2020) at around $200 \mu\text{g l}^{-1}$ whereas near location P8, the chlorophyll a concentration peaked between $40 \mu\text{g l}^{-1}$ (2020) and $60 \mu\text{g l}^{-1}$ (2018). The water temperature was similar for both sampling locations (P0 and P8), peaking in summer for all years (2018 to 2020) at around 25°C and dropped in winter to about 0°C (2018) to 5°C (2020).

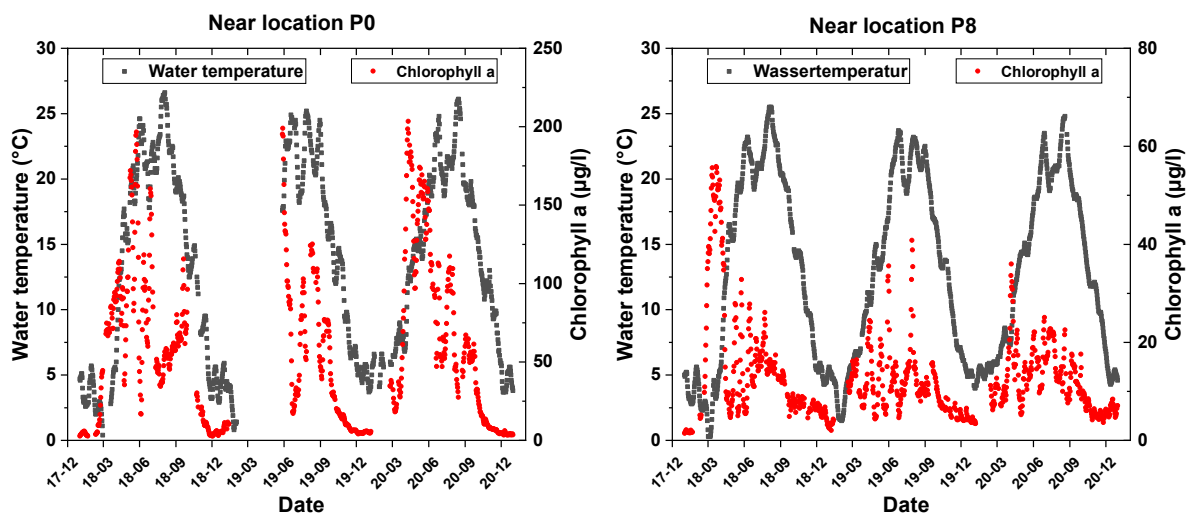
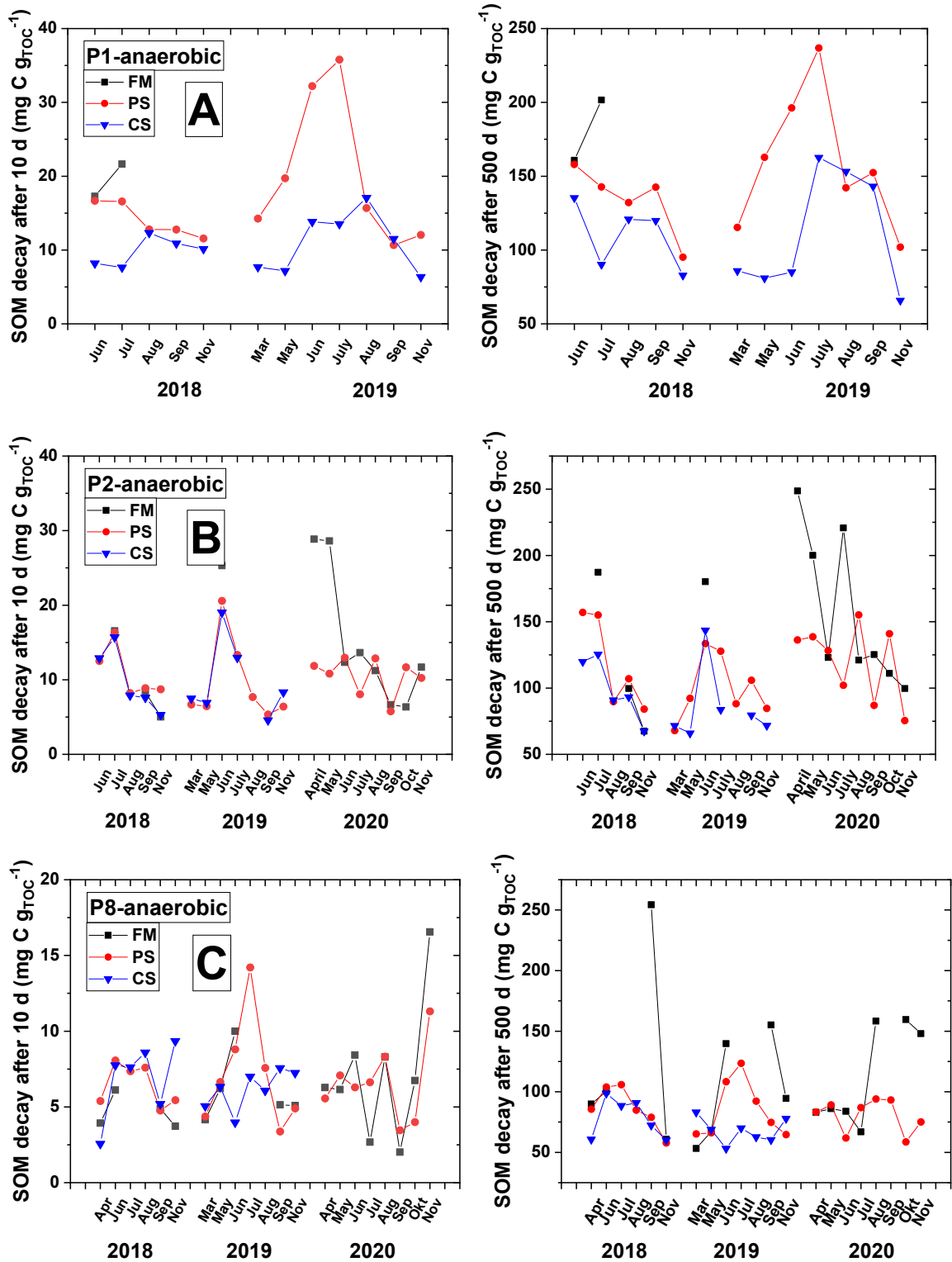


Figure 34 Temporal variability of the water temperature and the chlorophyll a near location P0 and P8, note the different right y-axes for chlorophyll a, data from Hamburg Serviceportal (2021).

Figure 35 shows the SOM decay after short-term (10 days) and long-term (500 days) anaerobic SOM decay for upstream locations P1 and P2 and downstream locations P8 and P9. Often, the anaerobic SOM decay peaked in summer (Figure 35). For some locations, the anaerobic SOM decay increased from spring to early summer (March to July) and decreased to the end of the year (November). For anaerobic SOM decay at location P1, a site with the least disruption in terms of dredging interventions and vessel traffic, PS and CS layers showed a clear pattern for 2019 with a peak in SOM degradability in July or August (Figure 35, A). For short-term anaerobic decay (10 days), the differences in the amount of SOM decay between summer and autumn were larger than for long-term SOM decay (500 days). In July, $35 \text{ mg C g}_{\text{TOC}}^{-1}$ were degradable and in September, $10 \text{ mg C g}_{\text{TOC}}^{-1}$ were degradable. After 500 days of incubation the SOM decay dropped from 240 to $100 \text{ mg C g}_{\text{TOC}}^{-1}$ from July to November (both Figure 35, A). To the end of the year 2020, the anaerobic SOM decay increased strongly by five-fold at location P2 (Figure 35, B) and by ten-fold at location P8 (Figure 35, C). The increasing trend of SOM decay at locations P2 and P8 in 2020 were less pronounced after the long-term decay (500 days of incubation,

Figure 35, B and C, left) compared to the short-term decay (10 days, Figure 35, B and C, right). In general, the upper sediment layers (FM and PS) showed a larger SOM decay than the lower CS layers. Some sediment layers were not present at some sampling dates; this was most often the case for FM layers. Aerobically incubated samples (not shown) showed a similar behaviour than anaerobically incubated samples.



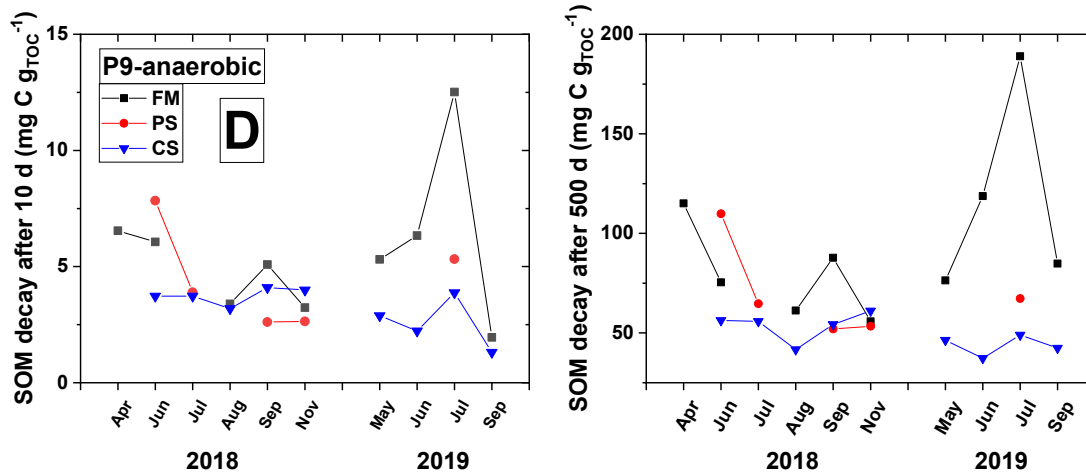


Figure 35 Temporal variability of anaerobic SOM decay after 10 and 500 days for FM, PS and CS layers from 2018-2019 (location P1 and P9) and from 2018-2020 (location P2 and P8).

In September 2020 for PS layers at upstream location P2, the DOC concentration was 220 mg l⁻¹ compared to around 100 mg l⁻¹ in June 2019 and July 2020 and to about 30 mg l⁻¹ in August and October 2020 (Figure 36, left). Therefore, the DOC concentration was about seven fold higher compared to baseline DOC concentrations and about twice as high compared to other peaked summer DOC concentrations at location P2. The same was true for the DOC concentration of the FM and PS layers at downstream location P8 in July 2020 with concentrations of about 80 mg l⁻¹ in July 2020 compared to about 30 to 40 mg l⁻¹ in April and May 2020 (Figure 36, right). This trend was also seen in 2019 at location P2 for PS layers with the DOC concentration increasing about three fold from in average 30 mg l⁻¹ to 100 mg l⁻¹ (Figure 36, left).

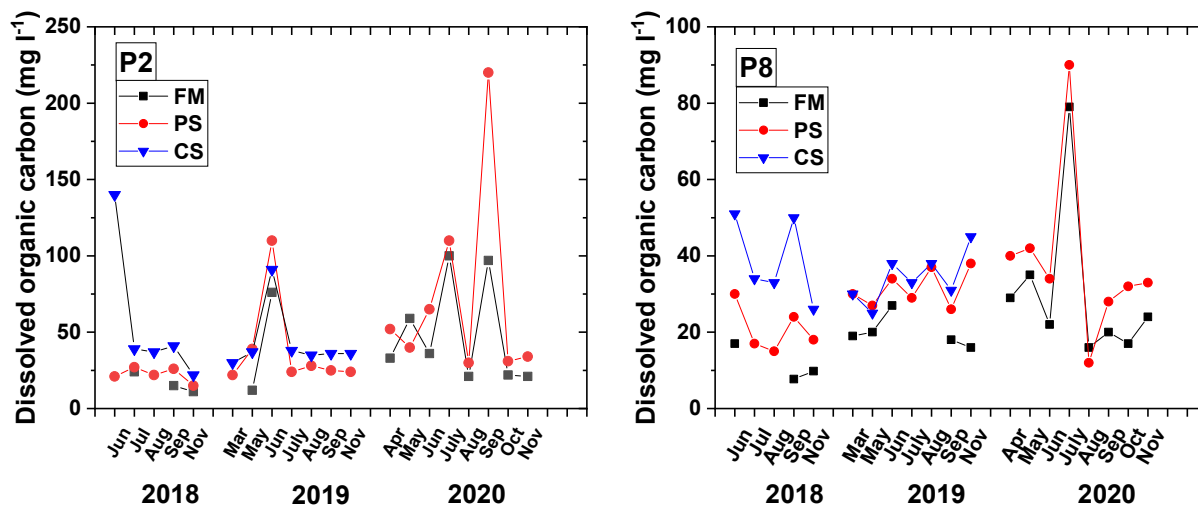


Figure 36 Dissolved organic carbon (DOC) concentration for FM, PS and CS layers from 2018-2020 at location P2 and P8.

9.3 Discussion

Seasonal trends, similar at all sampling sites along the investigated transect, indicate that the investigation area as a whole was affected by seasonal factors such as the availability of easily degradable organic matter. The SOM decay was affected by seasonally changing parameters like temperature, headwater and organic matter supply. For both aerobic (not shown) and anaerobic decay, clear patterns of temporal variability were observed with largest SOM decay in summer, dropping to autumn and winter (Figure 35). These results fit with the outcome of Zander et al. (2020);

2022a; 2022b) indicating the strong spatial variation of the input of labile organic matter. These patterns can be explained by the input of fresh, easily degradable SOM from upstream in spring and early summer, transported from terrestrial soils with the current into the harbour area (i.e., leaves, litter, nutrients from agricultural soils). Beside low primary production, light deficits led to lower SOM decay in winter (Kamjunke et al., 2021). Liu et al. (2015) investigated the distribution and sources (terrestrial and marine) of sediment organic matter in surface sea sediments and found that autochthonous organic matter was the dominant contribution to marine primary production. Lambert et al. (2017) found that land use was a major driver on fluvial organic matter composition at the regional scale of the Meuse Basin. Deininger and Friegstad (2019) also recognized terrestrial organic matter as a strong driver of aquatic productivity. The effect of land use on the Elbe River has been investigated by many researchers, among them Kersebaum et al. (2003), Heese and Krysanova (2016), Radinger et al. (2016) and Bierschenk et al. (2019).

The increase in anaerobic SOM decay in 2020 at location P8 (Figure 35, C) could neither be explained by the concentration of chlorophyll a nor by the temperature (Figure 34), excluding a higher input of fresh, biogenic organic matter as a possible cause of increased gas production potential. Also, aerobic carbon release did not show increased levels (data not shown). It is therefore assumed that the sampling sites received additional input of material with increased anaerobic enzymatic hydrolysis capacity. A possible cause could lie in the begin of capital dredging associated with the deepening of the Elbe River fairway, leading to increased disturbance and mobilization of sediment organic matter from other locations into the water phase and the ensuing settlement of this material in the sampled locations. The widening and deepening of the fairway near location P9 took place in spring and summer 2020. In May and June 2020, dredging work at location P8 caused turbidity in the water phase and activated sediment organic matter, presumably leading to larger SOM decay in summer and autumn (Hamburg Port Authority, 2021a). Moreover, from May 2020 on more dredging activity than usual happened in the whole harbour area with three Hopper dredgers, two Hopper barges and one large deep spoon dredger in use (Hamburg Port Authority, 2021a). This procedure resulted in sediment relocation in the downstream part of the Elbe River. Further, a lot of dredging activities happened for fairway deepening in the approaching area of the port. This led to increased sediment movement and further to an enhanced organic matter concentration in the water phase (DOC, Figure 35). The DOC concentration increased first in July 2020 at downstream locations P7 and P8 (Figure 36, centre and right) and two months later at upstream location P2 (Figure 36, left). This strengthened the hypothesis that artificial sediment movement increased the DOC concentration at downstream location. Further, the tide transported DOC in upstream direction. In 2019, an increased DOC concentration (Figure 36, left) possibly led to an increased SOM decay for all three layers (FM, PS, CS) at location P2 (Figure 35, B).

9.4 Conclusion

A clear temporal variability of the SOM decay was found. This was caused by changes in temperature, light level, input of easily degradable organic matter (phytoplankton) and large dredging maintenances, namely, the mobilization of easily degradable SOM.

10 Carbon flux in the Port of Hamburg

10.1 Introduction

Data on the degradability of sediment organic matter, its kinetics and the dependence on temperature can be used to estimate carbon fluxes from the investigation area, based on known sedimentation rates and in situ temperatures. These fluxes provide one aspect of the total carbon budget and can also be used in estimating for carbon-foot printing of port maintenance activities. Here, the carbon flux calculation focusses on the organic matter output, in other words, the flow from organic matter from the sediment to the atmosphere (solid to gas phase). Two fractions of degradable carbon are distinguished. Firstly, the *potentially* degradable carbon, using extrapolated laboratory data on exhaustive degradation of sediment organic matter (Zander et al., 2020), in other words, the maximum share of degradable carbon. Secondly, an estimation of the *actually* degradable carbon, considered SOM decay over one year (365 days) at the respective water temperature (Figure 39, Figure 40 and Table 9). The sediment temperature could be slightly different than the water temperature (measured near the water surface). The focus laid on the anaerobically degradable carbon fraction, because anaerobic conditions are prevailing in situ (Zander et al., 2020).

10.2 Approach

The values for SOM degradability of PS layers were taken from average values of the laboratory incubation experiments for the respective location (for an example, see Zander et al., 2020; 2022b). PS layers were chosen, because they were the most common layers in the harbour area, representing a rough average of the four layer system. The laboratory incubation values were adapted by the averaged in situ water temperatures per month according to the known temperature dependency of anaerobic SOM decay (Li, 2019). The temperature response under aerobic and anaerobic conditions for several temperatures is displayed in Figure 37. For the calculation, the first 365 days of the data in Figure 37 were used, with temperatures between roughly 5 and 20 °C as seen in Figure 40, right.

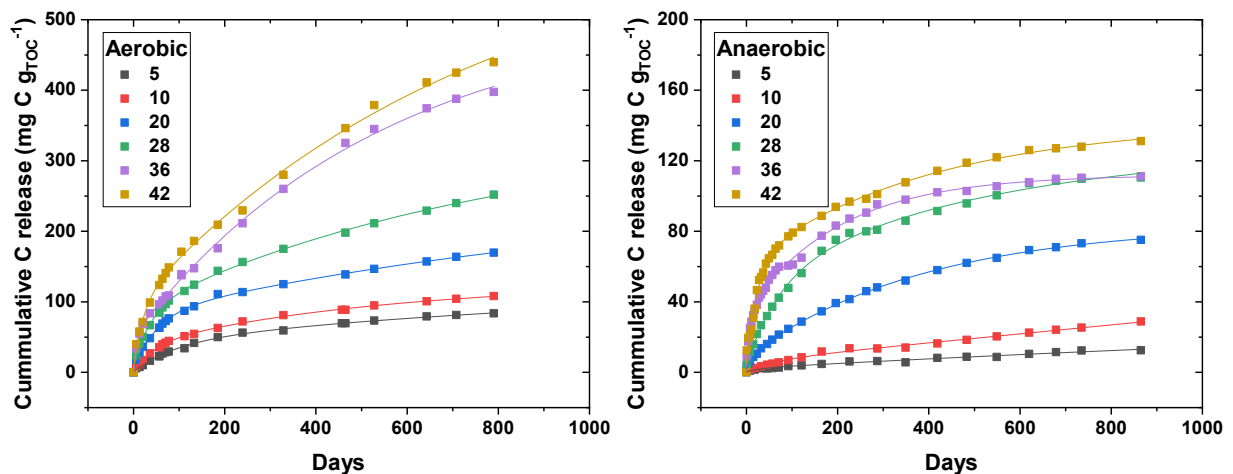


Figure 37 Cumulative carbon release for various temperatures (i.e., 5, 10, 20, 28, 36, 42 °C) under aerobic (left) and anaerobic (right) conditions.

According to Hamburg Port Authority (2021a), the sedimentation rates in the harbour area are the highest in May. Moreover, the chlorophyll concentration led to the assumption that the largest input of fresh, biogenic sediment organic matter enters the investigated locations in late spring (Figure 34). Therefore, the 1st of May was chosen for the first day of SOM decay. From day 1 (1st of May) to day 365 (30th of April), successive aging of the organic matter aging as evidenced by asymptotically declining degradation rates (Zander et al., 2020) was considered as well as the monthly changing water

temperature. New sedimentation of organic matter was not considered. The simplified approach for carbon flux estimation leads to smaller calculated carbon fluxes compared to in situ fluxes. In situ, the input of fresh sediment organic matter in months with high temperatures would lead to higher in situ carbon fluxes as calculated in chapter 10.3. The total mass of new sediments in the whole harbour area in 2020, as provided by Hamburg Port Authority (2021b, Table 9), was chosen as one-time input quantity. For the calculation of carbon released per mass unit of sediment, an exemplary mass of 100,000 t sediments were chosen for the locations P1 and P9 (Table 10). The number of samples per location is displayed in Table 7. Figure 38 and Table 9 show data from the potentially and actually degradable carbon.

Table 8 Number of samples per location for sediment organic matter decay from 2018 to 2020 for PS layers, samples used for the carbon flux calculation in chapter 10.3.

Location	Sample n SOM decay
P0	6
P1	13
P2	22
P3	5
P4	6
P5	12
P6	6
P7	13
P8	27
P9	5
P10	4

10.3 Results

Figure 38 shows a spatial gradient of cumulative potentially degradable carbon in PS layers from 2018 to 2020. Figure 38 and Figure 39 display the actual average of anaerobically degradable carbon for PS layers from 2018 to 2020 with consideration of the monthly water temperature (Figure 40, right). Table 9 considers both, potentially and actual SOM decay.

The TOC content per location varied between 2 % (location P9) and 7 % (location P1, both Figure 38, Zander et al., 2020). At upstream location P1, 42.8% of the TOC was degradable, namely 27.3% of TOC aerobically and 15.5% of TOC anaerobically (Zander et al., 2022b). 33% of TOC was anaerobically easily degradable, namely 21.5% of TOC aerobically and 11.5% of TOC anaerobically (pool 1). Whereas at downstream location P9 18.9% of the TOC was degradable (12.0% of TOC aerobically and 6.9% of TOC anaerobically, no easily degradable fraction). Comparing the redox state of the described analyses, the share of anaerobically degradable SOM for PS layers was about 39.5% whereas the share of aerobically degradable SOM was about 60.5%. The potentially aerobically degradable share of SOM was about 1.5 fold larger than the anaerobically degradable share.

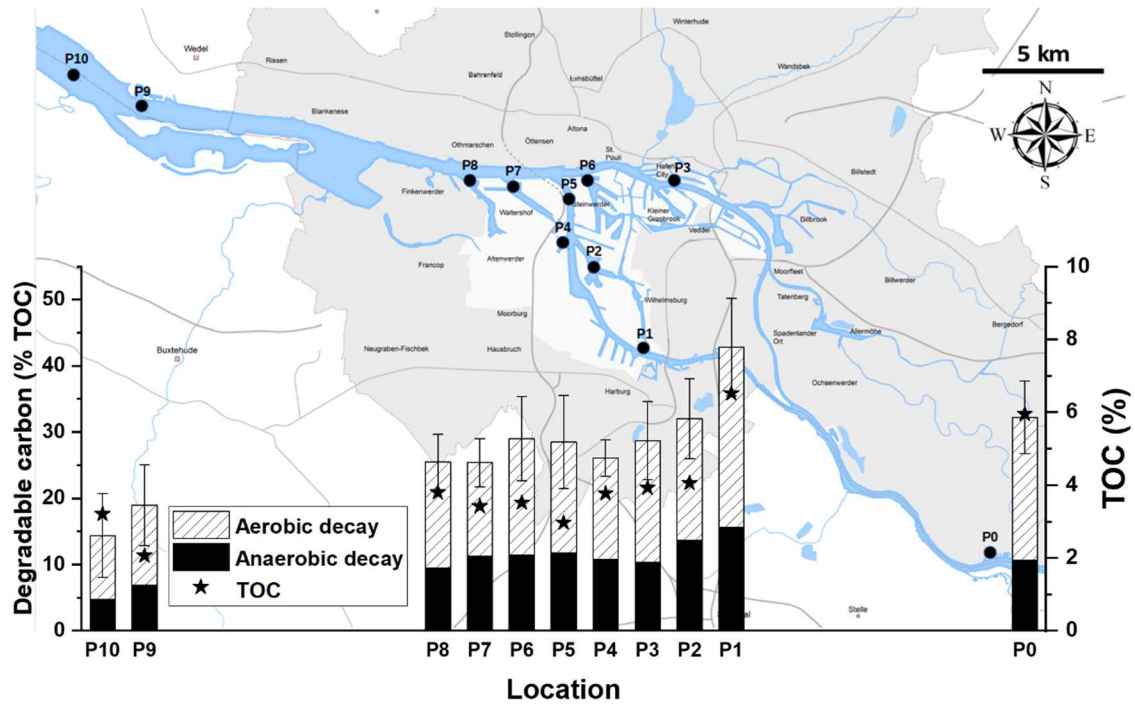


Figure 38 Sum of total (aerobically and anaerobically) cumulative degradable carbon (% TOC) for PS layers from 2018 to 2020 in the Port of Hamburg, stars show the average TOC content (% , right y-axis) error bars show the standard deviation for the sum of aerobic and anaerobic decay, number of samples per location are displayed in Table 2.

The spatial gradient of anaerobic SOM decay (Figure 39) showed a decrease from upstream location P0 to downstream location P10. In chapter 5, spatial gradients found in the harbour area are described. Sediments at location P1 showed three-fold larger potential SOM decay than sediments at location P10. During the months May, June and July, about two-thirds of the calculated cumulative anaerobically degradable carbon was decayed (Figure 39 and Figure 40, left), owing to the elevated water temperatures in combination with the presence of the easily degradable organic matter pool 1.

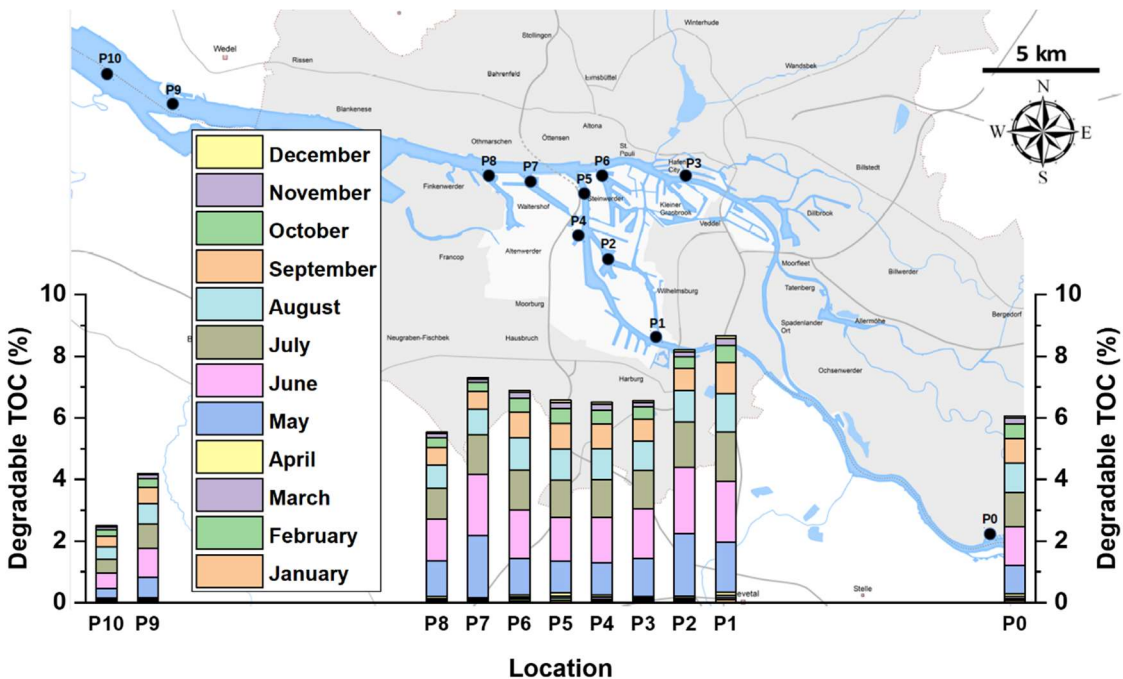


Figure 39 Sum of calculated cumulative anaerobically degradable carbon (% TOC) for one year (365 days) per month for PS layers from data between 2018 and 2020 with consideration of the monthly temperature (Figure 40, right), number of samples per location are displayed in 10.2.

The temporal changes of degradable SOM (Figure 40, left) clearly showed highest SOM decay in spring and summer decreasing to winter. In June, about 16 % of the TOC was degradable whereas in February only 0.5 % of TOC was degradable. After one year (365 days), about 61 % (2.5 % TOC of 4.1 % TOC) of the total potentially degradable carbon was degraded at location P9 (Figure 40, right) considering the in situ water temperature. The turquoise curve of the actual SOM decay increases similarly to the potential SOM decay until October, reaching a state of slight increase of SOM decay until April. The considered water temperature was the highest in August (above 20 °C) and decreased to 3 °C in January. The temperature was above 15 °C in May to September (Figure 40, right).

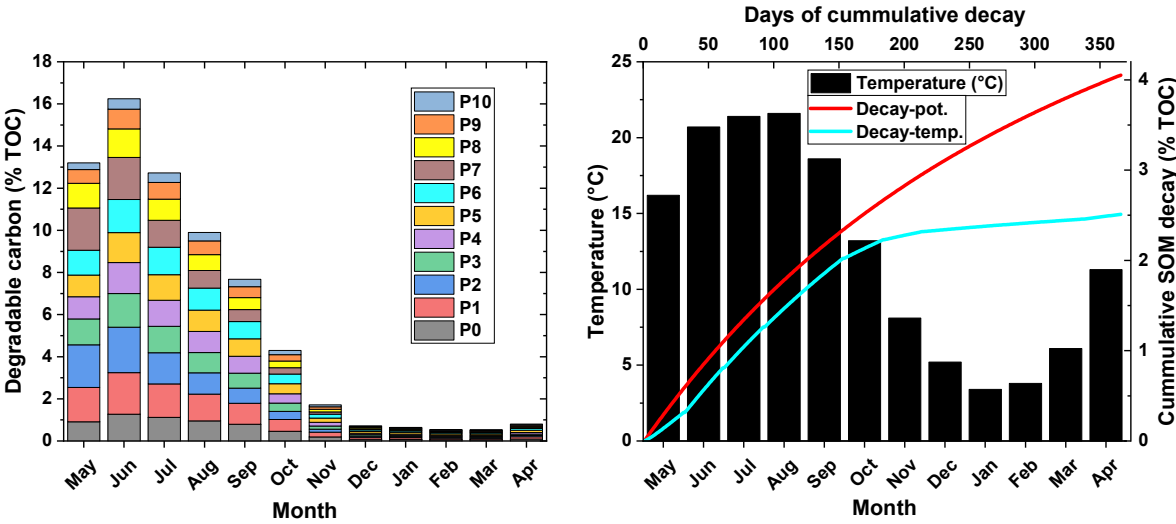


Figure 40 Left: Anaerobically cumulative degradable carbon (% TOC) for PS layers from 2018 to 2020 per month, considering the in situ temperature and the input of fresh SOM (in May), number of samples per location are displayed in Table 2. Right: Average monthly water temperature for the harbour area from 2015 to 2020 (bars, Hamburg Serviceportal, 2021) and potential (red line) as well as temperature-corrected SOM decay (turquoise line) at location P9.

The quantification of degradable carbon was performed exemplarily for the locations P1 and P9 considering the monthly water temperature. At upstream location P1, on average three times more carbon was potentially degradable (75 kg C m^{-3}) than at downstream location P9 (24 kg C m^{-3}). In total, about 44,500 t carbon were potentially degradable at a given dredged amount of 3,900,000 t sediments dry matter (DM) in 2020 (Hamburg Port Authority, 2021b). Considering SOM degradability per location, the mass of degradable carbon was about seven-fold larger at upstream location P1 compared to downstream location P9 (2,791 t C to 390 t C, Table 9). 10,465 t carbon were anaerobically degraded in the harbour area in one year. Therefore, the actual mass of anaerobic carbon emissions for one year was about one-fourth of the potential total carbon emissions (44,479 t C). The mass of degradable carbon was about seven-fold larger at upstream location P1 compared to downstream location P9 (565 t C to 86 t C, Table 9).

Table 9 Exemplary calculation of total potentially degradable carbon in the harbour area for a chosen amount of dredged sediment (HPA, 2021) with consideration of the degradability for location P1 and P9, both for PS layers from 2018 to 2020 and exemplarily calculation of the carbon emission by anaerobic SOM decay for one year with consideration of the monthly water temperature. DM dry matter, TOC total organic carbon, sample n and temperature shown in Table 8 and Figure 40.

Parameter	Number	Unit
Density	1.15	t m ⁻³
Volume sediments port, total	3,900,000	t DM
Exemp. volume sediments, P1	100,000	t DM
Exemp. volume sediments, P9	100,000	t DM
TOC, P1	6.5	% DM
TOC, P9	2.1	% DM
TOC port average, n = 121	4.0	% DM
<u>Total potentially degradable carbon</u>		
Degradable, TOC, P1	42.8	% TOC
Degradable, TOC, P9	19.0	% TOC
Degradable, TOC port average	28.5	% TOC
Degradable, P1	75	kg C m ⁻³ DM
Degradable, P9	24	kg C m ⁻³ DM
Degradable, port average	46	kg C m ⁻³ DM
Degradable, P1	2,791	t C
Degradable, P9	390	t C
Degradable, port average	44,479	t C
<u>Anaerobically degradable carbon in one year</u>		
1-year decay, P1	8.7	% TOC
1-year decay, P9	4.2	% TOC
1-year decay, port average	6.7	% TOC
1-year decay, P1	565	t C
1-year decay, P9	86	t C
1-year decay, port average	10,465	t C

10.4 Discussion

The largest shares of potentially degradable carbon (Figure 38) as well as actual degradable carbon (Figure 39, Figure 40 and Table 9) were found at upstream locations as described in Zander et al. (2020; 2022b). The spatial variability of degradable carbon is summarized in chapter 11.1. The locations P0 and P10 (Figure 38), upstream and downstream of the Port of Hamburg, showed a smaller amount of potentially degradable SOM compared with the (inner) harbour locations P1 and P9 which represent older, seldom dredged sediments. This leads to stronger (anaerobically) degraded SOM at locations P0 and P10 and therefore a lower share of easily degradable SOM measured in laboratory. The lower share of degradable SOM at P0 and P10 (Figure 38) was caused by less regular dredging maintenance and higher in situ SOM decay.

Knowing that in situ a strong increase in degradable SOM from May onwards was calculated (Figure 40) in relation to the assumed sedimentation of the total mass at one point in time in the beginning of May. The resulting time sequence of C fluxes is distorted as, of course, sedimentation and hence the decay of freshly settled SOM start before and continue after the 1st of May. The large share of actually degradable SOM in May to July (Figure 39 and Figure 40, left) can be explained by the higher temperatures (above 20 °C in June to August, Figure 40, right). This causes faster SOM decay as determined by temperature experiments given in Zander et al. (2022a). Further, the input of fresh SOM in spring is shown by the increasing chlorophyll a concentration (Figure 34). The decay gap between the potential and actual SOM decay after one year of SOM degradation (Figure 40, right) is a result of the low temperatures in autumn and winter (November to March). Moreover, the already aged organic matter showed lower SOM decay rates with time (Zander et al., 2020; 2022b). The large share of degradable carbon from May to July (Figure 40) fit well with the temporal results from Figure 35 (chapter 9), showing the largest SOM decay in summer. The actual anaerobically degradable mass carbon (Table 9) supported the spatial trends observed in Zander et al. (2020). They found up to seven fold larger mass of degradable carbon for location P1 compared to location P9.

10.5 Conclusion

The temperature corrected SOM decay was about 60% of the potential SOM decay within one year (location P9). From December to April, the SOM decay was more than 10-fold smaller than during summer, namely May to August. The calculated SOM flux was dependent on the input of easily degradable organic matter and on the in situ temperature. Moreover, other temporally changing parameters, as described in chapter 9, can influence the SOM decay (e.g., light deficits).

11 Overarching summary

In this chapter, the main findings are summarized and the generic research questions presented in chapter 2 are answered. Figure 41 illustrates the overarching findings.

11.1 Spatial variability of sediment organic matter decay

The input of easily degradable SOM into the harbour area was driven by upstream headwater and, to a lower share, from downstream tide (compare chapter 1.6). The carbon flux analyses (chapter 9.3) showed spatial gradients of total degradable SOM than described in Zander et al. (2020; 2022b). The investigation area was a transect of 30 river kilometres though the Elbe River around the Port of Hamburg. The area was characterised by a distinct gradient of sediment abiotic properties and organic matter lability, with higher degradability upstream and lower degradability downstream. The decrease of the biological parameters chlorophyll a (reflecting phytoplankton biomass), microbial biomass, silicic acid concentration, EPS concentration and oxygen consumption indicated a change in organic matter composition from upstream to downstream. SOM lability decreased from upstream to downstream, evidenced by an increased share of total SOM found in the acid-base-extractable fractions downstream. The light density fractions decreased strongly with older, more decayed and hence stabilized organic matter. The light density fraction decreased also from upstream to downstream, indicating the degraded state of the SOM at downstream locations.

The enrichment of ^{13}C in the organic matter at downstream locations strengthened the hypothesis of already degraded organic matter dominating at downstream locations. The hypothesis was also supported by the large enrichment of ^{13}C in long-term laboratory-decayed samples that indicated a higher extent of SOM decay. Thermometric pyrolysis (Rock Eval 6©) confirmed the trends indicated by the stable carbon isotope signatures and patterns in extractable SOM fractions. The Hydrogen Index, a proxy for more labile organic matter, related well to SOM decay rates. The I-index represents immature organic fraction and the R-index the stabilized fraction or persistent SOM (Sebag et al., 2006). The relationship between both indices supported the findings that a significant share of SOM was bound in organo-mineral complexes. These complexes showed an increased share of SOM at downstream locations. The slowly degradable pool 3 was assumed to be associated to more particle bound SOM. Pool 3 was spread more or less equally along the investigated transect and concluding a basis of hardly available SOM at all locations. Total degradability thus appears to be governed by the amount of SOM present in addition to this basis, which in turn follows a source gradient and an age gradient from upstream to downstream. The recalcitrant pool 4 was the largest pool in any part of the harbour and for both anaerobic and aerobic conditions.

The findings of this study are in line with the river continuum concept, presented by Vannote et al. (1980). For natural streams, the concept describes a temporal continuum of biological communities from headwater to mouth of the river. For shallow and eutrophic upstream parts of the Elbe River, Schoel et al. (2014) found super-saturation with oxygen due to enhanced net primary production. In the downstream part of the river, Schoel et al. (2014) described oxygen minimum zones induced by zooplankton decaying algal biomass and leading to light-deficiency.

Summary of the main differences between upstream and downstream locations

At *upstream locations*, sediments and organic matter predominantly originated from the Elbe catchment (i.e., location P0 and P1 were nourished primarily from upstream fluvial sediments). Upstream locations showed an additional greater share of autochthonous organic matter (planktonic biomass), earmarked by a lighter organic carbon (less ^{13}C). Upstream locations were characterised by

a higher concentration of DNA, a higher share of organic carbon in the light density fraction and lower $\delta^{13}\text{C}$ values. The suspended particulate matter contained more easily degradable components such as algal biomass. This was supported by higher chlorophyll a concentrations in the water column and reflected by a higher share of total mass in the sediment's lighter density fraction. The degradability was the largest at upstream locations, evidenced by the largest share of the easily degradable pool 1. It was assumed that a larger share of low molecular substances (i.e., cellulose) and a smaller share of high molecular substances (i.e., lignin) were found at upstream location. The gradient in the Zn concentration in the particle size fraction of $< 20 \mu\text{m}$ indicated that the upstream locations P0 and P1 being fed primarily from upstream fluvial sediments, whereas the other locations carried a stronger downstream signature as described in Kappenberg and Fanger (2007, in Beusekom et al., 2021).

At *downstream locations*, organic matter is mainly of allochthonous origin, entering the harbour mainly with the tidal flood current from the direction of the North Sea. Downstream, a higher level of mineralization and therefore of stabilization of the input organic matter was found. This is evidenced by an increased share of organic carbon bound to the mineral phase as well as by a lower aerobic and anaerobic degradability. The degradability was the lowest at downstream locations, evidenced by the lowest share of the easily degradable pool 1.

The *upper sediment layers* showed the highest amount of young organic matter and therefore the largest SOM degradability. Nevertheless, the upper layers showed a large share of the poorly degradable pool 3 and stabilized organic matter pool 4. Organic matter in the investigated system was already significantly degraded or stabilized in organo-mineral associations. This was also true for suspended and fluidic particle phases.

11.2 Influence of SOM decay on rheology under different redox conditions

Shakeel et al. (2019) found that not only the sediment density should be considered to predict the rheology of different mud. The sediment density is not the only parameter influencing the yield stress but also the share of organic matter.

The SOM degradability was larger under aerobic conditions compared to anaerobic conditions, as expected from recent literature. Degradation of organic matter significantly affected sediment strength, especially under anaerobic conditions. Although the mass of organic matter removed was little, here around 0.6% of dry matter, the decrease in sediment strength was significant. On average the decrease amounted to 70% for static yield stress under anaerobic conditions (chapter 8.3.1). Thus, in terms of nautical conditions, with increasing organic matter decay, the rheological conditions improve. In spite of the fact that the absolute amount of organic matter decayed aerobically was higher, shear strengths were lowered strongly after anaerobic SOM decay. Under aerobic conditions, precipitation of iron and manganese oxides support cementation processes and therefore the stabilization of particles leading to larger shear stresses. This was evidenced by the change of colour of the aerobically incubated sediment from dark grey to brown. The initial phases of degradation were assumed to be responsible for the break-down of organic bridging between mineral particles, thereby reducing the particle-particle interactions. This was seen in Figure 33 (left), displaying the strong decrease in yield stress already after 21 days. The SOM decay reduced the organic matter concentration and led to an entrapment of gas bubbles. Therefore, the SOM decay affected the shear strength biologically, chemically and physically.

A larger absolute change in yield stresses was seen with increasing depth. Gassy consolidated (CS) layers showed the largest absolute decrease in yield stresses. The relative changes for CS layers were similar to other layers. More consolidated sediments contained more mass and hence degradable

carbon per unit volume. CS layers showed the largest change in static and fluidic yield stresses from upstream to downstream, coinciding with a gradient of decreasing SOM degradability. Hence, larger changes in yield stresses were seen at locations with high SOM decay. Site-specific availability of easily degradable organic matter led to site-specific response of the rheological behaviour. Locations P2 and P8 had similar TOC and clay content (Zander et al., 2020). These locations showed different behaviour in yield stresses caused by different amounts of easily degradable organic matter available at these locations.

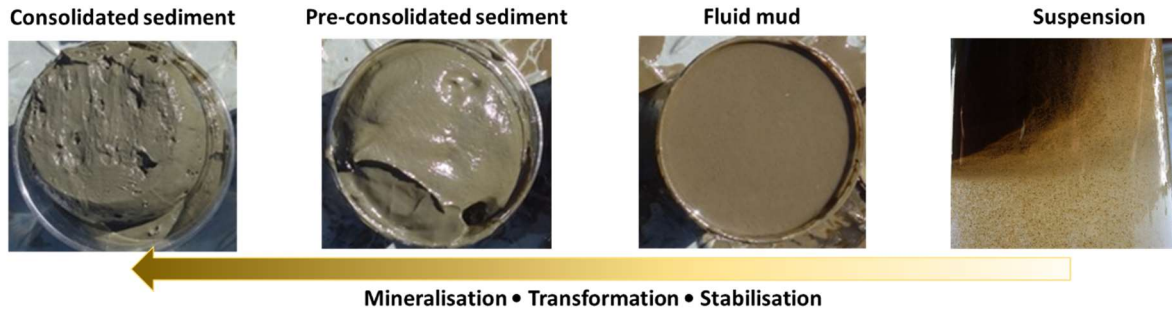
11.3 Organic matter metamorphosis and organic matter pools

The sedimentation and consolidation processes occur in situ from top to bottom of the sediment surface as briefly described in Zander et al. (2020). Chapter 1.1 describes processes of organic matter mineralization and stabilization. Figure 41 shows the proposed transition and stabilization processes of sediment organic matter (here termed metamorphosis) from the state of the sediment as suspended particulate matter (SPM) to consolidated sediment (CS, right to left). Further, Figure 41 shows the organic matter metamorphosis from upstream to downstream as described in chapter 11.1. From upstream to downstream, more (stable) biomass is stored in organo-mineral complexes, the heavy density fraction, carbon pool 4, shear stresses and the share of stable carbon isotopes are increasing whereas the SOM degradability, light density fraction, carbon pool 1 and 2, hydrophilic DOC fraction and Hydrogen Index (immature SOM) are decreasing. The size of carbon pool 3 is constant.

Labile organic matter in the upper sediment layers is mostly stabilized into mineral-complexes in deeper sediment layers, protected against further degradation. This was evidenced by increased shares of organic carbon in the heavy density fraction (Zander et al., 2020; 2022a; chapters 0 and 0). Zander et al. (2020; 2022a) used different methods of organic matter quantification to describe chemical and physical organic matter properties in different states of organic matter decay. Density fractionation and thermometric pyrolysis (i.e., Hydrogen Index) can be used to classify the share of available organic matter. The light density fraction represents the readily biological available labile organic matter. The heavy density fraction represents the stable organic matter, bound in organo-mineral complexes.

Organic matter metamorphosis in sediments

A - Depth



B - Transect

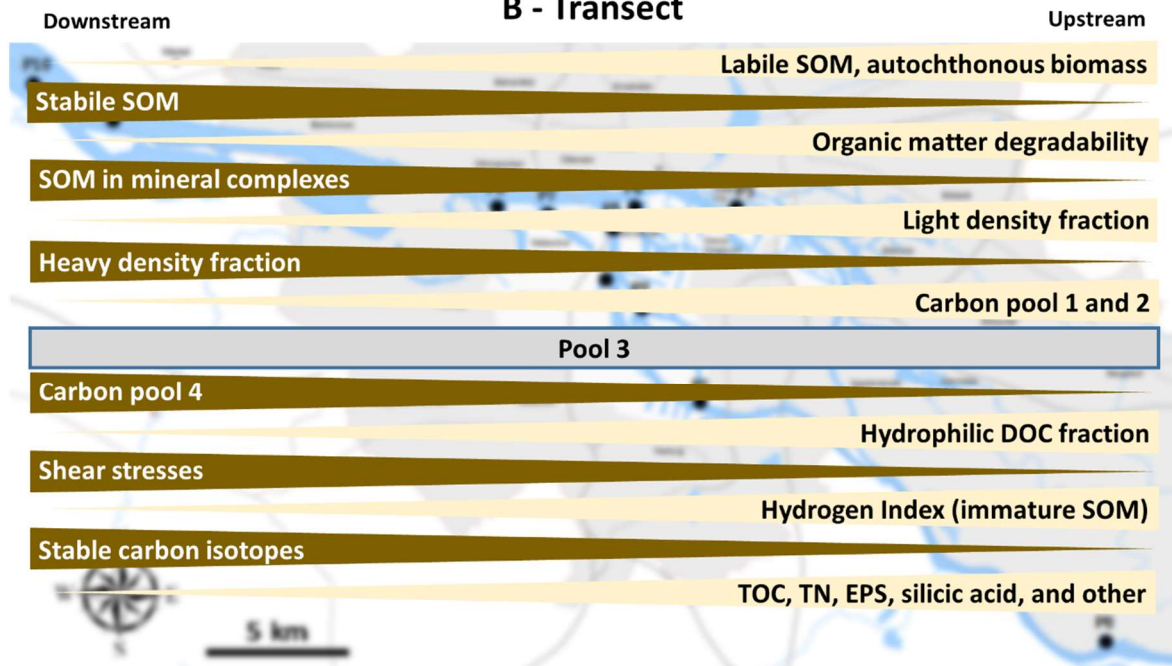


Figure 41: Schematic metamorphosis of sediment organic matter from suspension to consolidated sediment (A) as well as from upstream to downstream (B), adopted and added from Gebert (unpublished).

Zander et al. (2022b) described the quantification of labile and stabile organic matter using SOM decay rates to define differently degradable SOM pools, conceptually shown in Figure 42 (left). Total carbon (TC) separates into total inorganic carbon (TIC) and total organic carbon (TOC). Total organic carbon is found in a non-degradable (residual) and a degradable fraction. The degradable SOM was subdivided into three pools based on degradation rates: fast (pool 1), medium (pool 2) and slow (pool 3). The SOM degrade either aerobically or anaerobically, depending on in-situ conditions. While anaerobic and aerobic SOM pools overlap and cannot be viewed as separate entities, particular SOM shares do not degrade anaerobically but only under aerobic conditions. This was shown by higher total degradability of SOM under aerobic conditions (Zander et al. 2022b, chapter 7) were aerobically (larger share) and anaerobically (smaller share) degradable. Figure 42 (right) quantifies the size of these pools by example of average values for location P1 to P9.

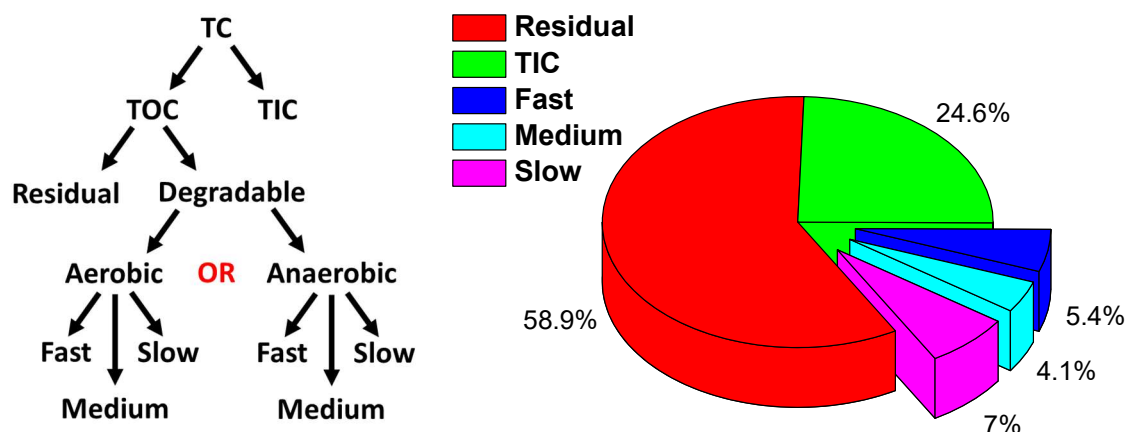


Figure 42: Schematic overview of carbon and organic matter pools (left) and exemplary shares (% TC) of the average organic matter (TOC) pools from location P1 to P9 for PS layers, samples from 2018 to 2020, data from Zander et al. (2022b) (right).

11.4 Answers to research questions

The anaerobic and aerobic degradation of organic matter in the investigation area showed pronounced spatial and seasonal patterns, both with respect to degradation rates, SOM pools, and physical and chemical SOM fractions (Zander et al., 2020; 2022a; 2022b). Also, a significant impact of SOM decay on the rheological properties was observed (Zander et al., 2022c; Shakeel et al., 2022a; 2022b). The characteristics of organic matter in the tidal harbour area of the Elbe River were described. Carbon fluxes were estimated as input for a carbon budget of the Port of Hamburg. The following overarching research questions (see also chapter 2) can be answered as follows:

1. Which spatial gradients are found in the Hamburg Port area?

Most of the easily degradable, plankton-derived sediment organic matter enters the harbour area from upstream. Older, more degraded organic matter originates from both, upstream and downstream sediments, namely, eroded soils or North Sea sediments. Short- and long-term SOM decay parameters (rates and pools) highlight the organic matter reactivity along the river transect with a larger recalcitrant organic matter pool at downstream areas. The share of organic matter that is stabilized in organo-mineral complexes increases towards downstream areas and also, at any one location, with age (depth). Conversely, upstream locations and upper sediment layers contain more easily degradable carbon. Analyses of DOM and density fractions, carbon stable isotopes and thermometric pyrolysis support the above mentioned trends of source and age gradient. The share of hydrophilic DOM decreasing in downstream direction, pool 1 and pool 2 are decreasing, light density fraction is decreasing whereas $\delta^{13}\text{C}$ values are increasing, pool 4 is increasing as illustrated in Figure 41. The following methods were considered as suitable to describe spatial variations of sediment and organic matter origin and properties, namely, the concentration of Zn in the particle size fraction $< 20 \mu\text{m}$, microbial biomass concentration of EPS, and the concentration of chlorophyll in the water phase.

2. What drives organic matter decay processes?

Labile organic matter enters the harbour mainly from upstream through algal biomass, adding a more rapidly degradable pool to the baseline pool of slowly degradable OM and the recalcitrant (non-degradable) pool. The SOM lability along the investigated transect is dependent on SOM origin and age. Chemical and physical organic matter fractions can be related to biological and physicochemical

sediment processes, namely, the hydrophilic DOC and the light density fraction to the upstream originated labile biomass as shown in Zander et al. (2022a). Dissolved organic matter (DOM) is a net product of organic matter decay, as seen from higher DOM concentrations with increasing incubation temperature and longer incubation time.

3. How can organic matter be classified in the harbour area?

Based on the biodegradation rates, reactivity of organic matter pools can be determined. The average degradable share of organic matter was about 25% of TOC (aerobic) and about 15% of TOC (anaerobic) with an averaged difference of about 10% of TOC. The size of the easily degradable organic matter pool 1 is about 10 to 15% of TOC. Most of the carbon in the harbour sediments is stored in a non-degradable form, indicated by the size of the recalcitrant pool 4 with about 75% to 85% of TOC. Spatial trends are seen in the highly reactive pool 1 (and pool 2) but not for the barely active pool 3, functioning as a baseline of slowly degradable organic matter that is present at in similar concentration in the entire investigation area.

4. What is the influence of organic matter decay on the rheological behaviour of sediments?

Yield stresses are strongly influenced by (anaerobic) organic matter decay. Already small extents of organic matter decay (i.e., carbon release of 0.6%DW) lead to large decreases of sediment yield stresses (i.e., on average about 70% for the static yield stress, SYS) due to proposed decrease of organic matter bridging between mineral particles. Yield stresses were dependent on spatial and seasonal trends of organic matter decay. Anaerobically decayed samples display greater changes in rheological properties than aerobically decayed samples. In view of the maintenance of the nautical depth, the state of organic matter decay influences the sediment strength and therefore the manoeuvrability of vessels in the Port of Hamburg.

5. What are the temporal patterns of biological parameters and organic matter decay in the investigated area?

A clear temporal variability is found for biological parameters such as chlorophyll a and silicic acid in the water column, representing the presence of fresh biomass (i.e. easily degradable organic matter) in the system and reflecting in a corresponding variability of organic matter degradation rates. The variability in net primary production upstream and hence SOM degradation rates within the Port of Hamburg can be explained by changes in light level and water discharge. The seasonal variability of in situ water and sediment temperature drive decay rates of the suspended and settled organic matter with the largest portion of the potential (i.e. degradable) annual carbon flux from SOM degradation being released in the months May to October.

12 Reflection and prospects of the research

For many estuaries, fundamental data gaps hamper the understanding of the connectivity of terrestrial, aquatic and marine carbon budgets (Ward et al., 2015). Estuaries should be better understood, because they can act as large carbon sources, relevant for global carbon budgets. The freshwater ecosystem in the Port of Hamburg should be incorporated in earth system models to understand terrestrial and marine organic matter degradation in freshwater bodies as suggested in Kothawala et al. (2021).

Combining analyses of organic matter decay with further microbial analyses (i.e., microbial biomass, EPS and DNA) will help understanding organic matter decay more deeply to reflect on differences in organic matter availability. Therefore, the composition of the microbial community can be investigated to enhance insight into the spatial composition of organic matter degrading microorganisms. Moreover, the diversity of microbial communities can be further analysed as done in Suominen et al. (2021), using DNA stable isotope probing incubation experiments.

Studying the effect of exposing anaerobic sediments to oxygen by dredging settled (i.e., anaerobic) sediments in the harbour can help to find answers for practical questions like the reduction of oxygen level by maintenance dredging.

For the improvement of maintenance dredging (moment and location of dredging) and the reduction of carbon emissions, a comprehensive carbon budget model for the Port of Hamburg should be implemented. Carbon budgets are not well represented in literature. The carbon flux analyses in chapter 9.3 gave first insights of a part of the total carbon budget. A comprehensive model should, however, consider terrestrial and marine carbon influx, net primary production, carbon storage and also out flux via the aqueous phase, as well as the biogeochemical boundary conditions. It is recommended to continue the investigation on organic matter in riverine sediments, connecting harbour maintenance with the environmental impact of organic matter decay.

Reflecting four years of doctoral work, it was helpful to decrease the amount of samples from 2018 to 2020. From 2019, there was more time to implement methods of further organic matter classification, namely, physical and chemical fractionation analyses. A stronger focus on international harbours in 2020 helped to get insight in the harbour management in other countries (i.e., Netherlands and Belgium).

References

- Adams JL, Tipping E, Thacker AS, Quinton JN (2018) An investigation of the distribution of phosphorus between free and mineral associated soil organic matter, using density fractionation. *Plant Soil* 427:139–148. doi.org/10.1007/s11104-017-3478-4
- Arndt S, Jørgensen BB, LaRowe DE, Middelburg JJ, Pancost RD (2013) Quantifying the degradation of organic matter in marine sediments: A review and synthesis. *Earth Sci Rev* 123:53-86. doi.org/10.1016/j.earscirev.2013.02.008
- Asaoka S, Jadoonb WA, Umeharac A, Takedad K, Otanie S, Ohnof M, Fujitakeg N, Sakugawad H, Okamura H (2020) Organic matter degradation characteristics of coastal marine sediments collected from the Seto Inland Sea, Japan. *Marine Chemistry* 225, 103854. doi.org/10.1016/j.marchem.2020.103854
- Baldock JA, Skjemstad JO (2000) Role of the soil matrix and minerals in protecting natural organic materials against biological attack. *Org Geochem* 31:697-710. doi.org/10.1016/S0146-6380(00)00049-8
- Berg B, McClaugherty C (2020) *Plant Litter*. Berlin Heidelberg Springer-Verlag. doi.org/10.1007/978-3-030-59631-6
- van Beusekom J, Sanders T, Fehling D, Schulz G, Minutolo F, Neumann A, Bold S, Dähnke K (2021) Long-term SPM dynamics in the Elbe estuary and adjacent coastal zone: Interactions with phytoplankton underestimated? *Helmholtz-Zentrum Geestacht. Mudnet conference 2021*
- Bierschenk AM, Mueller M, Pander J, Geist J (2019) Impact of catchment land use on fish community composition in the headwater areas of Elbe, Danube and Main. *Science of the Total Environment* 652: 66–74. doi.org/10.1016/j.scitotenv.2018.10.218
- Blume HP, Brümmer GW, Fleige H, Horn R, Kandeler E, Kögel-Knabner I, Kretschmar R, Stahr K, Wilke B-M, Scheffer F, Schachtschabel P (2016) *Soil Science*. Berlin Heidelberg Springer-Verlag. doi.org/10.1007/978-3-642-30942-7
- Boehlich MJ, Strotmann T (2008) *The Elbe Estuary*. Die Küste 74. Heide, Holstein: Boyens. S. 288-306.
- Burd AB, Frey S, Cabre A, Ito T, Levine NM, Lønborg C, Long M, Mauritz M, Thomas RQ, Stephens BM, Vanwalleghem T, Zeng N (2016) Terrestrial and marine perspectives on modeling organic matter degradation pathways. *Global Change Biology* 22, 121–136. doi.org/10.1111/gcb.12987
- Catalán N, Marcé R, Kothawala DN, Tranvik LJ (2016) Organic carbon decomposition rates controlled by water retention time across inland waters. *Nat Geosci* 9. doi.org/10.1038/NGEO2720
- Cheeke TC, Coleman DC, Wall DH (2016) *Microbial Ecology in Sustainable 122 Soil Biology & Biochemistry* 98:109-126 *Agroecosystems*. CRC Press, Boca Raton.
- Cui X, TS Bianchi, JA Hutchings, C Savage, JH Curtis (2016) Partitioning of organic carbon among density fractions in surface sediments of Fiordland, New Zealand. *J Geophys Res Biogeosci* 121:1016–1031. doi:10.1002/2015JG003225
- Datta R, Kelkar A, Baraniya D, Molaei A, Moulick A, Meena RS, Formanek P (2017) Enzymatic Degradation of Lignin in Soil: A Review. *Sustainability* 9:1163. doi.org/10.3390/su9071163
- Deininger A, Frigstad H (2019) Reevaluating the Role of Organic Matter Sources for Coastal Eutrophication, Oligotrophication, and Ecosystem Health. *Front. Mar. Sci.* 6:210. doi.org/10.3389/fmars.2019.00210

- Deng Z, He Q, Safar Z, Chassagne C (2019) The role of algae in fine sediment flocculation: In-situ and laboratory measurements. *Mar Geol* 413, 71–84. doi.org/10.1016/j.margeo.2019.02.003
- Devaux M-F, Jamme F, André W, Bouchet B, Alvarado C, Durand S, Robert P, Saulnier L, Bonnin E, Guillon F (2018) Synchrotron Time-Lapse Imaging of Lignocellulosic Biomass Hydrolysis: Tracking Enzyme Localization by Protein Autofluorescence and Biochemical Modification of Cell Walls by Microfluidic Infrared Microspectroscopy. *Front Plant Sci* 20. doi.org/10.3389/fpls.2018.00200
- Diochon A, Gillespie AW, Ellert BH, Janzen HH, Gregorich EG (2016) Recovery and dynamics of decomposing plant residue in soil: an evaluation of three fractionation methods. *European J Soil Sci* 67:196–205. doi10.1111/ejss.12316
- Dittmar T (2015) Reasons Behind the Long-Term Stability of Dissolved Organic Matter. *Biogeochemistry of Marine Dissolved Organic Matter*. dx.doi.org/10.1016/B978-0-12-405940-5.00007-8
- Fageria NK (2012) Role of Soil Organic Matter in Maintaining Sustainability of Cropping Systems. *Communications in Soil Science and Plant Analysis* 43(16):2063-2113. doi.org/10.1080/00103624.2012.697234
- Fernandes P, Souza AT, Tanaka M, Sebastiani R (2020) Decomposition and stabilization of organic matter in an old-growth tropical riparian forest: effects of soil properties and vegetation structure. *Research S*. doi.org/10.1186/s40663-021-00293-0
- Frouz J (2018) Effects of soil macro- and mesofauna on litter decomposition and soil organic matter stabilization. *Geoderma* 332:161–172. dx.doi.org/10.1016/j.geoderma.2017.08.039
- Gao J, Mikutta R, Jansen B, Guggenberger G, Vogel C, Kalbitz K (2019) The multilayer model of soil mineral–organic interfaces—a review. *J Plant Nutr Soil Sci* 000:1–15. doi.org/10.1002/jpln.201900530
- Gebert J, Köthe H, Gröngroft A (2006) Prognosis of Methane Formation by River Sediments. *J Soil Sediments* 6(2):75–83. doi.org/10.1065/jss2006.04.153
- Geerts L, Cox TJS, Maris T, Wolfstein K, Meire P, Soetaert K (2017) Substrate origin and morphology differentially determine oxygen dynamics in two major European estuaries, the Elbe and the Schelde. *Estuar Coast Shelf S* 191, 157-170. doi.org/10.1016/j.ecss.2017.04.009
- Gerbersdorf SU, Jancke T, Westrich B, Pasterson DM (2008) Microbial stabilization of riverine sediments by extracellular polymeric substances. *Geobiology* 6:57–69. doi.org/10.1111/j.1472-4669.2007.00120.x
- Grasset S, Moras S, Isidorova A, Couture R-M, Linkhorst A, Sobek S (2021) An empirical model to predict methane production in inland water sediment from particular organic matter supply and reactivity. *Limnol Oceanogr* 9999 1–13. doi.org/10.1002/lno.11905
- Hafen Hamburg (2021) hafen-hamburg.de/de/special/fahrrinnenanpassung/. Accessed: 9th December 2021
- Hamburg Port Authority (2021a) Personal communication on 10-12-2021.
- Hamburg Port Authority (2021b) Wassertiefenstandhaltung im Hamburger Hafen. Jahresbericht 2020. Internal document.
- Hamburg Serviceportal (2021) serviceportal.hamburg.de/HamburgGateway/. Accessed: 20th November 2021

- Hansell DA, Carlson CA, Repeta DJ, Schlitzer R (2009) Dissolved organic matter in the ocean: a controversy stimulates new insights. *Oceanography* 22, 202–211. www.jstor.org/stable/24861036
- Hayes MHB, McCarthy P, Malcolm RL, Swift RS (1989) *Humic Substances II in search of structure*. Wiley: New York
- Hayes MHB, Mylotte R, Swift RS (2017) Humin: Its Composition and Importance in Soil Organic Matter. *Advances in Agronomy* 143. [dx.doi.org/10.1016/bs.agron.2017.01.001](https://doi.org/10.1016/bs.agron.2017.01.001)
- Heese C, Krysanova V (2016) Modeling Climate and Management Change Impacts on Water Quality and In-Stream Processes in the Elbe River Basin. *Water* 8:40. doi.org/10.3390/w8020040
- Helfrich M, Flessa H, Mikutta R, Dreves A, Ludwig B (2007) Comparison of chemical fractionation methods for isolating stable soil organic carbon pools. *Eur J Soil Sci* 58:1316–1329. doi.org/10.1111/j.1365-2389.2007.00926.x
- Henin S, Turc L (1950) Studies in the fractionation of soil organic matter. *Transactions 4th Int. Cong. Soil Sci* 1:152-154. www.cabdirect.org/cabdirect/abstract/19501901354
- Heuck C, Spohn M (2016) Carbon, nitrogen and phosphorus net mineralization in organic horizons of temperate forests: stoichiometry and relations to organic matter quality. *Biogeochemistry* 131:229–242. doi.org/10.1007/s10533-016-0276-7
- Hoffland E, Kuyper TW, Comans RNJ, Creamer RE (2020) Eco-functionality of organic matter in soils. *Plant and Soil* 455:1–22. doi.org/10.1007/s11104-020-04651-9
- Jommi C, Murano S, Trivellato E, Zwanenburg C (2019) Experimental results on the influence of gas on the mechanical response of peats. *Géotechnique* 69(9):753–766. doi.org/10.1680/jgeot.17.P.148
- Kamjunke N, Rode M, Baborowski M, Kunz JV, Zehner J, Borchardt D, Weitere M (2021) High irradiation and low discharge promote the dominant role of phytoplankton in riverine nutrient dynamics. *Limnol and Oceano* 66:2648-2660.
- Kappenberg J, Fanger H-U (2007) *Sedimenttransportgeschehen in der tidebeeinflussten Elbe, der Deutschen Bucht und in der Nordsee*. GKSS report 2007/20; ISSN 0344–9629
- Ke Yaowei, Ning X-an, Liang J, Zou H, Sun J, Cai H, Lin M, Li R, Zhang Y (2018) Sludge treatment by integrated ultrasound-Fenton process: Characterization of sludge organic matter and its impact on PAHs removal. *J Hazardous Mat* 343:191–199. doi.org/10.1016/j.jhazmat.2017.09.030
- Kersebaum KC, Steidl J, Bauer O, Piorr H-P (2003) Modelling scenarios to assess the effects of different agricultural management and land use options to reduce diffuse nitrogen pollution into the river Elbe. *Physics and Chemistry of the Earth* 28:537–545. [doi.org/10.1016/S1474-7065\(03\)00090-1](https://doi.org/10.1016/S1474-7065(03)00090-1)
- Kögel-Knabner I (2000) Analytical approaches for characterizing soil organic matter. *Organic Geochemistry* 31:609-625. [doi.org/10.1016/S0146-6380\(00\)00042-5](https://doi.org/10.1016/S0146-6380(00)00042-5)
- Kögel-Knabner I, Guggenberger GM, Kleber M, Kandellar E, Kalbitz K, Scheu S, Eusterhaus K, Leinweber R (2008) Organo mineral associations in temperate soils: integrating biology, mineralogy and organic chemistry. *J.Plant Nutr.Soil Sci* 171:61-82. doi.org/10.1002/jpln.200700048
- Kögel-Knabner I, Rumpel C (2018) Advances in Molecular Approaches for Understanding Soil Organic Matter Composition, Origin, and Turnover: A Historical Overview. *Advances in Agronomy* 149:1-48. doi.org/10.1016/bs.agron.2018.01.003

- Kothawala DN, Kellerman AM, Catalán N, Tranvik LJ (2021) Organic Matter Degradation across Ecosystem Boundaries: The Need for a Unified Conceptualization. *Trends Ecology Evolution* 36:2. doi.org/10.1016/j.tree.2020.10.006
- Kristensen E, Ahmed, AI, Devol AH (1994) Aerobic and anaerobic decomposition of organic matter in marine sediment: Which is fastest? *Limnol Oceanogr* 40(8):1430-1437. doi.org/10.4319/lo.1995.40.8.1430
- Lagaly G, Dékány I (2013) Colloid Clay Science. *Dev. Clay Sci.* 5:243–345. doi.org/10.1016/B978-0-08-098258-8.00010-9
- Lambert T, Bouillon S, Darchambeau F, Morana C, Roland FAE, Descy J-P, Borges, AV (2017) *Biogeochemistry* 136:191–211. doi.org/10.1007/s10533-017-0387-9
- Lehmann J, Kleber M (2015) The contentious nature of soil organic matter. *Nature* 528. doi.org/10.1038/nature16069
- Li X (2019) Investigation of Gas Generation by Riverine Sediments: Production Dynamics and Effects of Sediment Properties. Master thesis TU Delft. <http://resolver.tudelft.nl/uuid:a56b5642-f1f8-4845-b24a-eea598967698>
- Li X, Lia Z, Zhangd X, Xiac L, Zhangf W, Maa Q, Hed H (2020) Disentangling immobilization of nitrate by fungi and bacteria in soil to plant residue amendment. *Geoderma* 374:114450. doi.org/10.1016/j.geoderma.2020.114450
- Li Z, Tian D, Wang B, Wang J, Wang S, Chen HYH, Xu X, Wang C, He N, Niu S (2019) Microbes drive global soil nitrogen mineralization and availability. *Glob Change Biol* 25:1078–1088. doi.org/10.1111/gcb.14557
- Lui D, Li X, Emeis K-C, Wang Y, Richard P (2015) Distribution and sources of organic matter in surface sediments of Bohai Sea near the Yellow River Estuary, China. *Estuarine, Coastal and Shelf Science* 165: 128-136. doi.org/10.1016/j.ecss.2015.09.007
- Liu Z, Xue J (2020) The lability and source of particulate organic matter in the northern Gulf of Mexico hypoxic zone. *J Geophys Res: Biogeosciences* 125 e2020JG005653. doi.org/10.1029/2020JG005653
- Von Lützw M, Kögel-Knabner I, Ekschmitt K, Flessa H, Guggenberger G, Matzner E, Marschner B (2007) SOM fractionation methods: Relevance to functional pools and to stabilization mechanisms. *Soil Biol Biochem* 39:2183–2207. doi.org/10.1016/j.soilbio.2007.03.007
- Malarkey J, Baas JH, Hope, J.A., Aspden RJ, Parsons DR, Peakall J, Paterson DM, Schindler RJ, Ye L, Lichtman ID, Bass SJ, Davies AG, Manning AJ, Thorne PD (2015) The pervasive role of biological cohesion in bedform development. *Nature Commun* 6:6257. doi.org/10.1038/ncomms7257
- Markgraf W, Watts CW, Whalley WR, Tomislav Hrkac T, Horn R (2012) Influence of organic matter on rheological properties of soil. *Applied Clay Science* 64:25–33. doi:10.1016/j.clay.2011.04.009
- Miryahyaei S, Olinga K, Ayub MS, Jayaratna SS, Othman M, Eshtiaghi N (2020) Rheological measurements as indicators for hydrolysis rate, organic matter removal, and dewaterability of digestate in anaerobic digesters. *Journal of Environmental Chemical Engineering* 8:103970. doi.org/10.1016/j.jece.2020.103970
- Mueller P, Schile-Beers LM, Mozdzer TJ, Chmura GL, Dinter T, Kuzyakov Y, de Groot AV, et al. (2017) Global Change Effects on Decomposition Processes in Tidal Wetlands: Implications from a Global

- Survey Using Standardized Litter. *Biogeosciences* 15:3189–3202. doi.org/10.5194/bg-15-3189-2018
- Nguyen TT, Marschner P (2016) Soil respiration, microbial biomass and nutrient availability in soil after repeated addition of low and high C/N plant residues *Biol Fertil Soils* 52:165–176. doi.org/10.1007/s00374-015-1063-7
- Parsons DR, Schindler RJ, Hope JA, Malarkey J, Baas JH, Peakall J, Manning AJ, Ye L, Simmons S, Paterson DM, Aspden RJ, Bass SJ, Davies AG, Lichtman ID, Thorne PD (2016) The role of biophysical cohesion on subaqueous bed form size. *Geophys Res Lett* 43:1566–1573. doi.org/10.1002/2016GL067667
- Paul EA (2016) The nature and dynamics of soil organic matter: Plant inputs, microbial transformations, and organic matter stabilization. *Soil Biol Biochem* 98:109-126. dx.doi.org/10.1016/j.soilbio.2016.04.001
- Plaza C, Giannetta B, Benavente I, Vischetti C, Zaccone C (2019) Density-based fractionation of soil organic matter: effects of heavy liquid and heavy fraction washing. *Scientific Reports* 9:10146. doi.org/10.1038/s41598-019-46577-y
- Poiriera V, Roumet C, Munson AD (2018) The root of the matter: Linking root traits and soil organic matter stabilization processes. *Soil Biol Biochem* 120:246–259. doi.org/10.1016/j.soilbio.2018.02.016
- Qiao N, Xu X, Hu Y, Blagodatskaya E, Liu Y, Schaefer D, Kuzyakov Y (2016) Carbon and nitrogen additions induce distinct priming effects along an organic-matter decay Continuum. *Scientific Reports* 6:19865. doi.org/10.1038/srep19865
- Rabalais NN, Diaz RJ, Levin LA, Turner RE, Gilbert D, Zhang J (2010) Dynamics and distribution of natural and human-caused hypoxia. *Biogeosciences* 7:585–619. doi.org/10.5194/bg-7-585-2010
- Radinger J, Hölker F, Horky P, Slavik O, Dendoncker N, Wolter C (2016) Synergistic and antagonistic interactions of future land use and climate change on river fish assemblages. *Global Change Biology* 22:1505–1522. doi.org/10.1111/gcb.13183
- Rahman MM, Castagneyrol B, Verheyen K, Jactel H, Carnol M (2018) Can tree species richness attenuate the effect of drought on organic matter decomposition and stabilization in young plantation forests? *Acta Oecologica* 93:30–40. doi.org/10.1016/j.actao.2018.10.008
- Reichenbach M, Fiener P, Garland G, Griepentrog M, Six J, Doetterl S (2021) The role of geochemistry in organic carbon stabilization against microbial decomposition in tropical rainforest soils. *Soil* 7:453–475. doi.org/10.5194/soil-7-453-2021
- Rice JA (2001) Humin. *Soil Science* 166:11. 0038-075C/01/16611-848–857
- Riggs CE, Hobbie SE, Bach EM, Hofmockel KS, Kazanski CE (2015) Nitrogen addition changes grassland soil organic matter decomposition. *Biogeochemistry* 125:203–219. doi.org/10.1007/s10533-015-0123-2
- Rolinski S (1999) On the dynamics of suspended matter transport in the tidal river Elbe: Description and results of a Lagrangian model. *J Geophysical Res* 104(CII):26043-26057. doi.org/10.1029/1999JC900230
- Schellekens J, Buurman P, Kalbitz K, van Zomeren A, Vidal-Torrado P, Cerli C, Comans RNJ (2017) Molecular Features of Humic Acids and Fulvic Acids from Contrasting Environments. *Environ Sci Technol* 51:1330–1339. doi.org/10.1021/acs.est.6b03925

- Schnecker J, Borken W, Schindlbacher A, Wanek W (2016) Little effects on soil organic matter chemistry of density fractions after seven years of forest soil warming. *Soil Biol Biochem* 103:300-307. doi.org/10.1016/j.soilbio.2016.09.003
- Schoel A, Hein B, Wyrwa J, Kirchesch V (2014) Modelling Water Quality in the Elbe and its Estuary - Large Scale and Long Term Applications with Focus on the Oxygen Budget of the Estuary. *Die Kueste* 81:203-232. https://hdl.handle.net/20.500.11970/101692. Accessed: 12th February 2022
- Schulz HD, Zabel M (2006) *Marine Geochemistry*. Berlin Heidelberg Springer-Verlag
- Sebag D, Disnar J-R, Guillet B, Di Giovanni C, Verrecchia EP, Durand A (2006) Monitoring organic matter dynamics in soil profiles by 'Rock-Eval pyrolysis': bulk characterization and quantification of degradation. *Eur J Soil Sci* 57(3):344–355. doi.org/10.1111/j.1365-2389.2005.00745.x
- Seelen LMS, Flaim G, Keuskamp J, Teurlincx S, Font RA, Tolunay D, Frankova M, Sumberova K, Temponeras M, Lenhardt M (2019) An affordable and reliable assessment of aquatic decomposition: Tailoring the Tea Bag Index to surface waters *Water Research* 151:31-43 doi.org/10.1016/j.watres.2018.11.081
- Shakeel A., Kirichek, A., Chassagne, C. 2019. Is density enough to predict the rheology of natural sediments? *Geo-Mar Lett* 39, 427–434, doi: doi.org/10.1007/s00367-019-00601-2
- Shakeel A, Zander F, de Kerk J-W, Kirichek A, Gebert J, Chassagne C (2022a) Effect of organic matter degradation in cohesive sediment: A detailed rheological analysis. *J Soil Sediment* doi.org/10.1007/s11368-022-03156-5 (accepted for publication 30 January 2022)
- Shakeel A, Zander F, Kirichek A, Gebert J, Chassagne C (2022b) Influence of anaerobic degradation of organic matter on the rheological properties of cohesive mud from different European ports. *J Mar Sci Eng* 10(3):446. doi.org/10.3390/jmse10030446
- Shen Q, Suarez-Abelenda M, Camps-Arbestain M, Pereira RC, McNally SR, Kelliherd FM (2018) An investigation of organic matter quality and quantity in acid soils as influenced by soil type and land use. *Geoderma* 328:44–55. doi.org/10.1016/j.geoderma.2018.05.006
- Sills GC, Gonzalez R (2001) Consolidation of naturally gassy soft soil. *Geotechnique* 51 7:629-639. doi.org/10.1680/geot.2001.51.7.629
- Six J, Paustian K (2014) Aggregate-associated soil organic matter as an ecosystem property and a measurement tool. *Soil Biol Biochem* 68:A4-A9. doi.org/10.1016/j.soilbio.2013.06.014
- Spieckermann M, Gröngröft A, Karrasch M, Neumann A, Eschenbach A (2021) Oxygen Consumption of Resuspended Sediments of the Upper Elbe Estuary: Process Identification and Prognosis. *Aquat Geochem* (2021). doi.org/10.1007/s10498-021-09401-6
- Stevenson MA, Faust JC, Andrade LL, Freitas FS, Gray ND, Tait K, Hendry KR, Hilton RG, Henley SF et al. (2020) Transformation of organic matter in a Barents Sea sediment profile: coupled geochemical and microbiological processes. *Phil Trans R Soc A* 378:20200223. dx.doi.org/10.1098/rsta.2020.0223
- Straathof AL, Chincarini R, Comans RNJ, Hoffland E (2014) Dynamics of soil dissolved organic carbon pools reveal both hydrophobic and hydrophilic compounds sustain microbial respiration. *Soil Biol Biochem* 79:109-116. doi.org/10.1016/j.soilbio.2014.09.004
- Straathof AL, Comans RNJ (2015) Input materials and processing conditions control compost dissolved organic carbon quality. *Bioresource Technol* 179:619–623. dx.doi.org/10.1016/j.biortech.2014.12.054

- Suominen S, Dombrowski N, Damsté JSS, Villanueva L (2021) A diverse uncultivated microbial community is responsible for organic matter degradation in the Black Sea sulphidic zone. *Environmental Microbiology* 23(6):2709–2728. doi.org/10.1111/1462-2920.14902
- Tadini AM, Nicolodelli G, Mounier S, Montes CR, Milori DMBA (2015) The importance of humin in soil characterisation: A study on Amazonian soils using different fluorescence techniques. *Science of the Total Environment* 537:152–158. dx.doi.org/10.1016/j.scitotenv.2015.07.125
- Totsche KU, Amelung W, Gerzabek MH, Guggenberger G, Klumpp E, Knief C, Lehndorff E, Mikutta R, Peth S, Pechtel A, Ray N, Kögel-Knabner I (2018) Review Article - Microaggregates in soils. *J Plant Nutr Soil Sci* 181:104–136. doi.org/10.1002/jpln.201600451
- Travnik LJ, Cole JJ, Prairie YT (2018) The study of carbon in inland waters—from isolated ecosystems to players in the global carbon cycle. *Limnology and Oceanography Letters* 3:41–48. doi.org/10.1002/lol2.10068
- Vannote RL, Minshall WG, Cummins KW, Sedell JR, Cushing CE (1980) The river continuum concept. *Can J Fish Aquat Sci* 37:130–137. doi.org/10.1139/f80-017
- Varma A, Buscot F (2005) *Microorganisms in Soils: Roles in Genesis and Functions*. Berlin Heidelberg: Springer-Verlag.
- Violante A, Caporale, AG (2015) Biogeochemical processes at soil-root interface. *Journal of Soil Science and Plant Nutrition* 15(2):422-448. dx.doi.org/10.4067/S0718-95162015005000038
- Viret F, Grand S (2019) Combined Size and Density Fractionation of Soils for Investigations of Organo-Mineral Interactions. *J. Vis. Exp.* 144:58927. doi.org./10.3791/58927 (2019).
- Wakeham SG, Canuel, EA (2016) The nature of organic carbon in density-fractionated sediments in the Sacramento-San Joaquin River Delta (California). *Biogeosciences* 13:567–582. doi.org/10.5194/bg-13-567-2016
- Waksman SA, Tenney FG, Stevens KR (1928) The Role of Microorganisms in the Transformation of Organic Matter in Forest Soils. *Ecology* 9(2):126-144. jstor.org/stable/1929350
- Wang L, Chen L, Tsang DCW, Li J-S, Yeung TLY, Ding S, Poona CS (2018) Green remediation of contaminated sediment by stabilization/solidification with industrial by-products and CO₂ utilization. *Science of the Total Environment* 631–632:1321–1327. doi.org/10.1016/j.scitotenv.2018.03.103
- Ward ND, Krusche AV, Sawakuchi HO, Brito DC, Cunha AC, Moura JMS, da Silva R, Yager PL, Keil RG, Richey JE (2015) The compositional evolution of dissolved and particulate organic matter along the lower Amazon River—Óbidos to the ocean. *Mar Chem* 177:244–256. doi.org/10.1016/j.marchem.2015.06.013
- Weilbeer H (2014) *Sediment Transport and Sediment Management in the Elbe Estuary*. Die Küste 81 Karlsruhe: Bundesanstalt für Wasserbau:409-426. hdl.handle.net/20.500.11970/101703
- Wieder WR, Allison SD, Davidson EA, Georgiou K, Hararuk O, He Y, Hopkins F, Luo Y, Smith MJ, Sulman B, Todd-Brown K, Wang Y-P, Xia J, Xu X (2015), Explicitly representing soil microbial processes in Earth systemmodels. *Global Biogeochem Cycles* 29:1782–1800. doi.org/10.1002/2015GB005188
- Wilkinson JF (1958) The extracellular polysaccharides of bacteria. *Bact Rev* 22:46–73

- Wolfstein K, Kies L (1999) Composition of suspended particulate matter in the Elbe estuary: implications for biological and transportation processes. *Deutsche Hydrografische Zeitschrift*, 51(4):453-463.
- Worden AZ, Follows MJ, Giovannoni SJ, Wilken S, Zimmerman AE, Keeling PJ (2015) Rethinking the marine carbon cycle: Factoring in the multifarious lifestyles of microbes. *Science* 347:1257594. doi.org/10.1126/science.1257594
- Wurpts R, Torn P (2005) 15 Years Experience with Fluid Mud: Definition of the Nautical Bottom with Rheological Parameters. *Terra et Aqua* 99:22-32
- Yang H, Yu S, Lu H (2021) Iron-Coupled Anaerobic Oxidation of Methane in Marine Sediments: A Review. *J Mar Sci Eng* 9:875. doi.org/10.3390/jmse9080875
- Yoshikawa T, Kanemata K, Nakase G, Eguchi M (2017) Microbial decomposition process of organic matter in sinking particles, resuspendable particles, and bottom sediments at a coastal fish farming area. *Fish Sci* 83:635–647. doi.org/10.1007/s12562-017-1098-9
- Zander F, Heimovaara T, Gebert J (2020) Spatial variability of organic matter degradability in tidal Elbe sediments. *J Soil Sediment* 20:2573-2587. doi.org/10.1007/s11368-020-02569-4
- Zander F, Comans RNJ, Gebert J (2022a) Linking patterns of density, thermometric and carbon stable isotope fractions of organic matter to its lability in sediments of the tidal Elbe river. *Appl Geochem* (submitted)
- Zander F, Gröngröft A, Eschenbach A, Heimovaara T, Gebert J (2022b) Organic matter pools in sediments of the tidal Elbe river. *Limnol* (accepted for publication on 8 June 2022)
- Zander F, Shakeel A, Kirichek A, Chassagne C, Gebert J (2022c) Effects of organic matter degradation in cohesive sediment: Linking sediment rheology to spatio-temporal patterns of organic matter degradability. *J Soil Sediment*. doi.org/10.1007/s11368-022-03155-6 (accepted for publication 30 January 2022)
- Zhang W, Jin X, Meng X, Tang W, Shan B (2018) Phosphorus transformations at the sedimentewater interface in shallow freshwater ecosystems caused by decomposition of plant. *Chemosphere* 201:328-334. doi.org/10.1016/j.chemosphere.2018.03.006
- Zhu D, Zhang P, Xie C, Zhang W, Sun J, Qian W-J, Yang B (2017) Biodegradation of alkaline lignin by *Bacillus ligniniphilus* L1. *Biotechnol Biofuels* 10:44. doi 10.1186/s13068-017-0735-y

A1

13 Effect of organic matter degradation in cohesive sediment: A detailed rheological analysis

A. Shakeel^{1,2}, F. Zander³, J.-W. de Klerk⁴, A. Kirichek¹, J. Gebert³, C. Chassagne¹

¹ Section of Rivers, Ports, Waterways and Dredging Engineering, Department of Hydraulic Engineering, Faculty of Civil Engineering & Geosciences, Delft, University of Technology, Stevinweg 1, 2628 CN Delft, The Netherlands

² Department of Chemical, Polymer and Composite Materials Engineering, University of Engineering & Technology, New Campus (KSK), Lahore 54890, Pakistan

³ Section of Geo-Engineering, Department of Geoscience and Engineering, Faculty of Civil Engineering & Geosciences, Delft University of Technology, Stevinweg 1, 2628 CN Delft, The Netherlands

⁴ Faculty of Mechanical, Maritime and Materials Engineering, Department of Dredging Engineering, Delft University of Technology, Mekelweg 2, 2628, CD, Delft, The Netherlands

Corresponding author: Ahmad Shakeel, A.Shakeel@tudelft.nl

Abstract

Purpose The presence of organic matter in cohesive sediment results in the formation of clay-organic flocs, which eventually imparts complex rheological behaviour including shear-thinning, viscoelasticity, thixotropy and two-step yielding to mud. In this study, the influence of microbial degradation of sediment organic matter on the rheological properties of mud samples, having similar densities, was examined.

Materials and methods The mud samples were collected from three different locations in the Port of Hamburg, Germany, displaying varying organic matter content. The rheological analysis of fresh and degraded mud samples was performed with the help of several tests including stress ramp-up tests, amplitude sweep tests, frequency sweep tests, time-dependence tests and structural recovery tests.

Results and discussion The results showed a significant decrease in rheological properties including yield stresses, complex modulus, etc. for degraded mud samples as compared to the fresh mud samples. The slopes of the line, correlating the change (degraded – fresh) in above mentioned rheological properties as a function of the same rheological property of the fresh mud, varied within the range of -0.28 to -0.49 . The structural recovery tests displayed a better recovery (i.e., stronger system) in mud after the pre-shearing step for the degraded mud samples as compared to the fresh mud samples. The effect of degradation time on the rheological properties of mud samples showed two critical time periods (3 days and 150 days) after which a significant change in rheological properties of mud samples was observed.

Conclusions This study provided a useful understanding about the influence of organic matter degradation on the rheological properties of mud, which can be used to optimize sediment management strategies in ports and waterways.

Keywords

Mud; Organic matter; Anaerobic degradation; Rheology; Two-step yielding; Moduli; Thixotropy

13.1 Introduction

Cohesive sediments (mud) typically consist of varying amounts of clay, silt, fine sand and organic matter. Organic matter (OM) in water-sediment systems originates from (i) natural sources including plant litter, eroded topsoils, pelagic and planktonic biomass, or (ii) anthropogenic sources such as surface runoff and urban sewage, as listed in Zander et al. (2020). Organic matter can be either suspended in the water phase, either as pure organic matter or bound to fine and still suspended mineral particles, or is bound to the already settled sediment. In suspensions, organic matter can interact with clay particles either by creating bridges between the particles or by charge neutralization (Lagaly and Dékány 2013), forming a flocculated system. Extensive research has been conducted on the measurements of floc size and settling rates in the laboratory for fine-grained sediments or sand/mud mixtures (Spearman and Manning 2017; Deng et al. 2019; Chassagne and Safar 2020; Chassagne 2021; Chassagne et al. 2021; Deng et al. 2021). The presence of these clay-organic flocs typically results in a complex rheological fingerprint of mud, including shear thinning, viscoelasticity, thixotropic behavior and two-step yielding (Coussot 1997; Van Kessel and Blom 1998; Shakeel et al. 2020d, b). For instance, a significant increase in rheological properties (i.e., yield stresses, moduli, thixotropy, etc.) was observed for mud samples having higher organic matter content, which may be attributed to the formation of stronger and higher number of clay-organic flocs (Shakeel et al. 2019).

Under anaerobic conditions, the microbial degradation of sediment organic matter results in the formation of carbon dioxide (CO₂) and methane (CH₄). These greenhouse gases are either released through the water column or remain entrapped in the mud layers. Entrapped gas bubbles are found to affect the density of mud and to be responsible for delayed consolidation. Given the role of clay-organic flocs for the rheological and cohesive properties of mud (Tolhurst et al. 2002; Wurpts and Torn 2005; Malarkey et al. 2015; Schindler et al. 2015; Parsons et al. 2016; Shakeel et al. 2019), it is hypothesized that the degradation of organic matter can significantly influence the rheological fingerprint of mud (as it weakens the mud). For the investigation area, Zander et al. (2021a) have shown that the organic matter present in the sediment can be separated into differently degradable pools based on their degradation kinetics and corresponding half-lives (Zander et al. 2021a). However, a systematic analysis of the hypothesized effect of organic matter degradation on rheological properties is still missing.

Therefore, the following research questions are addressed in this study: is there any significant influence of degradation of organic matter on the rheological properties of fine-grained sediments? Is this effect of organic matter degradation similar for different rheological properties (such as yield stress and moduli)? What is the effect of degradation time on the rheological properties of mud? To this end, the rheological properties of freshly sampled and thereafter further microbially degraded mud of similar densities, collected from three different locations of the Port of Hamburg, Germany, were analyzed. Rheological tests included stress ramp-up tests, amplitude sweep tests, frequency sweep tests, time-dependence tests and structural recovery tests. In the first part of study, the rheological analysis of fresh samples and samples degraded for 250 days was compared, while in the second part, the effect of degradation time on the rheological properties was studied.

13.2 Experimental methods

Mud samples were collected from locations Köhlfleet Hafen (KH), Rethe (RT) and Reiherstieg Vorhafen (RV) (Fig. S1, Table S1; see supplementary information) of the Port of Hamburg, Germany, using a 1 m core sampler. Based on previous studies (Zander et al. 2020; Shakeel et al. 2021a), these locations were

selected to cover a range of organic matter contents (Table S1). Directly after sampling, the core was divided into sublayers such as fluid mud, pre-consolidated and consolidated sediments, based on their visual strength and consistency. However, in this study, only pre-consolidated sediment (PS) (i.e., similar densities) was considered for rheological analysis. The sediment properties along with the rheological properties of other mud layers are reported in Zander et al. (2021b).

13.2.1 Water content and bulk density

The dry density (ρ_s) of the mud samples was measured using a gas pycnometer (ISO 17892-3:2015) and found to be within the range of 2375 – 2534 kg m⁻³. The bulk density ρ of the mud samples was then estimated by determining the content of water/solids after drying at 105 °C for 24 h (ISO 11465:1993). The change in excess bulk density ($\rho - \rho_w$), obtained by the difference between excess bulk density of degraded and fresh mud samples is plotted as a function of excess bulk density of fresh samples, where ρ_w is the density of water (Fig. S2). It is seen that the change in bulk density incurred during the long-term (250 days) incubation to degrade organic matter was lower than 5% of its original value. It was, therefore, assumed that changes in rheological properties between fresh and degraded samples were not related to the change in density or water content.

13.2.2 Degradation of organic matter

For the analysis of organic matter degradation under anaerobic conditions (typically prevailing in the investigated sediments (Zander et al. 2020)), 200 g of fresh mud was placed into 500 ml air tight glass bottles. The headspace above the sample was flushed with N₂ to establish anaerobic conditions and incubated at 36 °C in the absence of light for 250 days. All the samples were incubated in triplicate. Anaerobic carbon release was calculated from the increase in headspace pressure in combination with gas chromatographic analyses of headspace composition. The share of CO₂-C dissolved in the aqueous phase was calculated using the CO₂ concentration and the pressure in the bottle headspace and the temperature-corrected solubility of CO₂ in water as given by Henry's constant (given in Sander (2015)). Further details are reported in Zander et al. (2021b).

13.2.3 Impact of degradation time on rheological properties

In addition to the fixed degradation time of 250 days, the influence of varying degradation time on the rheological properties of mud was studied by parallel incubation of mud samples obtained from location RT, under the same conditions as mentioned before. After designated time intervals (i.e., 3 days, 7 days, 10 days, etc.), sample aliquots were sacrificed for the analysis of physical and rheological properties.

13.2.4 Rheological characterization

The rheological analysis of both fresh and degraded mud samples was performed using a HAAKE MARS I rheometer (Thermo Scientific, Germany) with Couette geometry (gap width = 1 mm). The mud samples were gently homogenized before each rheological experiment. After inserting the geometry into the sample, a waiting time of 3–5 min was adopted before the start of the experiment, in order to minimize the disturbances created by the bob while attaining the required measurement gap (i.e., between the bottom of the bob and the cup). The rheological experiments were performed at 20 °C, maintained by a Peltier controller system. In order to check the repeatability, all the experiments were performed in duplicate and the repeatability error was less than 2%.

Different types of rheological tests were performed to analyse the effect of organic matter degradation on the rheological properties of mud. Stress ramp-up tests were performed by linearly increasing the

stress at a rate of 1 Pa. s⁻¹, until the shear rate reached 300 s⁻¹ (Shakeel et al. 2020b). The corresponding rotation of the geometry was measured, which eventually provided the shear rate and apparent viscosity. The amplitude sweep test was carried out at a frequency of 1 Hz by applying an oscillatory stress, instead of a steady stress. The storage (G') and loss (G'') moduli (Shakeel et al. 2020d) were obtained as a function of oscillatory amplitude. The frequency sweep test was performed within the linear viscoelastic (LVE) regime, from 0.1 to 100 Hz. The LVE regime was determined from the amplitude sweep tests (i.e., the regime where moduli was almost constant as a function of amplitude). The outcome of frequency sweep tests was obtained in the form of storage and loss moduli as a function of frequency, which was then converted into complex modulus (G^*) and phase angle (δ). The time-dependence properties were obtained by performing the shear rate ramp up and ramp down experiment as follows: (i) shear rate ramp-up from 0 to 100 s⁻¹ for 50 s, (ii) constant shear rate of 100 s⁻¹ for 50 s, and (iii) shear rate ramp-down from 100 to 0 s⁻¹ for 50 s. In addition to the time-dependence experiment, a structural recovery test was carried out by using a three step protocol given in Shakeel et al. (2020c). In short, the first step provides the moduli of the mud sample (G'_0) before pre-shearing, by performing a small amplitude oscillatory time sweep experiment. The second step involves the application of a high shear rate (300 s⁻¹ for 500 s) to completely disturb the sample. The last step allows the sample to recover its structure by again performing a small amplitude oscillatory time sweep experiment for 500 s and recording the moduli as a function of time (G').

13.3 Results and discussion

13.3.1 Stress ramp-up tests

In order to investigate the influence of organic matter degradation on the yield stress of mud, stress ramp-up tests were performed. Figure S3 shows the behavior of apparent viscosity as a function of shear stress for fresh mud samples and mud samples that had been degraded for 250 days. A two-step yielding behavior was clearly identified from the two declines in viscosity. A similar two-step yielding behavior, in stress/shear rate sweep tests, has been previously reported for fine-grained sediments (Nie et al. 2020; Shakeel et al. 2020d).

Shakeel et al. (2021b) attributed the two-step yielding in mud samples to the (i) formation of interconnected network of flocs (first viscosity plateau), (ii) breakage of network of flocs (first viscosity decline), (iii) formation of cylinder/roll-like structures (second viscosity plateau), and (iv) collapse of reorganized flocs (second viscosity decline). The yield stress values, corresponding to the viscosity declines, were defined as the points of intersection of the extrapolated slopes of viscosity over stress before and after the decline (Fig. S3). The first yield point was denominated as static yield stress (τ_s) while the second decline was referred to as fluidic yield stress (τ_f). The example given in Fig. S3 shows that degraded mud had lower yield stress values than the fresh mud. This may be attributed to the presence of organic matter resulting in a stronger structure (i.e., higher yield stresses) of mud (Shakeel et al. 2019). The degradation/removal of this organic matter leads to a weaker system with lower yield stress values. A decrease in yield stress values by removing the organic matter content was also reported in literature for fine-grained sediments (Fass and Wartel 2006).

In order to further quantify the effect of organic matter degradation on the yield stress of mud samples from different locations, the change in static and fluidic yield stresses (degraded – fresh) was plotted as a function of yield stress of fresh samples in Fig. 1. A decrease in yield stress values is observed as a consequence of the degradation of organic matter, for all the investigated locations. Moreover, this decrease in yield stresses was found to be strongly correlated to the yield stress values of the original,

freshly sampled mud, i.e., the higher the original yield stress, the higher its reduction as a result of organic matter degradation (resulting in a negative slope). This shows that the effect of organic matter degradation on the yield stresses was more pronounced for the mud samples having higher yield stress values before degradation. The higher yield stress values of mud samples are typically associated to either higher density or higher organic matter content (Van Kessel and Blom 1998; Soltanpour and Samsami 2011; Xu and Huhe 2016; Shakeel et al. 2019, 2020d). In order to compare the effect of organic matter degradation on different rheological properties (i.e., yield stress, moduli, structural recovery, etc.), the following empirical equation was used to fit the experimental data of change in rheological property (degraded – fresh) as a function of the same rheological property before degradation, for all the locations:

$$y = a + bx \quad (1)$$

where a and b represent the intercept and slope of the line, respectively. For instance, the values of a and b were observed to be 0.99 and -0.37 for static yield stress and 1.73 and -0.28 for fluidic yield stress. The values of the slope clearly indicate that the yield stresses (static and fluidic) were reduced by almost 1/3 of its original value due to the degradation of organic matter. Furthermore, it is important to highlight that the main objective of using this simple linear relation (Eq. 1) is just to obtain a trend (particularly the slope of the line) for the change in rheological properties after degradation as a function of rheological properties of fresh sample, instead of giving a predictive correlation. However, the values of intercept (parameter a) are also provided for each rheological property, which can be useful for future studies.

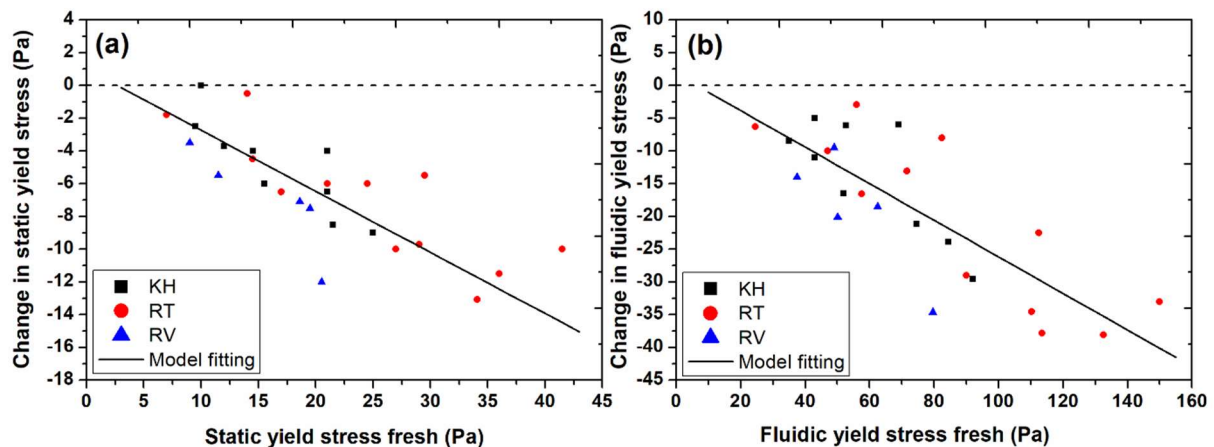


Figure 1. (a) Change in static yield stress (degraded – fresh) as a function of static yield stress of fresh mud sample from different locations, and (b) change in fluidic yield stress (degraded – fresh) as a function of fluidic yield stress of fresh mud sample from different locations. The dashed line represents the value where the degraded and fresh mud samples have same yield stresses. The solid line represents the empirical fitting using Equation 1.

13.3.2 Amplitude sweep tests

In addition to the yield stress of mud samples, the solid-liquid transition (a crossover between G' and G'') was studied by performing oscillatory amplitude sweep tests. A preliminary analysis was performed to select a suitable frequency for amplitude sweep tests (data not shown), which was found to be 1 Hz for all the selected mud samples. Figure 2a presents the storage and loss moduli as a function of oscillatory amplitude for fresh mud sample and mud sample degraded for 250 days. A linear viscoelastic (LVE) regime was identified from an almost independent behavior of moduli at smaller amplitudes, which also provided essential information to perform frequency sweep tests within LVE

regime. Apart from LVE regime, the solid-liquid transition was estimated from the crossover between G' and G'' and the corresponding amplitude was stated as crossover amplitude.

Figure 2a clearly depicts a decrease in crossover stress by the degradation of organic matter, which is in accordance with the yield stress analysis. Change in crossover amplitude (degraded – fresh) is plotted as a function of crossover amplitude of fresh mud sample for different locations (see Fig. 2b). The results again show the significant effect of organic matter degradation on the crossover amplitude for the mud samples having higher crossover amplitude before degradation. This experimental data was also fitted with Equation 1 and the values of a and b were found to be 0.49 and -0.35, respectively.

13.3.3 Frequency sweep tests

In order to analyze the strength of mud samples before and after degradation of organic matter, frequency sweep tests were performed within LVE regime (i.e., without affecting their structure) from 0.1 to 100 Hz. The outcome of frequency sweep tests is shown in terms of complex modulus and phase angle as a function of frequency for fresh mud sample and mud sample degraded for 250 days, see Fig. S4a and S4b. Both fresh and degraded mud samples showed solid-like character, i.e., an almost independence of complex modulus on frequency and significantly smaller values of phase angle (Lupi et al. 2016). In literature, a similar solid-like behavior of mud samples has been reported in frequency sweep tests (Van Kessel and Blom 1998; Soltanpour and Samsami 2011; Xu and Huhe 2016; Shakeel et al. 2020a). However, a weaker system (with lower complex modulus and higher phase angle values) was observed after the degradation of organic matter as compared to the fresh mud sample. The experimental data at higher frequencies was removed (for some samples) due to the inertial effects caused by the rheometer head.

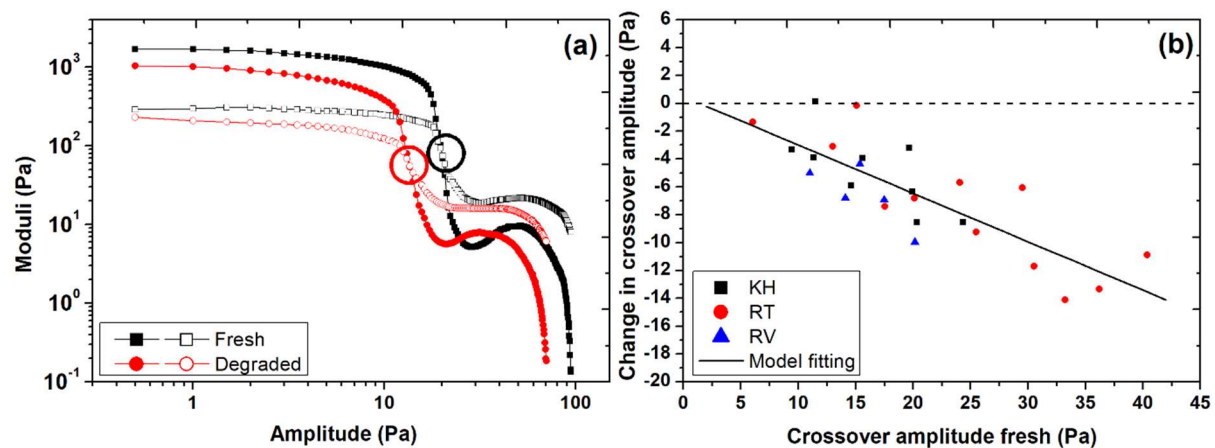


Figure 2. (a) Storage (filled symbols) and loss (empty symbols) moduli as a function of oscillatory amplitude for fresh mud sample and mud sample degraded for 250 days, collected from KH location. The circles represent the crossover amplitude. (b) change in crossover amplitude (degraded – fresh) as a function of crossover amplitude of fresh mud sample from different locations. The dashed line represents the value where the degraded and fresh mud samples have same crossover amplitude. The solid line represents the empirical fitting using Equation 1.

The values of complex modulus and phase angle at 1 Hz were selected to investigate the effect of organic matter degradation on the strength of mud samples from different locations. Figure 3a shows the correlation between the change in complex modulus (degraded – fresh) and the values of complex modulus of fresh mud samples for different locations. A decrease in complex modulus was observed due to the degradation of organic matter, which became more pronounced for the fresh samples having higher complex modulus, which may again be linked to the higher density of the samples. The empirical fitting of the experimental data of complex modulus using Equation 1 resulted in the values

of 92.9 and -0.49 for a and b , respectively. The correlation between the change in phase angle (degraded – fresh) and the values of phase angle of fresh mud samples, for different locations, was not very prominent (Fig. 3b). However, the degraded samples exhibited slightly higher values of the phase angle as compared to the fresh mud samples (i.e., positive values of change in phase angle), which indicated a weaker system, as already observed from other results.

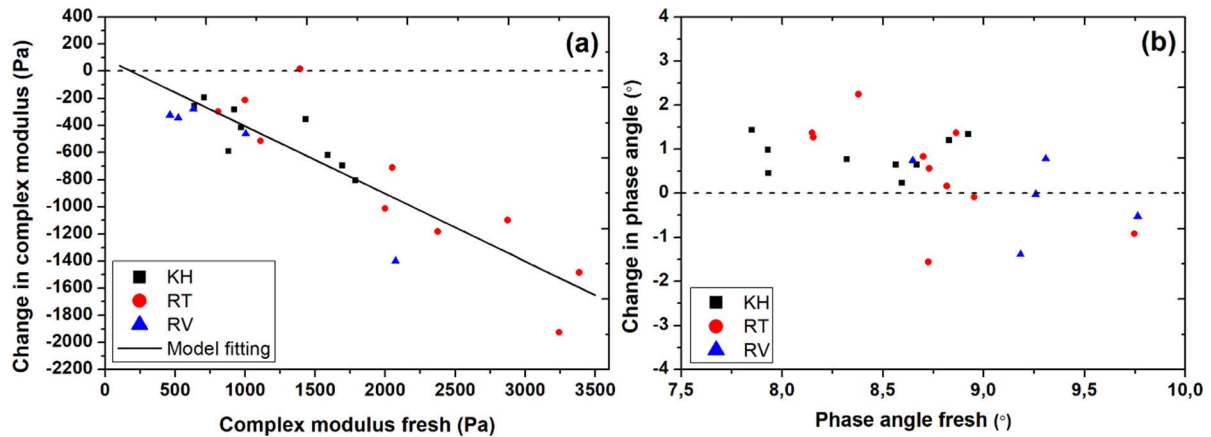


Figure 3. (a) Change in complex modulus (degraded – fresh) at 1 Hz as a function of complex modulus at 1 Hz of fresh mud sample from different locations. The solid line represents the empirical fitting using Equation 1, (b) change in phase angle (degraded – fresh) at 1 Hz as a function of phase angle at 1 Hz of fresh mud sample from different locations. The dashed line represents the value where the degraded and fresh mud samples have same hysteresis area. The solid line represents the empirical fitting using Eq. (1)

13.3.4 Time-dependence and structural recovery tests

The time-dependent behavior of fresh and degraded mud samples was analyzed by performing shear rate controlled ramp-up and ramp-down experiments from 0 to 100 s⁻¹. The time-dependent character is either observed in the form of clockwise hysteresis loop or counterclockwise hysteresis loop. The former is typically attributed to the faster structural breakdown in ramp-up step as compared to the structural buildup in ramp-down step while the latter is usually linked to the faster structural reformation in the ramp-down step as compared to the other phenomenon (Barnes 1997; Mewis and Wagner 2009). The outcome of shear rate ramp-up and ramp-down experiments show the existence of a typical clockwise loop at higher shear rates for both fresh mud sample and mud sample degraded for 250 days (Fig. 4a). However, at lower shear rates, a counterclockwise loop is observed, which may be attributed to a shear thickening phenomenon or the structural reorganization due to the shearing action (Shakeel et al. 2020d; Shakeel et al. 2021b). A similar combination of clockwise and counterclockwise loops as a function of shear rate has been reported in literature for fine-grained sediments (Yang et al. 2014).

Furthermore, the values of shear stress as a function of shear rate was significantly lower for the degraded mud sample as compared to the fresh mud sample, which is again in line with the previous results. The hysteresis area between the clockwise loop (i.e., typical thixotropic character) of the ramp-up and ramp down curves was estimated in order to investigate the effect of organic matter degradation on the time-dependent properties of mud samples. The change in hysteresis area (degraded – fresh) as a function of the values of hysteresis area of fresh mud samples, for different locations, is presented in Fig. 4b. A similar influence of organic matter degradation was observed on hysteresis area, as already observed for other rheological properties including yield stresses, moduli, etc. The empirical fitting of Equation 1 for time-dependency data resulted in the values of 39.84 and -0.29 for a and b , respectively. It is interesting to note that the value of parameter b (i.e., slope) is quite

similar, within the range of -0.28 to -0.49, for different rheological properties. This behavior suggests that the overall influence of organic matter degradation is quite similar on different rheological properties, i.e., the extent of decrease in rheological properties as a function of organic matter degradation is similar. This similar effect on different rheological properties is linked to the fact that these properties represent either the structure of mud samples at “rest” or the destruction of structure from an undisturbed state.

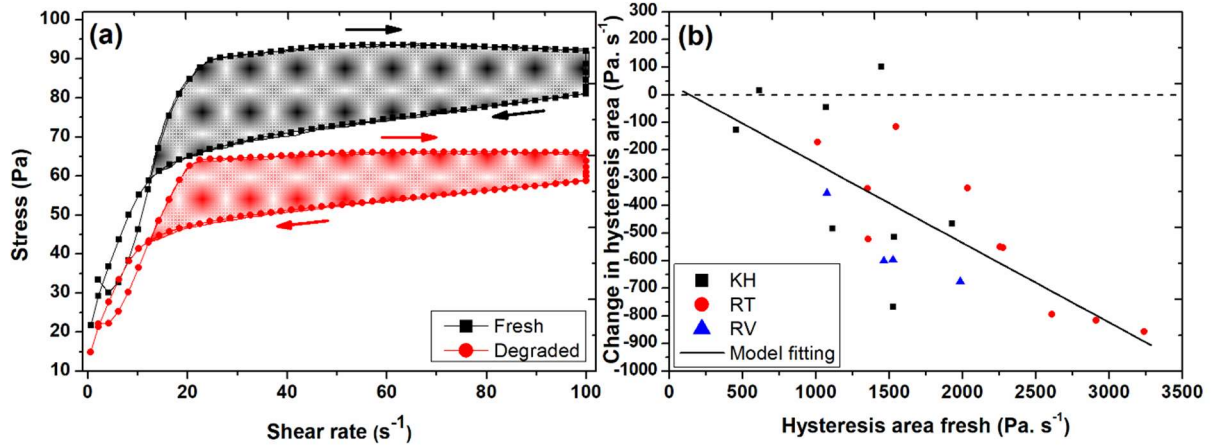


Figure 4. (a) Shear stress as a function of shear rate obtained by performing shear rate controlled ramp-up and ramp-down experiments for fresh mud sample and mud sample degraded for 250 days, collected from KH location. The direction of arrows represent the ramp-up or ramp-down curve. The filled region represent the hysteresis area, **(b)** change in hysteresis area (degraded – fresh) as a function of hysteresis area of fresh mud sample from different locations. The dashed line represents the value where the degraded and fresh mud samples have same hysteresis area. The solid line represents the empirical fitting using Equation 1.

In addition to the time-dependent properties of fresh and degraded mud samples, the structural recovery after intensive pre-shearing was investigated using a three step protocol explained in Section 2. The normalized time dependent storage modulus (G'/G'_0) as a function of time for fresh mud sample and mud sample degraded for 250 days is presented in Fig. S5. The oscillations in the storage modulus behavior, as a function of time, may be associated to the higher elasticity of the samples (Goudoulas and Germann 2016; Shakeel et al. 2020c). The results show higher normalized modulus values, at any particular time, for the degraded mud samples as compared to the fresh mud samples.

In order to further quantify the structural recovery behavior of fresh and degraded mud samples, a simple stretched exponential function, adapted from (Mobuchon et al. 2009), was used to fit the experimental data of third step of structural recovery protocol, written as follows:

$$\frac{G'}{G'_0} = \frac{G'_i}{G'_0} + \left(\left(\frac{G'_\infty - G'_i}{G'_0} \right) \left(1 - \exp \left[- \left(\frac{t}{t_r} \right)^d \right] \right) \right) \quad (2)$$

where G'_∞ and t_r represent the two most important parameters related to the structural recovery behavior of mud samples (Shakeel et al. 2020c). The change in normalized equilibrium storage modulus, G'_∞/G'_0 (degraded – fresh) as a function of the values of normalized equilibrium storage modulus of fresh mud samples is plotted in Fig. 5a for different locations. It can be seen that the values of normalized equilibrium storage modulus (G'_∞/G'_0) are higher for the degraded mud samples (i.e., positive values of change in normalized equilibrium storage modulus) than for the fresh mud samples. This may be attributed to the fact that the degradation of organic matter result in a weaker system, behaving as a purely mineral suspension without the bridging effect provided by organic matter, which eventually has a better structural recovery (i.e., higher values of modulus, higher strength) after pre-

shearing. A similar enhanced structural recovery was observed in literature for mud samples having lower organic matter content as compared to the samples having higher organic matter content (Shakeel et al. 2020c).

Furthermore, Fig. 5b shows a strong correlation between the change in characteristic time, t_r (degraded – fresh) and the values of characteristic time of fresh mud samples, for different locations, as already observed for other rheological properties. In this case, the values of the fitting parameters, a and b , were observed to be 206.7 and -1.06, respectively. It is clear that the slope (b) of the fitting line (Eq. 1) of the change of characteristic time over characteristic time found for the fresh sample is significantly different from the value of slope for the change of other investigated rheological properties. This could be attributed to the fact that other rheological properties (i.e., yield stresses, moduli, etc.) represented the strength of mud samples before any disturbance while the characteristic time showed the recovery behavior of structure/strength in mud after complete breakdown.

Moreover, it is interesting to note that below a certain characteristic time for the fresh mud sample (i.e., ~ 200 s), the value for characteristic time of degraded mud samples was higher than for the fresh samples while above this critical value of time, the characteristic time of degraded mud samples showed a decrease as compared to the fresh mud samples. This behavior may again be linked to the variable density of the mud samples, in addition to the organic matter degradation.

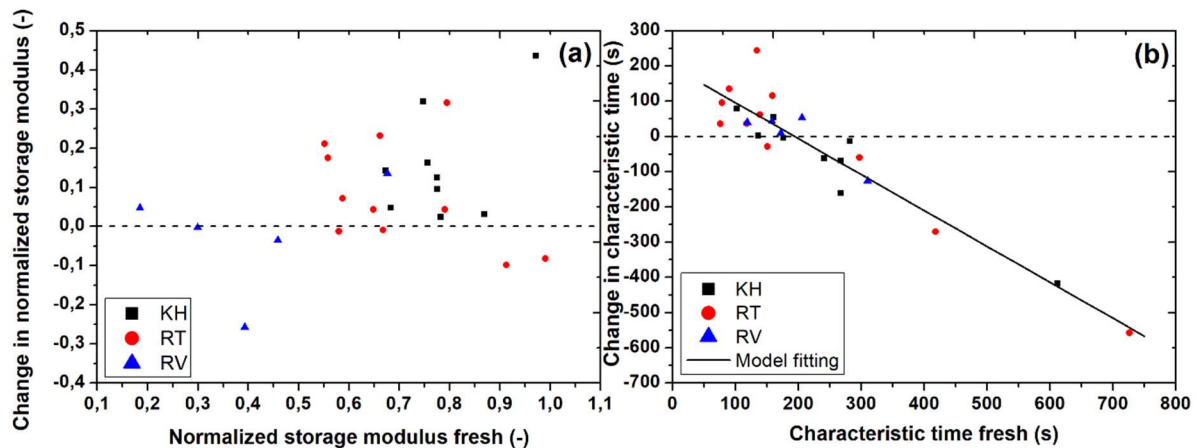


Figure 5. (a) Change in normalized equilibrium storage modulus, G'_{∞}/G'_0 (degraded – fresh) as a function of normalized equilibrium storage modulus, G'_{∞}/G'_0 of fresh mud sample from different locations, and (b) change in characteristic time, t_r (degraded – fresh) as a function of characteristic time, t_r , of fresh mud sample from different locations. The dashed line represents the value where the degraded and fresh mud samples have same normalized equilibrium storage modulus or characteristic time. The solid line represents the empirical fitting using Equation 1.

13.3.5 Effect of degradation time

The rheological analysis of degraded mud, discussed so far, was performed for the samples degraded for 250 days. The change in different rheological properties is plotted as a function of degradation time, see Fig. 6. For instance, the change in yield stresses (static and fluidic), crossover amplitude and complex modulus (degraded – fresh) as a function of degradation time showed two critical values of degradation time after which the change in rheological properties was quite significant (Fig. 6a and 6b). Initially, after 3 days of degradation, a significant decrease in above mentioned rheological properties was observed, which became more or less constant until 150 days, and after that a further decrease in rheological properties was evident. This behavior may be attributed to the presence of differently degradable organic matter pools which have also been identified by analysis of degradation kinetics (Zander et al. 2021a), which dominated degradation at different incubation time. Further

detailed analysis of the influence of short term degradation on the rheological properties of mud samples is reported in Zander et al. (2021b).

The extent of structural recovery after pre-shearing, represented by the normalized equilibrium storage modulus (G'_{∞}/G'_0), was higher for the degraded mud sample as compared to the fresh mud sample, for more or less all the investigated degradation time intervals (Fig. 6c). This behavior again suggested the better structural recovery in degraded mud due to the weaker system that upon degradation of bridging organic matter behaves like a purely mineral system, even after 3 days of degradation. The change in characteristic time (t_r), however, displayed a significant increase as a function of degradation time (Fig. 6d). This may be attributed to the fact that the characteristic recovery time of fresh mud sample was lower than 200 s, which resulted in longer characteristic time of degraded mud sample, as already explained in Fig. 5b.

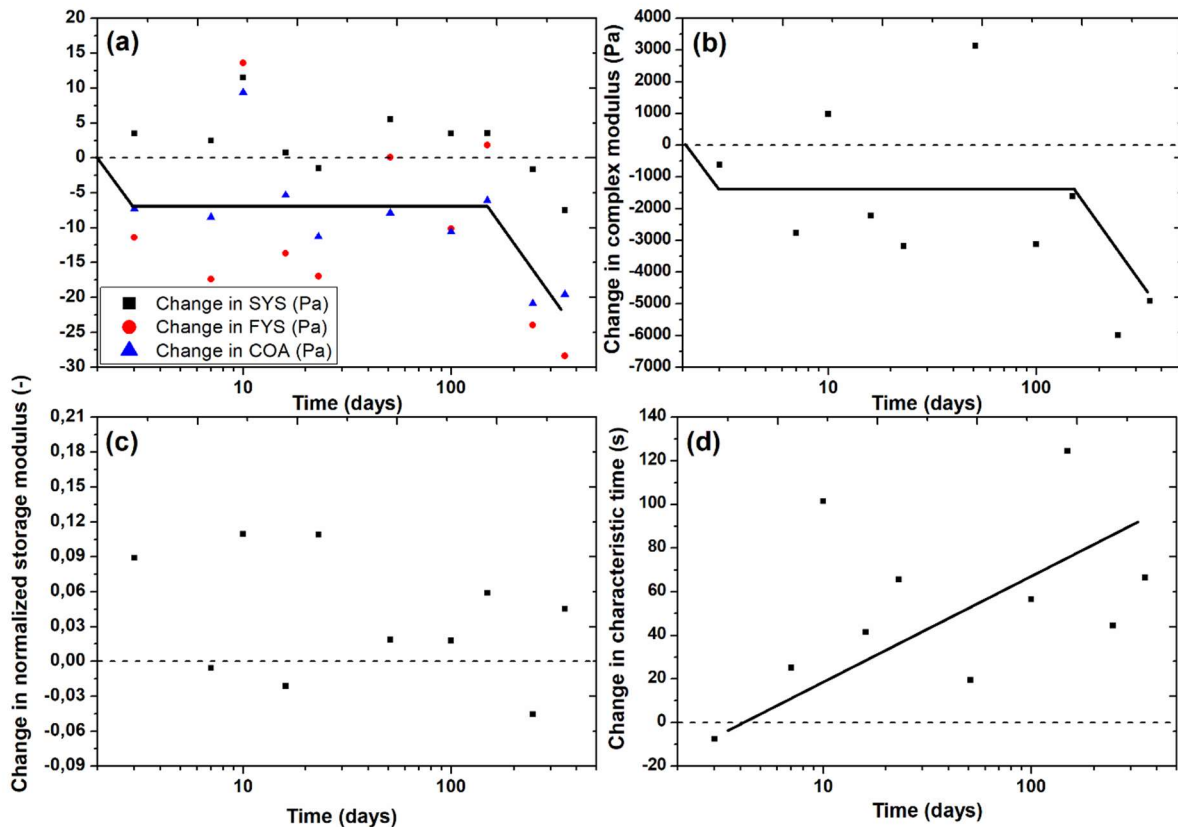


Figure 6. (a) Change in static yield stress (SYS), fluidic yield stress (FYS) and crossover amplitude (COA) as a function of degradation time, (b) change in complex modulus at 1 Hz as a function of degradation time, (c) change in normalized equilibrium storage modulus, G'_{∞}/G'_0 as a function of degradation time, and (d) change in characteristic time, t_r as a function of degradation time for the mud sample collected from RT location. The dashed line represents the value where the degraded and fresh mud samples have same rheological property. The solid line is a guide for the eye.

In this study, the influence of organic matter degradation on the rheological properties of mud is investigated by keeping the density of the mud constant, before and after degradation (by adding/removing water and by homogenizing to avoid dewatering). However, in in-situ conditions, settling and consolidation typically occur in different mud layers of varying density, in addition to organic matter degradation. Therefore, it would be interesting to analyze the combined effect of organic matter degradation and settling/consolidation phenomenon on the rheological properties of mud.

13.4 Conclusions

The presence of organic matter in cohesive sediments results in the formation of clay-organic flocs, which eventually leads to complex rheological behavior including shear-thinning, viscoelasticity, thixotropy and two-step yielding to mud. However, this organic matter undergoes microbial degradation under in-situ conditions and produces CO₂ and CH₄. Apart from producing greenhouse gases, organic matter degradation can significantly affect the rheological properties of mud by diminishing organic bridges between mineral particles and hence changing the clay-organic floc structures. Therefore, in this study, the influence of organic matter degradation on the rheological properties of mud samples, having similar densities, was examined. The mud samples were collected from three different locations of the Port of Hamburg, Germany, in order to have varying organic matter content. The rheological analysis of fresh and degraded mud samples was performed with the help of several tests including stress ramp-up tests, amplitude sweep tests, frequency sweep tests, time-dependent tests and structural recovery tests.

The results show a significant decrease in rheological properties including yield stresses (static and fluidic), crossover amplitude, complex modulus and hysteresis area for degraded mud samples as compared to the fresh mud samples. The slopes (b) of the lines, correlating the change (degraded – fresh) in above mentioned rheological properties as a function of the same rheological property of the fresh mud, are quite similar and vary within the range of -0.28 to -0.49 . This behavior shows that the influence of organic matter degradation is similar for all the rheological properties representing the strength of mud samples. Moreover, the fact that organic matter degradation results in a decrease in rheological properties of mud is an indirect proof of a concept that the organic matter interacts (either by bridging or charge neutralization) with the clay particles to form clay-organic flocs. The structural recovery tests displayed a higher extent of recovery in mud after pre-shearing for the degraded mud than for the fresh mud, which suggests the existence of a pure clay-dominated, OM-depleted system after organic matter degradation.

The behavior of the characteristic recovery time (t_r) shows that below a certain value for fresh mud sample (i.e., ~ 200 s), the characteristic time of degraded mud samples is higher than the fresh samples while above this critical value of time, the characteristic time of degraded mud samples show a decrease as compared to the fresh mud samples. The effect of degradation time on the rheological properties of mud samples display two critical time periods (3 days and 150 days) after which a significant change in rheological properties of mud samples is observed, which may be attributed to the presence of two differently degradable pools of organic matter in the considered mud sample. This study provided a useful understanding about the influence of organic matter degradation on the rheological properties of mud, which can be used to optimize the sediment management strategies in ports and waterways.

Acknowledgments

This study is carried out within the framework of the MUDNET academic network. <https://www.tudelft.nl/mudnet/>. The authors would like to acknowledge Deltares, The Netherlands for the use of the HAAKE MARS I rheometer, which was made possible thanks to the Memorandum of Understanding signed between Deltares and the TU Delft.

References

- Ahuja A, Gamonpilas C (2017) Dual yielding in capillary suspensions. *Rheol Acta* 56:801-810.
- Barnes HA (1997) Thixotropy—a review. *J Non-Newton Fluid Mech* 70:1-33.
- Chassagne C, Safar Z (2020) Modelling flocculation: towards an integration in large-scale sediment transport models. *Marine Geology* 430:106361.
- Chassagne C (2021) A simple model to study the flocculation of suspensions over time. *Chemical Engineering Research and Design* 172:302-311.
- Chassagne C, Safar Z, Deng Z, He Q, Manning AJ (2021) Flocculation in Estuaries: Modeling, Laboratory and In-situ Studies. In *Sediment Transport-Recent Advances*. IntechOpen.
- Coussot P (1997) *Mudflow Rheology and Dynamics*. CRC Press, Rotterdam, 272 pp.
- Deng Z, He Q, Safar Z, Chassagne C (2019) The role of algae in fine sediment flocculation: In-situ and laboratory measurements. *Marine Geology* 413:71-84.
- Deng Z, He Q, Chassagne C, Wang ZB (2021) Seasonal variation of floc population influenced by the presence of algae in the Changjiang (Yangtze River) Estuary. *Marine Geology* 440:106600.
- Fass RW, Wartel SI (2006) Rheological properties of sediment suspensions from Eckernforde and Kieler Forde Bays, Western Baltic Sea. *International Journal of Sediment Research* 21:24-41.
- Goudoulas TB, Germann N (2016) Viscoelastic properties of polyacrylamide solutions from creep ringing data. *Journal of Rheology* 60:491-502.
- ISO (11465:1993) Soil quality — Determination of dry matter and water content on a mass basis — Gravimetric method.
- ISO (17892-3:2015) Geotechnical investigation and testing — Laboratory testing of soil — Part 3: Determination of particle density.
- Lagaly G, Dékány I (2013) Chapter 8 - Colloid Clay Science. In: Bergaya F, Lagaly G (Editors), *Developments in Clay Science*. Elsevier, pp. 243-345.
- Lupi FR, Shakeel A, Greco V, Rossi CO, Baldino N, Gabriele D (2016) A rheological and microstructural characterisation of bigels for cosmetic and pharmaceutical uses. *Materials Science and Engineering: C* 69:358-365.
- Malarkey J, Baas JH, Hope JA, Aspden RJ, Parsons DR, Peakall J, Paterson DM, Schindler RJ, Ye L, Lichtman ID, Bass SJ, Davies AG, Manning AJ, Thorne PD (2015) The pervasive role of biological cohesion in bedform development. *Nature Communications* 6:6257.
- Mewis J, Wagner NJ (2009) Thixotropy. *Advances in colloid and interface science* 147:214-227.
- Mobuchon C, Carreau PJ, Heuzey M-C (2009) Structural analysis of non-aqueous layered silicate suspensions subjected to shear flow. *Journal of Rheology* 53:1025-1048.
- Nie S, Jiang Q, Cui L, Zhang C (2020) Investigation on solid-liquid transition of soft mud under steady and oscillatory shear loads. *Sedimentary Geology* 397:105570.
- Parsons DR, Schindler RJ, Hope JA, Malarkey J, Baas JH, Peakall J, Manning AJ, Ye L, Simmons S, Paterson DM, Aspden RJ, Bass SJ, Davies AG, Lichtman ID, Thorne PD (2016) The role of biophysical cohesion on subaqueous bed form size. *Geophys Res Lett* 43:1566-1573.
- Pham K, Petekidis G, Vlassopoulos D, Egelhaaf S, Poon W, Pusey P (2008) Yielding behavior of repulsion-and attraction-dominated colloidal glasses. *Journal of Rheology* 52:649-676.
- Potantin A (2019) Rheology of silica dispersions stabilized by polymers. *Colloids and Surfaces A: Physicochemical and Engineering Aspects* 562:54-60.
- Sander R (2015) Compilation of Henry's law constants (version 4.0) for water as solvent. *Atmos. Chem. Phys.* 15:4399-4981.
- Schindler RJ, Parsons DR, Ye L, Hope JA, Baas JH, Peakall J, Manning AJ, Aspden RJ, Malarkey J, Simmons S, Paterson DM, Lichtman ID, Davies AG, Thorne PD, Bass SJ (2015) Sticky stuff: Redefining bedform prediction in modern and ancient environments. *Geology* 43:399-402.
- Segovia-Gutiérrez J, Berli CLA, De Vicente J (2012) Nonlinear viscoelasticity and two-step yielding in magnetorheology: A colloidal gel approach to understand the effect of particle concentration. *Journal of rheology* 56:1429-1448.
- Shakeel A, Kirichek A, Chassagne C (2019) Is density enough to predict the rheology of natural sediments? *Geo-Marine Letters* 39:427-434.
- Shakeel A, Kirichek A, Chassagne C (2020a) Rheological analysis of natural and diluted mud suspensions. *Journal of Non-Newtonian Fluid Mechanics* 286:104434.
- Shakeel A, Kirichek A, Chassagne C (2020b) Yield stress measurements of mud sediments using different rheological methods and geometries: An evidence of two-step yielding. *Marine Geology* 427:106247.
- Shakeel A, Kirichek A, Chassagne C (2020c) Effect of pre-shearing on the steady and dynamic rheological properties of mud sediments. *Marine and Petroleum Geology* 116:104338.
- Shakeel A, Kirichek A, Chassagne C (2020d) Rheological analysis of mud from Port of Hamburg, Germany. *Journal of Soils and Sediments* 20:2553-2562.

- Shakeel A, Kirichek A, Talmon A, Chassagne C (2021a) Rheological analysis and rheological modelling of mud sediments: what is the best protocol for maintenance of ports and waterways? *Estuarine, Coastal and Shelf Science* 257: 107407.
- Shakeel A, MacIver MR, van Kan PJM, Kirichek A, Chassagne C (2021b) A rheological and microstructural study of two-step yielding in mud samples from a port area. *Colloids and Surfaces A: Physicochemical and Engineering Aspects* 624:126827.
- Shao Z, Negi AS, Osuji CO (2013) Role of interparticle attraction in the yielding response of microgel suspensions. *Soft Matter* 9:5492-5500.
- Shukla A, Arnipally S, Dagaonkar M, Joshi YM (2015) Two-step yielding in surfactant suspension pastes. *Rheologica Acta* 54:353-364.
- Soltanpour M, Samsami F (2011) A comparative study on the rheology and wave dissipation of kaolinite and natural Hendijan Coast mud, the Persian Gulf. *Ocean Dynamics* 61:295-309.
- Spearman J, Manning AJ (2017) On the hindered settling of sand-mud suspensions. *Ocean Dyn* 67:465–483.
- Tolhurst TJ, Gust G, Paterson DM (2002) The influence of an extracellular polymeric substance (EPS) on cohesive sediment stability. In: Winterwerp JC, Kranenburg C (Editors), *Proceedings in Marine Science*. Elsevier, pp. 409-425.
- Van Kessel T, Blom C (1998) Rheology of cohesive sediments: comparison between a natural and an artificial mud. *Journal of Hydraulic Research* 36:591-612.
- Wurpts R, Torn P (2005) 15 years experience with fluid mud: Definition of the nautical bottom with rheological parameters. *Terra et Aqua* 99:22-32.
- Xu J, Huhe A (2016) Rheological study of mudflows at Lianyungang in China. *International Journal of Sediment Research* 31:71-78.
- Yang W, Yu G-l, Tan Sk, Wang H-k (2014) Rheological properties of dense natural cohesive sediments subject to shear loadings. *International Journal of Sediment Research* 29:454-470.
- Zander F, Heimovaara T, Gebert J (2020) Spatial variability of organic matter degradability in tidal Elbe sediments. *Journal of Soils and Sediments* 20:2573-2587.
- Zander F, Groengroeft A, Eschenach A, Heimovara T, Gebert J (2021a) Organic matter pools in sediments of the tidal Elbe river. *Limnology and Oceanography* (Submitted).
- Zander F, Shakeel A, Kirichek A, Chassagne C, Gebert J (2021b) Effect of organic matter degradation in cohesive sediment: A spatiotemporal analysis of yield stresses. *Journal of Soils and Sediments* (Submitted).

A2

14 Influence of anaerobic degradation of organic matter on the rheological properties of cohesive mud from different European ports

A. Shakeel^{1,2}, F. Zander³, J. Gebert³, C. Chassagne¹, A. Kirichek⁴

¹ Section of Environmental Fluid Mechanics, Department of Hydraulic Engineering, Faculty of Civil Engineering & Geosciences, Delft University of Technology, Stevinweg 1, 2628 CN Delft, The Netherlands

² Department of Chemical, Polymer and Composite Materials Engineering, University of Engineering & Technology, New Campus (KSK), Lahore 54890, Pakistan

³ Section of Geo-Engineering, Department of Geoscience and Engineering, Faculty of Civil Engineering & Geosciences, Delft University of Technology, Stevinweg 1, 2628 CN Delft, The Netherlands

⁴ Section of Rivers, Ports, Waterways and Dredging Engineering, Department of Hydraulic Engineering, Faculty of Civil Engineering & Geosciences, Delft University of Technology, Stevinweg 1, 2628 CN Delft, The Netherlands

Corresponding author: Ahmad Shakeel, A.Shakeel@tudelft.nl

Abstract

The presence of clay-organic flocs in cohesive mud results in a complex rheological behavior of mud, including viscoelasticity, shear-thinning, thixotropy and two-step yielding. In this study, the effect of microbial degradation of organic matter on the rheological properties of mud samples, collected from different ports, was examined. The mud samples were collected from five different European ports (Port of Antwerp (PoA), Port of Bremerhaven (PoB), Port of Emden (PoE), Port of Hamburg (PoH) and Port of Rotterdam (PoR)), displaying varying sediment properties. The rheological analysis of fresh and degraded mud samples was performed with the help of several tests, including stress ramp-up tests, amplitude sweep tests, frequency sweep tests, time-dependent tests and structural recovery tests. The results showed: (i) a significant decrease in yield stresses and complex modulus after organic matter degradation for mud samples from PoA, PoH and PoR, (ii) a negligible change in rheological properties (yield stresses, crossover amplitude and complex modulus) for mud samples from PoB, and (iii) a significant increase in rheological properties for mud samples from PoE. For time-dependent tests, mud samples from PoB showed a substantial increase in hysteresis (~50% mean value) as compared to the changes in yield stresses and crossover amplitude. The analysis of gas production during degradation of organic matter showed a (i) significant release of carbon per g dry matter for mud samples from PoA, PoH and PoR, (ii) lower carbon release per g dry matter for mud samples from PoB, and (iii) a negligible carbon release per g dry matter for mud samples from PoE, which corresponded well with the change in rheological properties.

Keywords: mud; organic matter; anaerobic degradation; two-step yielding; yield stress; European ports

14.1 Introduction

Cohesive mud is composed of varying amount of fine-grained mineral particles (clay, silt and fine sand) and of organic matter (OM). Particulate organic matter is typically suspended in the water phase (as pure, biogenic organic matter or bound to suspended mineral particles) or attached to the already settled sediment. The existence of organic matter creates flocculated systems due to the interactions (bridging or charge neutralization) between the clay particles and organic matter [1]. The complex rheological fingerprint of cohesive mud such as viscoelasticity, shear thinning, thixotropy and two-step yielding is attributed to the formation of a clay-organic flocculated network [2–5]. For example, the mud samples having higher organic matter content displayed larger values of rheological properties (i.e., yield stresses and moduli), which were linked to the formation of a stronger and large number of clay-organic flocs [6].

The microbial degradation of organic matter, under anaerobic conditions, produces methane (CH₄) and carbon dioxide (CO₂) gases [7], which are either trapped in the mud layers or released via the water column. The density and settling–consolidation behavior of mud are known to be significantly influenced by the presence of entrapped gas bubbles. Moreover, owing to the significant influence of clay-organic flocs on the rheological and cohesive properties of mud [6,8–12], anaerobic degradation of organic matter is observed to significantly reduce the rheological properties of mud from Port of Hamburg, Germany [13,14]. However, as the sediment properties including type and content of organic matter, salinity, clay type and content, and particle size distribution, along with the sediment management techniques vary for different ports, different rheological responses to organic matter and its decay can be expected. A systematic analysis of the influence of organic matter degradation on the rheological properties of mud from different ports is still missing.

The main objective of the present study was, therefore, to analyze the effect of organic matter degradation on the rheological properties of mud samples from different European ports (Antwerp, Bremerhaven, Emden, Hamburg and Rotterdam). To this end, the rheological properties of fresh samples and microbially degraded samples, collected from different ports, were analyzed. Rheological tests included stress ramp-up tests, amplitude sweep tests, frequency sweep tests, time-dependent tests and structural recovery tests. In the first part of study, the results of gas production due to the anaerobic degradation of organic matter are discussed for mud samples from different ports, while in the second part, different rheological properties of fresh samples and samples degraded for 250 days were compared..

14.2 Experimental Methods

14.2.1 Sample Collection

Mud samples were collected from different European ports, including PoA, PoB, PoE, PoH and PoR (see Table S1, Supporting information) using either a core sampler or a grab sampler. Directly after sampling, the core was divided into sublayers such as fluid mud, pre-consolidated and consolidated sediments, based on their visual strength and consistency. However, in this study, only the top mud layer (fluid mud or pre-consolidated mud layer) was considered for analysis. PoA, PoB, PoE and PoR mud samples were collected from different locations within the port (see Table S1 for WGS coordinates and sample IDs). Conversely, the mud samples from PoH were collected from only one location (Köhlfleet mit Köhlfleethafen) due to the large number of samples collected from this particular location for our previous analysis [13]. Moreover, for comparison with PoE mud samples, only fluid

mud samples were considered from PoH, while for comparing with other ports, pre-consolidated mud samples were selected from PoH.

14.2.2 Wet Bulk Density, Particle Size Distribution and TOC Content

The specific gravity of the mineral particles was taken to be 2.65 [2]. The wet bulk density ρ of the mud samples was then estimated by determining the content of water/solids after drying at 105 °C for 24 h [15] (see Table S1). The particle size distribution of the mud samples was measured by using the static light scattering (SLS) technique. The total organic carbon (i.e., TOC content) of the mud samples was determined using an ISO standard [16] (see Table S1).

14.2.3 Anaerobic Degradation of Organic Matter

The anaerobic degradation of organic matter was performed by placing the fresh mud samples into 500 mL airtight glass bottles. The anaerobic conditions were maintained by flushing the headspace above the samples with N₂, and samples were incubated at 36 °C in the absence of light for 250 days. Anaerobic carbon release was estimated from the increase in headspace pressure and headspace composition, as analyzed by gas chromatography (GC-WLD; Da Vinci Laboratory Solutions). The share of CO₂-C dissolved in the aqueous phase was calculated using the CO₂ concentration, the pressure in the bottle headspace, and the temperature-corrected solubility of CO₂ in water as given by Henry's constant (given by Sander [17]). All the samples were incubated and analyzed in triplicate.

14.2.4 Rheological Characterization

The rheological analysis of both fresh and degraded mud samples was performed using a HAAKE MARS I rheometer (Thermo Scientific, Karlsruhe, Germany) with Couette geometry (gap width = 1 mm). The mud samples were gently homogenized before each experiment. After inserting the geometry into the sample, a waiting time of 3–5 min was adopted, in order to minimize the disturbances created by the bob. The rheological experiments were performed at 20 °C, maintained by a Peltier controller system. In order to check the repeatability, all the experiments were performed in duplicate, and the repeatability error was less than 2%.

Different types of rheological tests were performed in order to analyze the effect of organic matter degradation on the rheological properties of mud. Stress ramp-up tests were performed by linearly increasing the stress at a rate of 0.1–1.0 Pa s⁻¹, until the shear rate reached 300 s⁻¹ [4,18]. The corresponding rotation of the geometry was measured, which eventually provided the shear rate and apparent viscosity. The amplitude sweep tests were carried out at a frequency of 1 Hz by applying an oscillatory stress/amplitude. The storage (G') and loss (G'') moduli [3] were obtained as a function of oscillatory amplitude. The frequency sweep test was performed within the linear viscoelastic (LVE) regime, from 0.1 to 100 Hz. The outcome of frequency sweep tests was obtained in the form of storage and loss moduli as a function of frequency, which was then converted into complex modulus (G^*) and phase angle (δ). The time-dependent test was conducted by performing the shear rate ramp up and ramp down experiment as follows: (i) shear rate ramp-up from 0 to 100 s⁻¹ over 50 s, (ii) constant shear rate of 100 s⁻¹ over 50 s, and (iii) shear rate ramp-down from 100 to 0 s⁻¹ over 50 s. In addition to the time-dependent test, a structural recovery test was performed by using a three-step protocol given in Shakeel et al. [19]. In short, the first step provides the moduli of the mud sample (G'_0) before pre-shearing, by performing a small amplitude oscillatory time sweep experiment. The second step involves the application of a high shear rate (300 s⁻¹ for 500 s) to completely disturb the sample. The last step allows the sample to recover its structure by again performing a small amplitude oscillatory time sweep experiment for 500 s and recording the moduli (G') as a function of time.

14.3 Results and Discussion

14.3.1 Anaerobic Degradation Tests

The cumulated release of carbon after 250 days of degradation time is shown in Figure 1a for mud samples from different ports. It is evident that the mud samples from PoA, PoH and PoR showed significant release of carbon per g dry matter while lower carbon release per g dry matter was observed for mud samples from PoB, which corresponded well with the change in rheological properties. The comparison between PoE mud samples and fluid mud samples from PoH for cumulated release of carbon after 250 days of degradation time is presented in Figure 1b. It is evident that the mud samples from PoE displayed a negligible carbon release, while in the case of PoH fluid mud samples, a pronounced carbon release was observed, which is again in line with the rheological results.

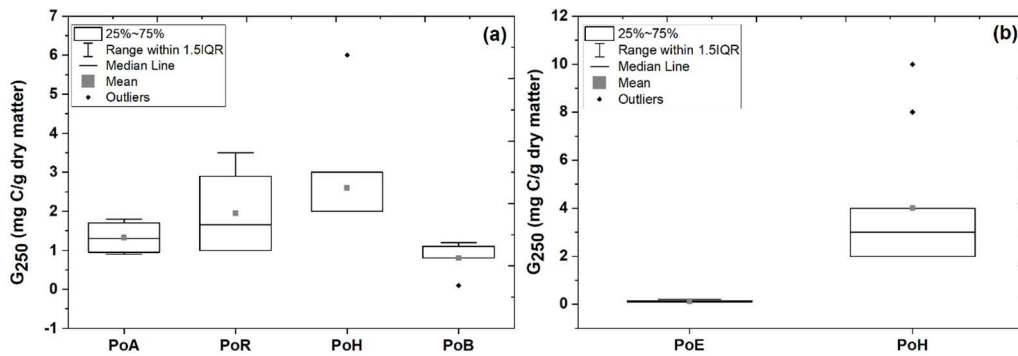


Figure 1. Cumulative carbon release after 250 days of degradation normalized to dry mass for mud samples (a) from different ports, and (b) from PoE and fluid mud samples from PoH. 1.5IQR, factor 1.5 of the interquartile range (25~75%).

14.3.2 Wet Bulk Density, Particle Size Distribution and TOC Content

The change in excess wet bulk density ($\rho - \rho_w$, with ρ_w = density of water), obtained by the difference between excess wet bulk density of degraded and fresh mud samples, is plotted as a function of excess wet bulk density of fresh mud samples (Figure S1). It is seen that the change in wet bulk density incurred during the long-term (250 days) incubation to degrade organic matter was generally lower than 5% of its original value. It was, therefore, assumed that changes in rheological properties between fresh and degraded samples were not related to the change in density or water content.

Mud samples obtained from PoB, PoE, PoH and PoR showed quite similar particle size distribution (Figure S2a) along with the similar D50 values (see Table S2). Conversely, the mud samples collected from PoA displayed two different behaviors (Figure S2b), i.e., one was similar to the other ports while another one showed bimodal particle size distribution along with the higher D50 values (see samples A2 and A4 in Table S2), which was linked with the presence of a significant amount of sand sized particles. For these two samples (A2 and A4), the higher sand content was also found in the particle size distribution obtained by the sieving technique [20], which verified the SLS results (see Table S3). Some other sediment properties such as TOC content, electrical conductivity and pH of mud samples from different ports are presented in Table S1.

14.3.3 Stress Ramp-Up Tests

Stress ramp-up tests were performed to analyze the effect of organic matter degradation on the yield stresses of mud from different ports. Figure S3 shows the outcome of stress ramp-up tests in terms of apparent viscosity as a function of shear stress for fresh mud samples and degraded mud samples from various ports. A two-step yielding behavior was evident from the two declines in viscosity. A similar two-step yielding behavior has already been reported in the literature for fine-grained sediments

[3,21]. This two-step yielding behavior in mud samples was associated with the structural reorganization during shearing, i.e., breakage of interconnected networks of flocs, formation of rolls/cylinder-like structures and collapse of cylinder-like structures [22]. The yield stress values, corresponding to these viscosity declines, were defined as static yield stress (τ_s) and fluidic yield stress (τ_f).

Figure S3 shows that the degraded mud samples had lower yield stress values as compared to the fresh mud samples, except for mud samples from PoB and PoE. This decrease in yield stress values may be associated with the degradation of organic matter and the corresponding decline of the extent of mineral bridging, which eventually results in a weaker system [6]. A similar decrease in yield stress values by chemically removing the organic matter from mud was also reported in the literature [23]. The mud samples from PoB and PoE showed either similar yield stress values or even higher yield stress values after organic matter degradation.

In order to further quantify the influence of organic matter degradation on the yield stress of mud samples from different ports, the change in static and fluidic yield stresses (degraded–fresh) was plotted as a function of yield stress of fresh samples (see Figure 2a and 2c). A strong inverse correlation was observed between the change in yield stresses and the yield stresses of fresh mud samples, i.e., the higher the original yield stress, the higher its reduction after organic matter degradation (i.e., negative slope) [13,14]. Moreover, the following empirical equation was used to fit the experimental data of change in the rheological property (degraded–fresh) as a function of the same rheological property before degradation:

$$y = a + bx \tag{1}$$

where a (Pa or Pa s⁻¹) and b (–) represent the intercept and slope of the line, respectively. The values of these fitting parameters are presented in Table S4. The values of the slope indicated that the yield stresses (static and fluidic) were significantly reduced for mud samples from PoA and PoH due to the degradation of organic matter. In the case of mud samples from PoB and PoR, the reduction in yield stresses after organic matter degradation was less significant, as evident from the smaller values of negative slope (Table S4). The mud samples collected from PoE exhibited smaller densities as compared to the samples collected from other ports (see Table S1). Therefore, the change in yield stresses (degraded–fresh) as a function of yield stresses of fresh mud samples for PoE is compared with the fluid mud samples collected from PoH with similar densities (Figure 2b and 2d, static and fluidic yield stresses). It is observed that the mud samples from PoE displayed an increase in both static and fluidic yield stress values after organic matter degradation (i.e., positive slope), while in the case of PoH, a pronounced negative slope was found with significant reduction in both static and fluidic yield stresses (Table S4).

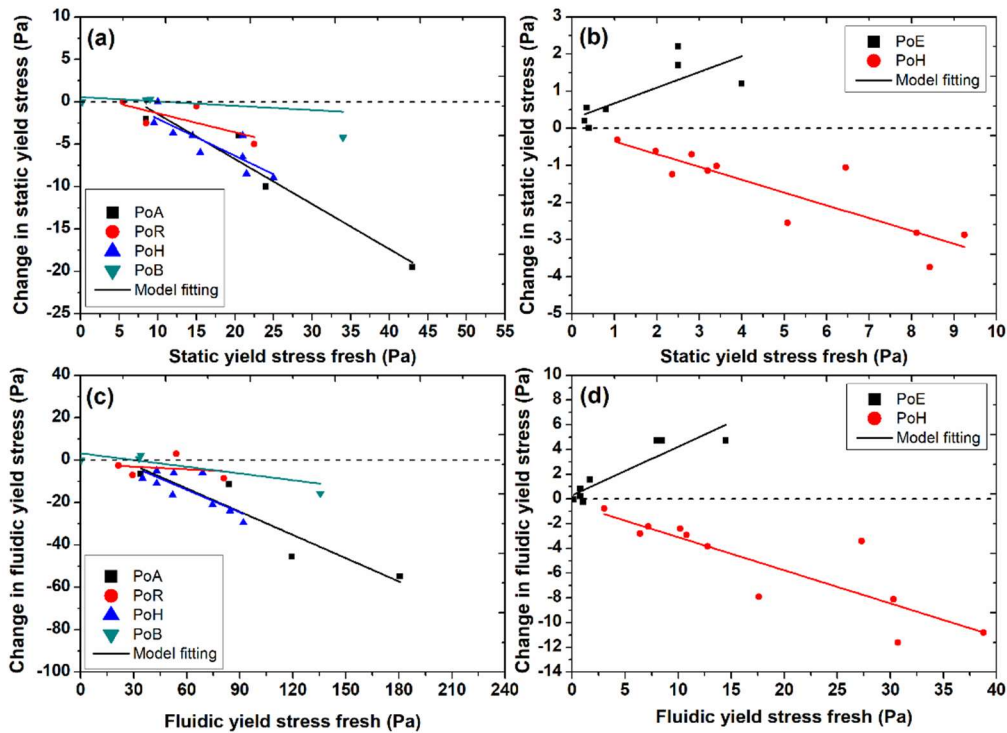


Figure 2. Change in static yield stress (degraded–fresh) as a function of static yield stress of fresh mud samples (a) from different ports and (b) from PoE and fluid mud samples from PoH; (c) change in fluidic yield stress (degraded–fresh) as a function of fluidic yield stress of fresh mud samples (c) from different ports and (d) from PoE and fluid mud samples from PoH. The dashed line represents the value where the degraded and fresh mud samples have the same yield stresses. The solid line represents the empirical fitting using Equation (1).

The aforementioned results were plotted in terms of percent change in yield stresses $\left(\frac{\text{degraded} - \text{fresh}}{\text{fresh}} \times 100\right)$ after organic matter degradation for different ports (Figure 3). These results identified a significant reduction in yield stresses for PoA and PoH (~20–40% mean value), a less pronounced decrease in yield stresses for PoR (~10–20% mean value), a negligible change in yield stresses for PoB (~0–5% mean value), and a significant increase in yield stresses for PoE (~40–70% mean value). The significant decrease in yield stresses for mud from PoA and PoH may be attributed to the active nature of the organic matter, particularly for PoH [14], which degrades under suitable conditions. The small or negligible changes in yield stresses after degradation for PoB may be associated with the lower organic matter decay as compared to the other ports. Conversely, the increase in yield stresses after degradation of organic matter in mud from PoE is quite unexpected. It is hypothesized that under laboratory conditions, i.e., in a closed incubation system with no addition of fresh new carbon and favorable conditions of temperature, the composition of the microbial community, its abundance, and thereby the floc/biofilm architecture also change. This means that as organic matter (OM) is decayed, and is released as CH₄ and CO₂, the remaining OM undergoes a transformation toward more stable organo-mineral associations with concurrent changes of the microbial community composition, compared to the fresh sample. As a result, different floc and biofilm properties change, which could result in a different strength. It is assumed that this effect also occurs in the samples from the other ports but might be masked due to the high OM decay and the significant mass loss of carbon, which dominate the rheological response by disrupting mineral bridging. Hence, due to low mass loss and OM decay rates in PoE (see Figure 1), other processes changing the physical architecture of flocs and biofilms might become more relevant.

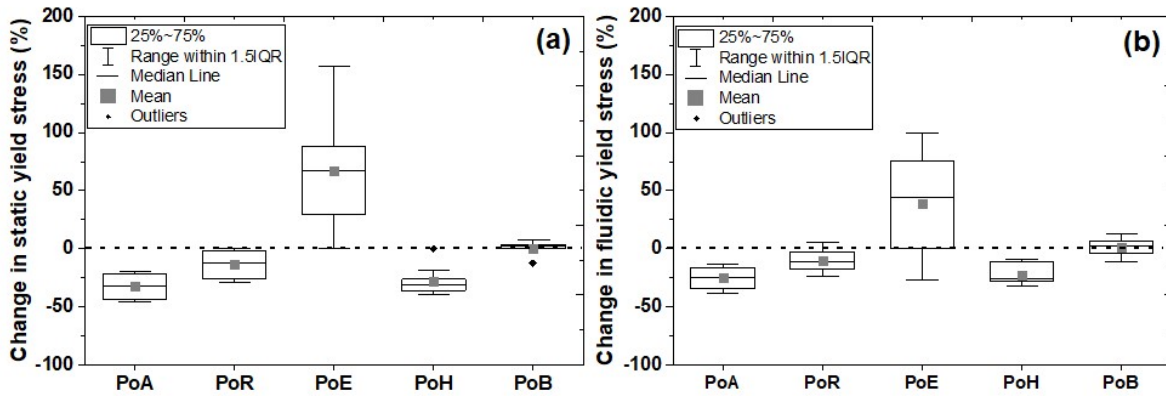


Figure 3. Percent change in (a) static and (b) fluidic yield stresses $\left(\frac{\text{degraded} - \text{fresh}}{\text{fresh}} \times 100\right)$ of mud samples from different ports. 1.5IQR, factor 1.5 of the interquartile range (25~75%). Negative values represent the percent decrease in yield stresses after degradation, while positive values represent the percent increase in yield stresses after degradation.

14.3.4 Amplitude Sweep Tests

In addition to the yield stress, the transition between solid-like and liquid-like behavior of mud samples was investigated by performing oscillatory amplitude sweep tests. Figure S4 shows the phase angle as a function of oscillatory amplitude for fresh and degraded mud samples. The solid-liquid transition point was estimated when the phase angle became equal to 45° (i.e., crossover point between G' and G''), and the corresponding stress amplitude was demonstrated as crossover amplitude. Figure S4 illustrates a decrease in crossover amplitude by the degradation of organic matter, except for samples from PoE and PoB, which is in agreement with the yield stress analysis.

Change in crossover amplitude (degraded–fresh) is now plotted as a function of crossover amplitude of fresh mud samples from different ports (see Figure 4a). The organic matter degradation again showed a significant influence on the crossover amplitude for the mud samples having higher crossover amplitude before degradation. The experimental data were then fitted with Equation (1), and the values of a and b are given in Table S4. The slope values are quite similar in the case of crossover amplitude and yield stresses for mud samples from different ports. This behavior shows that the influence of organic matter degradation on the extent of decrease in rheological properties (crossover amplitude and yield stresses) is quite similar, because both these properties involve the application of a shearing action to disturb the intact structure. The change in crossover amplitude (degraded–fresh) as a function of crossover amplitude of fresh mud samples for PoE was again compared with the fluid mud samples collected from PoH with similar densities (Figure 4b). It is again evident that the mud samples from PoE displayed an increase in crossover amplitude values after organic matter degradation (i.e., positive slope), while in the case of PoH, a pronounced negative slope was observed with significant reduction in crossover amplitude (Table S4).

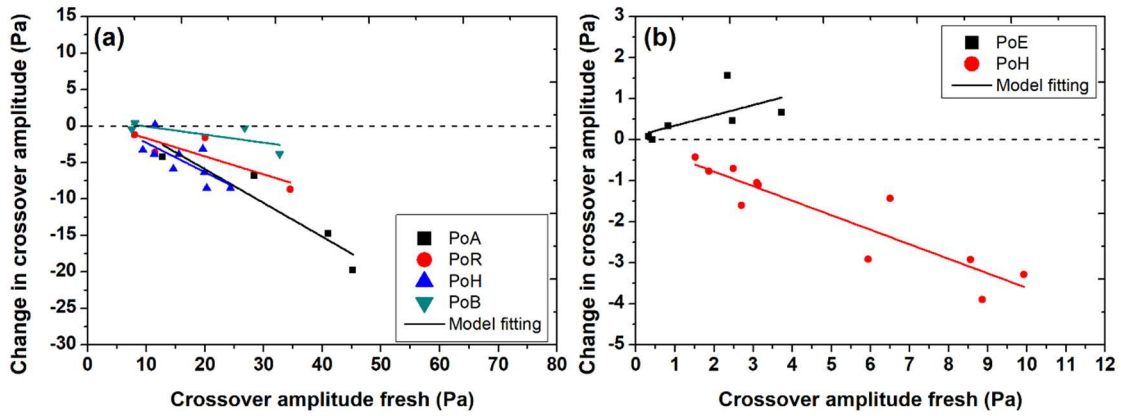


Figure 4. Change in crossover amplitude (degraded–fresh) as a function of crossover amplitude of fresh mud samples (a) from different ports and (b) from PoE and fluid mud samples from PoH. The dashed line represents the value where the degraded and fresh mud samples have the same crossover amplitude. The solid line represents the empirical fitting using Equation (1).

The percent change in crossover amplitude $\left(\frac{\text{degraded} - \text{fresh}}{\text{fresh}} \times 100\right)$ after organic matter degradation for mud samples from different ports is shown in Figure 5. These results again identified a significant reduction in crossover amplitude for PoA, PoH and PoR (~20–30% mean value), a negligible decrease in crossover amplitude for PoB (~0–5% mean value), and a significant increase in crossover amplitude for PoE (~30% mean value). These results verified the outcome of yield stress analysis and can be attributed to the processes changing the physical architecture of flocs and biofilms.

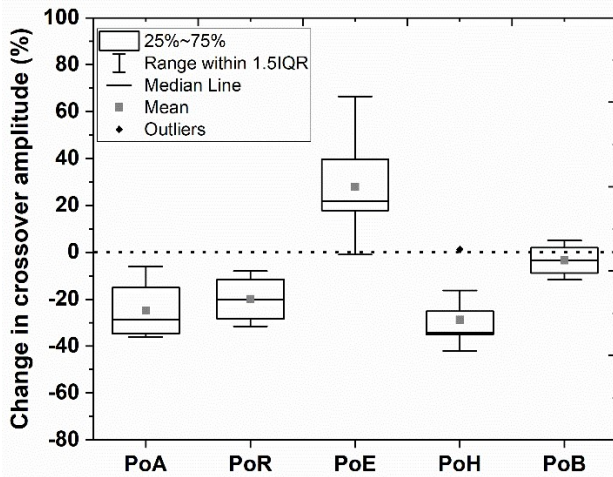


Figure 5. Percent change in crossover amplitude $\left(\frac{\text{degraded} - \text{fresh}}{\text{fresh}} \times 100\right)$ of mud samples from different ports. 1.5IQR, factor 1.5 of the interquartile range (25~75%). Negative values represent the percent decrease in crossover amplitude, while positive values represent the percent increase in crossover amplitude after degradation.

14.3.5 Frequency Sweep Tests

Frequency sweep tests were performed within the LVE regime from 0.1 to 100 Hz in order to analyze the strength of mud samples, without disturbing their structure, and before and after degradation of the organic matter. Figure S5 shows the complex modulus and phase angle as a function of frequency for fresh and degraded mud samples for different ports. A solid-like behavior was observed for both fresh and degraded mud samples, i.e., an almost independence of complex modulus on frequency and significantly smaller values of phase angle [24]. A similar solid-like character of mud samples has already been reported in the literature [5,25–27]. However, the organic matter degradation resulted in a weaker system (i.e., lower complex modulus values), particularly for PoA and PoH mud samples.

The experimental data at higher frequencies were excluded from the graphs due to the inertial effects caused by the rheometer head.

Figure 6a shows the correlation between the change in complex modulus at 1 Hz (degraded–fresh) and the values of complex modulus at 1 Hz of fresh mud samples collected from different ports on a semi-log scale. A significant decrease in complex modulus was observed due to the degradation of organic matter, which became more pronounced for the fresh samples having higher complex modulus, particularly for PoA and PoH mud samples. For PoB and PoR mud samples, the complex modulus remains almost the same after the organic matter degradation. This behavior was also evident from the values of the fitting parameters (i.e., slope) of Equation (1) for the experimental data of complex modulus (Table S4). The comparison between PoE and fluid mud samples from PoH for change in complex modulus at 1 Hz due to the organic matter degradation is presented in Figure 6b. It is again evident that the mud samples from PoE displayed an increase in complex modulus values after organic matter degradation (i.e., positive slope), while in the case of PoH, a pronounced negative slope was observed with significant reduction in complex modulus (Table S4).

The correlation between the change in phase angle at 1 Hz (degraded–fresh) and the values of phase angle at 1 Hz of fresh mud samples, obtained from different ports, was not prominent (Figure S6). However, the degraded samples from PoA, PoB and PoH exhibited positive values of change in phase angle (i.e., higher phase angle values of degraded samples as compared to the fresh samples), which indicated the weakening of these mud samples. However, for mud samples from PoE and PoR, negative values of change in phase angle were observed, which highlighted the strengthening of mud samples.

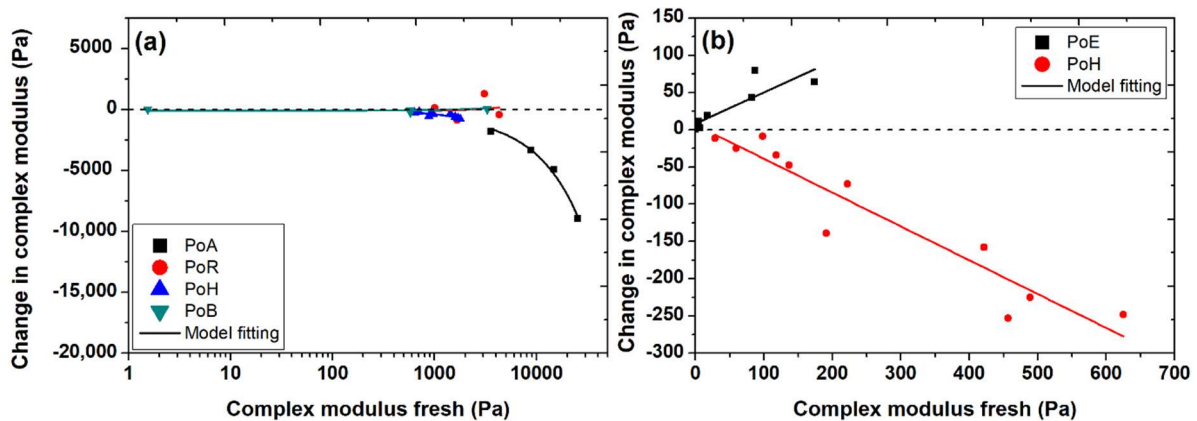


Figure 6. Change in complex modulus (degraded–fresh) at 1 Hz as a function of complex modulus at 1 Hz of fresh mud samples (a) from different ports and (b) from PoE and fluid mud samples from PoH. The solid line represents the empirical fitting using Equation (1). The dashed line represents the value where the degraded and fresh mud samples have the same complex modulus at 1 Hz.

The percent change in complex modulus $\left(\frac{\text{degraded} - \text{fresh}}{\text{fresh}} \times 100\right)$ after organic matter degradation for mud samples from different ports is shown in Figure 7. These results identified a significant reduction in complex modulus for PoA and PoH (~30–40% mean value), a negligible increase in complex modulus for PoB (~0–5% mean value), and a significant increase in complex modulus for PoE (~80% mean value). These results corresponded well to the outcome of yield stress and crossover amplitude. However, for mud samples from PoR, a negligible change in complex modulus was observed as compared to the changes in yield stresses and crossover amplitude. This behavior shows that the organic matter degradation strongly influenced the rheological property, which involves the destruction of structure (i.e., yield stress and crossover amplitude). While the effect of organic matter degradation on the rheological property, which is typically measured by having undisturbed structure (i.e., complex

modulus within LVE regime), was negligible for the mud samples from PoR. This behavior may be attributed to the higher salinity (see Table S1 for conductivity values) of these samples, which results in stronger flocculated structure and compensates the decrease in modulus values due to the organic matter degradation. However, this compensation offered by the salt-induced flocculation was negligible for yield stresses and crossover amplitude due to the application of higher shearing action for these rheological properties and the weaker nature of salt-induced flocs [28].

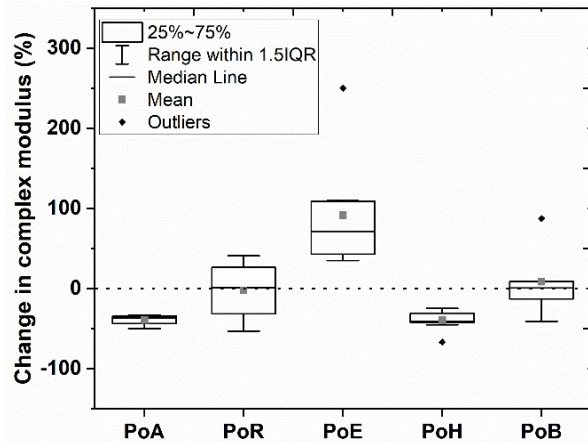


Figure 7. Percent change in complex modulus at 1 Hz $\left(\frac{\text{degraded} - \text{fresh}}{\text{fresh}} \times 100\right)$ of mud samples from different ports. 1.5IQR, factor 1.5 of the interquartile range (25~75%). Negative values represent the percent decrease in the complex modulus, while positive values represent the percent increase in the complex modulus after degradation.

14.3.6 Time Dependent and Structural Recovery Tests

Shear rate-controlled ramp-up and ramp-down experiments were performed from 0 to 100 s⁻¹, in order to investigate the time-dependent behavior of fresh and degraded mud samples from different ports. The results of the time-dependent experiments revealed the existence of a typical clockwise loop at higher shear rates for both fresh and degraded mud samples (Figure S7). However, at lower shear rates, a counterclockwise loop was observed, which may be associated with a shear thickening phenomenon or a structural reorganization due to the shearing action [3,22]. A similar combination of clockwise and counterclockwise loops has already been reported in the literature for mud samples [29].

Furthermore, the hysteresis loop was significantly lower for the degraded mud samples as compared to the fresh mud samples, which is again in line with the previous results. The hysteresis area between the clockwise loop (i.e., shaded region in Figure S7) was estimated. The change in hysteresis area (degraded–fresh) as a function of the values of hysteresis area of fresh mud samples, for different ports, is presented in Figure 8a. A similar decrease in hysteresis area was found as a function of organic matter degradation as already observed for other rheological properties, except for mud samples from PoB. This behavior is also evident from the values of fitting parameters of Equation (1) for time-dependent experiment (Table S4). The mud samples from PoB displayed an increase in hysteresis area after the organic matter degradation, as also observed for PoE mud samples (Figure 8b).

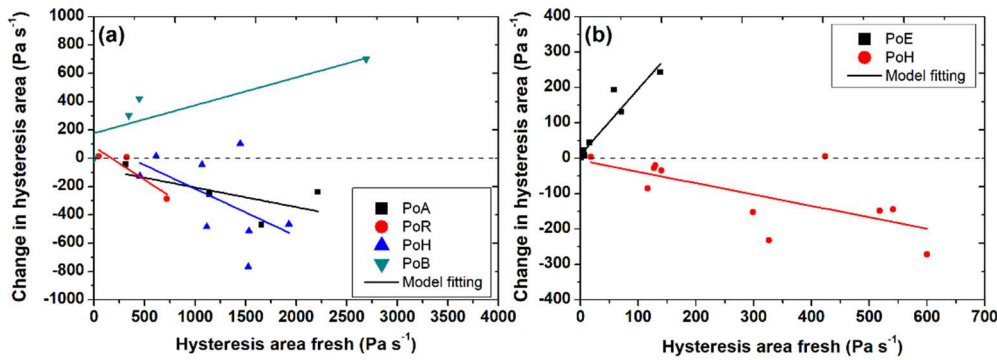


Figure 8. Change in hysteresis area (degraded–fresh) as a function of hysteresis area of fresh mud samples (a) from different ports and (b) from PoE and fluid mud samples from PoH. The dashed line represents the value where the degraded and fresh mud samples have the same hysteresis area. The solid line represents the empirical fitting using Equation (1).

The percent change in hysteresis area $\left(\frac{\text{degraded} - \text{fresh}}{\text{fresh}} \times 100\right)$ after organic matter degradation for mud samples from different ports is shown in Figure 9. These results identified a significant reduction in hysteresis area for mud samples from PoA, PoH and PoR (~20–30% mean value) and a significant increase in hysteresis area for PoE mud samples (~210% mean value). These results again corresponded well to the outcome of yield stress and crossover amplitude. However, for mud samples from PoB, a substantial increase in hysteresis area (~50% mean value) was observed as compared to the changes in yield stresses and crossover amplitude. This behavior shows that the influence of organic matter degradation on the rheological property, which involves the destruction of structure (i.e., yield stress and crossover amplitude), was negligible for PoB mud samples. However, the organic matter degradation significantly affected the rheological property, which involves the measurement of a time-dependent response (i.e., stress/viscosity) of the mud samples from PoB. This behavior may be attributed to the different size and type of organic matter present in the mud samples from PoB, which needs further investigation.

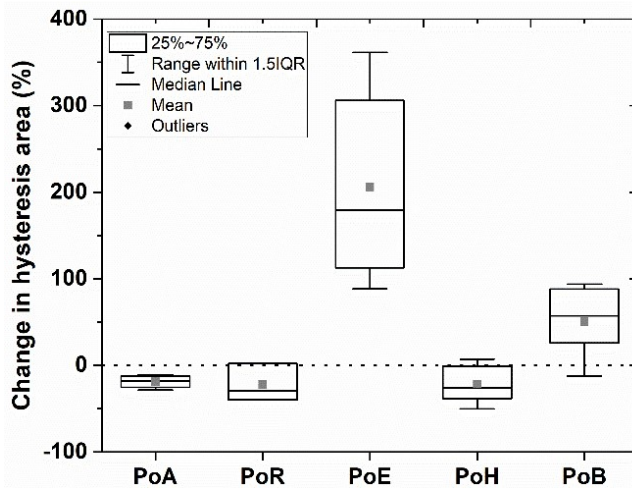


Figure 9. Percent change in the hysteresis area $\left(\frac{\text{degraded} - \text{fresh}}{\text{fresh}} \times 100\right)$ of mud samples from different ports. 1.5IQR, factor 1.5 of the interquartile range (25~75%). Negative values represent the percent decrease in the hysteresis area, while positive values represent the percent increase in the hysteresis area after degradation.

In addition to the time-dependent characteristic of fresh and degraded mud samples, the structural recovery after intensive pre-shearing was investigated using a three-step protocol, as explained in Section 2.4. The normalized time-dependent storage modulus (G'/G'_0) as a function of time for fresh and degraded mud samples is presented in Figure S8. The oscillations in the storage modulus behavior

as a function of time may be associated with the higher elasticity of the samples, which is typically stated as creep ringing [19,30]. A simple stretched exponential function, adapted from Mobuchon et al. [31], was further used to fit the experimental data of the third step of structural recovery protocol, written as follows:

$$\frac{G'}{G'_0} = \frac{G'_i}{G'_0} + \left(\left(\frac{G'_\infty - G'_i}{G'_0} \right) \left(1 - \exp \left[- \left(\frac{t}{t_r} \right)^d \right] \right) \right) \quad (2)$$

where G'_∞ and t_r represent the two most important parameters of equilibrium storage modulus and characteristic time of the material, respectively. G' is the time-dependent storage modulus of mud after shearing, G'_0 is the storage modulus before structural breakup, G'_i is the storage modulus right after pre-shearing (at $t \rightarrow 0$) and d is the stretching exponent. The change in normalized equilibrium storage modulus, G'_∞/G'_0 (degraded–fresh) as a function of the values of normalized equilibrium storage modulus of fresh mud samples is plotted in Figure 10a for different ports. It can be seen that the values of normalized equilibrium storage modulus (G'_∞/G'_0) are higher for the degraded mud samples than for the fresh mud samples (i.e., positive values of change in normalized equilibrium storage modulus). This may be attributed to the fact that the degradation of organic matter results in a weaker system, behaving as a purely mineral suspension without the bridging effect provided by organic matter, which eventually has a better structural recovery (i.e., higher values of modulus, higher strength) after pre-shearing. A similar enhanced structural recovery was observed in the literature for mud samples having lower organic matter content as compared to the samples having higher organic matter content [19].

Furthermore, Figure 10b shows a correlation between the change in characteristic time, t_r (degraded–fresh) and the values of characteristic time of fresh mud samples, for different ports. It is evident that for some samples the characteristic time was higher for degraded samples as compared to fresh mud samples (i.e., positive value of change), while for other samples it was lower for degraded samples than the fresh samples (i.e., negative value of change). This behavior may again be linked to the variable density of the mud samples, in addition to the organic matter degradation.

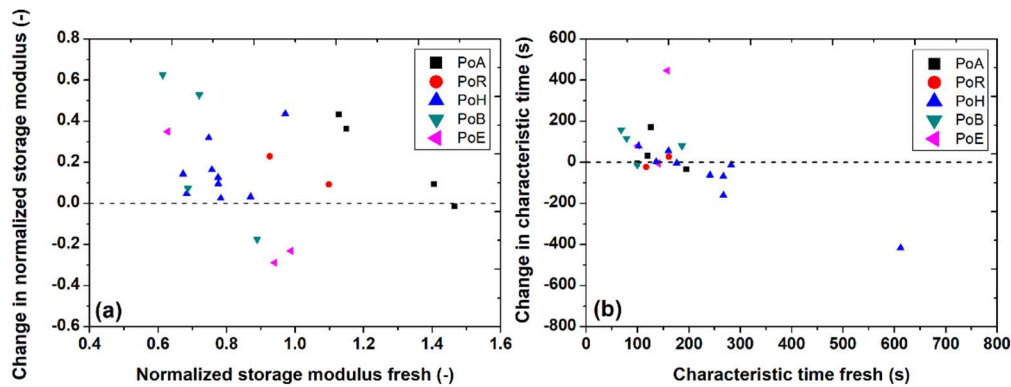


Figure 10. (a) Change in normalized equilibrium storage modulus, G'_∞/G'_0 (degraded–fresh) as a function of normalized equilibrium storage modulus, G'_∞/G'_0 of fresh mud samples from different ports, and (b) change in characteristic time, t_r (degraded–fresh) as a function of characteristic time, t_r of fresh mud samples from different ports. The dashed line represents the value where the degraded and fresh mud samples have same normalized equilibrium storage modulus or characteristic time.

14.4 Conclusions

The presence of clay-organic flocs in cohesive mud results in a complex rheological behavior of mud including viscoelasticity, shear-thinning, thixotropy and two-step yielding. The degradation of this

organic matter, under anaerobic conditions, results in the formation of greenhouse gases (CO₂ and CH₄) and influences the rheological properties of mud by breaking/weakening the organic bridges between mineral particles. Hence, in this study, the effect of organic matter degradation on the rheological properties of mud samples, collected from different ports, was examined. The mud samples were collected from five different European ports (Port of Antwerp (PoA), Port of Bremerhaven (PoB), Port of Emden (PoE), Port of Hamburg (PoH) and Port of Rotterdam (PoR)), in order to have samples with varying sediment properties. The rheological analysis of fresh and degraded mud samples was performed with the help of several tests, including stress ramp-up tests, amplitude sweep tests, frequency sweep tests, time-dependent tests and structural recovery tests.

The results showed a significant reduction in yield stresses for PoA and PoH (~20–40% mean value), a less pronounced decrease in yield stresses for PoR (~10–20% mean value), a negligible change in yield stresses for PoB (~0–5% mean value), and a significant increase in yield stresses for PoE (~40–70% mean value). This varying behavior is attributed to the nature of organic matter and its degradability, port maintenance strategies and sediment properties. Moreover, in order to understand the increase in yield stresses after degradation of organic matter for mud samples of low gas production potential, such as from PoE, it is recommended to study the change in floc and biofilm structure that results from long-term laboratory incubations of organic mud suspensions, for example by using a floc camera setup. The similar trend was also observed for other rheological properties, including crossover amplitude and complex modulus for mud samples from different ports. For time-dependent tests, mud samples from PoB showed a substantial increase in hysteresis area (~50% mean value) as compared to the changes in yield stresses and crossover amplitude. This behavior may be attributed to the different size and type of organic matter present in the mud samples from PoB, which needs further investigation. Moreover, the structural recovery was higher for the degraded mud samples than for the fresh mud samples from different ports. This may be attributed to the fact that the degradation of organic matter results in a weaker system, behaving as a purely mineral suspension with better structural recovery. The analysis of gas production during degradation of organic matter showed a (i) significant release of carbon per g dry matter for mud samples from PoA, PoH and PoR, (ii) lower carbon release per g dry matter for mud samples from PoB, and (iii) a negligible carbon release per g dry matter for mud samples from PoE, which corresponded well with the change in rheological properties. This study provided a useful understanding about the influence of organic matter degradation on the rheological properties of mud from different European ports, which can be used to optimize sediment management strategies in ports and waterways.

Supplementary Materials

The following supporting information can be downloaded at: www.mdpi.com/xxx/s1, Table S1: Details of the mud samples collected from different European ports; Table S2: Particle size distribution, obtained by static light scattering technique, of the mud samples collected from different European ports; Table S3: Particle size distribution, obtained by sieving technique (DIN ISO 11277 2009), of the mud samples collected from different European ports; Table S4: The values of the fitting parameters of Eq. 1 for different ports; Figure S1: Change in excess bulk density (degraded – fresh) as a function of excess bulk density ($\rho - \rho_w$) of fresh mud sample from different ports. The dashed line represents the value where the degraded and fresh mud samples have the same bulk densities; Figure S2: Particle size distribution of (a) mud samples from PoA, PoR, PoE, PoH and PoB; (b) mud samples from different locations of PoA obtained using static light scattering technique; Figure S3: Apparent viscosity as a function of shear stress for fresh mud samples (filled symbol) and mud samples degraded for 250 days

(empty symbols) collected from different ports. The dashed lines represent the static (τ_s) and fluidic (τ_f) yield stresses; Figure S4: Phase angle as a function of oscillatory stress amplitude for fresh mud samples (filled symbol) and mud samples degraded for 250 days (empty symbols) collected from different ports. The dashed line represents the crossover amplitude (i.e., $G' = G''$ or phase angle = 45°); Figure S5: (a) Complex modulus and (b) phase angle as a function of frequency for fresh mud samples (filled symbol) and mud samples degraded for 250 days (empty symbols) collected from different ports. The dashed lines represent the complex modulus and phase angle at 1 Hz, which is typically used for comparative analysis of different samples; Figure S6: Change in phase angle (degraded – fresh) at 1 Hz as a function of phase angle at 1 Hz of fresh mud samples from different ports. The dashed line represents the value where the degraded and fresh mud samples have same phase angle at 1 Hz; Figure S7: Shear stress as a function of shear rate obtained by performing shear rate controlled ramp-up and ramp-down experiments for fresh mud sample and mud sample degraded for 250 days, collected from PoH. The direction of arrows represent the ramp-up or ramp-down curve. The filled region represents the hysteresis area; Figure S8: Normalized time dependent storage modulus, G'/G'_0 as a function of time obtained from the structural recovery step for fresh mud sample and mud sample degraded for 250 days, collected from PoH. The solid line represents the empirical fitting using Eq. 2.

Acknowledgments

This study is carried out within the framework of the MUDNET academic network: <https://www.tudelft.nl/mudnet/> (accessed on 26 January, 2022). The authors would like to acknowledge Deltares, the Netherlands, for the use of the HAAKE MARS I rheometer, which was made possible thanks to the Memorandum of Understanding signed between Deltares and the TU Delft.

Conflicts of Interest: The authors declare no conflict of interest.

References

- Lagaly, G.; Dékány, I. Chapter 8—Colloid Clay Science. In *Developments in Clay Science*; Bergaya, F., Lagaly, G., Eds.; Elsevier: Amsterdam, The Netherlands, 2013; Volume 5, pp. 243–345.
- Coussot, P. *Mudflow Rheology and Dynamics*; CRC Press: Rotterdam, The Netherlands, 1997; p. 272.
- Shakeel, A.; Kirichek, A.; Chassagne, C. Rheological analysis of mud from Port of Hamburg, Germany. *J. Soils Sediments* 2020, 20, 2553–2562. <https://doi.org/10.1007/s11368-019-02448-7>.
- Shakeel, A.; Kirichek, A.; Chassagne, C. Yield stress measurements of mud sediments using different rheological methods and geometries: An evidence of two-step yielding. *Mar. Geol.* 2020, 427, 106247. <https://doi.org/10.1016/j.margeo.2020.106247>.
- Van Kessel, T.; Blom, C. Rheology of cohesive sediments: Comparison between a natural and an artificial mud. *J. Hydraul. Res.* 1998, 36, 591–612. <https://doi.org/10.1080/00221689809498611>.
- Shakeel, A.; Kirichek, A.; Chassagne, C. Is density enough to predict the rheology of natural sediments? *Geo-Mar. Lett.* 2019, 39, 427–434. <https://doi.org/10.1007/s00367-019-00601-2>.
- Zander, F.; Heimovaara, T.; Gebert, J. Spatial variability of organic matter degradability in tidal Elbe sediments. *J. Soils Sediments* 2020, 20, 2573–2587. <https://doi.org/10.1007/s11368-020-02569-4>.
- Malarkey, J.; Baas, J.H.; Hope, J.A.; Aspden, R.J.; Parsons, D.R.; Peakall, J.; Paterson, D.M.; Schindler, R.J.; Ye, L.; Lichtman, I.D.; et al. The pervasive role of biological cohesion in bedform development. *Nat. Commun.* 2015, 6, 6257. <https://doi.org/10.1038/ncomms7257>.
- Parsons, D.R.; Schindler, R.J.; Hope, J.A.; Malarkey, J.; Baas, J.H.; Peakall, J.; Manning, A.J.; Ye, L.; Simmons, S.; Paterson, D.M.; et al. The role of biophysical cohesion on subaqueous bed form size. *Geophys. Res. Lett.* 2016, 43, 1566–1573. <https://doi.org/10.1002/2016GL067667>.
- Schindler, R.J.; Parsons, D.R.; Ye, L.; Hope, J.A.; Baas, J.H.; Peakall, J.; Manning, A.J.; Aspden, R.J.; Malarkey, J.; Simmons, S.; et al. Sticky stuff: Redefining bedform prediction in modern and ancient environments. *Geology* 2015, 43, 399–402. <https://doi.org/10.1130/G36262.1>.
- Tolhurst, T.J.; Gust, G.; Paterson, D.M. The influence of an extracellular polymeric substance (EPS) on cohesive sediment stability. *Proc. Mar. Sci.* 2002, 5, 409–425.
- Wurpts, R.; Torn, P. 15 years experience with fluid mud: Definition of the nautical bottom with rheological parameters. *Terra Aqua* 2005, 99, 22–32.
- Shakeel, A.; Zander, F.; De Klerk, J.; Kirichek, A.; Gebert, J.; Chassagne, C. Effect of organic matter degradation in cohesive sediment: A detailed rheological analysis. *J. Soils Sediments* 2022. <https://doi.org/10.1007/s11368-022-03156-5>.
- Zander, F.; Shakeel, A.; Kirichek, A.; Chassagne, C.; Gebert, J. Effect of organic matter degradation in cohesive sediment: A spatiotemporal analysis of yield stresses. *J. Soils Sediments* 2022. <https://doi.org/10.1007/s11368-022-03156-6>.
- ISO 11465; Soil Quality—Determination of Dry Matter and Water Content on a Mass Basis—Gravimetric Method. International Organization for Standardization: Geneva, Switzerland, 1993.
- ISO 10694; Soil Quality—Determination of Organic and Total Carbon after Dry Combustion (Elementary Analysis). International Organization for Standardization: Geneva, Switzerland, 1995.
- Sander, R. Compilation of Henry's law constants (version 4.0) for water as solvent. *Atmos. Chem. Phys.* 2015, 15, 4399–4981. <https://doi.org/10.5194/acp-15-4399-2015>.
- Shakeel, A.; Kirichek, A.; Talmon, A.; Chassagne, C. Rheological analysis and rheological modelling of mud sediments: What is the best protocol for maintenance of ports and waterways? *Estuar. Coast. Shelf Sci.* 2021, 257, 107407. <https://doi.org/10.1016/j.ecss.2021.107407>.
- Shakeel, A.; Kirichek, A.; Chassagne, C. Effect of pre-shearing on the steady and dynamic rheological properties of mud sediments. *Mar. Pet. Geol.* 2020, 116, 104338. <https://doi.org/10.1016/j.marpetgeo.2020.104338>.
- ISO 11277; Soil Quality—Determination of Particle Size Distribution in Mineral Soil Material—Method by Sieving and Sedimentation. International Organization for Standardization: Geneva, Switzerland, 2009.
- Nie, S.; Jiang, Q.; Cui, L.; Zhang, C. Investigation on solid-liquid transition of soft mud under steady and oscillatory shear loads. *Sediment. Geol.* 2020, 397, 105570. <https://doi.org/10.1016/j.sedgeo.2019.105570>.
- Shakeel, A.; MacIver, M.R.; van Kan, P.J.M.; Kirichek, A.; Chassagne, C. A rheological and microstructural study of two-step yielding in mud samples from a port area. *Colloids Surf. A Physicochem. Eng. Asp.* 2021, 624, 126827. <https://doi.org/10.1016/j.colsurfa.2021.126827>.
- Fass, R.W.; Wartel, S.I. Rheological properties of sediment suspensions from Eckernforde and Kieler Forde Bays, Western Baltic Sea. *Int. J. Sediment Res.* 2006, 21, 24–41.
- Lupi, F.R.; Shakeel, A.; Greco, V.; Oliviero Rossi, C.; Baldino, N.; Gabriele, D. A rheological and microstructural characterisation of bigels for cosmetic and pharmaceutical uses. *Mater. Sci. Eng. C* 2016, 69, 358–365. <https://doi.org/10.1016/j.msec.2016.06.098>.
- Shakeel, A.; Kirichek, A.; Chassagne, C. Rheological analysis of natural and diluted mud suspensions. *J. Non-Newton. Fluid Mech.* 2020, 286, 104434.
- Soltanpour, M.; Samsami, F. A comparative study on the rheology and wave dissipation of kaolinite and natural Hendijan Coast mud, the Persian Gulf. *Ocean Dyn.* 2011, 61, 295–309. <https://doi.org/10.1007/s10236-011-0378-7>.
- Xu, J.; Huhe, A. Rheological study of mudflows at Lianyungang in China. *Int. J. Sediment Res.* 2016, 31, 71–78. <https://doi.org/10.1016/j.ijsrc.2014.06.002>.
- Mietta, F.; Chassagne, C.; Winterwerp, J.C. Shear-induced flocculation of a suspension of kaolinite as function of pH and salt concentration. *J. Colloid Interface Sci.* 2009, 336, 134–141. <https://doi.org/10.1016/j.jcis.2009.03.044>.
- Yang, W.; Yu, G.-I.; Tan, S.k.; Wang, H.-k. Rheological properties of dense natural cohesive sediments subject to shear loadings. *Int. J. Sediment Res.* 2014, 29, 454–470. [https://doi.org/10.1016/S1001-6279\(14\)60059-7](https://doi.org/10.1016/S1001-6279(14)60059-7).
- Goudoulas, T.B.; Germann, N. Viscoelastic properties of polyacrylamide solutions from creep ringing data. *J. Rheol.* 2016, 60, 491–502.
- Mobuchon, C.; Carreau, P.J.; Heuzey, M.-C. Structural analysis of non-aqueous layered silicate suspensions subjected to shear flow. *J. Rheol.* 2009, 53, 1025–1048.

Acknowledgements

I want to thank my daily supervisor and promotor Julia Gebert for uncountable amount of helpful discussions and great support during my four years.

I thank my promotor Timo Heimovaara for the fruitful discussions about my papers.

I want to thank Alexander Gröngröft for the great discussions during my PhD as well as for forwarding me the vacancy that brought me into this PhD.

I want to thank the technicians of TU Delft who supported me always when I needed help in the laboratory.

Thanks also to the student assistants Ties, Daan, Bart, Laurant and Luica for their help with the thousands of measurements.

I also want to thank Rob Comans and Gerlinde Vink for the help during my time in Wageningen and the introduction to the field of organic matter fractionation – I enjoyed working with you.

I want to thank the crew of the Hamburg Port Authority for the great field work with 21 sampling campaigns including hail, rain, wind, fog and sometimes sun.

I also want to thank Deborah Harms and Sumita Rui for their support in the laboratory of the Soil Science Institute in Hamburg for the help of the measurement of hundreds of aerobically incubated samples – the “Bunker” still feels like home!

I want to thank dr. Susan Buisma-Yi and my former roommate Dean for proofreading the thesis.

Further, I want to thank all my friends and colleagues in Den Haag, Delft and Hamburg who supported me during this time.

I want to thank my mum and dad who supported me with great food, a warm bed and anything else I needed when I was on a field trip in Hamburg.

This thesis was conducted within the project BIOMUD, funded by Hamburg Port Authority. BIOMUD is member of the MUDNET academic network (www.tudelft.nl/mudnet/). MUNDNET is a platform created by scientists for knowledge exchange on diverse aspects regarding fine grained sediment.

Curriculum Vitae

Florian Zander

14-03-1992 Born in Hamburg, Germany

Education

2018-2022 PhD student
Delft University of Technology

2014-2017 Master Degree in Soil Science
University of Hamburg, Germany

2011-2014 Bachelor Degree in Geoscience
University of Hamburg, Germany

Work experience

2017 - 2018 Visiting Researcher at School of Urban and Regional Planning
University of the Philippines, Manila

2014 Engineering office, melchior + wittpohl
Hamburg, Germany

2013 - 2016 Student assistant at Institute of Soil Science
University of Hamburg, Germany

List of publications

Zander F, Comans RNJ, Gebert J (2022) Linking patterns of density, thermometric and carbon stable isotope fractions of organic matter to its lability in sediments of the tidal Elbe river, *submitted*

Zander F, Gröngröft A, Eschenbach A, Heimovaara T, Gebert J (2022) Organic matter pools in sediments of the tidal Elbe river. *Limnol*, *accepted for publication on 8 June 2022*

Zander F, Shakeel A, Kirichek A, Chassagne C, Gebert J (2022) Effects of organic matter degradation in cohesive sediment: Linking sediment rheology to spatio-temporal patterns of organic matter degradability. *J Soil Sediment*. doi.org/10.1007/s11368-022-03155-6, *accepted for publication 30 January 2022*

Shakeel A, **Zander F**, de Kerk J-W, Kirichek A, Gebert J, Chassagne C (2022) Effect of organic matter degradation in cohesive sediment: A detailed rheological analysis. *J Soil Sediment* doi.org/10.1007/s11368-022-03156-5, *accepted for publication 30 January 2022*

Shakeel A, **Zander F**, Kirichek A, Gebert J, Chassagne C (2022) Influence of anaerobic degradation of organic matter on the rheological properties of cohesive mud from different European ports. *J Mar Sci Eng* 10(3):446. doi.org/10.3390/jmse10030446

Zander F, Heimovaara T, Gebert J (2020) Spatial variability of organic matter degradability in tidal Elbe sediments. *J Soil Sediment* 20:2573-2587. doi.org/10.1007/s11368-020-02569-4